



Copernicus Climate Change Service



# **Summary report of the coordinated comparison between pan-European and regional datasets in support of the user guidance**

## **D311a\_Lot4.4.2.2**

Issued by: MeteoSwiss / M.Bandhauer, F. Isotta and C. Frei;

MetNO / C. Lussana, O. E. Tveito;

OMSZ / M. Lakatos, Z. Bahari;

Date: 5/28/2020

Ref: C3S\_D311a\_Lot4.4.2.2\_v1

Official reference number service contract: 2017/C3S\_311a\_Lot4\_KNMI/SC1



IMPLEMENTED BY  
 ECMWF



*This document has been produced in the context of the Copernicus Climate Change Service (C3S). The activities leading to these results have been contracted by the European Centre for Medium-Range Weather Forecasts, operator of C3S on behalf of the European Union (Delegation Agreement signed on 11/11/2014). All information in this document is provided "as is" and no guarantee or warranty is given that the information is fit for any particular purpose. The user thereof uses the information at its sole risk and liability. For the avoidance of all doubts, the European Commission and the European Centre for Medium-Range Weather Forecasts has no liability in respect of this document, which is merely representing the authors view.*



## Contributors

### Meteoswiss

M. Bandhauer  
F. Isotta  
C. Frei

### MetNO

C. Lussana  
O. E. Tveito  
L. Båserud

### OMSZ

M. Lakatos  
Z. Bahari  
B. Izsák  
O. Szentes  
L. Hoffmann  
A. Kircsi  
T. Szentimrey (*Varimax Limited Partnership, Hungary*)



## Table of Contents

Abstract	8
1. Scope of this document	8
Parameters and used evaluation datasets	9
E-OBS	10
ERA5	11
COSMO-REA6	12
Reference datasets used	12
NGCD	13
APGD	14
LAPrec	15
CARPATCLIM	16
Data specifications	17
2. Domains	18
2.1 Fennoscandian region	19
2.2 Alpine region	22
2.3 Carpathian region	23
3. Precipitation	24
3.1 Fennoscandia	26
3.1.1 Climate Indices	26
3.1.2 Yearly cycle	33
3.1.3 Temporal Trends	34
3.1.4 Extreme event: Flood on 30 September to 2 October 2017	35
3.1.5 Verification scores	36
3.1.5.1 SEEPS	36
3.1.5.2 ETS	41
3.1.5.3 LINEAR REGRESSION	42
3.1.6 Frequency Distribution Function	42
3.1.7 Main outcomes – precipitation in Fennoscandia	43
E-OBS	43



ERA5	44
GENERAL COMMENTS	44
3.2 Alpine region	44
3.2.1 Mean annual precipitation	44
3.2.2 Yearly cycle	46
3.2.3 Wet-day frequency	47
3.2.4 95th quantile	48
3.2.5 Example of an extreme event: Flood on 21st/22nd August 2005	50
3.2.6 Theil-Sen Trend	52
3.2.7 RMSE	54
3.2.8 MSESS	55
3.2.9 SEEPS	56
3.2.10 Rank histogram	56
3.2.11 Frequency distribution function	57
3.2.12 BSS	58
3.2.13 Main outcomes – precipitation in the Alpine region	59
E-OBS	59
ERA5	59
GENERAL COMMENTS	59
3.3 Carpathian region	59
3.3.1 Mean annual precipitation	60
3.3.2 Yearly cycle and Catchments based studies	61
3.3.3 Wet-day frequency	66
3.3.4 95th quantile	67
3.3.5 Example of an extreme event: daily precipitation on 15 and 16 May 2010	68
3.3.6 RMSE	70
3.3.7 MSESS	75
3.3.8 Analysis of Variance (ANOVA)	79
3.3.9 Maxima of daily precipitation	88
3.3.10 Trends	90
3.3.11 Homogeneity test	91
3.3.12 Main outcomes – precipitation in the Carpathians	94



E-OBS	95
ERA5	95
4. Temperature	96
4.1 Fennoscandia	97
4.1.1 Climate Indices	97
4.1.2 Yearly Cycle	103
4.1.3 Verification scores	107
4.1.4 Case study. Tropical nights in 2018	119
4.1.5 Main outcomes – temperature in the Fennoscandia	120
E-OBS	120
ERA5	121
4.2 Carpathian region	121
4.2.1 Analysis of Variance (ANOVA)	121
4.2.2 Yearly cycle	139
4.2.3 Mean annual DTR	141
4.2.4 Quantiles TX and TN	142
4.2.5 Climate indices	148
4.2.6 RMSE	154
4.2.7 MESS	160
4.2.8 Trends	164
4.2.9 Homogeneity test	166
4.2.10 Main outcomes – temperature in the Carpathians	173
E-OBS	174
ERA5	175
5. Conclusion	176
E-OBS	176
PRECIPITATION	176
TEMPERATURE	176
ERA5	177
PRECIPITATION	177
TEMPERATURE	177
6. References	179



## Appendix

182



## Abstract

In recent years, E-OBS has proven to be a state-of-the-art pan-European dataset based on in-situ measurements. With the new update, including increased spatial resolution, more observations, a new homogenization approach and an ensemble dataset, an evaluation becomes necessary. Consequently, E-OBS, as well as the newly available global reanalysis ERA5 and the regional reanalysis COSMO-REA6, are being tested against regional gridded datasets. Given the higher spatial resolution of both compared to their predecessors, daily precipitation and temperature are investigated on a mesoscale. By calculating climate indices and several statistical tests in three European sub-regions, namely in the Carpathians, Fennoscandia and the Alpine region, information about the spatial distribution, intra- and inter-annual variation and extreme behavior of these parameters is gained. The improvements and the limitations of E-OBS and of ERA5 are hence highlighted in this deliverable. Overall, E-OBS performs best in flat areas with a high station density, as opposed to complex topography. E-OBS tends to underestimate precipitation compared to all regional high-resolution datasets. ERA5, on the other hand, realistically represents precipitation and temperature patterns in general. However, the magnitude of precipitation is overestimated and the coarser original grid resolution leads to misrepresentation of temperature in transitive regimes and of small catchments prone to heavy precipitation.

## 1. Scope of this document

The pan-European observational dataset E-OBS has been considered as a reference for several European climate analyses until today. After having received a major update and now being available as an ensemble dataset, an evaluation is necessary to find out about the suitability of E-OBS. In order to do so, the new E-OBS dataset is compared to several regional high-resolution climate datasets in this deliverable. In addition to that, the newly available global reanalysis ERA5 and the regional reanalysis COSMO-REA6 is tested against these regional datasets and then compared to E-OBS. To examine the performance of both datasets under different circumstances, European subregions are considered: Fennoscandia, the Alpine region and the Carpathian region. The improvements, as well as the limitations of the new E-OBS datasets will be carved out with the help of several statistical tests. These statistical tests include the calculation of climate indices, which show the general, seasonal and extreme behavior and the deviations between the examined datasets. The update of E-OBS and its evaluation are performed in the framework of the COPERNICUS C3Surf project work package 4 (WP4) (C3S\_311a\_Lot4), ending in 2021.

After an overview on all datasets used in this report, the three European regions are described in more detail in Section 2. At the beginning of Section 3, the examined precipitation indices and statistical measures are explained, followed by the evaluation results for all regions separately. Analogously, in Section 4, the examined indices and statistical measures of mean, maximum and minimum temperature and the evaluation results are presented for all regions separately.



## Parameters and used evaluation datasets

The focus of the evaluation has been on precipitation as it is still a challenge for climate datasets to correctly represent this climate variable, especially in complex terrain. Given that the main dataset of interest, E-OBS, also provides near-ground temperature, it was included in the evaluation, where the reference datasets also include this variable. All investigated parameters are listed in Table 1.1, together with their abbreviations and their definitions. Furthermore, in Table 1.2 the two evaluation datasets, E-OBS and ERA5 (including its different setups), and the supplementary COSMO-REA6 are listed together with their domains, coordinate system (CRS), spatial resolution and time coverage. Additionally, the considered variables are denoted for every reference dataset.

Abbreviation	Name	Definition
RR	Precipitation	Daily precipitation sum (mm) aggregated between 06:00 UTC of the day specified in the time-stamp attached to a field and 06:00 UTC of the day previous to that.
TG	Mean Temperature	Daily mean temperature (°C) aggregated between 06:00 UTC of the day specified in the time-stamp attached to a field and 06:00 UTC of the day previous to that.
TX	Maximum Temperature	Daily maximum temperature (°C) is the highest temperature between 18:00 UTC of the day specified in the time-stamp attached to a field and 18:00 UTC of the previous day.
TN	Minimum Temperature	Daily minimum temperature (°C) is the lowest between 18:00 UTC of the day specified in the time-stamp attached to a field and 18:00 UTC of the previous day.

Table 1.1: List of investigated parameters with their abbreviations and the exact definition.



Name	Domain	CRS	Grid res.	Time coverage/ ensemble size	Variables
COSMO-REA6	Alps	rotpol	0.055°	1997-2008	RR
E-OBS	EU	latlon	0.1°	1950-2018	RR, TG, TX, TN
E-OBS-Ens	EU	latlon	0.1°	1950-2018 / 100 ensemble members	RR, TG, TX, TN
ERA5-HRES	EU	latlon	0.25°	1979-2018	RR, TG, TX, TN
ERA5-ENDA	EU	latlon	0.5°	1979-2018 / 10 ensemble members	RR, TG, TX, TN
ERA5-LAND	EU	latlon	0.125°	2000-2018	RR, TG, TX, TN

Table 1.2: List of evaluation datasets considered. CRS (coordinate system): latlon = regular latitude/longitude; rotpol = rotated pole.

## E-OBS

E-OBS version 19.0 (Cornes et al., 2018) has been downloaded from the Copernicus website (<http://surfobs.climate.copernicus.eu/dataaccess/index.php>) and the variables considered are RR, TG, TX and TN. E-OBS is an observational gridded dataset that covers Europe with a grid resolution of 0.1°. This corresponds to a grid spacing of roughly 10 km in both meridional and zonal directions. E-OBS consists of a dense, regionally different station network, which is depicted in Figure 1.1. Since its first version from 2008 (Haylock et al., 2008) it has been extensively used for climate model evaluation and climate monitoring in Europe (e.g. Isotta et al., 2015) and regularly updated. The dataset only encompasses quality-controlled in-situ measurements based upon the station series of the European Climate Assessment Dataset (ECA&D) initiative (Klok and Klein Tank, 2008). Aside from changes regarding the gridding technique, which are described in detail in Cornes et al. 2018, a

new homogenization method has been applied for this version (Squintu et al., 2019; Squintu et al., 2020). Despite the strongly varying station density over the domain, E-OBS today can be regarded as the main reference dataset on European scale thanks to its unique amount of station data involved on a large-scale. Furthermore, the dataset was extended toward a probabilistic dataset, consisting of 100 ensemble members. This is done via a conditional simulation procedure, where each ensemble member represents a spatially correlated random field, derived from a global variogram, which is calculated for every day (Cornes et al. 2018).

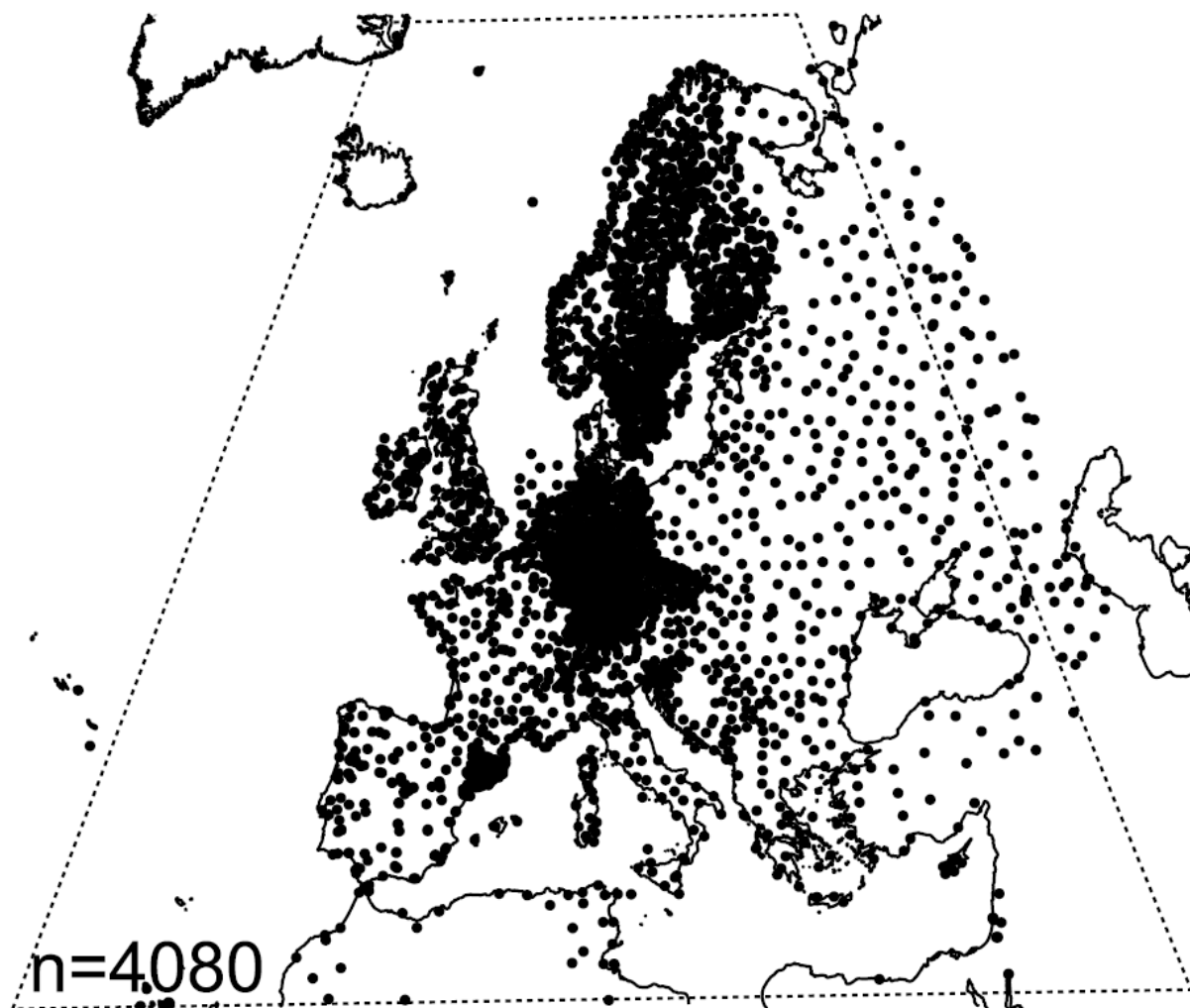


Figure 1.1: Map showing the n=4080 stations from which temperature measurements between 1950 and 2017 are available in the pan-European E-OBS dataset (Cornes 2018).

## ERA5

With ERA5, a new global reanalysis is investigated in order to show the potential of ad-hoc reanalyses compared to observational datasets (Copernicus Climate Change Service (C3S), 2017; Hersbach et al. 2020). Here, we have considered the high-resolution realization (ERA5-HRES), the



reduced resolution ten member ensemble (ERA5-EDA) and in the case of Fennoscandia, also the replay of the land component of ERA5 (ERA5-LAND) has been investigated. The three different ERA5 datasets have different characteristics and they are produced over three different grids. The data can be downloaded from the Climate Data Store (CDS) onto regular grids covering the whole of Europe in the geographical coordinate reference system with different spacing: ERA5-EDA 0.5 degree (in both zonal and meridian directions), ERA5-HRES 0.25 degree and ERA5-LAND 0.125 degree. The time period considered ranges from 1979 to 2018. Since we have chosen to download the data at the finest time resolution available, the time resolution of the three datasets were different: hourly data for ERA5-HRES and ERA5-LAND, three-hourly data for ERA5-EDA (at e.g., 09:00 UTC, 12:00 UTC, ...). The variables downloaded were also different among the datasets. For ERA5-HRES and ERA5-EDA we have downloaded: total precipitation amounts (precipitation\_amount\_acc), 2 meter temperature (air\_temperature\_2m), maximum temperature at 2 meters since previous post-processing (mx2t), minimum temperature at 2 meters since previous post-processing (mn2t).

## COSMO-REA6

As supplement to the relatively coarsely resolved ERA5, the regional reanalysis, COSMO-REA6 is taken into account. COSMO-REA6 has a spatial resolution of  $0.055^\circ$ , which equals to a grid spacing of around 6 km, it has an hourly temporal resolution and it covers the entire European continent, corresponding to the COordinated Regional climate Downscaling EXperiment (CORDEX) EUR-11 domain (Giorgi et al., 2009) (see Bollmeyer et al. 2015 Figure 1). Despite covering entire Europe, it is hereafter only used to provide insight on smaller scale parts of the evaluation in the Alpine region. As COSMO-REA6 only covers the time period between 1997 and 2008, it is only considered in analyses which do not strongly depend on the length of the data availability. For this study, daily aggregated precipitation (RR) has been used.

## Reference datasets used

To evaluate the above listed datasets, reference datasets from three European sub-regions were investigated. In the Alpine region, only the precipitation dataset is examined, whereas in the Fennoscandian and the Carpathian regions both climate variables are investigated. All used reference datasets are listed in Table 1.3 together with their domains, coordinate system (CRS), spatial resolution and time coverage. Also, the considered variables are denoted for every reference dataset.

Name	Domain	CRS	Grid res.	Time coverage/ ensemble size	Variables
APGD	Alps	Iaea	5 km	1971-2008	RR



APGD-Ens	Alps	Iaea	catchments	1971-2008 / 100 ens. members	RR
CARPATCLIM	Carpathians	lonlat	0.1°	1961-2010	RR, TX, TN
LAPrec	Alps	Iaea	5 km	1871/1901-2010	RR
NGCD-1	Fennoscandia	Iaea	1 km	1961-2019	RR, TG, TX, TN
NGCD-2	Fennoscandia	Iaea	1 km	1957-2017	RR, TG, TX, TN

Table 1.3: List of reference datasets. CRS (coordinate system): latlon = regular latitude/longitude; Iaea = ETRS89 Lambert Azimuthal Equal-Area projection coordinate reference system.

## NGCD

The Nordic Gridded Climate Dataset (NGCD) is a regional observational gridded dataset covering Fennoscandia (Finland, Sweden and Norway) with a grid resolution of 1 km in both meridional and zonal directions. Analogously to E-OBS, the data is freely available via Copernicus (<http://surfobs.climate.copernicus.eu/dataaccess/index.php>). The observational datasets used for the production of the gridded field consist mostly of the in-situ measurements provided by the European Climate Assessment Dataset (ECA&D: Klein Tank et al., 2002), with the exception of Norway where some more stations have been included. The additional stations of temperature and precipitation have been made available by the MET Norway's climate database (frost.met.no). For the gridding process, the Lambert azimuthal equal-area coordinate (LAEA) reference system is used. The variables produced are RR, TG, TX and TN. For each of the variables, NGCD offers two alternative datasets (NGCD-1 and NGCD-2). For RR, NGCD-1 is based on a triangulation procedure with an elevation-dependent systematic adjustment of the precipitation field; NGCD-2 implements a successive correction method over multiple spatial scales. For temperature, NGCD-1 is based on a residual kriging approach, applying five external predictors to describe the large scale trend (background) field: elevation, mean elevation within a 20 km circle, lowest elevation within a 20 km circle, longitude, latitude; NGCD-2 implements a scale-separation approach based on Optimal Interpolation (OI).

## APGD

The Alpine Precipitation Grid Dataset (APGD) is used as a reference throughout the precipitation analysis in the Alpine region and is described in detail in Isotta et al. (2014) (Figure 1.2). APGD has an original grid resolution of 5 km in meridional and zonal direction and provides daily precipitation from 1971 to 2008. The effective grid spacing, which equals the average distance between neighboring stations, is in the order of 10-20 km and thus tends to be slightly larger than grid resolution of APGD. This limitation is especially important in regions like Northern Italy where the station density is comparatively low.

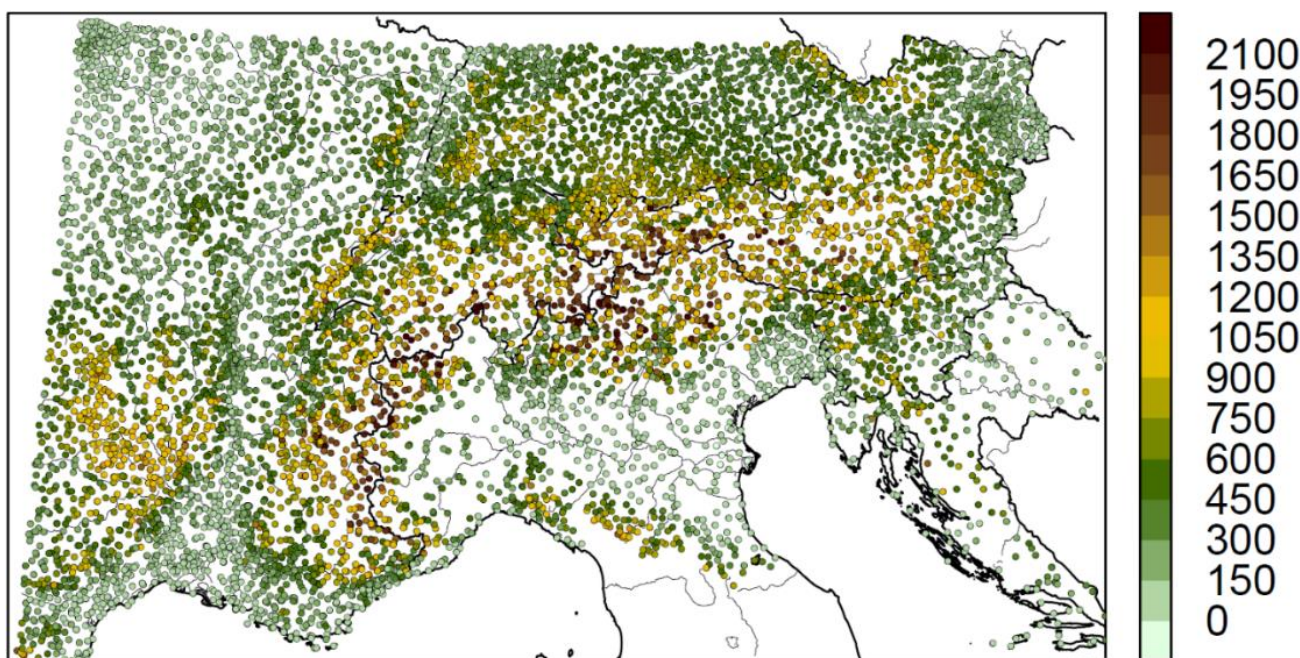


Figure 1.2: Map showing the stations from which precipitation measurements between 1971 and 2008 are available in the high-resolution reference dataset (APGD). The location bullets of each station are colored according to their altitude [m a.s.l.].

A special focus of the evaluation is on the representation of precipitation depending on the region and scale. To achieve the latter, a scale separation approach is applied by using an additional dataset as reference, named “APGD-Ens” hereafter. Starting from the same observations as APGD (Figure 1.2), a probabilistic spatial analysis of daily precipitation that is capable of quantifying uncertainties was developed. Instead of a regular grid, daily precipitation is represented for hydrological units of different sizes according to the European Catchment Dataset to account for aspects of scale separation (European Environment Agency, 2016) (Figure 1.3). In this evaluation study, 15 out of a total of 325 of these hydrological catchments were subsequently used (Figure 1.3). In order to represent different kinds of catchments, the middle sized are of Black Forest in Southwestern Germany, the middle sized Upper Aare catchment from Alpine Switzerland and the smaller sized Tagliamento catchment from the precipitation intense Julian Alps between Italy and Slovenia were chosen for a closer investigation. The first one represents a catchment with a typical

moderate climate from a relatively flat area, where E-OBS has a high station density (Figure 1.1), the second one represents a catchment reaching into the Central Alps and has a comparatively large size and finally the third one represents an extraordinarily wet catchment, which lies in the Mediterranean zone and is still in the middle of mountains.

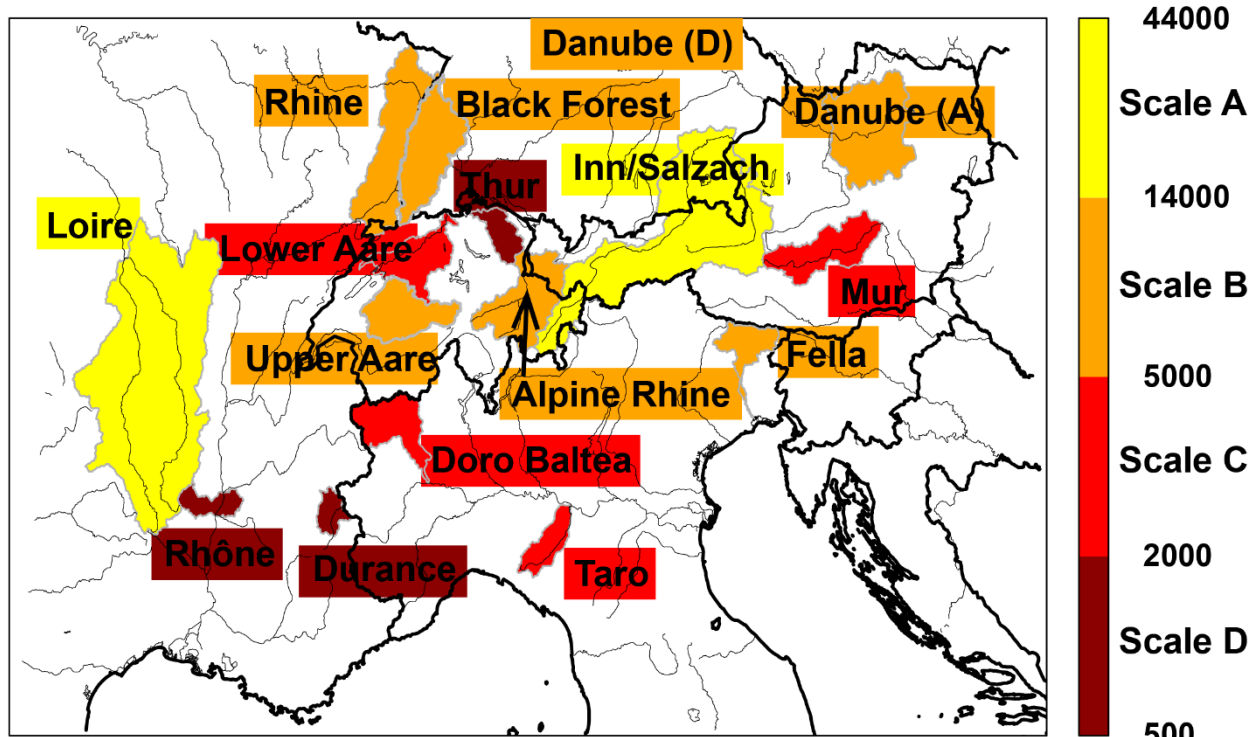


Figure 1.3: Map showing the 15 hydrological catchments used for the evaluation of E-OBS. The color scale ranges from bordeaux to yellow with the color depending on the size of the catchments (given in square kilometers).

### LAPrec

In addition to that, the new gridded precipitation dataset LAPrec (long-term Alpine precipitation reconstruction), developed in the framework of the Copernicus Climate Change Service Project C3Surf (C3S\_311a\_Lot4), was partly included in this evaluation (Isotta 2020). The dataset extends back until 1871 and was specifically constructed to satisfy high standards in climate consistency. LAPrec has a less dense station network due to the long-term time consistency and is only available on a monthly basis, which is why it is only considered for the monthly/yearly indices. It covers the mountain range of the European Alps with territory from eight countries. Overall, LAPrec is less suited for applications where the interest is in small-scale spatial patterns (scales smaller than ~20 km), or when high absolute precision is required.



## CARPATCLIM

To overcome the lack of a dense long-term dataset based on in-situ measurements for the Carpathian region because of strict data policy, the CARPATCLIM dataset has been developed. CARPATCLIM is a gridded dataset encompassing daily observations (Figure 1.4). It is available on a  $0.1^\circ$ ( $\sim 10 \text{ km} \times 10 \text{ km}$ ) grid and includes homogenized, gridded daily time series of various meteorological parameters from 1961 to 2010. The method and software used for data quality control, homogenization, data completion were the Multiple Analysis of Series for Homogenization software (MASH version 3.03; Szentimrey 1999, 2008). Interpolation of the homogenized time series were carried out by applying the MISH (Meteorological Interpolation Based on Surface Homogenized Data Basis version 1.03; Szentimrey and Bihari, 2007) method. The near border data exchange before and after homogenization ensured the harmonization between countries. The homogenization and interpolation were carried out by the participating countries themselves and the harmonized country grids were merged in the end. CARPATCLIM is a daily dataset for TN, TG, TX, RR, wind direction and speed, sunshine duration, cloud cover, global radiation, relative humidity, vapour pressure, air pressure, snow depth, several climate indicators and drought indices from 1961 to 2010. The complete procedure is described in detail on the webpage of CARPATCLIM. An overview of the applied procedures and trend analysis of the basic variables can be found in Spinoni et al. (2015). The daily grids with the metadata are freely accessible on the website of the project: [www.carpatclim-eu.org](http://www.carpatclim-eu.org). The temperature and precipitation grids are available also via Copernicus: [https://surfobs.climate.copernicus.eu/dataaccess/access\\_carpatclim.php](https://surfobs.climate.copernicus.eu/dataaccess/access_carpatclim.php). The climate indices derived from CARPATCLIM are available via Copernicus too: [https://surfobs.climate.copernicus.eu/dataaccess/access\\_carpatclim\\_indices.php](https://surfobs.climate.copernicus.eu/dataaccess/access_carpatclim_indices.php)

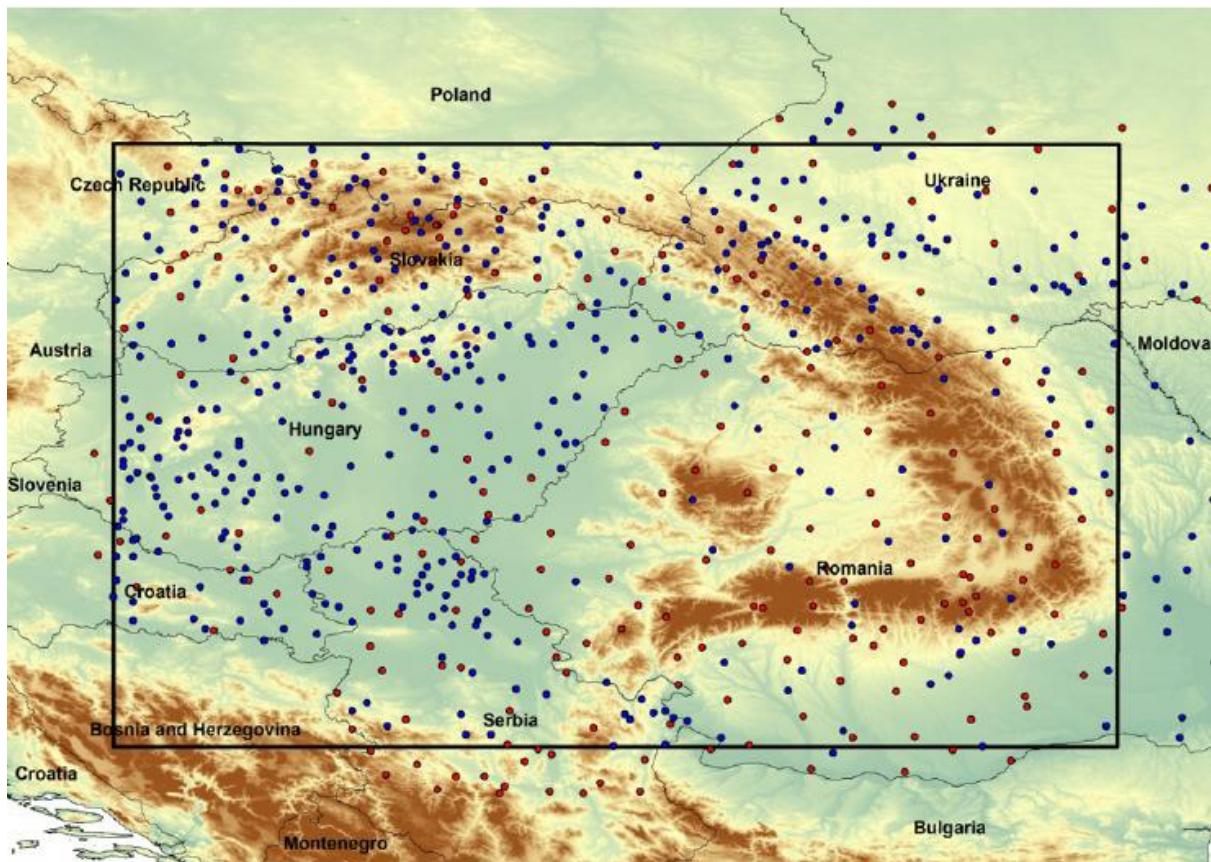


Figure 1.4. Stations with both precipitation and temperature data (red dots) and stations with precipitation data only (blue dots). The black rectangle encloses the Carpathian region.

## Data specifications

The datasets have been generated by different institutions over grids with different specifications and with different time resolutions. First, the sub-daily fields have been aggregated to get daily RR, TG, TX and TN as previously defined, for all datasets except for the monthly resolved LAPrec. However, two different definitions of “day” have been used. In fact, for total accumulated precipitation (RR) and mean temperature (TG), the data has been aggregated between 06:00 UTC of the day specified in the time-stamp attached to a field and 06:00 UTC of the day previous to that. For minimum (TN) and maximum (TX) temperature, the data has been considered between 18:00 UTC of the day specified in the time-stamp attached to a field and 18:00 UTC of the previous day (Table 1).

Second, we have decided to regrid all datasets onto the  $0.1^\circ \times 0.1^\circ$  regular latitude-longitude grid of E-OBS to establish comparability between the various datasets. In the case of NGCD and APGD, the conversion is done by transforming the grid coordinates from the native LAEA reference coordinate system, measured in meters, into the geographical system used by E-OBS, measured in degrees of longitude and latitude. The upscaled RR values of one E-OBS grid point are derived with the help of



bilinear interpolation and hence by averaging the four corresponding grid points from the finer grids. The same was done for ERA5 in the Alpine region, in Fennoscandia and in the Carpathians, namely the data was downscaled from  $0.25^\circ$  to  $0.1^\circ$  with a bilinear interpolation. When regridding CARPATCLIM to E-OBS grid, a  $0.05^\circ$  shift between the grid systems was found. In order to use the same grid points in all analyses, E-OBS was hence regridded onto CARPATCLIM grid by applying the nearest neighbor method. Considering temperature in Fennoscandia, the values were downscaled by taking into account the elevation of E-OBS grid points. In particular, for each E-OBS grid point only ERA5 points lying within a small neighborhood surrounding it were considered. It needs to be noted that the exact size of this neighboring area depends on ERA5 dataset considered and it was set according to a visual inspection of the final fields. Those grid points have been used to locally compute a vertical profile of near-surface temperature, which has then been used to extract the temperature value corresponding to E-OBS grid point elevation.

The grid resolution of  $0.1^\circ$ , which roughly equals to  $10 \text{ km} \times 10 \text{ km}$ , is assumed to be statistically reasonable, given that for some regions and datasets the distance between available measurement stations is larger than the finest available grid spacing. While E-OBS ensemble (E-OBS-Ens) is available on a  $0.1^\circ$ -grid, ERA5 ensemble (ERA5-Ens) is only available on a  $0.5^\circ$ -grid and hence too coarse for a statistically reasonable regridding.

For Fennoscandia it is worth remarking that the reference datasets and E-OBS are based on very similar sets of observational data, the main difference being that NGCD uses more observations over Norway. For CARPATCLIM the number of stations behind the daily grids are substantially higher than in E-OBS. All involved observational datasets have in common that they implement spatial analysis techniques through statistical methods. On the contrary, ERA5 is based on a sophisticated mixture of statistical methods (4D-Var data assimilation) with atmospheric dynamics (numerical models), which uses a totally different set of observations. For this reason, the evaluation of ERA5 against the reference datasets needs to be treated individually. By evaluating ERA5 against the reference datasets and E-OBS against the reference datasets, it is possible to qualitatively assess the significance of the deviations of E-OBS and ERA5 and to infer the added value of a continental dataset such as E-OBS with respect to a global reanalysis.

## 2. Domains

In this Section, the three European regions that were investigated in order to evaluate E-OBS, are shown and described. At first, the region of Fennoscandia is presented, including the partition into subregions. Secondly, the Alpine region including its split-up into hydrological catchments, is shown and finally the Carpathian region is shown.



## 2.1 Fennoscandian region

Fennoscandia extends from 2 to 17.5°E and from 43 to 49°N and consists of Finland, Sweden and Norway. The variety of climates is a challenge for climate modeling and gridded observational datasets. While the westernmost coast along Norway has a precipitation intense oceanic climate, the continental parts of Sweden and Finland oppose a rather cold and dry climate. These different climates are divided by the Scandinavian mountain ridge.

Figure 2.1.1 shows the domain considered for NGCD, the three countries considered are delimited by the national borders (black lines). Oceans, lakes and rivers are shown in blue. The topography is shown with the color shades. The complex topography of the Scandinavian mountains, with the highest peaks above 2000 m in southern Norway and in northern Sweden, is known to cause pronounced orographic enhancement of precipitation along the Norwegian coast, especially along the western coast.

Figures 2.1.2 and 2.1.3 show the subregions chosen for precipitation and temperature, respectively, in the analyses reported in Sections 3 and 4. In addition to the entire Fennoscandia, we have considered three subregions within Norway showing three distinct climates. The meridional part of Norway has been divided in two regions: western Norway (No-West, pink) and eastern Norway (No-East, blue), then the central and the northern part of Norway is considered as a single subregion (No-North, yellow). In fact, the more we move towards higher latitudes, the more the station network becomes sparser, then the region No-North has been used to achieve more robust and significant statistical results.

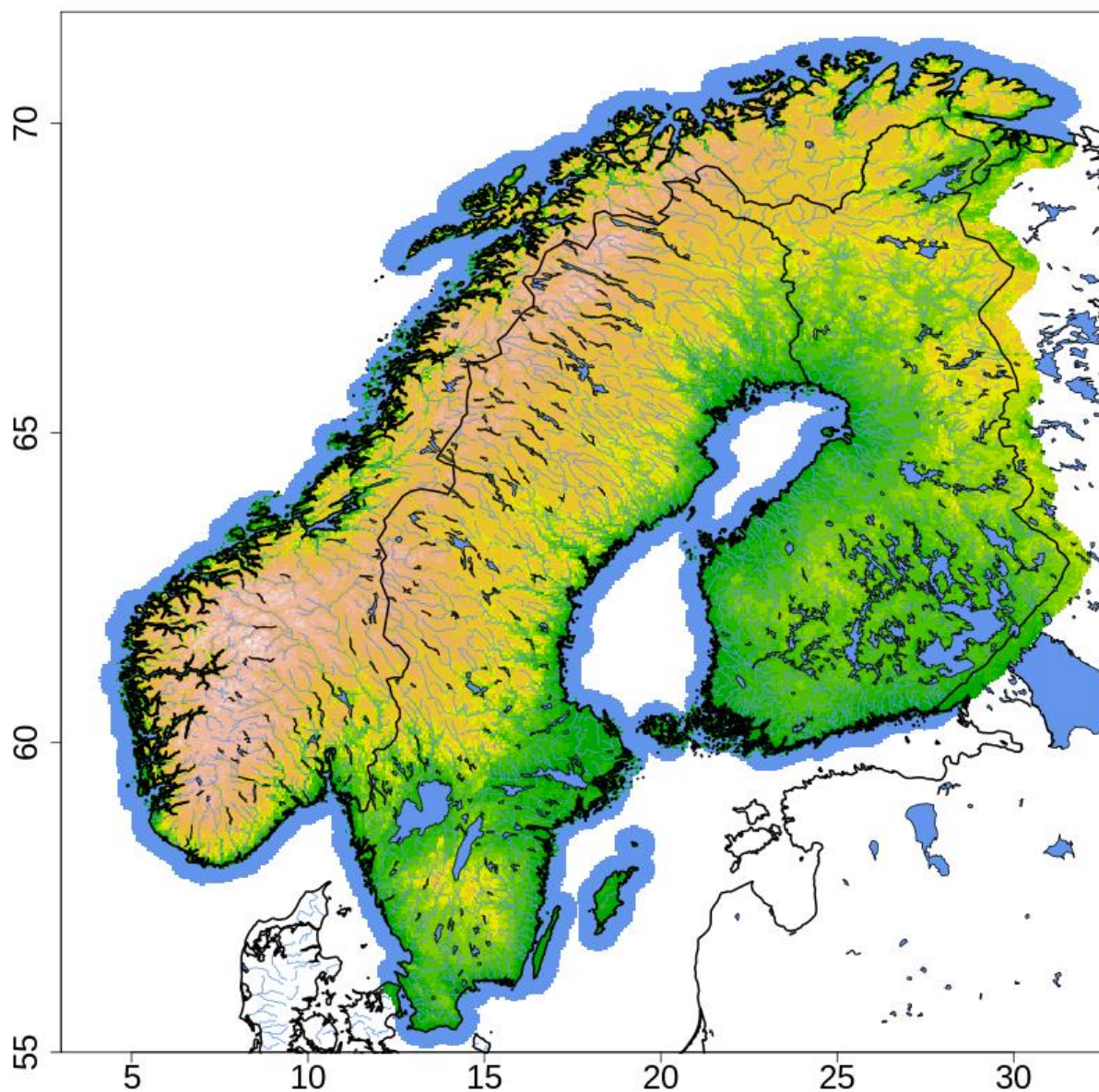


Figure 2.1.1. Fennoscandian domain considered for NGCD.

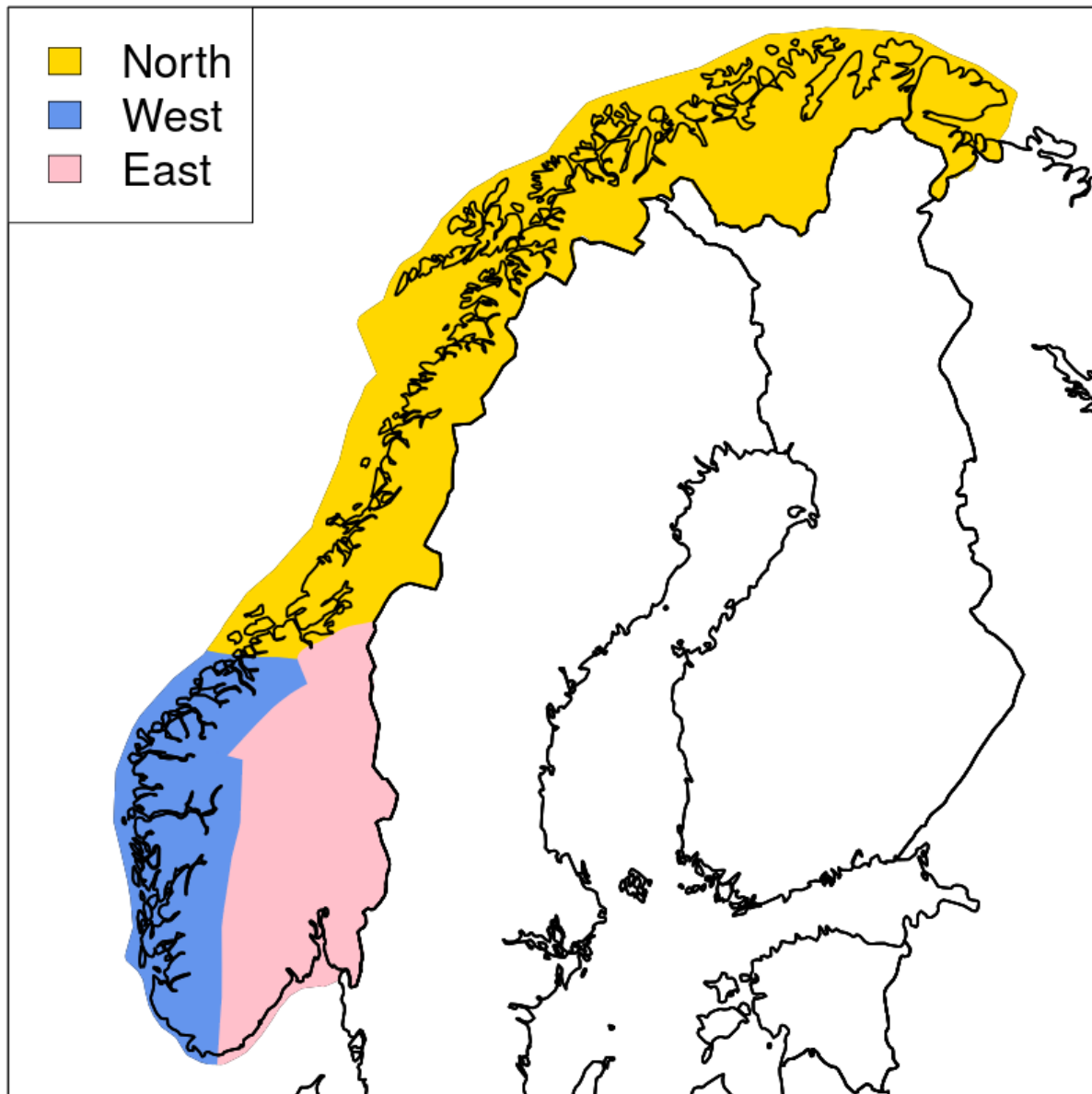


Figure 2.1.2. Map of the subregions used for precipitation. Fennoscandia (Figure 7) is the domain of our study and it is identified as the region “All”. The subregions used in our analyses are: western Norway (“No-West”), eastern Norway (“No-East”) and northern Norway. In addition, the abbreviation “No-All” is used for the entire Norwegian mainland.

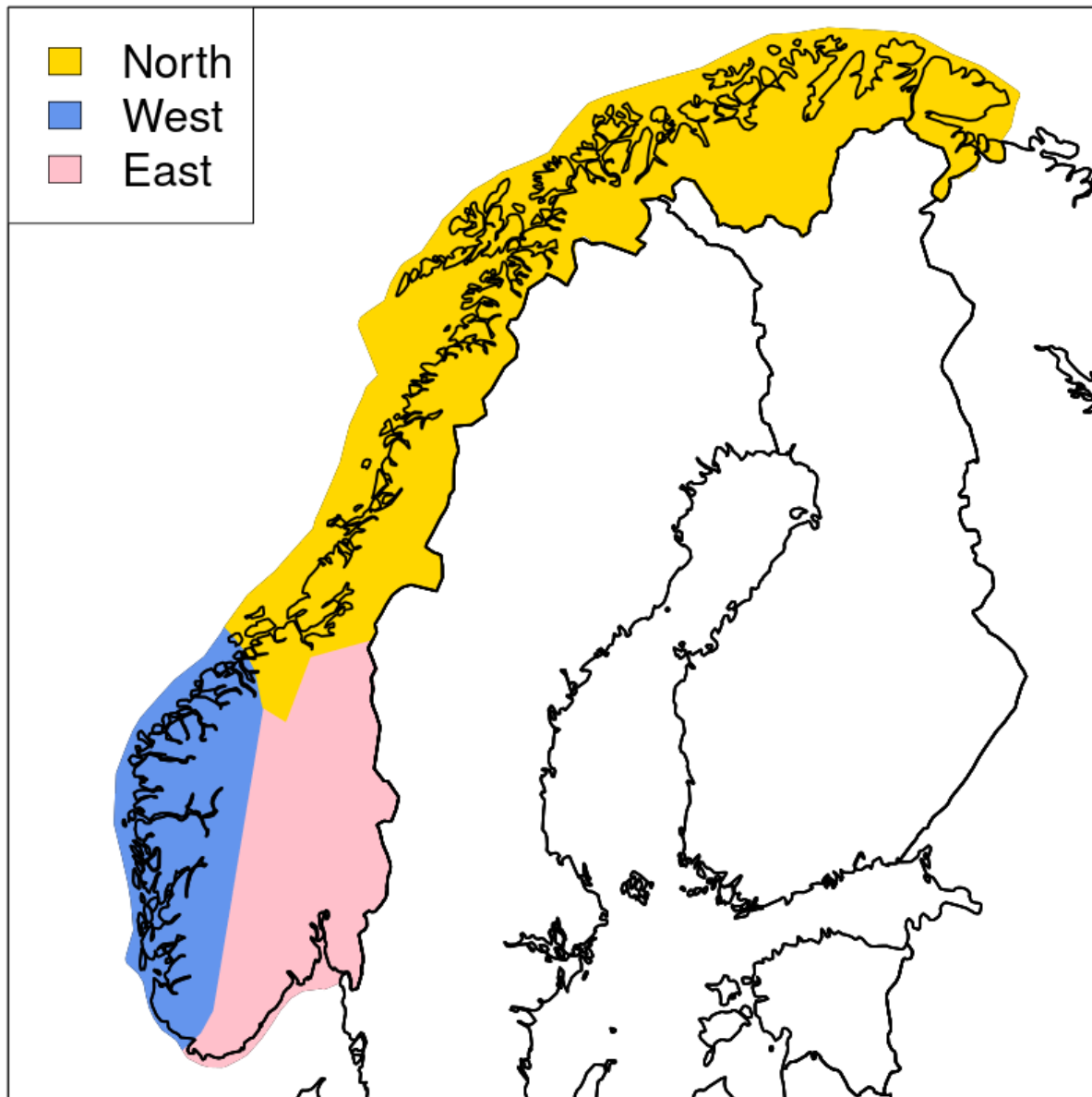


Figure 2.1.3. Map of the subregions used for temperature. Fennoscandia (Figure 7) is the domain of our study and it is identified as the region "All". The subregions used in our analyses are: western Norway ("No-West"), eastern Norway ("No-East") and northern Norway. In addition, the abbreviation "No-All" is used for the entire Norwegian mainland.

## 2.2 Alpine region

The study region extends from 2 to 17.5°E and from 43 to 49°N, comprising the entire mountain range of the European Alps as well as adjacent flatland and smaller hill ranges. The domain includes the area of Switzerland, Liechtenstein, Austria, Slovenia and Croatia, as well as parts of France, Germany, Italy, Czech Republic, Slovakia, Hungary and Bosnia and Herzegovina. Several mountainous areas are involved, namely the Massif Central in Southeastern France, the Vosges and Black Forest along the Upper Rhine valley, the Bohemian Forest, the Apennine in Northern Italy as well as the

Julian and the Dinaric Alps in the Southeast. Because of this complex topography and the strongly varying local climates encompassed by it, the Alpine region is challenging for climate modelling.

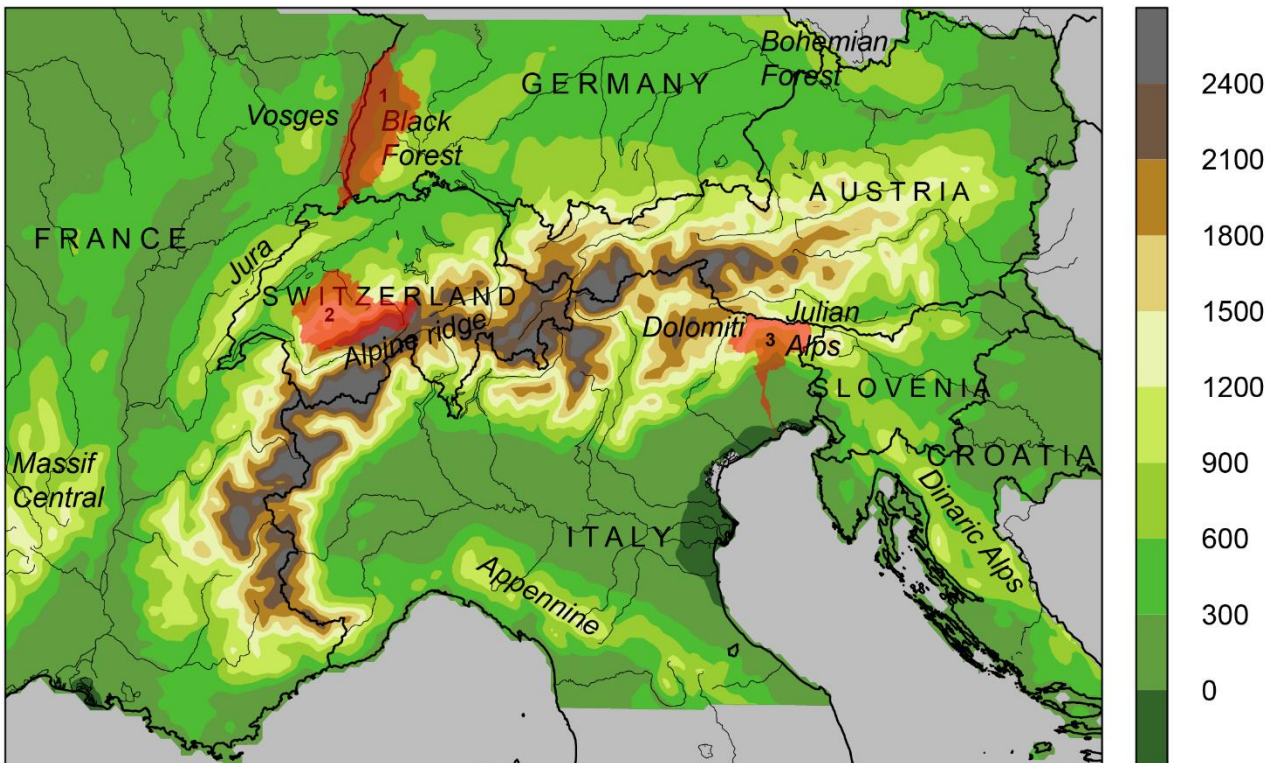


Figure 2.2.1: Map showing the topography [m.a.s.l.], the rivers and the lakes in the Alpine region on a 5km grid (ETRS-LAEA). Marked in red are the three in-depth examined catchments: 1: Black Forest (D), 2: Upper Aare (CH) and 3: Tagliamento (I).

### 2.3 Carpathian region

The Carpathians are the longest mountain range and the geographic barrier between central Europe, Eastern Europe and the Balkans. Bordered by the Alps in the northwest, the Dinaric Alps in the southwest and by the Carpathians in northeastern direction, and divided by the Danube river on the central Carpathian Basin. The Carpathian region is a transition area between Mediterranean, Atlantic and continental climates. The study region extends from 17-27°E and 44- 50°N., covering the entire Carpathian region and thus parts of the Czech Republic, Slovakia, Poland, Ukraine, Romania, Serbia, Croatia, Austria and Hungary. The mixture between a large basin of continental climate surrounded by mountains is a challenge for climate modeling and also for gridded observational datasets.

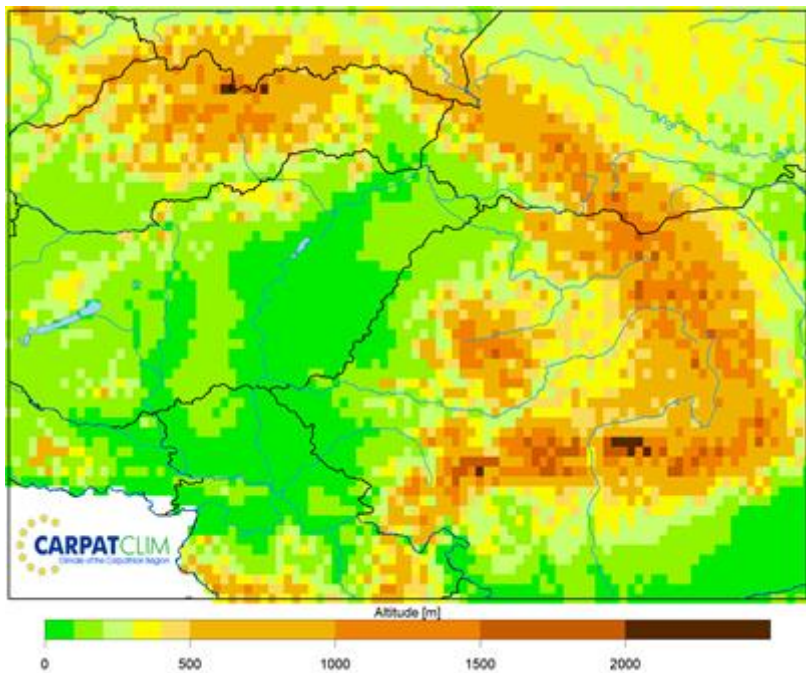


Figure 2.3.1: The domain of CARPATCLIM

### 3. Precipitation

Before the evaluation results of precipitation (RR) of the investigated datasets E-OBS and ERA5 are presented, each of the examined climate indices and statistical measures of RR are explained. As a first step, the mean annual precipitation is calculated to get an overview on the precipitation climatology over regions and to find out about the main characteristics of those datasets. Principal patterns like regions of strong orographic precipitation or continental, dry plains should be thereof detected as well as general insights regarding the wetness of each dataset.

To depict the seasonal behavior of all compared datasets, the monthly averages are calculated and depicted as time series. By looking at the yearly cycle precipitation, a geographic region can be easily characterized in terms of precipitation climate. Also, the distribution of precipitation throughout the year reveals the origin of each dataset, whether it is prone to large precipitation amounts or not and whether these amounts are likely or not. By furthermore splitting up regions into smaller catchments, to capture the yearly cycle of mesoscale precipitation climates can be tested.

A more general characteristic of a precipitation dataset is its wetness. The wetness can be derived by calculating the amount of days with more precipitation than 1 mm ( $>1 \text{ mm/d}$ ) and then dividing this number through the number of all days. This results in a property, which informs about the frequency of rainy days, the so-called Wet-day frequency (WDF).



Because extreme events occur very rarely and locally they are often not represented in large-scale datasets. But, in order to characterize a dataset completely, a look at intense and heavy precipitation is essential. Therefore, the 95th quantile (Q95), “i.e. the daily precipitation amount which is exceeded on average every 20 days” (Isotta et al. 2015), is calculated and examined in this evaluation study.

In order to give insight on the error structure of the datasets, the Root Mean Square Error (RMSE) is examined. It is an easily interpretable measure for the uncertainty of E-OBS and ERA5 compared directly to the reference datasets.

A more sophisticated measure of a dataset’s performance is the Mean Square Error Skill Score (MSESS). The aim of this measure is to depict the amount of explained variation in each dataset. Once again this is done by referencing E-OBS and ERA5 to the regional state-of-the-art datasets.

For Fennoscandia and for the Alpine region, several other verification scores and statistic measures have been considered that do not focus only on the averages or systematic errors but that evaluate also the ability of the datasets in representing extreme values. Among them are the SEEPS (Stable Equitable Error in Probability Space). SEEPS is used to investigate the magnitude depending performance and therefore involves a three-categorial approach. It distinguishes between dry days (< 1mm/day), days with light and days with heavy precipitation. Light precipitation accounts for two thirds of all wet days and heavy precipitation for one third of all wet days. This score is considered as an error score instead of a skill score because it treats anomalous behavior in the probability space. Consequently, this score is robust when skewed data like precipitation is involved. Furthermore, it is stable regarding the sampling uncertainty “by applying ‘strong perfect forecast’ constraints” and equitable thanks to lower and upper boundaries for ‘constant forecasts’ and ‘perfect forecasts’ (Rodwell et al. 2014).

Also, the Brier Skill Score (BSS) is calculated in the Alpine region. With the help of BSS, the improvement of a probabilistic forecast relative to a reference forecast can be measured. Its calculation exhibits the probability for each day and grid point for the precipitation to be bigger than a certain threshold.

Among the other analyses are the Equitable Threat Score (ETS) linear regression, rank histogram and frequency distribution function.

Additionally, the ETCCDI (Expert Team on Climate Change Detection) indices were calculated for Fennoscandia. The reference time period, used for some of the ETCCDI indices is Expert Team on Climate Change Detection and Indices (ETCCDI) for the datasets. The 30-year period 1981-2010.

For the Carpathian region, the Analysis of Variance (ANOVA) method was applied, which is an adequate statistical methodology to explore the statistical structure of different datasets. ANOVA can be used effectively for the characterization of the spatio-temporal statistical properties of CARPATCLIM, E-OBS and ERA5. The datasets with different spatial resolution can be compared by analyzing the spatio-temporal means and variances. The main principles of the ANOVA method is



that the total variance can be partitioned into the sum of the spatial variance of the temporal means and the spatial mean of the temporal variances on one hand; and the sum of the temporal variance of the spatial means and the temporal mean of the spatial variances on the other hand. The comparison of the magnitude and spatial distribution of the specific components of the total variance can be analyzed for different time periods, years and seasons for example. The spatial means and spatial variances at the moment “t” are illustrated on graphs and temporal mean and temporal variance at specific locations “s”, corresponding to the grid points illustrated on maps (see the Appendix for details of ANOVA methodology).

Also, an exponential trend model was applied for precipitation for CARPATCLIM in this comparative study. The estimated changes over the period (1979-2010) were computed and expressed in %.

These methods used in the comparison of the Carpathian region is described in detail in Szentimrey (2019).

### 3.1 Fennoscandia

This Section contains results of the comparison of precipitation (RR) from NGCD against E-OBS and from NGCD against ERA5. The evaluation period is 1979-2018, which corresponds to the maximum overlap of all datasets and the reference. In the following Sections, the results of the analysis are presented and discussed.

#### 3.1.1 Climate Indices

The dictionary of climate indices can be found at

<https://surfobs.climate.copernicus.eu/userguidance/indicesdictionary.php>.

**Mean total annual precipitation.** E-OBS, ERA5 and NGCD fields over Fennoscandia are rather similar, as can be seen from Figure 3.1.1.1. The highest values are along the Norwegian coastline and the lowest values are in the inland regions in Northern Fennoscandia, corresponding roughly to the Lapland region. All the datasets place the absolute maxima in western Norway with values ranging from around 2500 mm/year for the coarser global reanalyses (ERA5-EDA) to approximately 4000 mm/year for NGCD-1. One of the significant differences between the finer resolution observational datasets and the global reanalyses is that the first ones represent more accurately the regions with the lowest precipitation values, while global reanalyses tend to overestimate the precipitation there. With respect to the monthly values averaged over Fennoscandia, ERA5 datasets have higher values than the observational datasets and E-OBS is comparable to NGCD-2. In Figure 3.1.1.5, the analysis over monthly precipitation fields is presented.

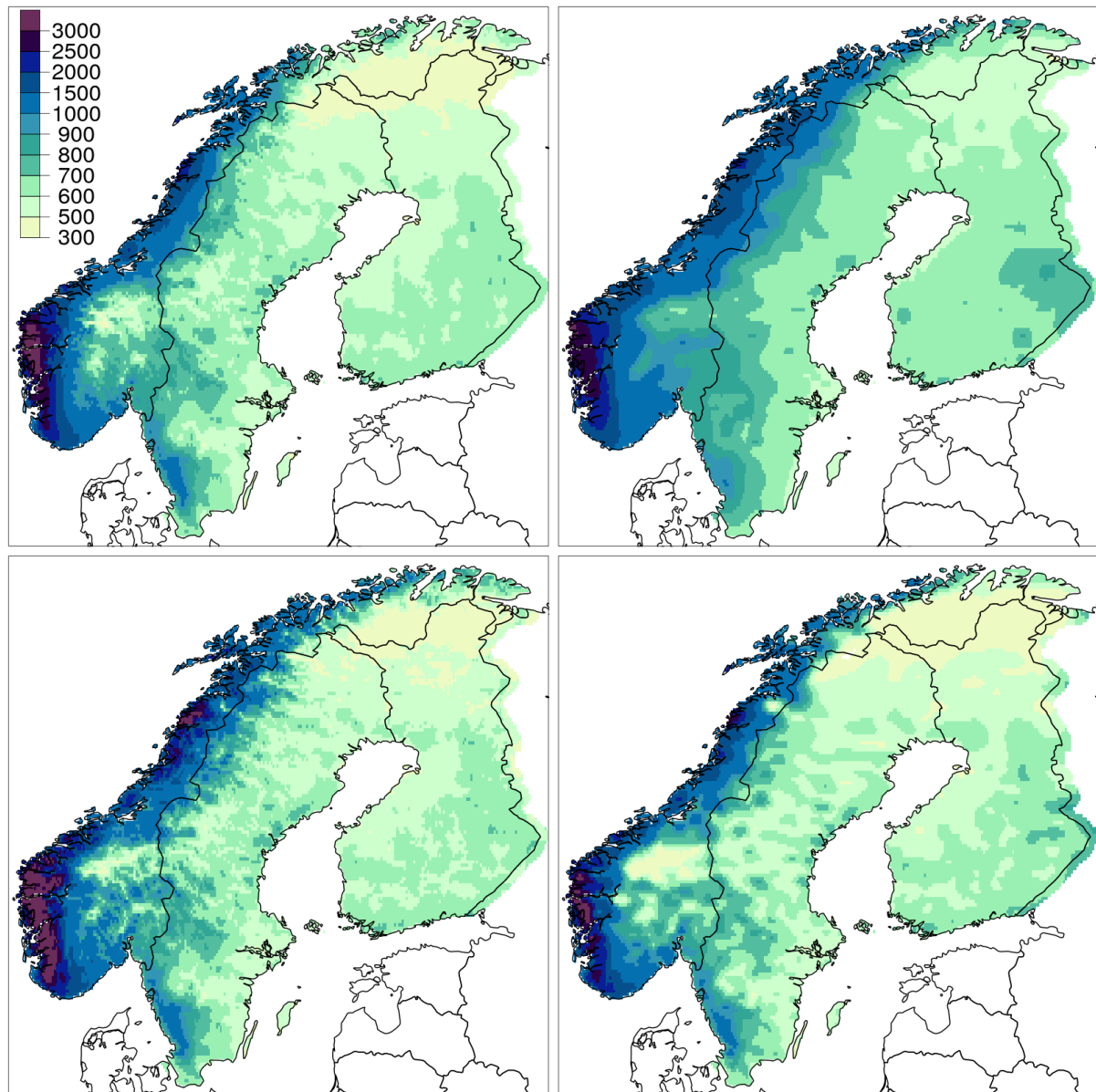


Figure 3.1.1.1: Mean annual precipitation (mm) in the time period 1979-2018 for the datasets: E-OBS (top-left), ERA5-HRES (top-right), NGCD-1 (bottom-left), NGCD-2 (bottom-right).

**Intense precipitation.** R75pFRAC, R95pFRAC (Figure 3.1.1.2) and R99pFRAC show that E-OBS is behaving differently from both ERA5 and NGCD along the watershed between western and eastern Norway and along the coast in northern Norway. The precipitation fraction due to moderate, wet and very wet days (the reference period is 1981-2010) in those regions is systematically smaller in E-OBS than for the other datasets. Note that those regions are characterized either by complex topography or heterogeneous land use. The result might indicate some problems in E-OBS with the representation of intense precipitation where the station network is sparse and the precipitation field is highly variable due to variations in geographical conditions.

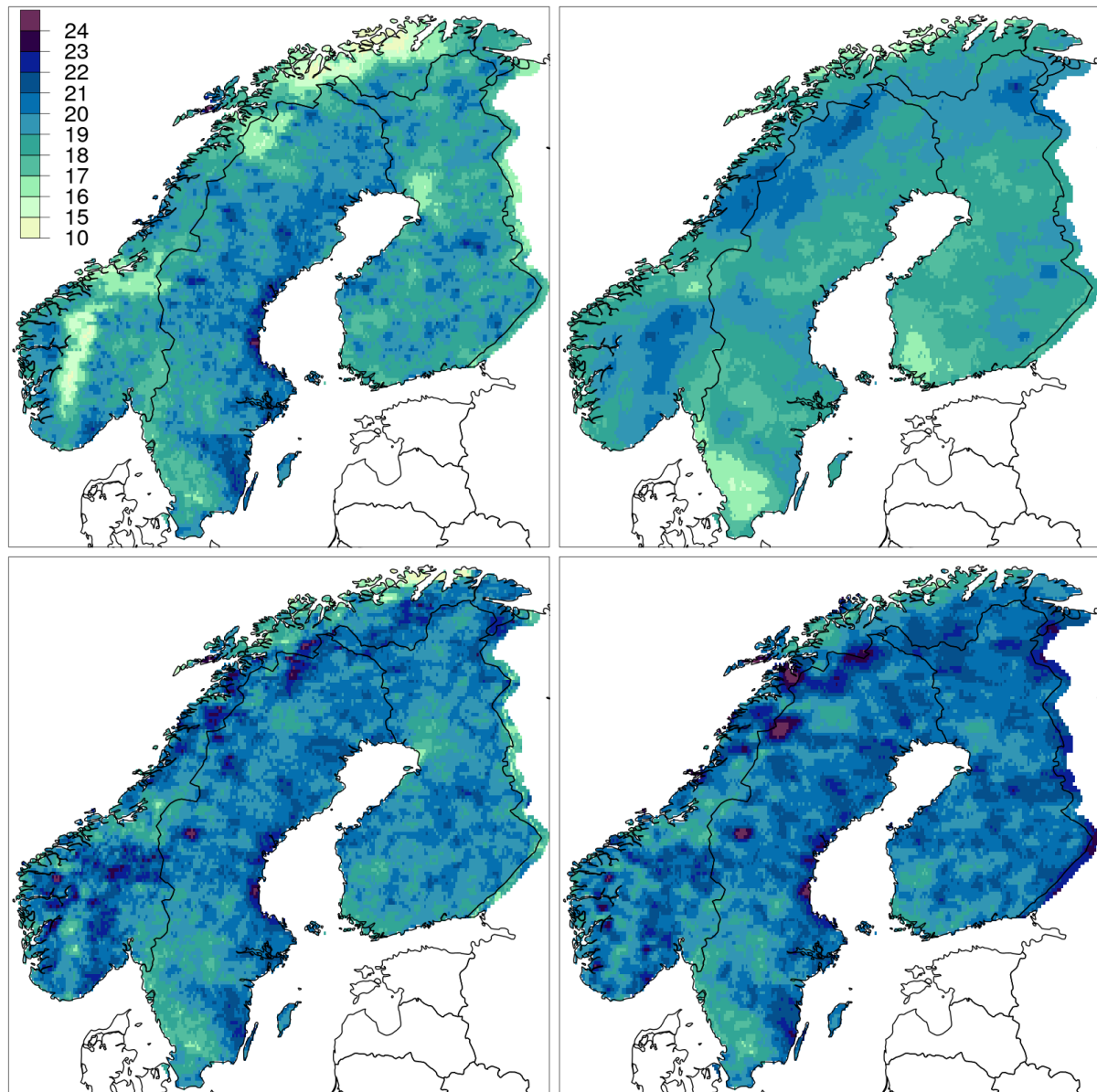


Figure 3.1.1.2: Mean annual R95pFRAC (%) in the time period 1979-2018 for the datasets: E-OBS (top-left), ERA5-HRES (top-right), NGCD-1 (bottom-left), NGCD-2 (bottom-right).

With respect to the **Simple daily intensity index** (SDII, mm/wet day), the annual mean in 1978-2018 of E-OBS is similar to NGCD-2, with about 15 mm/wet day in the regions where the highest annual totals are registered. NGCD-1 has higher values than E-OBS and ERA5 lower values. The annual SDII time series (not shown here, it is similar to Figure 3.1.1.6) of E-OBS is more comparable to ERA5-HRES than to NGCD. As a matter of fact, the monthly averaged SDII for a typical year over Fennoscandia shows that E-OBS is characterized by a greater variability than ERA5 and NGCD. During winter, when SDII reaches its minimum value, E-OBS behaves like ERA5-EDA while in spring and early summer, when SDII reaches its maximum, E-OBS is closer to NGCD-1. Then, in autumn E-OBS SDII drops quickly to values comparable to ERA5 again. E-OBS has an annual cycle of



precipitation that during winter is comparable to ERA5, while during spring and early summer better matches NGCD.

The SDII components are precipitation frequency and intensity. Those two components are considered separately in the following.

**Frequency.** With respect to the **number of wet days** (R1mm), the spatial distribution of the annual averaged values of E-OBS is rather similar to NGCD-1, as shown in Figure 3.1.1.3. Note that ERA5 is significantly overestimating R1mm in a wide portion of the domain, such as Finland, large part of Sweden and northern Fennoscandia, while the overestimation is less dramatic in those regions of Norway where the precipitation frequency is higher. The time series of annual averaged R1mm over Fennoscandia shows that E-OBS is much closer to NGCD than ERA5, though NGCD systematically presents highest values. In Figure 3.1.1.6, the time series of R1mm are shown.

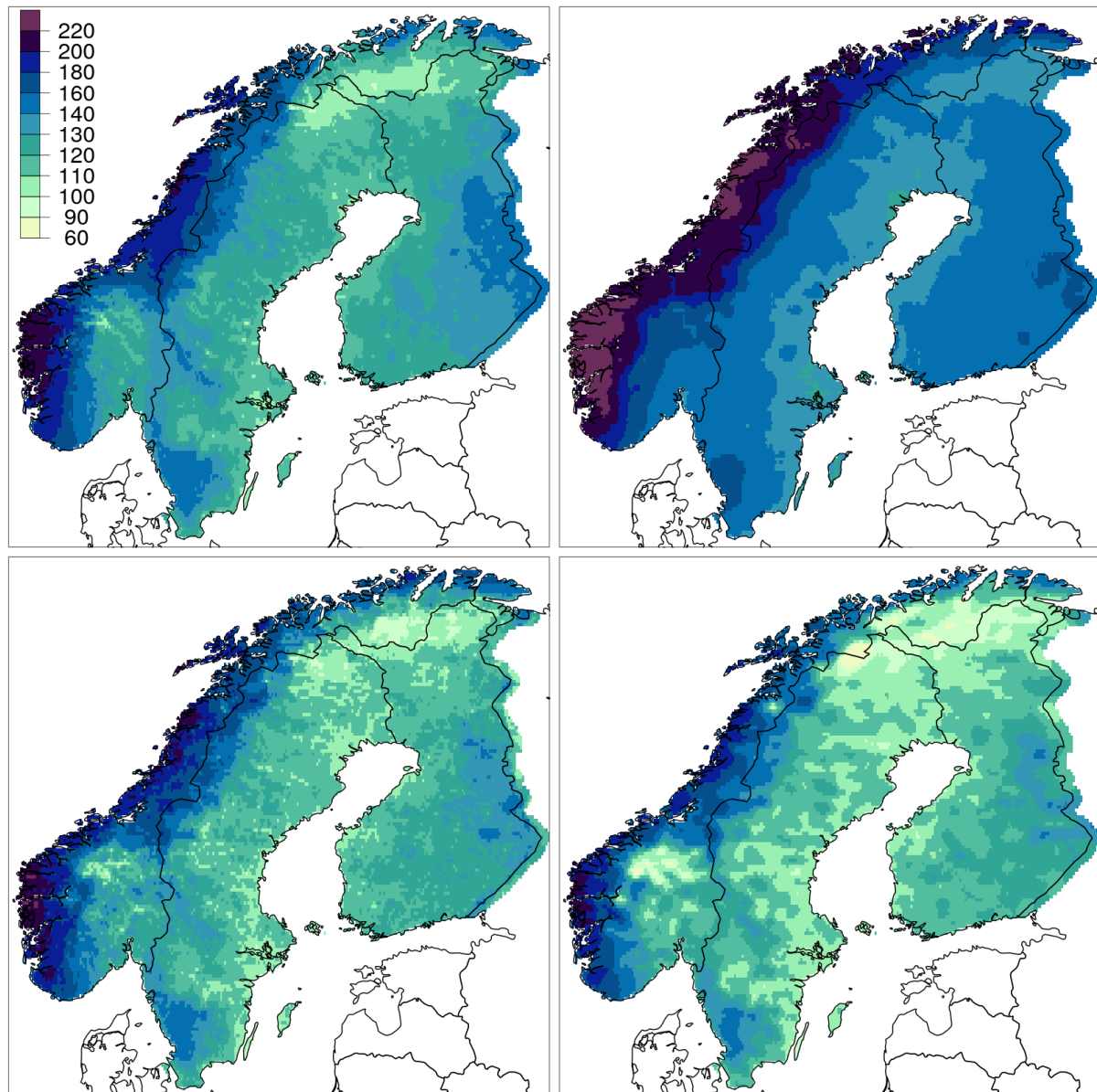


Figure 3.1.1.3: Mean annual R1mm (days) in the time period 1979-2018 for the datasets: E-OBS (top-left), ERA5-HRES (top-right), NGCD-1 (bottom-left), NGCD-2 (bottom-right).

The annual average number of **heavy precipitation days** (R10mm) in the time period 1979-2018 is much more similar for all the datasets than R1mm, notably the differences between the global reanalysis and the observational datasets are significantly smaller than for R1mm. E-OBS seems to systematically underestimate R10mm in Lapland and northern Finland. The time series of the annual R10mm aggregated over Fennoscandia show that E-OBS presents systematically smaller values than NGCD and ERA5-HRES (the differences are approximately 2-4 days), while it is rather similar to ERA5-EDA.

The maps of the annual average of **very heavy precipitation days** (R20mm) in the time period 1978-2018 for E-OBS is similar to NGCD in Norway and part of Sweden, while it is more comparable to



ERA5 in Finland and northern Fennoscandia. The time series of the R20mm annual averages aggregated onto Fennoscandia show that E-OBS, if compared to NGCD, systematically underestimates this parameter and the difference is approximately between 2-3 days. On the other hand, E-OBS time series resembles quite closely ERA5-HRES.

**Precipitation Extremes 95% and 99%.** The ability of the models to reconstruct the climatologies of extreme precipitation is investigated by means of the computation of the ETCCDI indices of precipitation: RX1day, RX5dy, R20mm, R95pTOT and R99pTOT. As an example, Figure 3.1.1.4 shows the maps for R95pTOT. The patterns are well reconstructed by all datasets. NGCD-1 is the dataset that reproduces the highest precipitation extremes. E-OBS and NGCD-2 are rather similar. ERA5-HRES underestimates the precipitation extremes, though not in a dramatic way. The underestimation is more pronounced for ERA5-EDA.

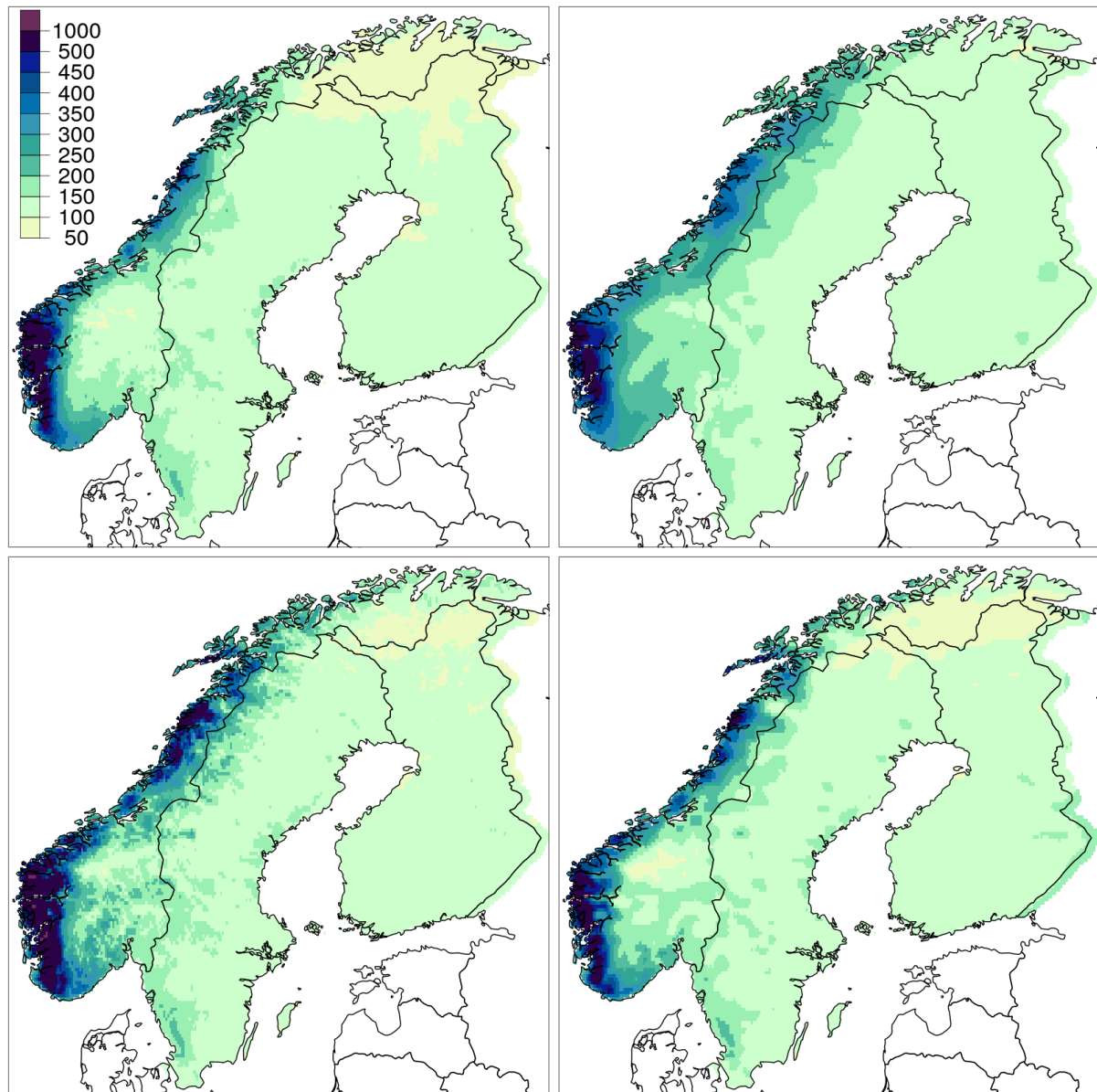


Figure 3.1.1.4: Mean annual R95pTOT (mm) in the time period 1979-2018 for the datasets: E-OBS (top-left), ERA5-HRES (top-right), NGCD-1 (bottom-left), NGCD-2 (bottom-right).

### 3.1.2 Yearly cycle

The yearly cycle of precipitation is shown in Figure 3.1.2.1 over Fennoscandia. The distinction between ERA5 datasets and the regional datasets is evident for all seasons. ERA5 presents more precipitation, as expected because of its coarser resolution that tends to “spread out” precipitation amounts over too large regions. On the other hand, the timing of precipitation is similar to all datasets, this might suggest that it could be possible to downscale ERA5 data to finer grids by using more sophisticated tools than bilinear interpolation and to consequently reduce its bias. ERA5-HRES is the dataset with the highest total precipitation amounts. The different members of ERA5-EDA do show some spread in their values, and in winter and autumn their total monthly amounts are not too different from those of the regional datasets.

E-OBS monthly amounts of precipitation are well in line with NGCD. E-OBS fits better NGCD-2 for most of the months, while NGCD-1 often shows higher amounts. However, for May, June and July E-OBS agrees better with NGCD-1.

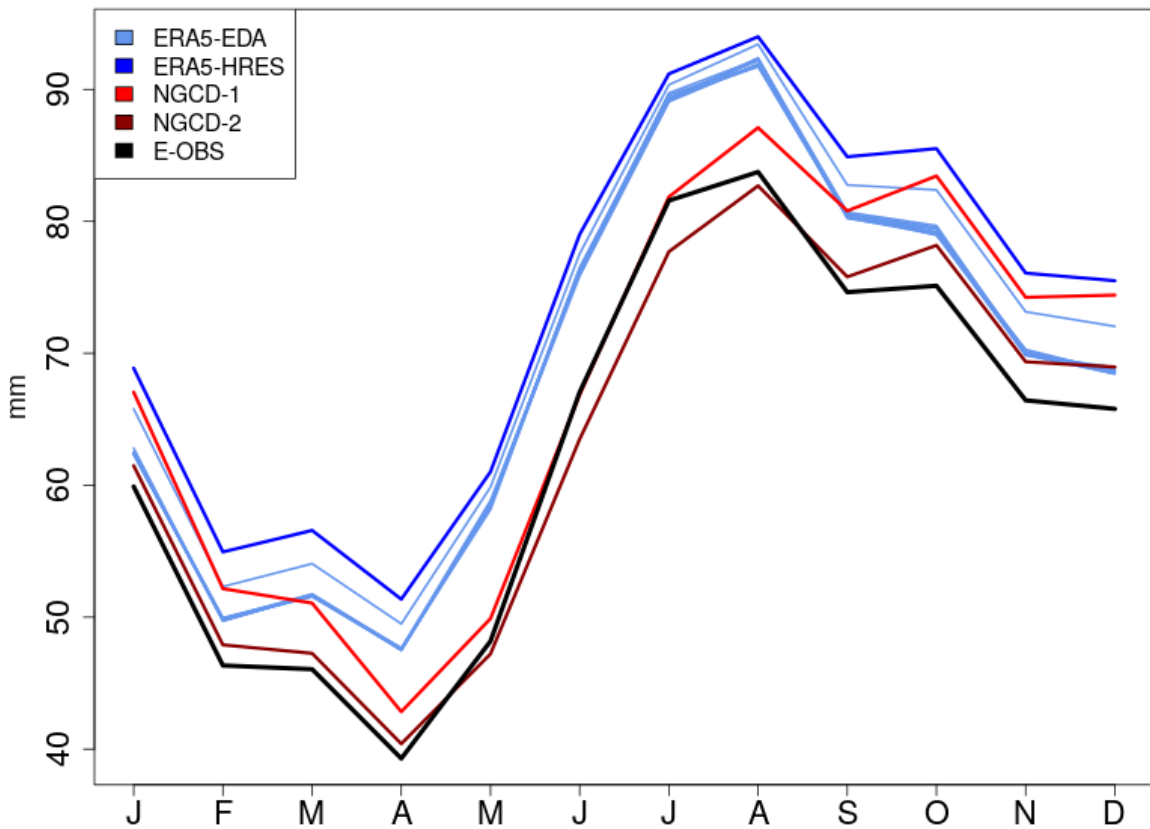


Figure 3.1.2.1: Monthly totals of precipitation over Fennoscandia for the gridded datasets considered.

### 3.1.3 Temporal Trends

We have also compared the temporal trends of the ETCCDI climate indices derived from the datasets considered. Since the observational dataset E-OBS and NGCD are not based on a fixed station network, the temporal trends presented have been computed for the values aggregated over the entire Fennoscandia.

As an example, Figure 3.1.3.1 shows the time series of R1mm for the datasets considered in our study. Note that the green line shows the result obtained for ERA5-Land, which at the time we downloaded the data was available from 2001 onwards. In the case of R1mm, as for most of the climate indices considered, it is possible to identify two clusters, the one of the global reanalyses and the one of the regional datasets. E-OBS closely follows the time series of the two NGCD datasets.

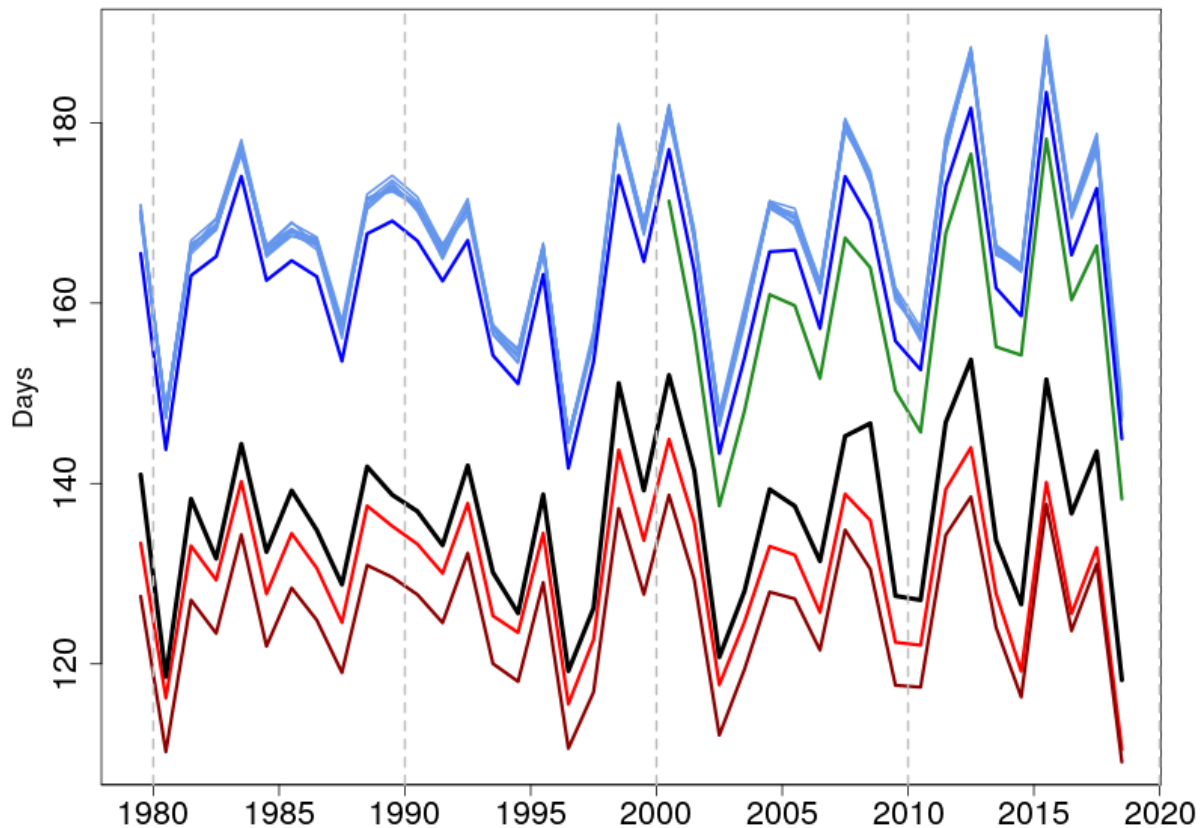


Figure 3.1.3.1: Time series of spatially averaged number of wet days ( $RR \geq 1 \text{ mm}$ ) (R1mm) in a year over Fennoscandia. Models: E-OBS (black), NGCD-1 (red), NGCD-2 (darkred), ERA5-HRES (blue), ERA5-EDA (lightblue), ERA5-LAND (green).



### 3.1.4 Extreme event: Flood on 30 September to 2 October 2017

The performances of the different models have been evaluated for a case study of extreme precipitation over Southern Norway, that caused a serious flood in the region as described in details in the report of The Norwegian Water Resources and Energy Directorate ([http://publikasjoner.nve.no/rapport/2017/rapport2017\\_80.pdf](http://publikasjoner.nve.no/rapport/2017/rapport2017_80.pdf), in Norwegian)

Figure 3.1.4.1 shows the total amount of precipitation accumulated over three days in Southern Norway, between 2017-09-29 06:00 UTC and 2017-10-02 06:00 UTC. NGCD-1 and 2 are the references, while E-OBS and ERA5 are the datasets under evaluation. According to NGCD, the total precipitation amount over a part of the region is greater than 250 mm, though NGCD-1 and 2 disagree on the patterns. NGCD-1 shows three distinct maxima, closely following the topography of the region, while NGCD-2 has one single maxima representing the amount observed by the station network. E-OBS precipitation maxima are greater than 200 mm but generally not as high as NGCD, the pattern is very similar to NGCD-2. ERA5-HRES show a remarkable agreement with the observational datasets, though no observation of precipitation has been used in the product generation. As expected, ERA5 smooths out the precipitation extreme values quite a bit, since the maxima are just above 150 mm.

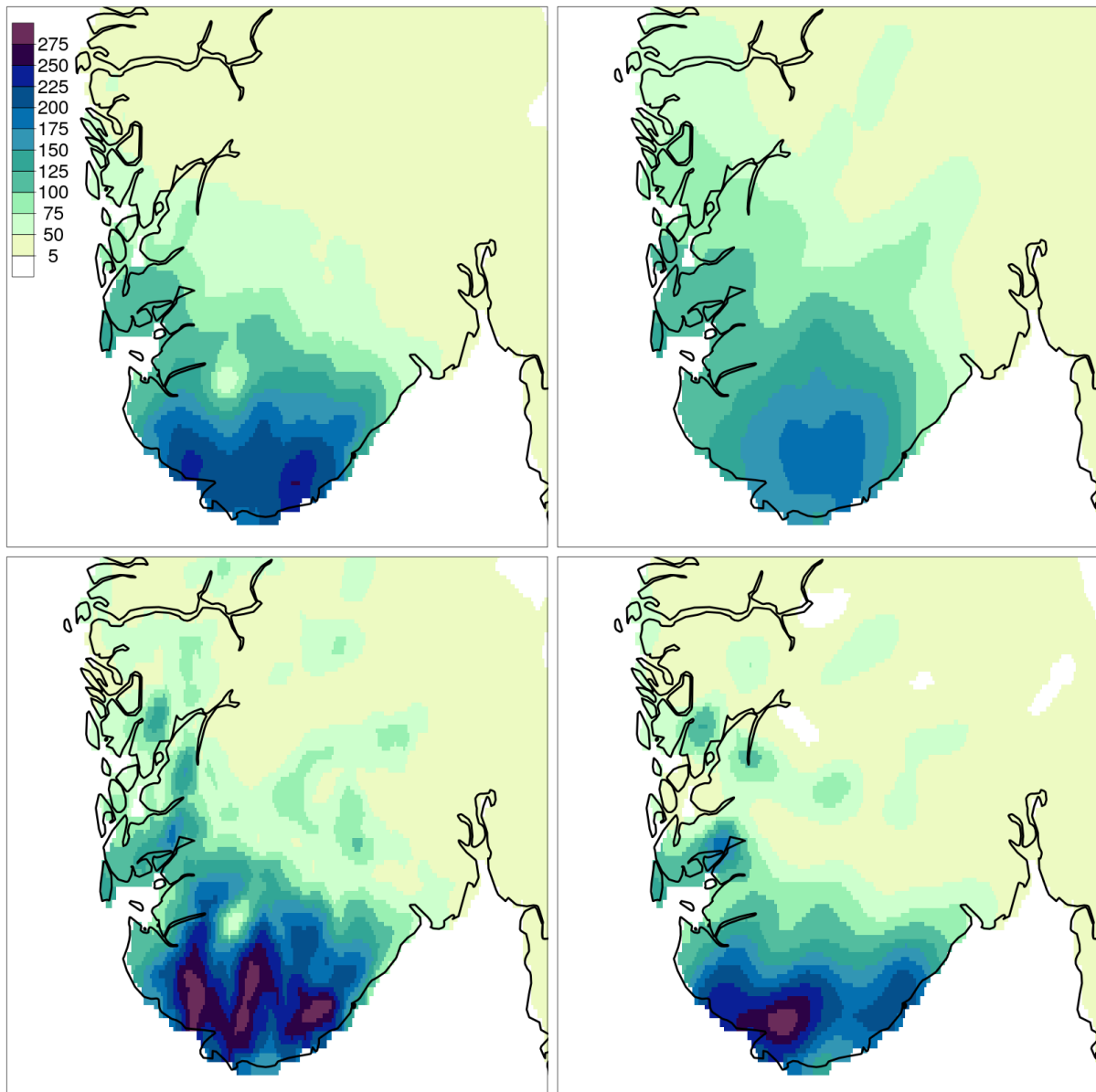


Figure 3.1.4.1: Total precipitation accumulated between 2017-09-29 06:00 UTC to 2017-10-02 06:00 (mm/72 hours) over southern Norway. Top row: E-OBS (left) and ERA5-hres (right). Bottom row: NGCD-1 (left) and NGCD-2 (right).

### 3.1.5 Verification scores

#### 3.1.5.1 SEEPS

The first verification score applied is the SEEPS. This score ranges from 0 to 1 and the perfect score is 0. The verification of E-OBS against NGCD-1 is shown in Figure 3.1.5.1.1 and against NGCD-2 is shown in Figure 3.1.5.1.2. The color scale has been chosen in such a way that: the blue-ish colors represent the lower  $\frac{1}{3}$  of the possible values, with cyan marking the mean of this interval; the green

colors indicate the center of the distribution; the warm colors (red to yellow) indicate values in the upper third of the distribution. SEEPS does not show pronounced seasonal trends and the patterns are similar among seasons, however E-OBS performances are slightly worse in winter than in summer. The verifications against the two NGCD references also shows similar patterns and values. It is worth remarking that the color scale chosen allows for a detailed visual inspection of the SEEPS fields and it is evident that the values are close to zero close at station locations shared by NGCD and E-OBS.

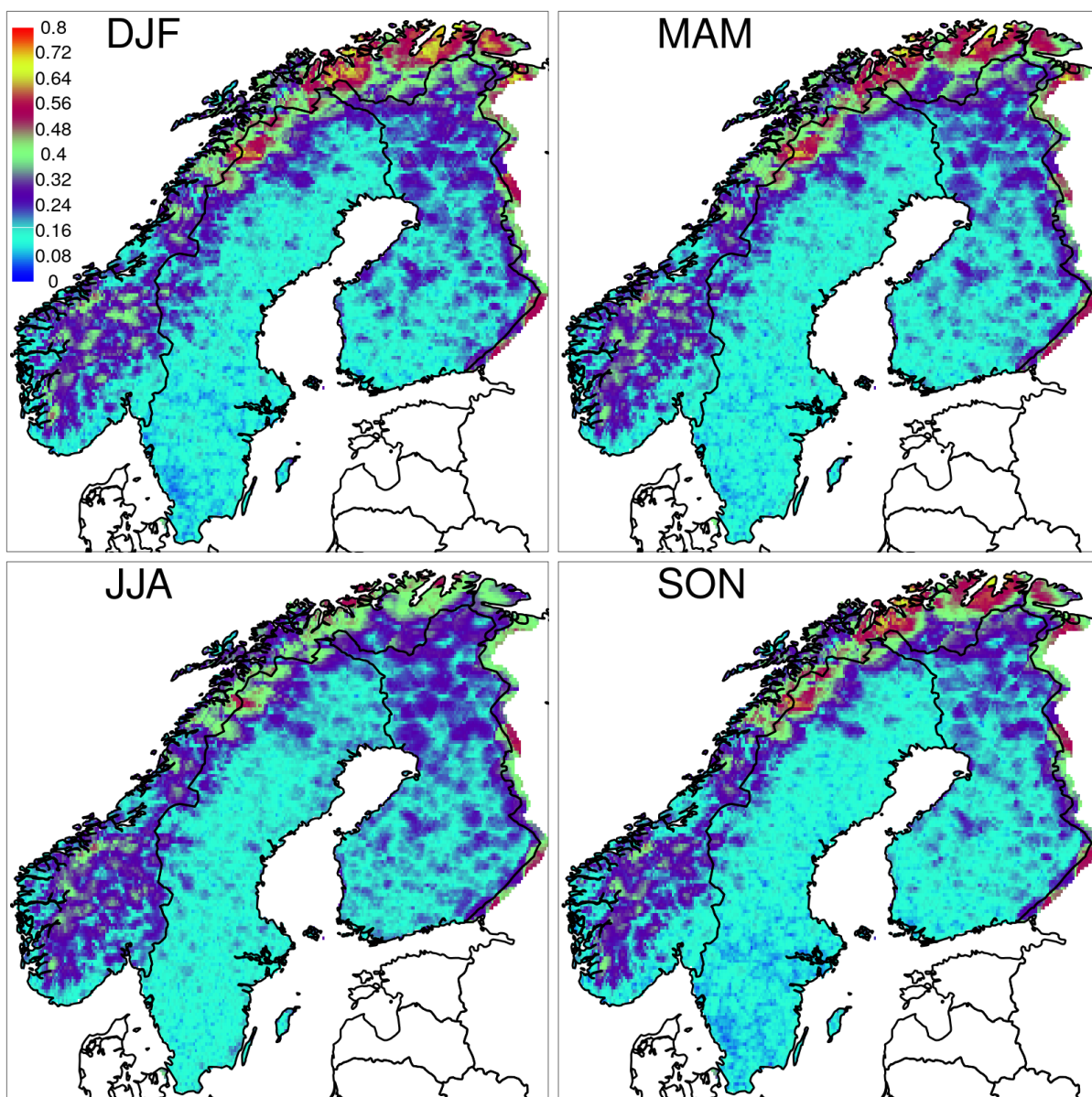


Figure 3.1.5.1.1: SEEPS for the daily precipitation. E-OBS is evaluated against NGCD-1 over the time period 1979-2018.

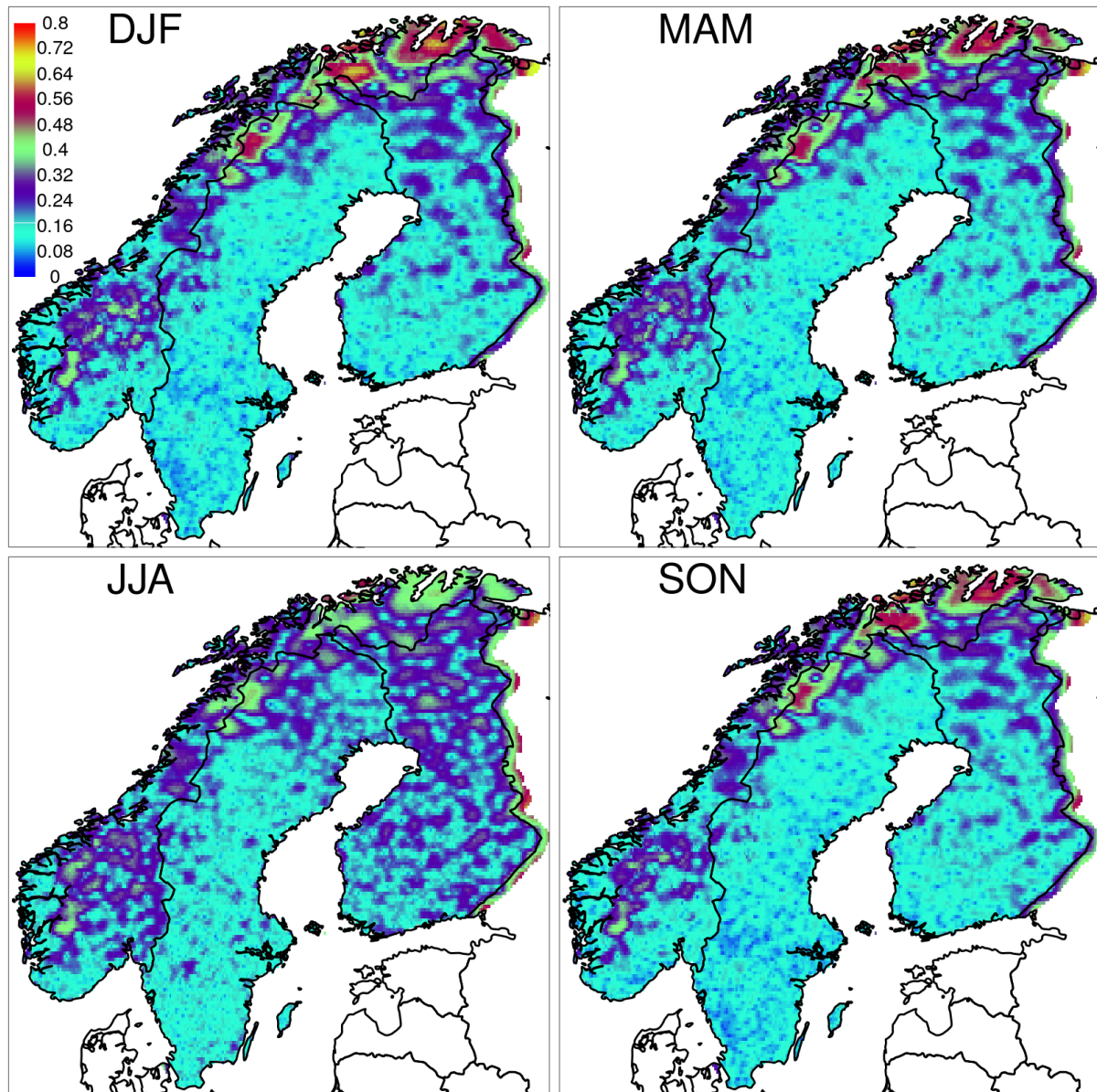


Figure 3.1.5.1.2: SEEPS for the daily precipitation. E-OBS is evaluated against NGCD-2 over the time period 1979-2018.

If we consider the three macro-region of Sweden, Finland and Norway, the SEEPS score is close to zero over a large part of Sweden, except for the mountainous region close to the Norwegian border where SEEPS values greater than 0.5 can be found. Over Finland, the SEEPS values are mostly within 0 and 0.3, with a tendency towards the highest values in the data sparse regions of the north. In Norway, the SEEPS score shows a greater variability and it is possible to distinguish the three main climatic regions: western Norway; eastern Norway and northern Norway. In western Norway, E-OBS performs better along the coast where the SEEPS is around 0.1 for all seasons and the performances degrade in the mountains with SEEPS of 0.4. In eastern Norway, the situation is similar as in the West, however the worst E-OBS performances are registered during summer, where convection



takes place more often. The northern part of Norway is the region where E-OBS and NGCD differs the most, this is partially due to the complex topography and partially due to lack of observations, especially in the northernmost regions.

The statistics of the SEEPS score for ERA5-HRES compared against NGCD-1 and 2 are shown in Figures 3.1.5.1.3 and 3.1.5.1.4, respectively. The same color scale of Figures 3.1.5.1.1 and 3.1.5.1.2 have been used, so to make the comparison between E-OBS and ERA5 easier. ERA5 evaluations against NGCD-1 and 2 are consistent and similar between each other. Summer is the season where the deviations of ERA5 from NGCD are more pronounced. The maps show similar patterns as those for E-OBS, however the SEEPS values are significantly worse for ERA5. For example, over Sweden and Finland E-OBS often reports values between 0.08 and 0.16, while ERA5 has values between 0.24 and 0.32.

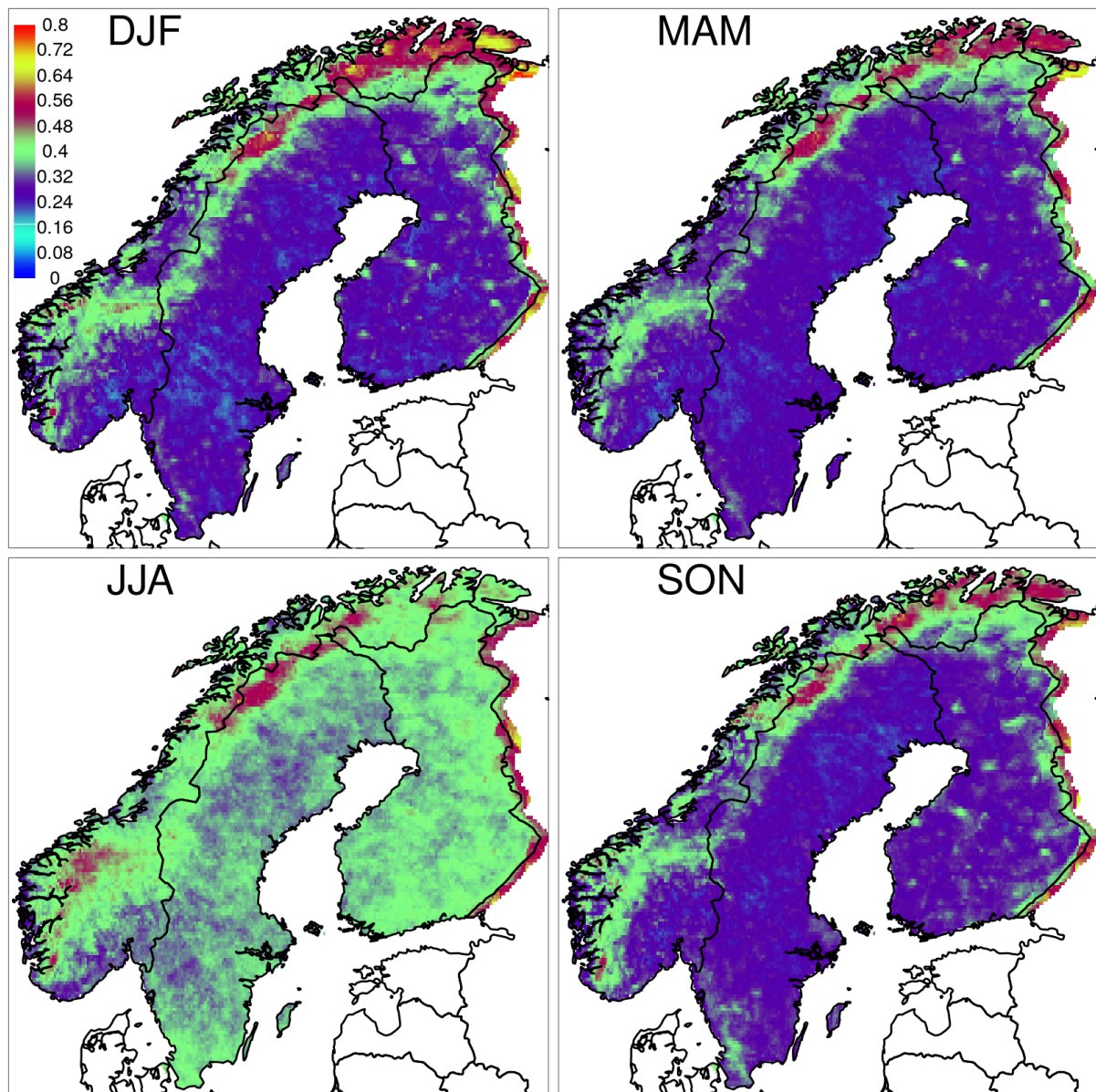


Figure 3.1.5.1.3: SEEPS for the daily precipitation. ERA5-HRES is evaluated against NGCD-1 over the time period 1979-2018.

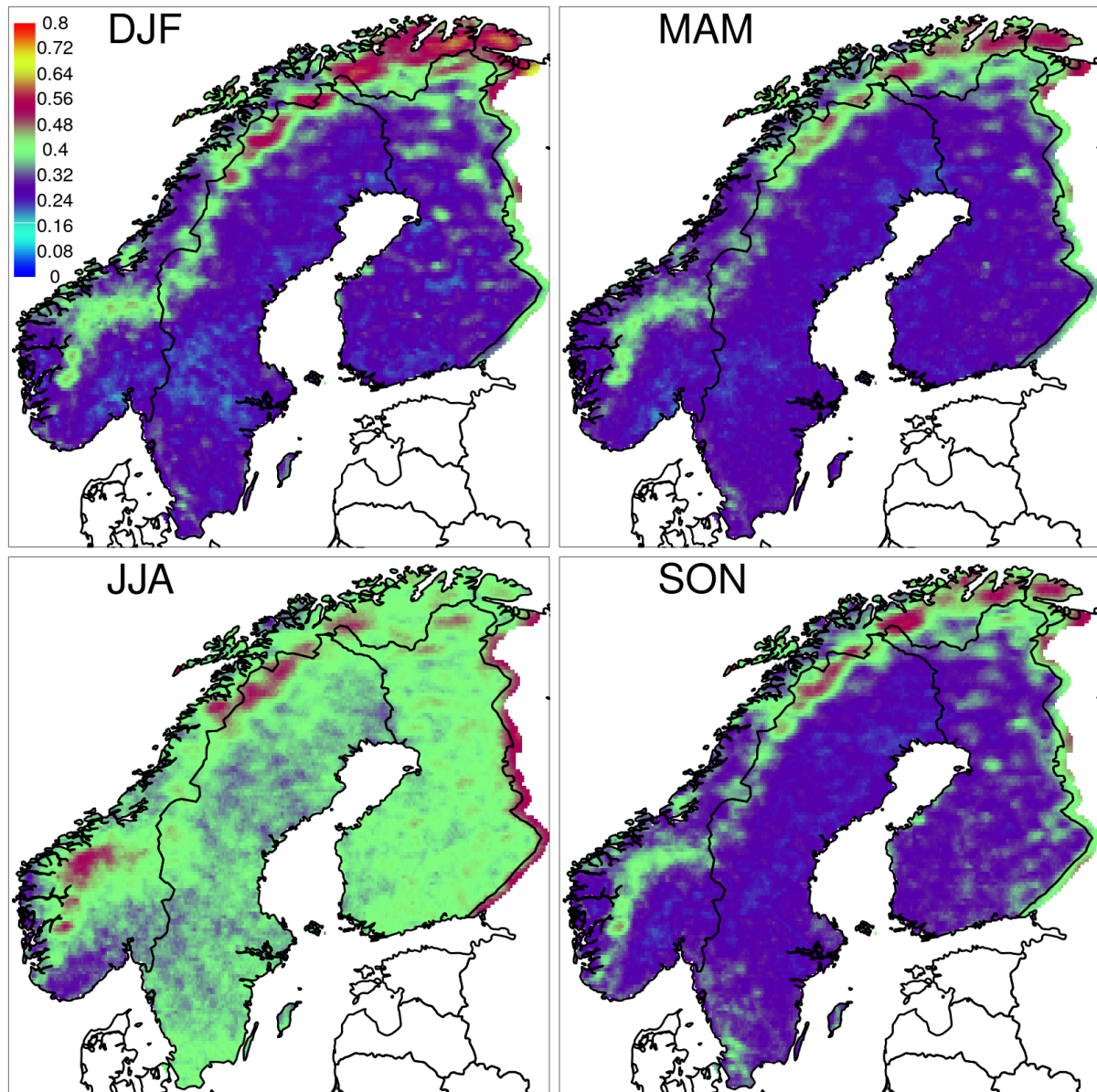


Figure 3.1.5.1.4:SEEPS for the daily precipitation. ERA5-HRES is evaluated against NGCD-2 over the time period 1979-2018.

### 3.1.5.2 ETS

The Equitable threat score (ETS) has been used to assess the ability of the datasets to correctly distinguish between precipitation yes/no events. The ETS threshold used for the definition of a precipitation yes event is 0.5 mm/day, which is a threshold that is normally used to distinguish between a wet and a dry day in Scandinavia. Note that ETS is a positively oriented score.

ETS and SEEPS show similar patterns, such that we have decided not to add Figures on ETS but to describe the main results. ETS does add the information that for those regions where SEEPS is worse, E-OBS often is different from NGCD with respect to the reconstruction of wet and dry days. Again, this distinction becomes more challenging during summer. For ERA5, the ETS shows two



distinct situations: in summer and spring it is mostly around 0.3, with the smaller values in the north and in the mountains of 0.2 and the best performances in the southernmost part of the domain with values of 0.5; winter and autumn are seasons where ERA5 is performing better with large parts of the domain with values around 0.5.

### 3.1.5.3 LINEAR REGRESSION

We have also performed a grid point by grid point linear regression considering those cases where both E-OBS and NGCD present daily precipitation greater than 1 mm/day. The linear regression is  $E\text{-OBS} = m * NGCD$ . We have called it a “robust” linear regression because the regression line is forced to have 0 mm/day as the intercept, then we have divided the NGCD values in bins of 1 mm/day width and the angular coefficient is optimized so to better fit the medians of the distributions E-OBS values falling in each bin. Bins with few values are not considered in the fitting. The situation over Sweden and Finland show that E-OBS and NGCD reconstruct similar values ( $m$  around 1, smaller values in the mountains and in the north of Finland). In Norway, E-OBS tends to underestimate the precipitation amounts, in the worst cases the underestimation reaches 50% of the precipitation. However, the situation is significantly different if we consider NGCD-1 or NGCD-2, in this last case the underestimation is less pronounced and there are small regions in western Norway where E-OBS overestimates precipitation by 20%.

### 3.1.6 Frequency Distribution Function

The ability of the different datasets to reproduce extreme values of precipitation is investigated in this Section. We have computed the frequency at which daily precipitation amounts exceed a threshold and the graphs are shown in Figure 3.1.6.1 for the regions of Norway shown in Figs. 2.1.2 and 2.1.3. NGCD has a slightly higher frequency of occurrence for intense precipitation than E-OBS, which in turn has a statistics not too different from ERA5-HRES. The coarser-grid ERA5-EDA is the dataset that more underestimates the frequency of occurrence of intense precipitation. Note that the eastern region of Norway is the region where the datasets show more similar values, while in the west, where the highest precipitation values are registered, there is a distinct difference between E-OBS and NGCD and ERA5. ERA5 underestimates the frequencies. NGCD-1 is always the dataset with the highest frequency of intense precipitation, however in the west this characteristic (with respect to the others) is more pronounced.

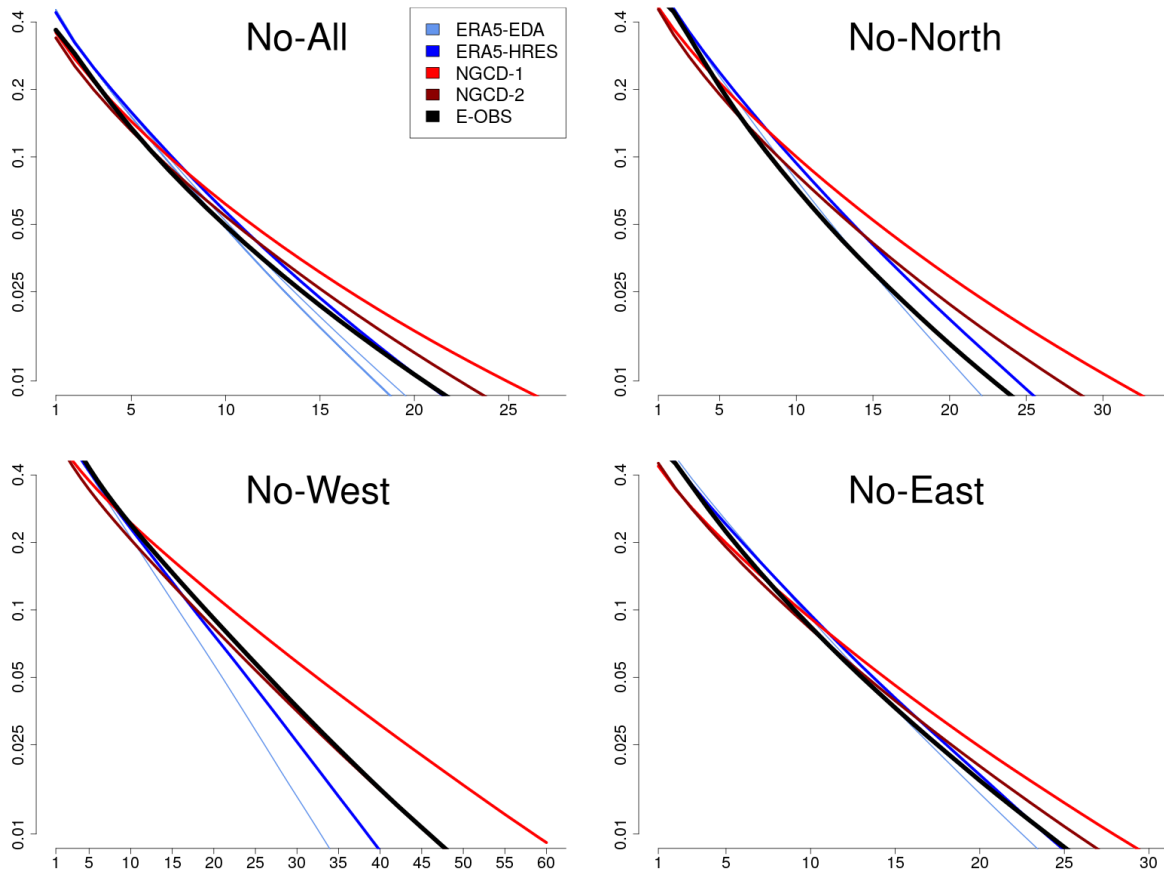


Figure 3.1.6.1: Frequency (y-axis, fraction of days, log-scale) at which daily precipitation amounts (values at 0.1 degree resolution grid points) exceed a threshold (x-axis, mm). Results are based on data over the time period 1979-2018 and for different subdomains (see Figures 2.1.1b and c). The Norwegian mainland is shown in the top-left graph, northern Norway in the top-right, western Norway in the bottom-left and eastern Norway in the bottom-right. Note the different scales (x-axes).

### 3.1.7 Main outcomes – precipitation in Fennoscandia

#### E-OBS

E-OBS precipitation climatology over Fennoscandia is very similar to those of NGCD-1 and NGCD-2 datasets. In this sense, it can be stated that E-OBS is able to represent the mesoscale features of precipitation over Fennoscandia. The main differences are found for the representation of the precipitation fraction due to moderate, wet and very wet days in some regions, such as: in Norway, along the watershed dividing eastern and western Norway; in northern Norway, along the coast; in Sweden, in the region of the highest mountain peaks. For extreme precipitation events, E-OBS presents smaller precipitation amounts than NGCD but similar patterns. E-OBS daily precipitation fields over Finland and Sweden are very similar to NGCD. E-OBS daily precipitation fields over Norway tend to differ more from NGCD than in the other two Countries, partially due to the



contribution of Norwegian stations used in NGCD and not in E-OBS and partially due to the complex topography of some Norwegian regions.

## ERA5

ERA5 represents the moist climate over Fennoscandia relatively well, especially if used for studies on climatology at the synoptic and Meso-alpha scales. The monthly precipitation amounts are generally overestimated compared to NGCD, as it is the frequency of wet days. The extreme precipitation values are filtered out, but the patterns represented are realistic. It is worth remarking that ERA5 provides areal averages over grids having a larger resolution than those of E-OBS ( $0.1^\circ$ ), used in this study. Nonetheless, the daily fields are still able to provide useful information over large portions of Fennoscandia, except perhaps those regions where the real topography and land area fraction deviate the most from those of ERA5, such as the Scandinavian mountains and the northern part of Norway. In addition, ERA5 struggles in representing the summer precipitation, probably because of the prevalence of convective processes, which occurs over scales unresolved by ERA5.

## GENERAL COMMENTS

With respect to drought and precipitation ETCCDI indices aggregated over the entire Fennoscandia, E-OBS is -on average- more similar to ERA5 datasets than NGCD, especially for those indices where the reconstruction of the frequency of occurrence of intense events is more important. A remarkable feature is that temporal trends of the aggregated ETCCDI indices over Fennoscandia seem to be well correlated, despite biases due to different grid resolutions.

## 3.2 Alpine region

In the following subSections, the quality of precipitation (RR) in E-OBS in the Alpine region is being assessed. At the same time the global reanalysis ERA5 and the regional reanalysis COSMO-REA6 are being tested. This is done by evaluating them against two regional climate datasets, APGD and LAPrec, that are specifically designed to model precipitation in the Alpine region. The evaluation period is 1979-2008 for most of the analysis, only if the COSMO-REA6 is involved the evaluation period is shortened to 1997-2008. This time period corresponds to the maximum overlap of all examined datasets. In the following chapters, different indices and scores are discussed. After an overview of the general precipitation climatology, inter-annual and seasonal differences and the behavior of extreme values are highlighted. To statistically assess the performance of the different datasets, several measures and skill scores are used. As stated in Section 1, the monthly LAPrec dataset is only shown in the context of monthly indices.

### 3.2.1 Mean annual precipitation

Figure 3.2.1.1 shows the mean annual precipitation for the datasets on a  $0.1^\circ$  grid. The reference dataset APGD clearly shows the topographical imprint of the domain: the Apennine, the Massif Central, the Jura, the Vosges, the Black Forest, the Julian and the Dinaric Alps exhibit comparatively



high precipitation sums of more than 1700 mm per year on average. Generally, precipitation amounts range between 600 mm per year in the Po valley up to more than 2500 mm in the Julian Alps along the border of Italy and Slovenia. Similar precipitation patterns emerge from E-OBS: The Alpine arc is well visible with just slightly lower values of around 1600 mm and also, the outstanding wet area in the Julian Alps with an average annual sum of up to 2000 mm is captured in Figure 3.2.1.1. In contrast to that, the enhanced orographic precipitation along the Alpine ridge seems to stop over Central Austria, while in APGD the precipitation band reaches further into the Vienna Basin. Also, E-OBS misses the precipitation band over Northeastern Italy and shows significantly lower values around the Massif Central and in the area of Jura mountains. The behavior of E-OBS obviously strongly depends on the number of available in-situ measurements, which is significantly lower in Northern Italy and in parts of Austria, France and Switzerland.

While E-OBS thus tends to underestimate mean annual precipitation, ERA5 clearly overestimates precipitation throughout the whole domain (Figure 3.2.1.1). All elevated areas and the flatland adjacent to the Alps exhibit yearly precipitation values of more than 1400 mm. The pronounced precipitation hotspot in the Ossola valley, south of Switzerland, is slightly shifted westwards compared to APGD and shows values of more than 2500 mm per year. One possible explanation for this shift is that the smoothing of the topography due to the coarser original grid resolution of ERA5 leads to a wrong representation of the southern Alpine slopes. The precipitation mechanism subsequently would hence form precipitation at the wrong location. Furthermore, the rather dry region of Southern Tyrol exhibits too large values in ERA5 compared to APGD. Apart from these features the precipitation pattern seems to be in good agreement with APGD, with the highest values arising along the Alpine ridge and in the Julian Alps. Also, all the other orographic regions show higher than average precipitation amounts, as suggested by theory and the APGD.

To shortly also mention COSMO-REA6, the coincidence of its annual precipitation pattern with the one from APGD is striking (Appendix 1). The main difference arises over Central Austria, where values of up to 2500 mm per year are visible for COSMO-REA6. This overestimation is too large in order to be reasonable. Also remarkable are the higher precipitation sums in the area of the southwesternmost Alpine ridge. This difference could be reasonable as the station network is relatively sparse in APGD in this region. In the other high precipitation areas, however, the precipitation amounts of COSMO-REA6 are in general slightly lower than in APGD. Most pronounced is this underestimation over the Swiss plateau.

When looking at the spatial precipitation distribution of LAPrec there are only negligible differences visible compared to APGD, which is not surprising as most of the included measurement stations are shared and as LAPrec has been calibrated with the mean over a short reference period from APGD.

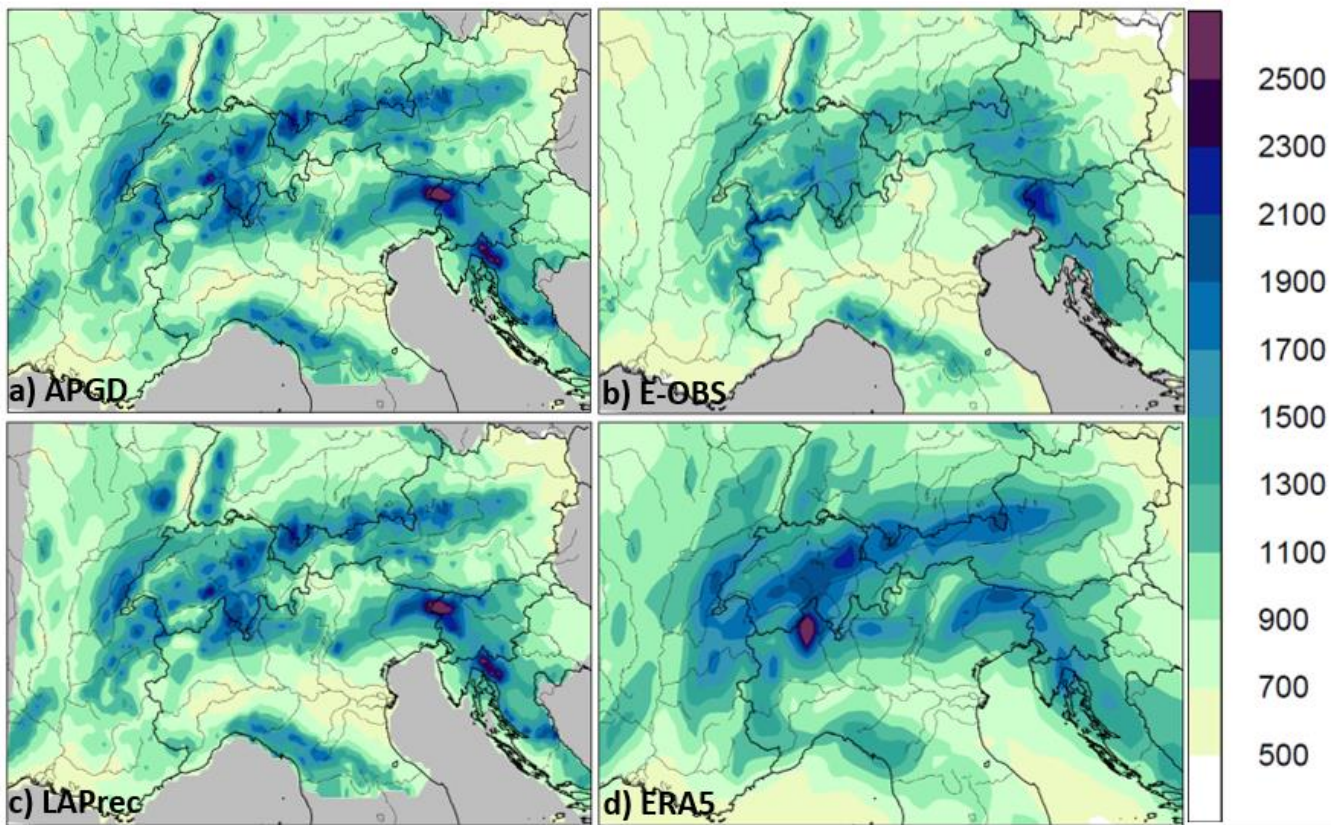


Figure 3.2.1.1: Mean annual precipitation (mm per year; 1979–2008). In panels a) – d), datasets are shown on a  $0.1^\circ$  regular grid. Reference: APGD.

### 3.2.2 Yearly cycle

When looking at the yearly cycle in the three different regions, typical temporal distributions are reproduced (Figure 3.2.1.2). Notably, the catchment in Southern Germany (panel (a)) shows a first peak in late spring, which equals convective precipitation, and a second peak in early winter due to topographically enhanced frontal precipitation. The Swiss catchment (panel (b)) in the Alps shows a dominant summer (convective) maximum, whereas the catchment in the southern Julian Alps (panel (c)) shows a maximum in late autumn and a minimum in late winter. While E-OBS ensemble (E-OBS-Ens) reproduces the yearly cycle very well for the German catchment, there is a clear underestimation in the mountainous, Swiss catchment. For the smaller, and more precipitation intense catchment of Tagliamento in the Julian Alps, E-OBS underestimates precipitation, the larger the monthly precipitation sum. The differences are most pronounced during summer and less in winter months. Considering the spread of both ensembles, E-OBS-Ens has a slightly smaller spread throughout the whole year than ERA5-Ens, except for the Alpine catchment of Aare (panel (b)). The global reanalysis ERA5-Ens overestimates precipitation for nearly every month. The surplus is especially high during summer for the two catchments on the Northern Alpine side. When the catchment of Tagliamento is considered, though, a slight underestimation is visible. Looking at the yearly cycle of COSMO-REA6, most often the expected yearly cycle is not met, except for the Tagliamento catchment. While a strange yearly cycle emerges at Black Forest, it agrees with E-OBS

at Aare catchment, underestimating the summer peak heavily. LAPrec, on the other hand, unsurprisingly fully agrees with the yearly cycle of APGD.

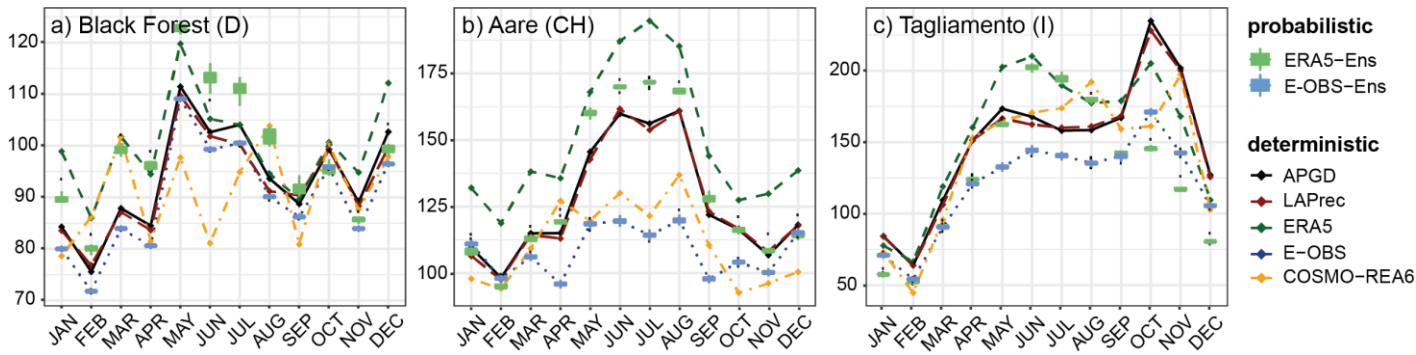


Figure 3.2.2.1: Yearly cycle depicted by average monthly precipitation sums [mm] for the catchments of Black Forest (D) (a), Aare (CH) (b) and Tagliamento (I) (c). The analysis on a  $0.1^\circ$  grid are shown for the deterministic datasets APGD (black line), LAPrec (darkred stipplings), ERA5 (green stipplings) and E-OBS (blue stipplings) and for the probabilistic datasets of ERA5-Ens (green boxplots) and E-OBS-Ens (blue boxplots).

### 3.2.3 Wet-day frequency

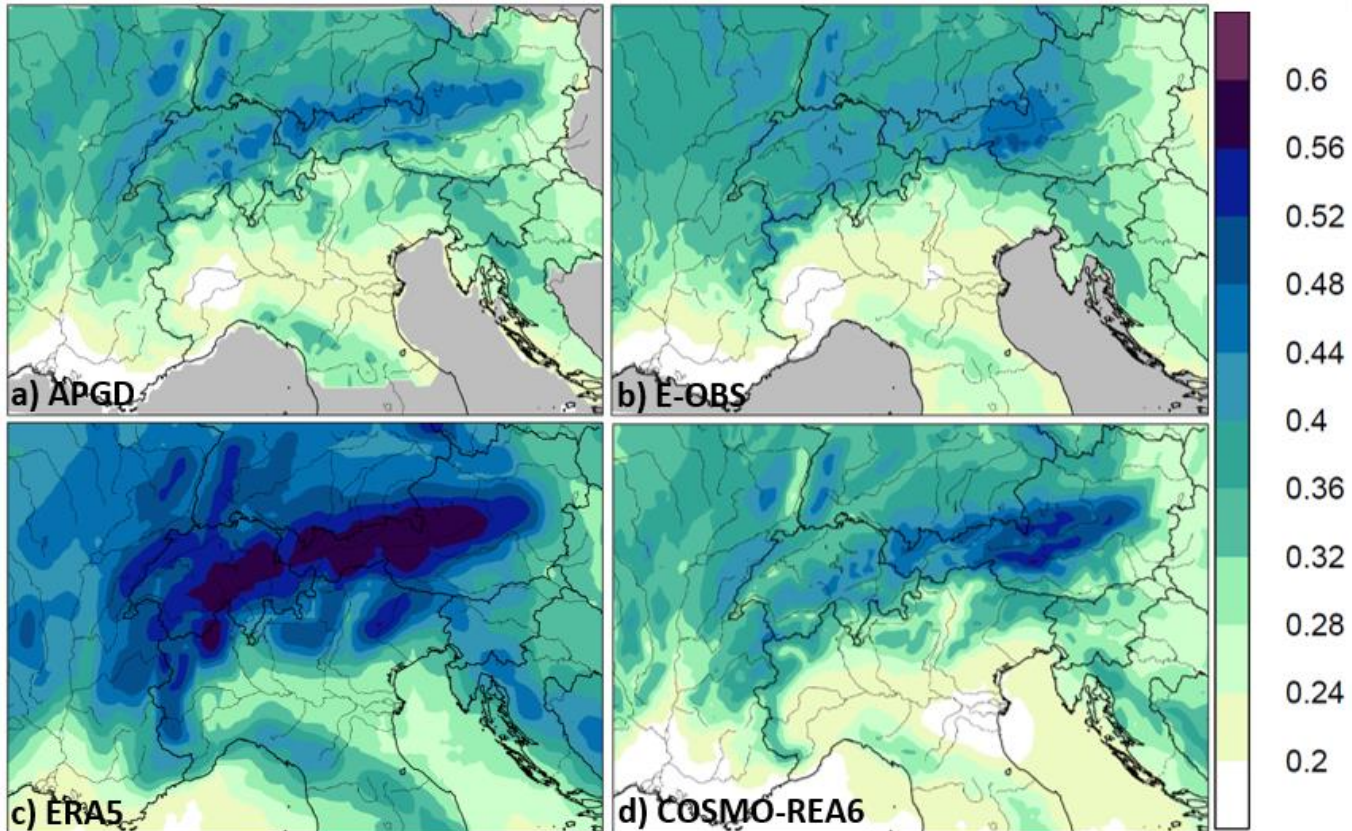


Figure 3.2.3.1: Wet-day frequency showing the frequency of days in the datasets with more than 1 mm of precipitation. The plots show the analysis on a  $0.1^\circ$  grid for APGD (a), E-OBS (b), ERA5 (c) and COSMO-REA6 (d).



In Figure 3.2.3.1, the higher frequency of wet days along the Alpine rim and over the northern and western foreland of the Alps in Germany and France is clearly visible in APGD. The average WDF of nearly 0.5 corresponds to roughly one rainy day out of two. While the northern orographic areas of Jura, Vosges, Black Forest and Bavarian Forest show similar frequencies, the elevated areas south of the crest, like the Julian Alps and the Apennine, show slightly smaller frequencies with roughly one rainy day out of three. This quantity is lowered even more in the southern flatlands, where e.g. in the Po valley precipitation occurs only on every fifth day. Relatively lower frequencies are also found in the inner-Alpine regions. Although the mean annual precipitation, as provided in Figure 3.2.3.1, reaches similarly high values in the South as in the North, the WDF is different. This suggests that precipitation in the southern mountainous regions seems to be occurring less often but more intense, whereas along the Alpine ridge and on the Northern Alpine side precipitation is dispersed more constantly throughout the year. These precipitation patterns are qualitatively evident in all evaluated datasets, however there are substantial differences regarding the magnitude and single maxima. For E-OBS, (panel (b)), the WDF along the Alpine ridge and on the Northern Alpine slope reaches very similar values compared to APGD. Significant differences arise, though, when looking at the Apennine, the easternmost part of the Alps in Austria and Northeastern Italy. This difference in rainy days seems to be clearly linked to the already mentioned reduced availability of stations in these areas (Figure 1). Overall, the difference between APGD and E-OBS is less accentuated for WDF than in Section 3.2.1.

For the global reanalysis (ERA5), a heavy overestimation of WDF over the whole domain gets evident. Frequencies of more than 0.5 are visible over the whole Alpine ridge and even in the adjacent flatlands of France, Germany and northernmost Italy precipitation is abundant on nearly every second day. In the Julian Alps and the Apennine, however, slightly smaller frequencies with roughly one rainy day out of three are visible. Also, ERA5 constantly overestimates the wetness to a strong degree in these areas. For the regional reanalysis, COSMO-REA6, the situation looks different with an overall good coincidence of wetness in the considered domain. Although, there is a remarkable maximum of WDF in Central Austria of more than 0.5, which is not visible in APGD to that extent. In the Apennine, on the other hand, WDF is smaller compared to APGD with precipitation occurring on around every third day.

The WDF of COSMO-REA6 agrees very well with APGD, apart from an underrepresented wetness in the Apennine and an overrepresentation in Central Austria, at the eastern end of the Alpine ridge.

### 3.2.4 95th quantile

Figure 3.2.4.1, panel (a) shows the daily 95th quantile (Q95) of APGD. The region of highest precipitation lies in the Julian Alps with values over 37 mm per day. Other hotspots of heavy precipitation are the Dinaric Alps and Southern Switzerland, followed by the Alpine ridge in general and the other orographic elevations, mentioned in Section 3.2.1. In the adjacent flatlands, the Q95 is considerably lower with values between 10 and 15 mm per day compared to more than 20 mm per day in APGD. E-OBS, at first sight underestimates the Q95 over the whole domain. However, the outstanding maxima in the Julian Alps is clearly visible, which suggests that observations from this



area are included in E-OBS. Enhanced high quantiles in the Massif Central, on the other hand, are totally missed in E-OBS. In general, the behavior of E-OBS coincides with the picture drawn from the mean annual precipitation analysis in Section 3.2.1.

In panel (c), a striking maximum (>37 mm per day) of the global reanalysis (ERA5) is visible in the region of Ossola valley in Northern Italy. The maximum seems to be shifted westwards compared to the high precipitation area in Southern Switzerland apparent in APGD. This wrong representation might arise due to the steep slopes of the Southern Alps in the topography of ERA5, which then probably urges the reanalysis to form precipitation. Or alternatively, the underrepresentation of the Apennine in ERA5 and thus of an important precipitation barrier depending on the moisture flow is missing. Nevertheless, in this Q95 analysis, the geographical difference between APGD and ERA5 is less distinct compared to precedent analyses involving ERA-Interim (Isotta et al. 2015). The Alpine ridge, as well as the Dinaric Alps are generally well represented in ERA5, apart from the missing heavy precipitation spot at the border of Italy and Slovenia. When considering the regional reanalysis, COSMO-REA6 (panel (d)), the spatial distribution of Q95 looks very similar to the one from APGD. Significant differences are mainly visible again in Central Austria, where COSMO-REA6 slightly overestimates heavy precipitation. In all drier regions (Po valley, Southern France, Danube region and Vienna Basin), on the other hand, the regional reanalysis slightly underestimates Q95. Furthermore, even if the remarkable maximum in the Julian Alps is clearly underestimated, the Q95 value belongs among the highest of COSMO-REA6 in this domain.

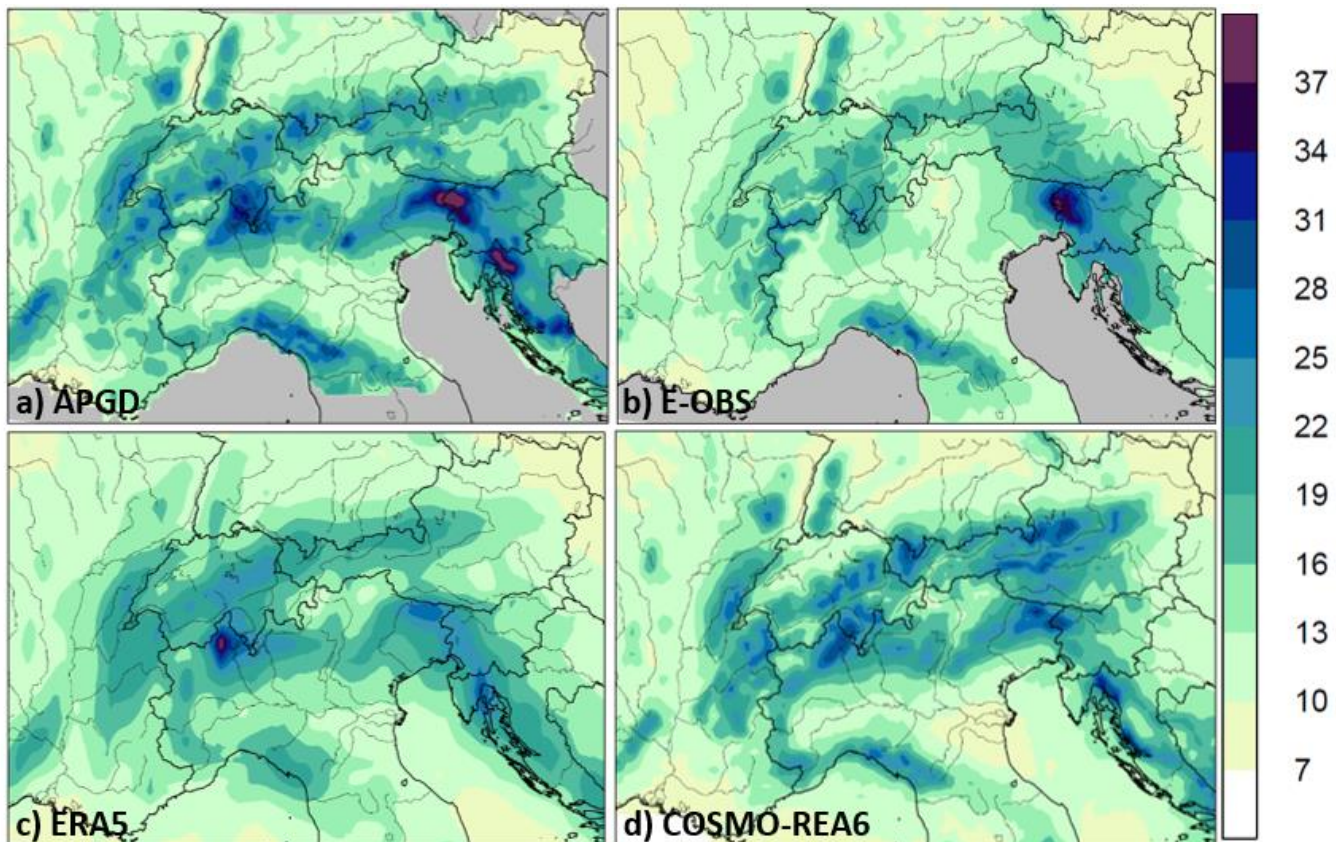


Figure 3.2.4.1: 95% quantile of daily precipitation in [mm/d]. The plots show the analysis on a  $0.1^\circ$  grid for APGD (a), E-OBS (b), ERA5 (c) and COSMO-REA6 (d).

### 3.2.5 Example of an extreme event: Flood on 21st/22nd August 2005

To illustrate the correspondence between the investigated datasets and to depict the behavior of extreme precipitation values, an extraordinary superregional precipitation event is chosen: the flood on 21st and 22nd August 2005. This flood occurred more or less in all of the Northern pre-Alpine regions of Switzerland, Germany and Austria. The devastating extent of the flood was a consequence of constant precipitation in the days before, during and after the event.

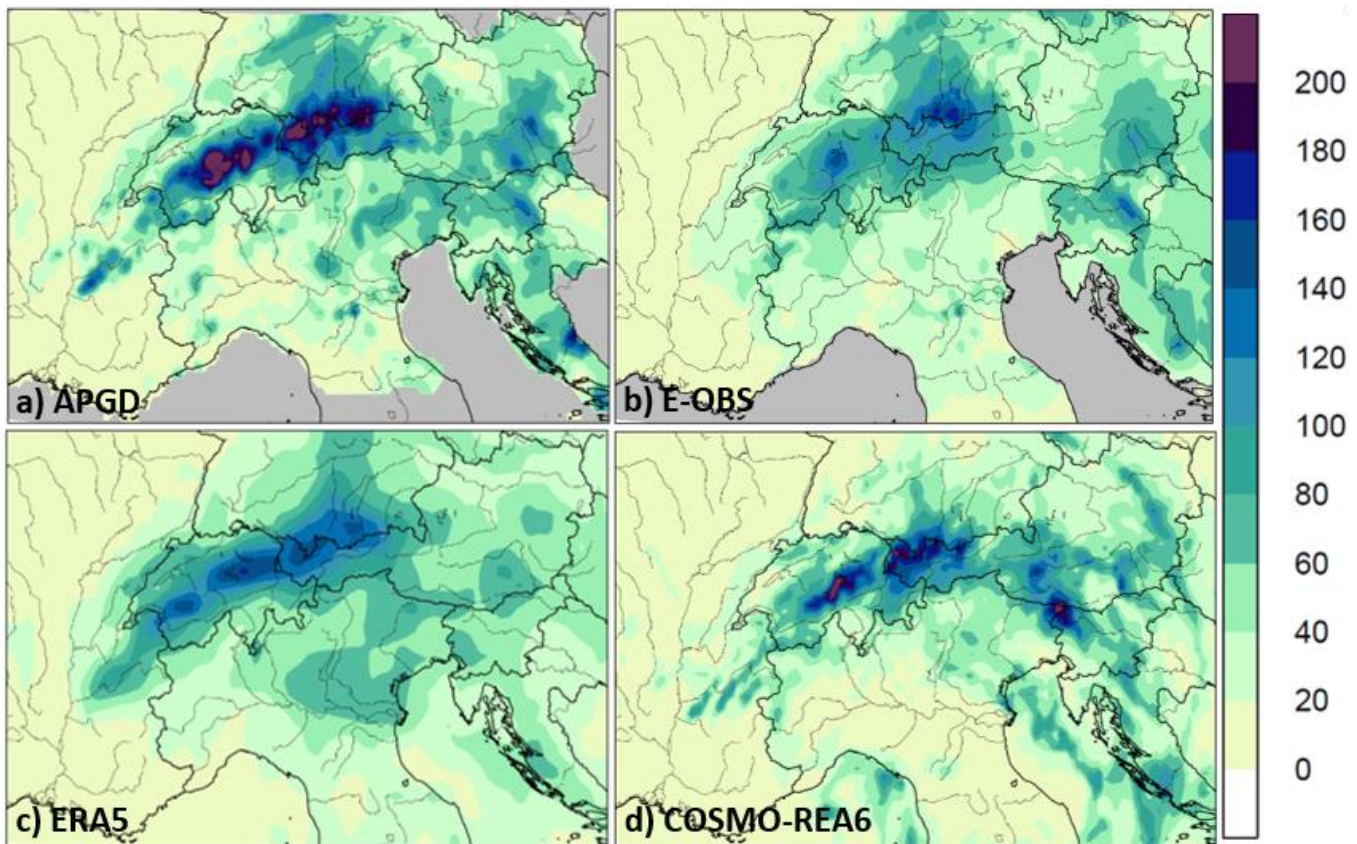


Figure 3.2.5.1: Precipitation sum [mm] from 20th to 23rd of August 2005 of APGD (a), E-OBS (b), ERA5 (c) and COSMO-REA6 (d). The investigated datasets are shown on a  $0.1^\circ$  grid.

Figure 3.2.5.1 represents the precipitation sum between 20th and 23rd August 2005 of the four investigated datasets. In the output of APGD, the heavy precipitation event, which has led to widely spread floodings, is well visible along the Alpine ridge with a strong emphasis on the Central Swiss Alps and the Western Austrian Alps. In both regions, the precipitation sum is higher than 200 mm over the course of four days. Furthermore, large parts of Southern Germany and the area between Austria, Slovenia and Italy show precipitation sums of 80-120 mm. When looking at E-OBS, it clearly reproduces this extreme event with two maxima, one over the Central Swiss Alps and the other at the border between Bavaria and Western Austria. Also, relatively high precipitation sums are visible in large parts of Southern Germany and in the Julian Alps. However, the magnitude of the event in general is underestimated by E-OBS, compared to APGD.

The global reanalysis, ERA5, shows nearly the same spatial precipitation distribution as APGD with the center of the event being over Alpine ridge. The largest difference between APGD and ERA5 is a relatively high precipitation sum in the Eastern Po valley where APGD only shows single spots of similar magnitude. Similarly to that, the main deviation of the regional reanalysis COSMO-REA6 is a precipitation peak in the Julian Alps where APGD doesn't show heavy precipitation. Another

difference regarding the spatial pattern is that the precipitation band which covers large parts of Southern Germany in APGD is much weaker in COSMO-REA6.

In Figure 3.2.5.2, the temporal evolution of the event is shown by means of daily precipitation sums of all considered datasets between 11th and 23rd of August 2005. Unsurprisingly, the extraordinary event is mainly visible in the German and the Swiss catchment, whereas in the Tagliamento catchment (Julian Alps) the precipitation sums are somewhat lower. It is nicely visible that all datasets correctly position the peak intensity, however, again the magnitude is underestimated by both E-OBS and ERA5 for the Aare catchment. At Black Forest, however, ERA5 shows even enhanced values throughout the course of the event compared to APGD. Well visible is that E-OBS shows nearly the same amount of precipitation on every day, which is of no surprise as the Black Forest lies in an area where E-OBS draws relatively many observations from (Figure 1.1). The spread of ERA5-Ens is significantly smaller compared to APGD-Ens, except for the German catchment. The light underestimation of E-OBS and ERA5 could be explained by the fact that single heavy precipitation events (as occurred especially on the 21st August) are most often only caught by observations and hence do not necessarily appear in reanalyses or they might not be included in E-OBS.

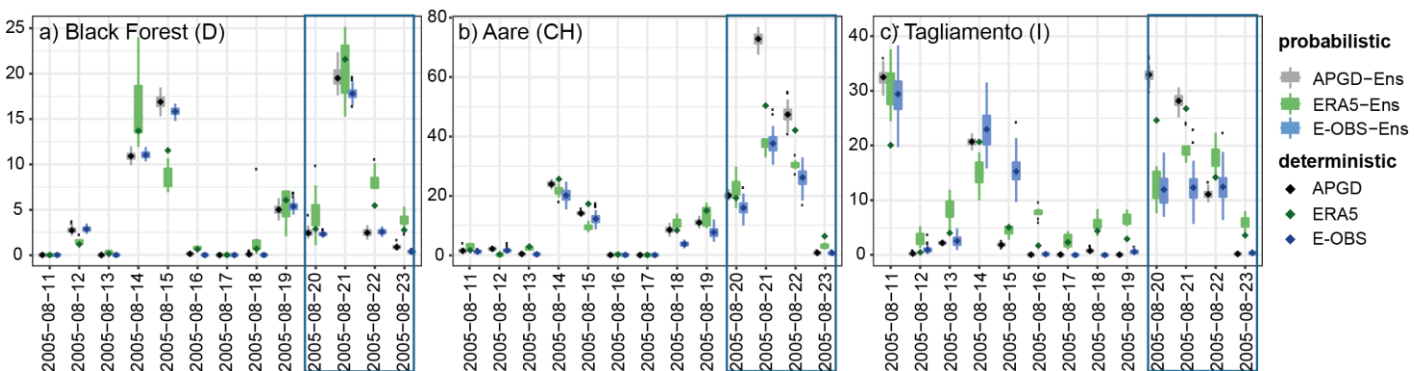


Figure 3.2.5.2: Daily precipitation sums for the catchments of Black Forest (D) (left), Aare (CH) (centre) and Tagliamento (I) (right) between 11th and 23rd of August 2005. The analysis is shown for the deterministic datasets APGD (black dots), ERA5 (green dots) and E-OBS (blue dots) and for the probabilistic datasets of APGD-Ens (grey boxplots), ERA5-Ens (green boxplots) and E-OBS-Ens (blue boxplots). The extreme event between 20th and 23rd of August is temporally marked with a blue box.

### 3.2.6 Theil-Sen Trend

Information about a possible trend signal is provided in Figure 3.2.6.1. Given that LAPrec nearly perfectly coincides with APGD, as shown in Figure 3.2.1.1 and 3.2.2.1, and that it spans a substantially longer time period it is considered as reference in this analysis. Therefore, a Theil-Sen trend test has been calculated over period of 1950 - 2017, which corresponds to the maximum overlap of E-OBS and LAPrec. Linear trends are computed using the robust method by Theil-Sen (Sen, 1968; Theil, 1950), which determines the slope as the median of all possible slopes between data pairs. Statistical significance is verified by means of Multiple Hypothesis Testing and the method of Hochberg and Benjamini, respectively (Hochberg 1995). Over the considered period, only

E-OBS shows a statistically significant trend signal in some regions. Namely, the local and highly positive trend signal (up to + 20 mm per 67 years) over Southwestern Switzerland and the relatively strong negative trend signal (up to - 20 mm per 67 years) over the Apennine are significant. Aside from the single “hot-spots”, larger areas of significant trend signals emerge along the border of Austria and Italy with a maximum in the Julian Alps (positive) and in the Po valley (negative). Less strong but nevertheless statistically significant trend signals are detected over broad areas in the south-westernmost Alps of France (positive), in the Dinaric Alps (positive), Massif Central (negative) and also in some parts of the flatlands adjacent to orographic regions.

When looking at panel (c) in Figure 3.2.6.1, the slope of Theil-Sen trend test of the difference between E-OBS and LAPrec is visible. By taking the square root and then subtracting the two datasets common variance and “noise” should be erased and subsequently an otherwise “lost” trend signal could emerge. As has already been shown in various articles (e.g. Frei 2014), the temporally inconsistent station density of E-OBS could explain why there are relatively strong trend signals opposed to no significant trend signals at all in LAPrec, which is a temporally consistent long-term climate dataset. Increasing station density over time leads to a conditional bias, especially at the low and high quantiles, and hence to an artificial trend.

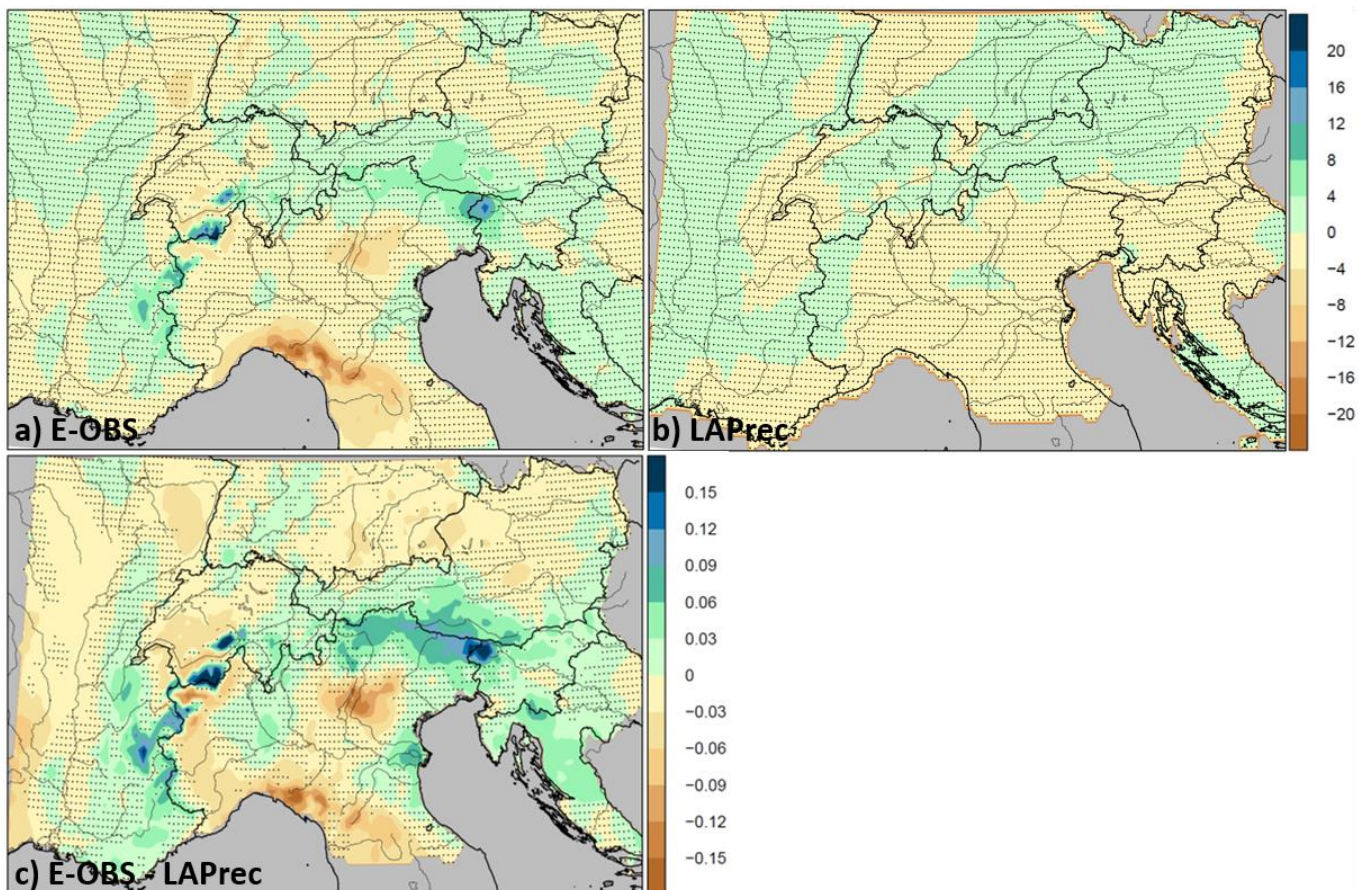


Figure 3.2.6.1: Theil-Sen Trend estimate in [mm/ 67 years] for (a) and (b) and dimensionless for (c). The trend is calculated for (a) E-OBS and (b) LAPrec over the period 1950 – 2017 on 0.1° grid. In (c), a Theil-Sen trend

test is calculated over the difference between E-OBS and LAPrec ( $\text{VE-OBS} - \text{VLAPrec}$ ) on a  $0.1^\circ$  grid. The stippling indicates that the statistical significance of the trend signal is not met at 0.05 (Hochberg 1995).

### 3.2.7 RMSE

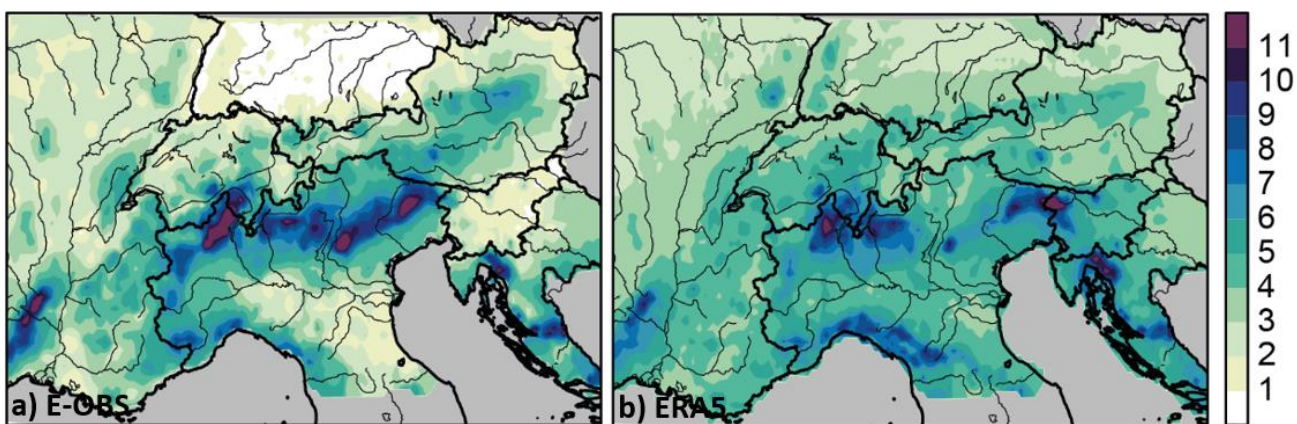


Figure 3.2.7.1: Daily root mean squared error (RMSE) in [mm] of (a) E-OBS and (b) ERA5. The statistical measure is computed on a  $0.1^\circ$  grid and with the reference of APGD.

On the one hand, a surprisingly low RMSE of nearly zero mm per day is visible over the entire area of Germany and Slovenia (Figure 3.2.7.1). Similarly, the error approximates 1 mm per day over Northeastern France, Northern Switzerland, the Vienna basin and northern parts of Central Italy. On the other hand, the largest errors for E-OBS arise just south of Switzerland, where in APGD a relatively wet area is visible. This hotspot of precipitation is clearly missed by E-OBS with a RMSE of more than 10 mm per day in this area. Other areas of high errors are the already mentioned precipitation band over Northeastern Italy, which is totally neglected in E-OBS as well as enhanced precipitation in the Massif Central. Very generally, precipitation in the westernmost part and in the easternmost part of the Alpine ridge, as well as along the Apennine, is clearly underestimated. This misbehavior of E-OBS compared to APGD can be easily explained by looking again at the distribution of station data in E-OBS (Figure 1.1): While the measurement density in Germany and Slovenia is very high, the density over Eastern Austria, Northern Italy, parts of Switzerland and parts of France is comparatively low..

For the global reanalysis, ERA5, a partly different picture arises when looking at the RMSE. North of the Alpine region, the error approximates zero, whereas along the Alpine ridge the clear overestimation of precipitation in ERA5 leads to a relatively larger error. Also, larger errors are visible in the area of Massif Central, the easternmost part of the Alps, the Apennine and the Dinaric Alps over Croatia. Most strikingly, the error in the Ossola valley, a region prone to heavy precipitation lying just south of Switzerland, is spatially again very limited and very high. This obvious misrepresentation of true precipitation has already been explained in Section 3.2.4.

Overall, RMSE thus tends to be larger in areas which are well known for heavy precipitation, like the Julian Alps, Southern Switzerland, Massif Central and Apennine, because a similar relative error is more heavily weighted in case of high compared to low intensities (Isotta et al. 2015). Another

factor which strongly impacts the RMSE is the smoothing effect, an effect mostly occurring when the average distance between stations is lower than the grid spacing.

### 3.2.8 MESS

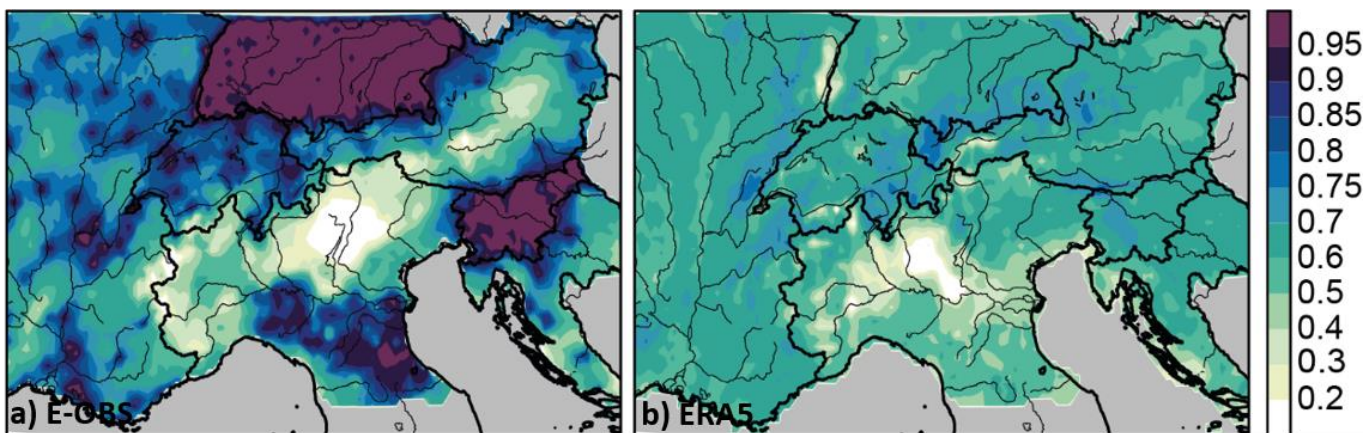


Figure 3.2.8.1: Mean Squared Error Skill Score (MESS) over time and for every grid point in [mm]. The score is computed for (a) E-OBS and (b) ERA5, on 0.1° grid and with the reference of APGD.

Unsurprisingly, the MESS for E-OBS is the highest in the well-represented areas of Germany and Slovenia, where values uniformly approximate a perfect skill of 1 (Figure 3.2.8.1). In the area of Apennine and in some areas of Switzerland, Central France and Southern France the explained variance also reaches a similar level. A rather diverse spatial pattern of MESS is visible over France in general: spots of high MESS alternate with areas of less explained variance. A worse MESS is visible throughout most parts of Northern Italy with a minimum over eastern Po valley and just slightly higher MESS over Central and Southern Austria.

A smaller amount of explained variance is apparent by means of a lower MESS, when looking at ERA5. However, apart from the Po valley, the MESS is very uniformly distributed over the whole domain (0.5-0.7). The only areas of higher MESS are the orographic areas along the Alpine ridge and north of the Alps (Jura, Vosges, Black Forest, Bavarian Forest). Parts of this comparatively bad performance of ERA5 can be explained with reanalyses generally overestimating precipitation over the whole domain due to a strict mass balance which urges moisture to precipitate although precipitation is not likely in reality. Furthermore, this worse performance compared to APGD can be explained with missing in-situ measurements in reanalyses.

### 3.2.9 SEEPS

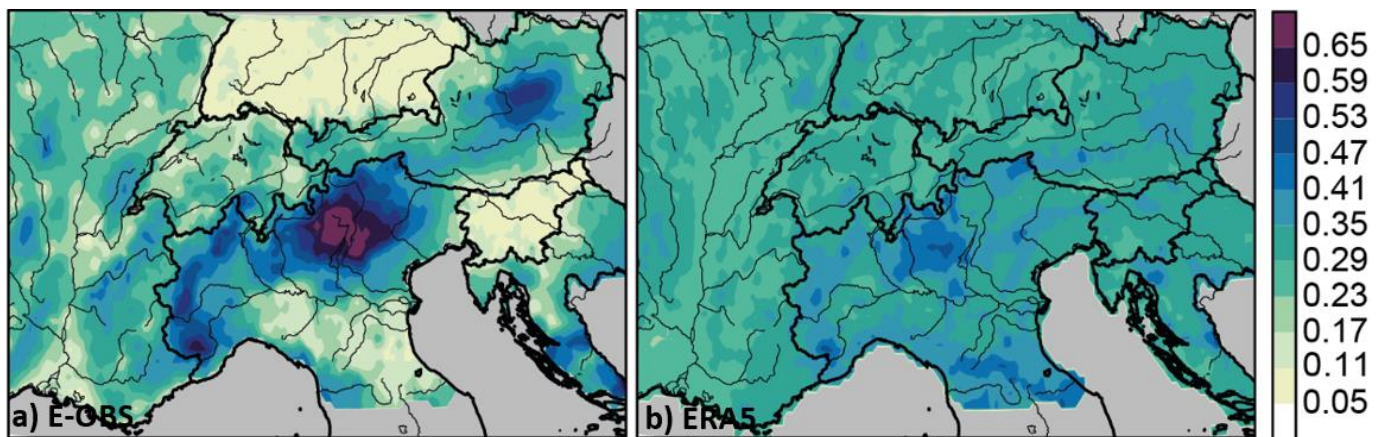


Figure 3.2.9.1: SEEPS (Stable equitable error in probability space) for every grid point and for three categories: dry days ( $< 1\text{mm/day}$ ), days with light and days with heavy precipitation. This score is computed for (a) E-OBS and (b) ERA5, on a  $0.1^\circ$  grid and with the reference of APGD.

The magnitude depending SEEPS is hereafter presented to quantify and hence compare the correspondence among different regions of the domain. In Figure 41, the distribution of SEEPS again shows how strongly the correspondence of E-OBS compared to APGD depends on the regional availability of stations. This manifests in clear contrasts of SEEPS between Germany and Slovenia on the one hand, and France and Italy on the other hand. For ERA5, SEEPS produces a very similar picture as MSESS (Figure 3.2.8.1) only that the spatial correspondence is in general worse along the entire Alpine ridge. The regional varying performance might arise due to the stronger penalty of SEEPS when wrongly representing the intensity of rain. Overall, ERA5 has the highest SEEPS north of the Alpine crest and over nearly whole Eastern France. This is in good agreement with the precedent analyses.

### 3.2.10 Rank histogram

In order to assess whether a deterministic dataset could be an equiprobable member of a probabilistic reference dataset, the PITs (Probability Integral Transforms) are calculated. If the ensemble members of the probabilistic dataset and the observations of the deterministic dataset all have been drawn from the same distribution, the rank of the observations within this value range is equally likely to be any of the ranks. If the observation is smaller than all members, then it would have rank = 1, if it is larger than all members it would have rank =  $n(\text{ens})+1$ . Thereby, systematic errors in one direction could be detected and therefore the need of a bias correction or other transformations can be investigated. In this analysis, the ensemble of the APGD dataset is considered as reference.

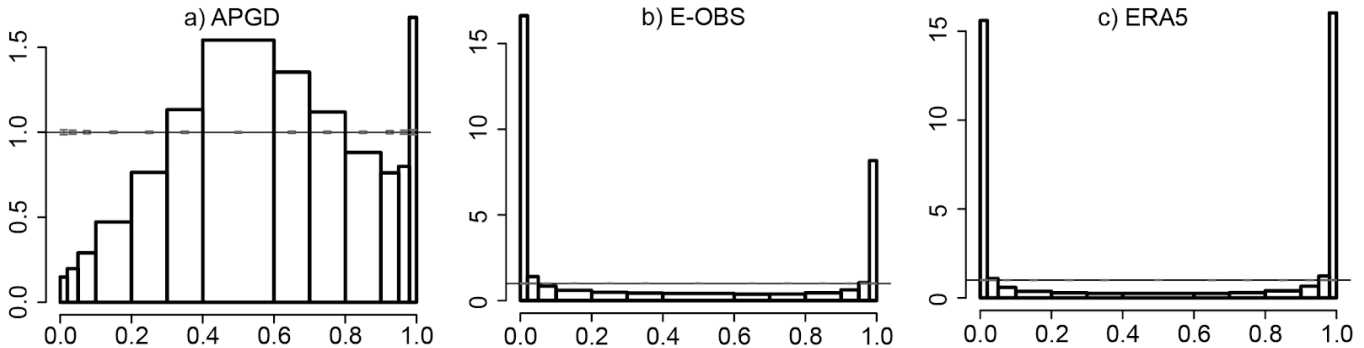


Figure 3.2.10.1: Rank histograms of deterministic E-OBS (left), ERA5 (center) and APGD (right) with the reference of APGD-Ens, calculated on a  $0.1^\circ$  grid. The horizontal line in the diagram equals the relative frequency of all members  $(n(\text{ens})+1)^{-1}$ .

In Figure 3.2.10.1, the rank histogram is shown for both deterministic datasets, E-OBS (center panel), and ERA5 (right panel). For both, central ranks seem to be constantly underestimated, whereas the extreme ranks are overpopulated in comparison to the probabilistic APGD dataset. E-OBS and ERA5 tend to be out of the uncertainty range of APGD-Ens and consequently both datasets are too misrepresenting precipitation compared to the reference. Consequently, both deterministic datasets of interest, namely E-OBS and ERA5, cannot be considered as equiprobable members of APGD-Ens. In other words the  $n(\text{ens})$  members and the single observations obviously have not been drawn from the same distribution.

### 3.2.11 Frequency distribution function

The frequency distribution function is a way to depict the frequency of a dataset to exceed a certain threshold. The quantiles are calculated for every value, so that the cumulated frequencies can be displayed in a decreasing order. As an example, if a daily precipitation value of 5mm/d equals the frequency of 0.6, in 60% of all cases precipitation will be higher than 5mm/d.

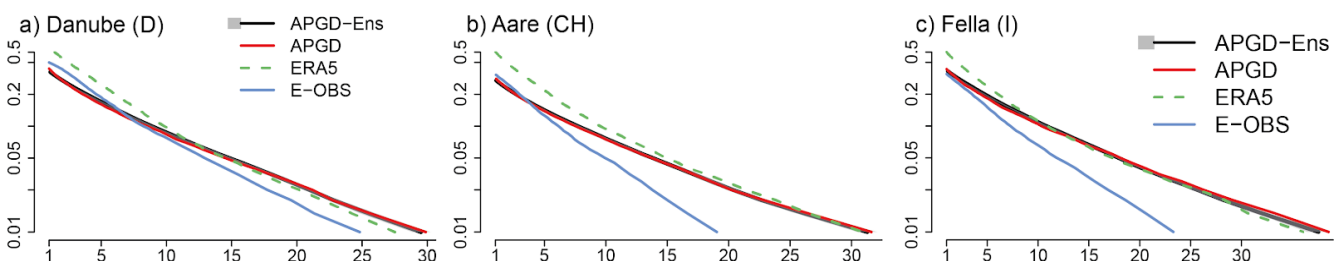


Figure 3.2.11.1: Frequency distribution function of the catchments Danube (D) (left), Tagliamento (I) (center) and Aare (CH) (right), calculated on a  $0.1^\circ$  grid. The red line corresponds to the deterministic APGD, the green line to ERA5 and the blue line to E-OBS. The reference is APGD-Ens depicted by the black curve.

As visible in Figure 3.2.11.1, the higher the precipitation amount, the stronger the underestimation of E-OBS for all catchments. Although, this underestimation is much smaller for the German catchment of Danube, compared to Aare (CH) and Tagliamento (I). This different behavior can be explained to some extent by the already above mentioned high station density in Germany. Also not

surprising is the overestimation of small precipitation sums in ERA5, which has already been seen throughout the whole evaluation. On the other side, the higher precipitation sums tend to be slightly underestimated, except for the heavy precipitation catchment of Tagliamento. Interesting is that the quantile depending behavior of ERA5 does not vary significantly among the investigated catchments.

### 3.2.12 BSS

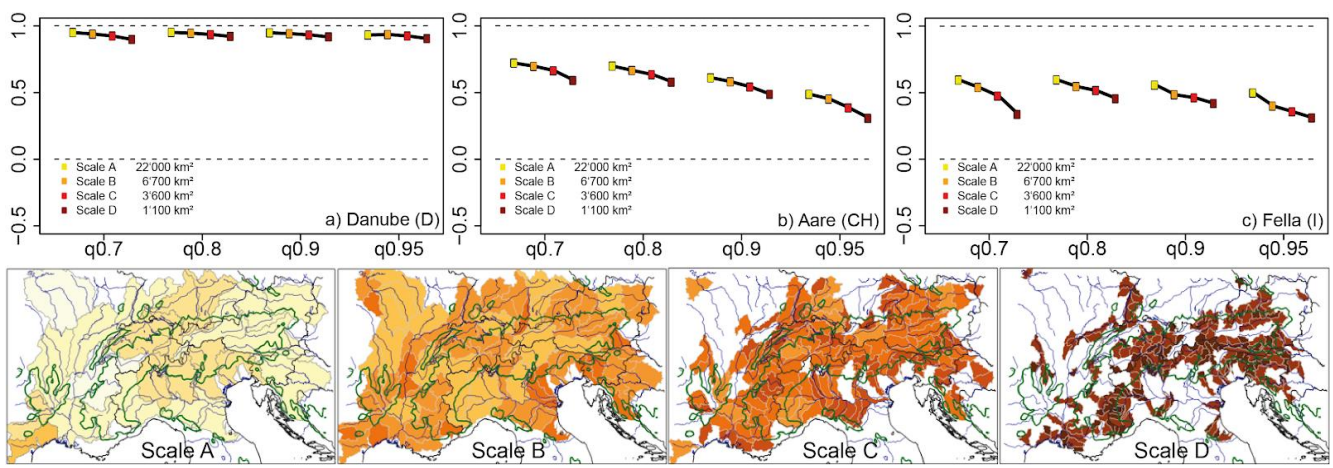


Figure 3.2.12.1: Brier Skill Score (BSS) in the period 1979-2008 of APGD (left), E-OBS (center) and ERA5 (right). The abscissa axis is the threshold used for the score, corresponding to the 70%, 80%, 90% and 95% quantile (for each catchment). The point chain represents the score for different scales (from A, the biggest catchments to D, the smallest, see legend in the panel of the APGD dataset). Each scale is composed of several catchments, as illustrated in the bottom panels. The reference for the score is the probabilistic dataset APGD-Ens.

To have a more profound look at the scale-dependent behavior of the investigated datasets, the BSS has been calculated for the higher quantiles of Q70, Q80, Q90 and Q95, as visible in Figure 3.2.12.1. At first sight, BSS unsurprisingly is the highest for APGD (left panel) for all scales and quantiles with scores ranging between 0.8 and 1 depending on the scale. Also obvious is that the smaller the scale and the higher the quantile, the lower the score. This makes sense because extreme values in general are more difficult to adequately represent and because on small scales less data is available which could correctly influence the values. This effect is well visible when looking at E-OBS (center panel), nevertheless the BSS for the 70% and the 80% quantile is above 0.5 for all scales. The same is valid for the 90% quantile at all scales, except for the smallest scale (D). ERA5 (right panel) generally shows the smallest BSS of all investigated datasets. Moreover, it shows an extraordinary strong decline of BSS for the Q70 depending on the scale. While the largest scale (A) has a BSS of roughly 0.6 the smallest scale (D) has a BSS of roughly 0.3. For the other three displayed quantiles (Q80, Q90, and Q95), this quantile and scale dependent decrease is less pronounced. As a consequence of that, the highest investigated quantile (Q95) shows an equally high BSS as E-OBS, apart from scale B.



### 3.2.13 Main outcomes – precipitation in the Alpine region

#### E-OBS

E-OBS represents orographic precipitation patterns in the Alpine region generally well, though it tends to underestimate the precipitation magnitude. Also, several mesoscale precipitation anomalies are reproduced and the precipitation “hot-spot” in the Julian Alps is satisfactorily visible. However, E-OBS also lacks some of the outstanding moist anomalies like the Massif Central, the Jura, the westernmost Alpine ridge in Central Austria and a precipitation band over Northeastern Italy. Thus, the performance of E-OBS obviously strongly depends on the data availability, which is in some countries still limited. For small catchment sizes and for higher precipitation quantiles, the biggest differences compared to the reference and the lowest skill scores are found. Furthermore, the deviation from the reference of APGD enhances with increasing magnitude of precipitation.

#### ERA5

ERA5 reproduces enhanced precipitation along the Alpine crest and at the other elevated areas realistically. However, it tends to generally overestimate the magnitude of precipitation and especially the frequency of light precipitation. Because of spatial smoothing inherent to the coarser grid resolution of ERA5 ( $0.25^\circ$ ) and as there are no in-situ measurements included in ERA5, local precipitation extremes are furthermore not displayed or underestimated. ERA5 should thus not be considered for the investigation of local heavy precipitation. Overall, the performance of ERA5 is surprisingly good, compared to the reference dataset of APGD. In regions of sparse station density it even outperforms E-OBS, unless the wet days frequency is considered, which is strongly overestimated in ERA5.

#### GENERAL COMMENTS

Users should be aware of the effective resolution of datasets, which corresponds to the average distance between neighbouring measurement stations. While the spatial resolution of the reference APGD is finer than the chosen evaluation grid resolution, it is coarser for ERA5. Also, the effective resolution of E-OBS can be coarser than its nominal grid resolution and investigations on single grid cells thus should be considered with caution.

## 3.3 Carpathian region

This Section draws up the results of the comparison of precipitation (RR) between CARPATCLIM, E-OBS and ERA5 for the period 1979-2010, which corresponds to the maximum overlap of all datasets and the reference. In the following chapters, the results of the analysis are presented and discussed.

### 3.3.1 Mean annual precipitation

Precipitation is a climate parameter with high temporal and spatial variability in the Carpathian region. Its spatial distribution is determined by distance from the seas, continentality and topography. However, the Carpathian chain is very long (more than 1500 km, but only the Tatra Mountains are above 2000 m altitude) and it has a curved shape, consequently the Carpathians do not always stop the air masses that can cross above the mountains or can be deviated towards the south. Similarly, the Carpathians are not always able to stop the humid oceanic air masses coming from north-west. Topography also plays a role in the modification of the air flows in the large central plain, the Carpathian basin.

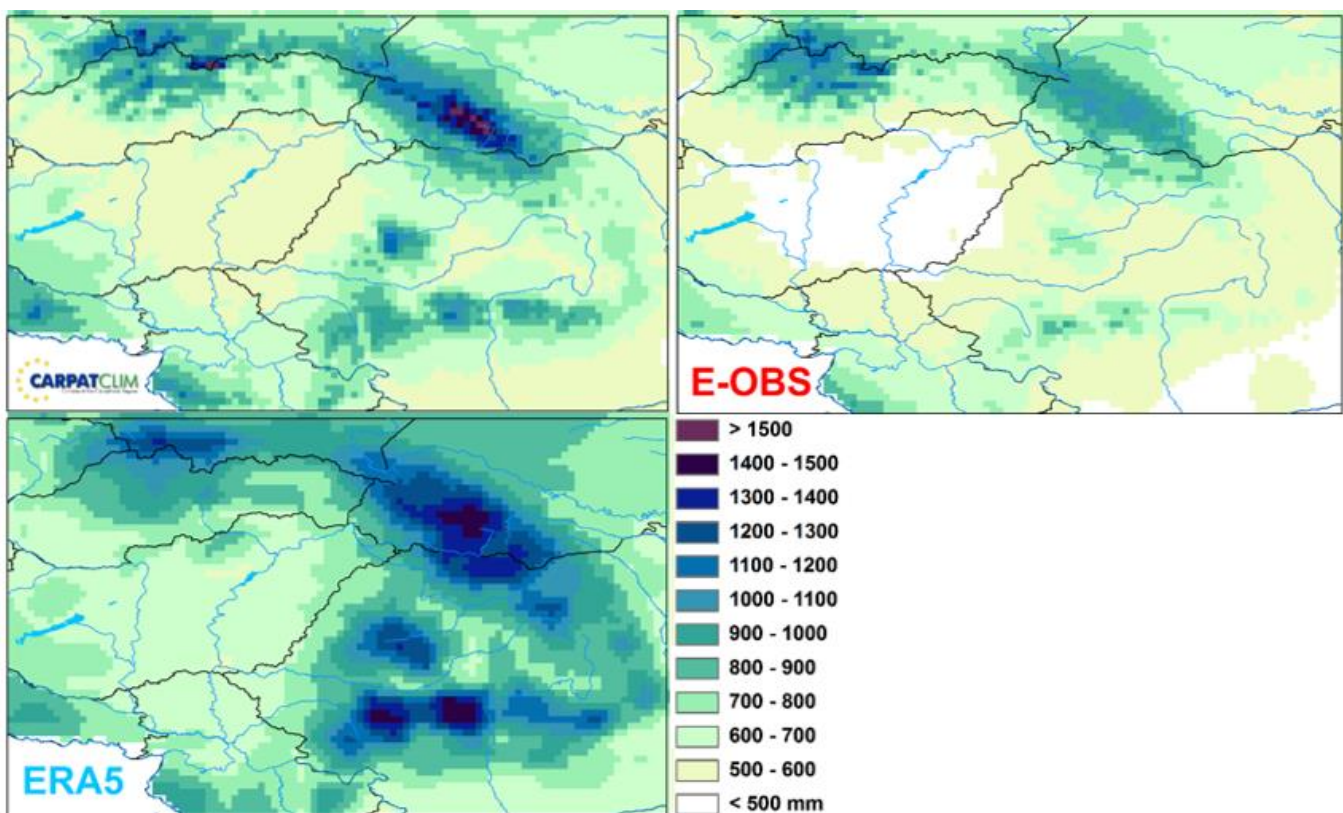


Figure 3.3.1.1 Mean annual precipitation for the period 1979–2010.

The mean annual precipitation is shown first to get an overview on the precipitation climatology over the Carpathian region for each dataset. Principal patterns like areas of strong orographic precipitation or continental, dry plains should be thereof detected as well as general insights regarding the wetness of the datasets. Figure 3.3.1.1 shows the gridded average annual precipitation values for the period 1979–2010 for the datasets involved in the examinations. According to precipitation climatologies, the rainy season lasts from May to July. In every season, there is more precipitation over the mountains (up to 1650 mm in the Ukrainian Carpathians and in the Tatra Mountains) than in the plains. The lowest annual precipitation totals occur in eastern Hungary (550 mm). The averages computed for the entire region and for different ranges can be found in Table 3.3.1.1 According to the Table 3.3.1.1 E-OBS is drier and ERA5 is wetter than



CARPATCLIM at each elevation. E-OBS underestimates the yearly sum with 81.4 mm for the entire region, particularly at higher elevation above 1500 m, where the underestimation is 215.4mm in average. Similarly, even higher overestimation can be found in ERA5 at the highest mountainous areas (249.1 mm). The overall overestimation is 143.1 mm for the entire region, which is more than half as much compared to the underestimated precipitation in E-OBS.

1979-2010	entire region	$h < 200m$	$200 < h < 500m$	$500 < h < 1500m$	$h > 1500m$
<b>CARPATCLIM</b>	699.4	609.7	696.6	848.5	965.6
<b>E-Obs</b>	618.0	540.1	630.7	727.5	750.2
<b>ERA5</b>	842.5	707.9	851.1	1047.0	1214.7

Table 3.3.1.1 Annual average precipitation (mm) for the period 1979–2010 at different altitudes.

### 3.3.2 Yearly cycle and Catchments based studies

Considering the annual course, less precipitation falls in the winter half year in the Carpathian region. The distribution of the precipitation throughout the year is similar in all three examined datasets although there is a substantial overestimation in ERA5 in each month. E-OBS resulted in less amount of precipitation throughout the year than CARPATCLIM. ERA5 provides 143.1 mm more on an annual basis. The differences from February to August are greater than 10 mm in every month. Approximately 20 mm of overestimation in April is the largest in ERA5. The averages in October are similar for all three datasets, the deviations from CARPATCLIM are below 7 mm averaged over all regions. The monthly average overestimation is 11.92 mm in ERA5 compared to CARPATCLIM. For E-OBS and CARPATCLIM the monthly averages coincide relatively well, but the monthly amounts derived from E-OBS coursing under CARPATCLIM on the chart in the Figure 3.3.2.2 The overall monthly average underestimation is 6.7 mm for E-Obs, the largest (10.15 mm) departure from CARPATCLIM arises is in June. The standard deviation of the time series of regionally averaged monthly precipitation is similar (Figure 3.3.2.2), with lowest values in E-OBS (winter half year) and highest values in ERA5 (summer half year) with CARPATCLIM between them.

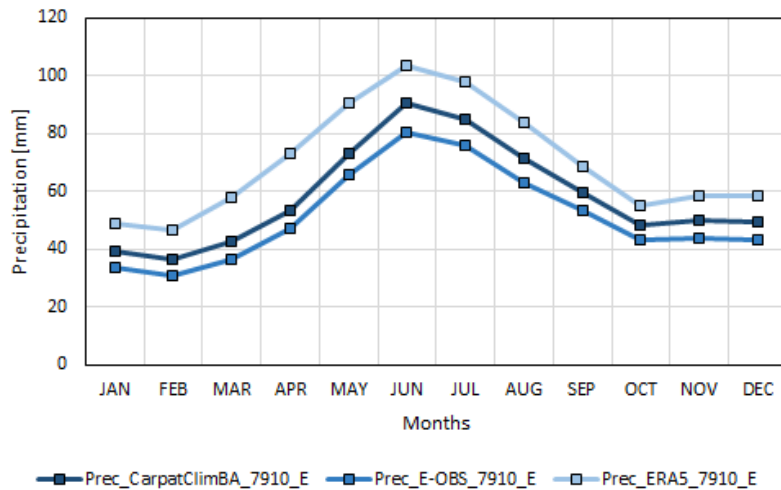


Figure 3.3.2.1 Monthly averaged precipitation (1979–2010) showing the annual cycle for different datasets.

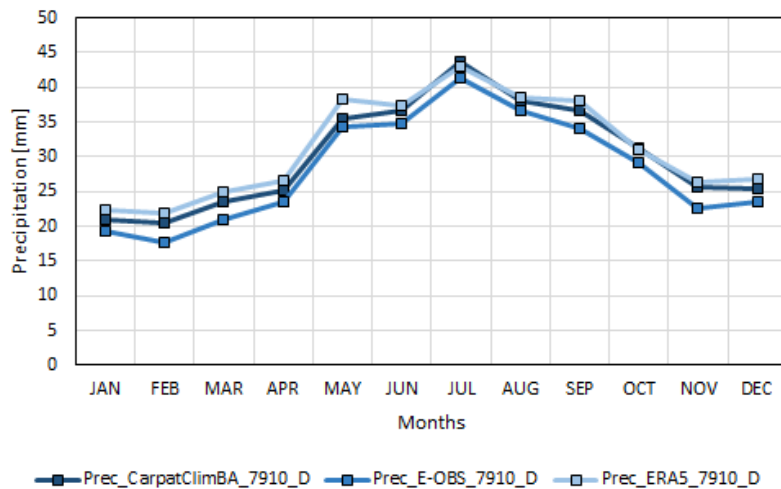


Figure 3.3.2.2 Monthly averaged standard deviation of daily precipitation (1979–2010) showing the annual cycle for different datasets.

## Catchments based studies

Four sub-catchments of the Danube catchment were selected for this comparison in the Carpathian region. The selected watersheds are large enough in order to be realistically resolved by ERA5 and some of them small enough to represent mesoscale phenomena (Figure 3.3.2.3). The sub-catchments represent different precipitation climates. The larger ones are involved in this sub-catchment studies to emphasize the importance of the availability of cross border data and data exchange strategic planning of the flood control. The role of the smaller ones are to reveal possible differences in representation of the mesoscale processes in the data tests.



Sub-catchments analysed here:

a) Zala, Balaton: 5 737 km<sup>2</sup>

Balaton is the largest freshwater lake in the Transdanubian region of Hungary. The Zala river provides the largest inflow of water to the lake, and the canalised Sió is the only outflow. Lake Balaton affects the local precipitation in the area. The area receives approximately 50–70 mm more precipitation than most of Hungary, resulting in more cloudy days and less extreme temperatures. Balaton is a shallow lake, typical shallow lakes with their average depth remaining below 5 m. An important feature of the shallow lakes in the moderate climate zone is the high quantitative and qualitative sensitivity to the changes of environmental factors (including climate factors) in space and time.

b) Felső-Tisza (Upper Tisza): ~ 10 000 km<sup>2</sup>

About 60% of the whole Upper Tisza River Basin gets more than 1000 mm of precipitation annually. Warm air masses from the Mediterranean Sea and the Atlantic Ocean cause cyclones with heavy rainfall on the southern and western slopes. The catchment b), the upper parts of the Tisza river, outside Hungary, in Ukraine, (8% of the Tisza river basin) suffers from flash flooding.

c) Zagyva: 5677 km<sup>2</sup>

Mesoscale atmospheric phenomena lasting often for 12-24 hours only, but involving heavy rainfall over smaller catchments, like the Zagyva river, may trigger floods. Flash floods often of considerable magnitude may rush down the small streams like Zagyva and creeks and cause violent local storms in a few hours duration. The flood wave retreat is rapid because of the large slope of the watercourses in the mountainous regions.

d). Körösök, Berettyó: 27 537 km<sup>2</sup>

The Körösök has three source rivers, all of which have their origin in the Apuseni Mountains in Transylvania, Romania. The Tisza River Basin where the catchment d) is located is influenced by the Atlantic, Mediterranean and Continental climates, which impact regional precipitation. The multi-annual mean values of annual precipitation vary within the Tisza River Basin from 500 to 1600 mm/yr. The highest values (around 1600 mm/yr) occur in the northwestern Carpathians and in the Apuseni Mountains in Transylvania, Romania.

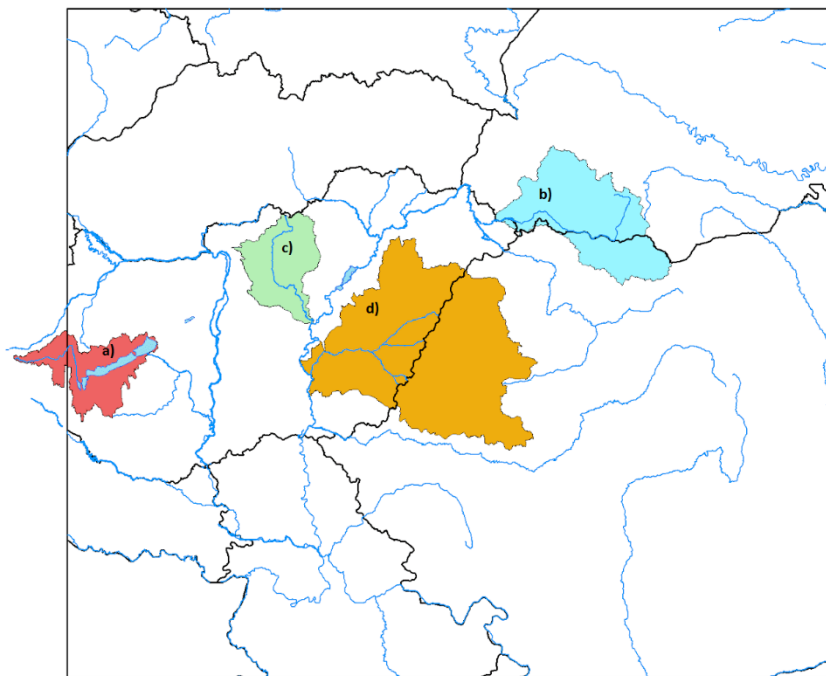
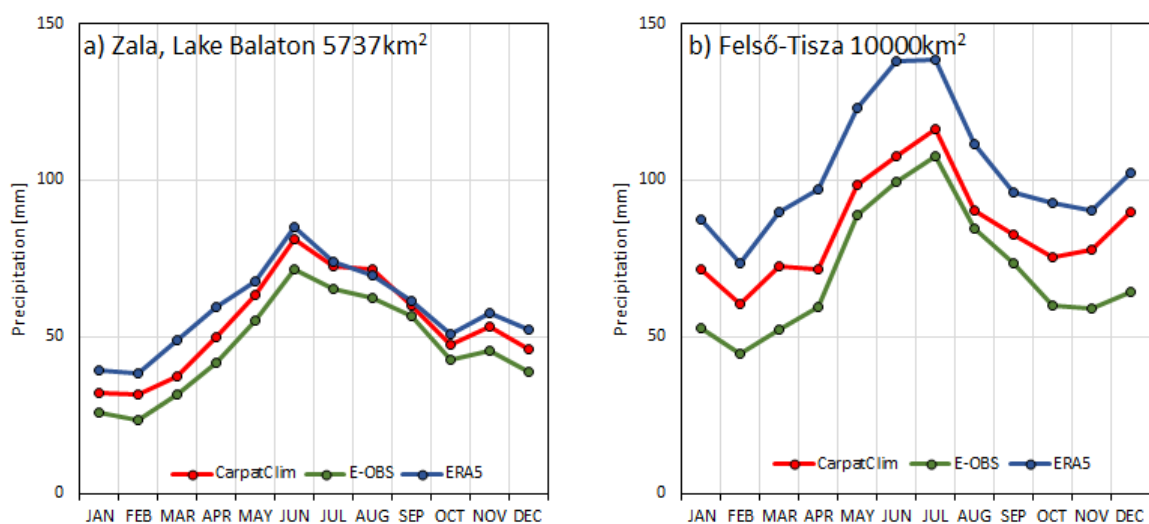


Figure 3.3.2.3 Geographical location of the 4 different investigated sub-catchments of the Danube river on area of CarpatClim dataset. a) Zala, Lake Balaton, b) Felső-Tisza, c) Zagyva d) Körösök, Berettyó based on Mátrai (2015).



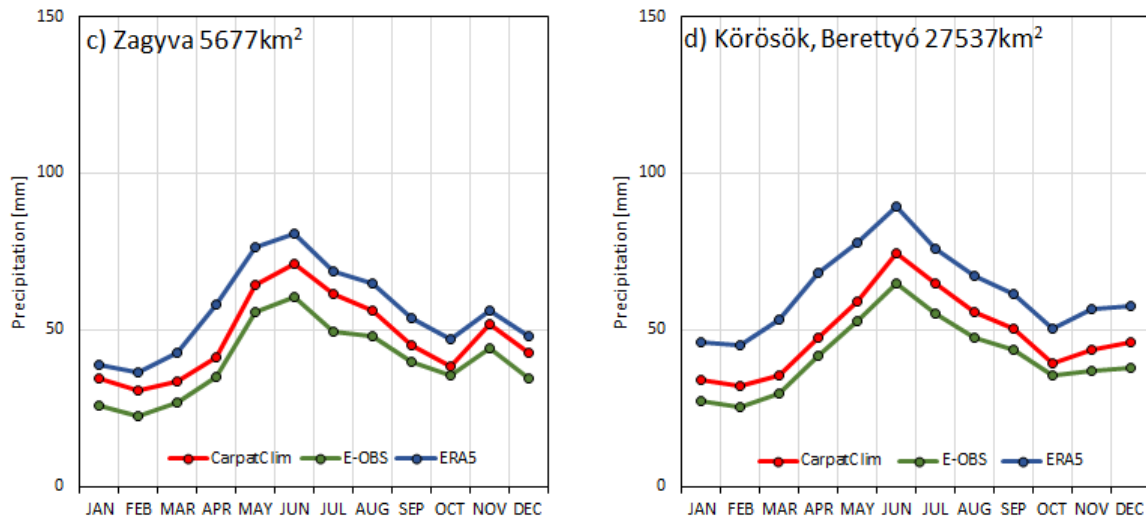


Figure 3.3.2.4 Yearly cycle depicted by average monthly precipitation sums [mm] for the 4 different sub-catchments of the Danube river. a) Zala, Lake Balaton, b) Felső-Tisza, c) Zagyva d) Körösök, Berettyó.

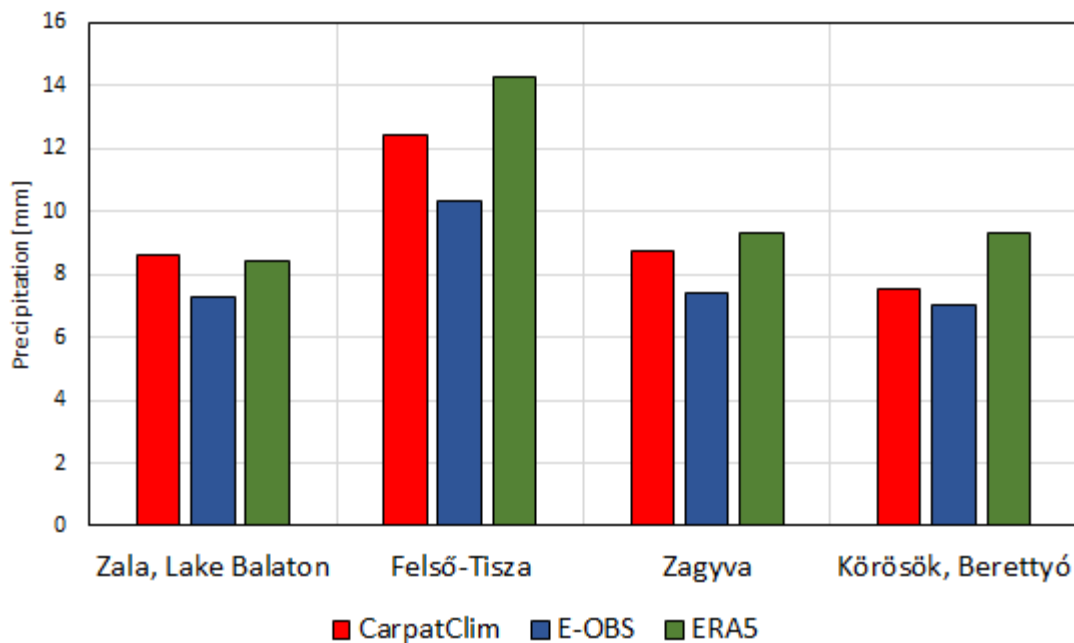


Figure 3.3.2.5 The 95th quantile the average precipitation [mm] of the 4 different sub-catchments of the Danube river.

The monthly mean precipitation fell at the selected watersheds (Figure 3.3.2.4) confirm the general overestimation of ERA5 and underestimation of E-OBS in the territory of the sub-catchments,

particularly for b), c) and d). In the case of catchment a) (which is situated in the wettest part of Hungary) ERA5 and CARPATCLIM monthly averages are similar from May to October, in other respects, E-OBS monthly values are fewer by around 7 mm on average. The monthly values are the closest in September in the catchment a) for all three dataset. The largest overestimation comes into view the region of Upper-Tisza (b) sub-catchment in Ukraine in ERA5 related to CARPATCLIM during the whole year, between 13 mm and 30 mm, with largest differences in the convective season.

The Figure 3.3.2.5 shows the 95th precipitation quantiles where higher extreme quantiles appear in ERA5 and lower in E-OBS. than in CARPATCLIM (2-3 mm more in ERA5 and less in E-OBS) at all sub-catchments. The similarities in Q95 quantiles can be explored also in the watershed a) of Lake Balaton.

### 3.3.3 Wet-day frequency

Empirical probability of wet days showing the frequency of days in the datasets with equal or more than 1 mm of precipitation. The plots show an analysis on CARPATCLIM, E-OBS and ERA5.

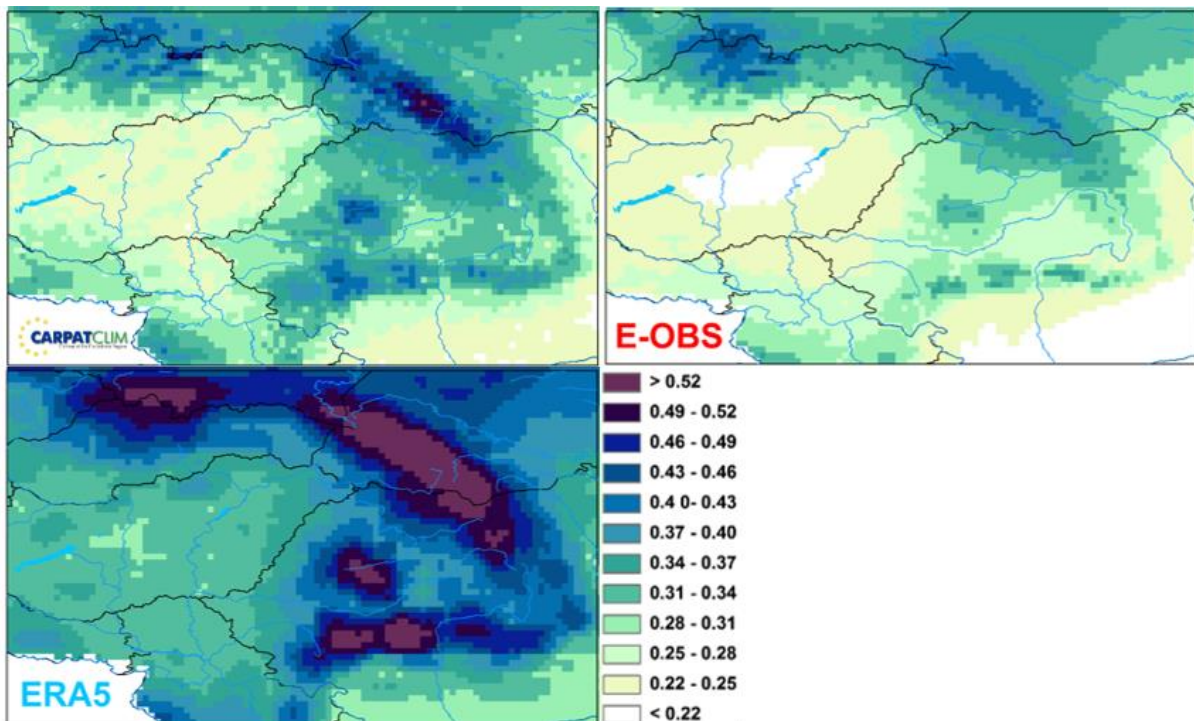


Figure 3.3.3.1 Empirical probability of wet days showing the frequency of days in the datasets with equal or more than 1mm of precipitation (WDF). Plots show CARPATCLIM (upper left panel), E-OBS (upper right panel) and ERA5 (lower panel).

In CARPATCLIM (Figure 3.3.3.1, upper panel, left) higher frequency of wet days appears along the Carpathian Chain and in the Bihor Massif in Romania. The northwestern Carpathians and extended



regions in the eastern Carpathians and also southern Carpathians can be characterized by 0.5 of the wet day's frequency. The average frequency of nearly 0.5 corresponds to roughly one rainy day out of two. The areas in the Inner Western Carpathians at the north bound of the region and the Transylvanian Plateau to the east and the ridge of the Dinaric Alps in south-east of CARPATCLIM region show frequency of wet days between 0.3 and 0.4. The fewest rainy days with at least 1 mm occur in the flatlands with elevations lower than 200 m in the Carpathian basin on the central Great Plain, in the Wallachia out of the range of the Carpathians in Romania and in the Romanian Plain at the southeastern edge of the domain. In general, precipitation occurs only on every fifth day in the flatland in CARPATCLIM dataset.

E-OBS (Figure 3.3.3.1, upper panel, right) is obviously drier than CARPATCLIM, particularly in plane regions in the center and in the southeastern border of the domain. The higher amount of rainy days in elevated parts of the southern Carpathians is completely absent in E-OBS. This difference in rainy days seems to be linked to the reduced availability of stations in these areas. Analyzing the yearly cycle of WDF the highest underestimation in E-OBS occurs from May to September in the convective season, otherwise the monthly averages of the WDF are similar.

Considerable overestimation of the frequency of wet days over the whole CARPATCLIM domain is obvious for the whole year in ERA5 (Figure 3.3.3.1, lower panel). The empirical probability of wet days in regional average is 0.31, 0.29 and 0.39 for CARPATCLIM, E-OBS and ERA5, respectively.

### 3.3.4 95th quantile

Figure 3.3.4.1 (upper panel, left) shows the 95% quantile of daily precipitation (Q95) in CARPATCLIM. The most intense precipitation falls in the High Tatras at the Slovak and Polish border and the northeastern Carpathians. The Q95 is around 20 mm/day in those regions. The impact of the orography is clearly visible in CARPATCLIM dataset. The Q95 values above 18mm/day are present in the southern Carpathians and, limited to smaller regions, in the Dinaric Alps. The magnitude of precipitation is underrepresented in E-OBS. However, the spatial distribution of the Q95 in E-OBS agrees well with the precipitation patterns in CARPATCLIM. A lack of higher expected values in the southern Carpathians is obvious. Also in the Great Plain in Hungary, small Q95 values (8mm/days or below) can be found. On the other hand, in the case of ERA5 an overall overestimation of Q95 is apparent, most of all in higher altitudes, although the most intense precipitation in the northeastern Carpathians are lower than in CARPATCLIM.

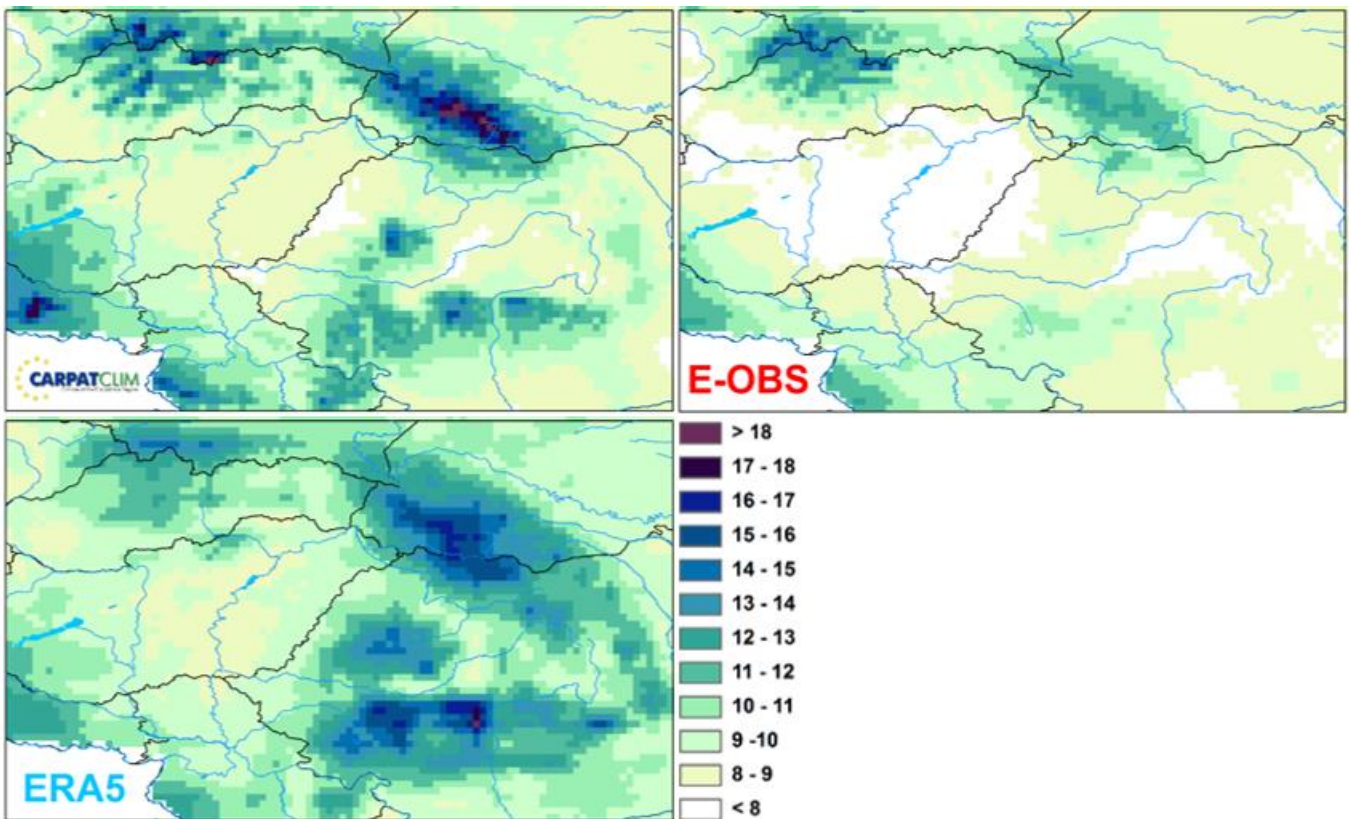


Figure 3.3.4.1 95% quantile of daily precipitation in [mm/d]. The plots show the analysis on 0.1° grid for CARPATCLIM, E-OBS and ERA5 in the period 1979-2010.

### 3.3.5 Example of an extreme event: daily precipitation on 15 and 16 May 2010

An extremely strong and long-lasting storm, caused by a Mediterranean cyclone, devastated the Carpathian Basin between 15 and 18 May 2010. The strongest wind gusts exceeded 120 km/h in many places, but there were measurement sites where wind gusts above 130 km/h were measured. In the central part of Transdanubia, especially in the Lake Balaton region, there were wind gusts above 80 km/h in every hour for 24 hours. The storm also caused a huge amount of precipitation, so in the Transdanubia the amount of precipitation in 72 hours exceeded 150 mm in more places, and in the Bakony Mountain above 250 mm was measured, but in the Bodrog and Hernd river basins (north eastern part of Hungary) the amount of precipitation exceeded even the 100 mm. The storm caused very significant material damage, partly due to wind-induced tree falls and building damages, and due to sudden floods. The Figure 3.3.5.1 show how the analyzed datasets could catch the precipitation fallen during this event.

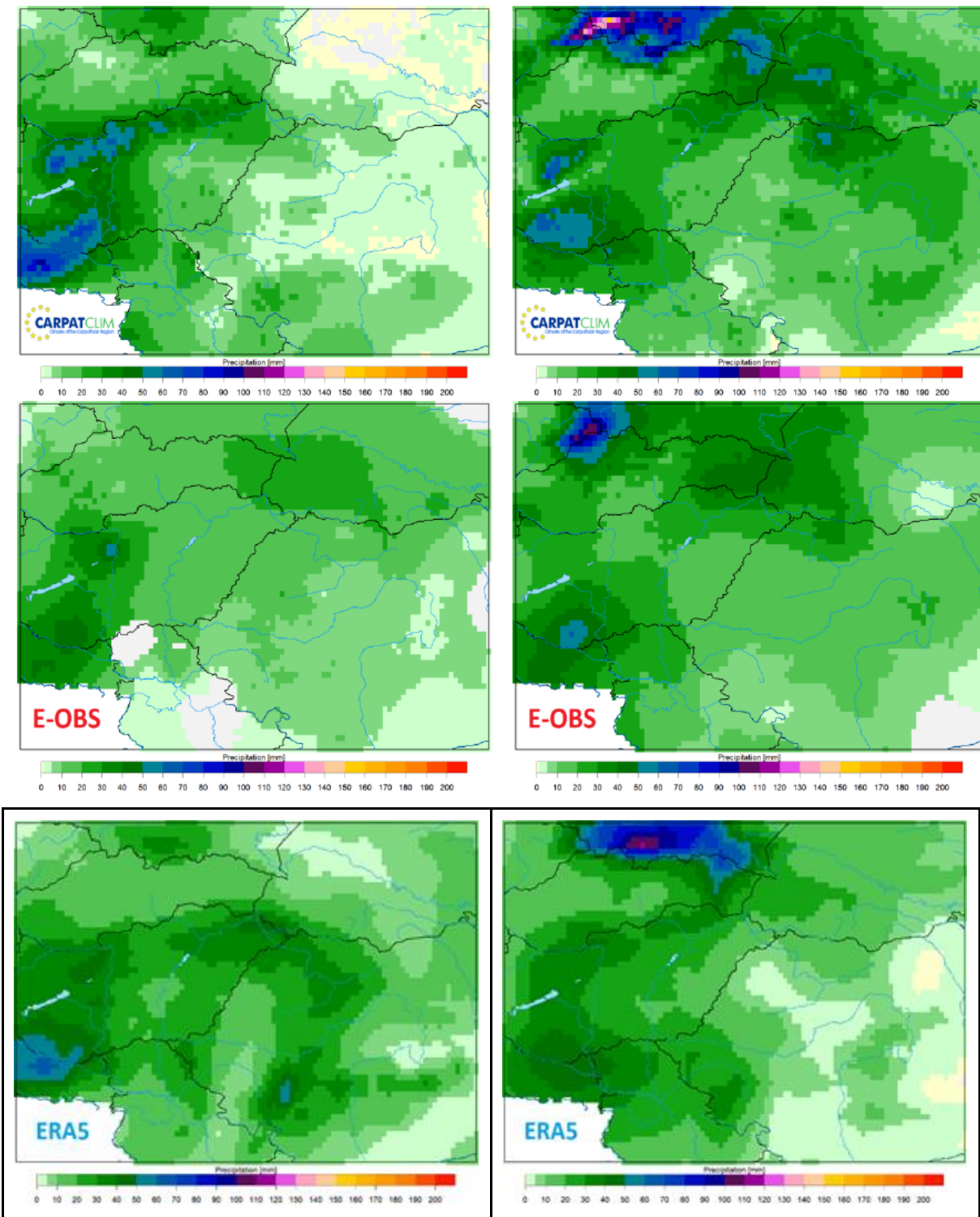


Figure 3.3.5.1 Daily precipitation sum (mm) on 15th (left) and 16th May (right) 2010 in the Carpathian region. The plots show the analysis on 0.1° grid for CARPATCLIM, E-OBS and ERA5 in the period 1979-2010.

### 3.3.6 RMSE

A frequently used measure of the differences of datasets is the Root Mean Square Error (RMSE). In our case E-OBS and ERA5 datasets were compared to CARPATCLIM as a reference dataset in the analysis. Besides, ERA5 was compared to E-OBS for the domain of CARPATCLIM. Thus, both observational datasets were compared to reanalysis data for CARPATCLIM domain. The monthly RMSE maps are also shown for seeing the spatial patterns of these statistics.

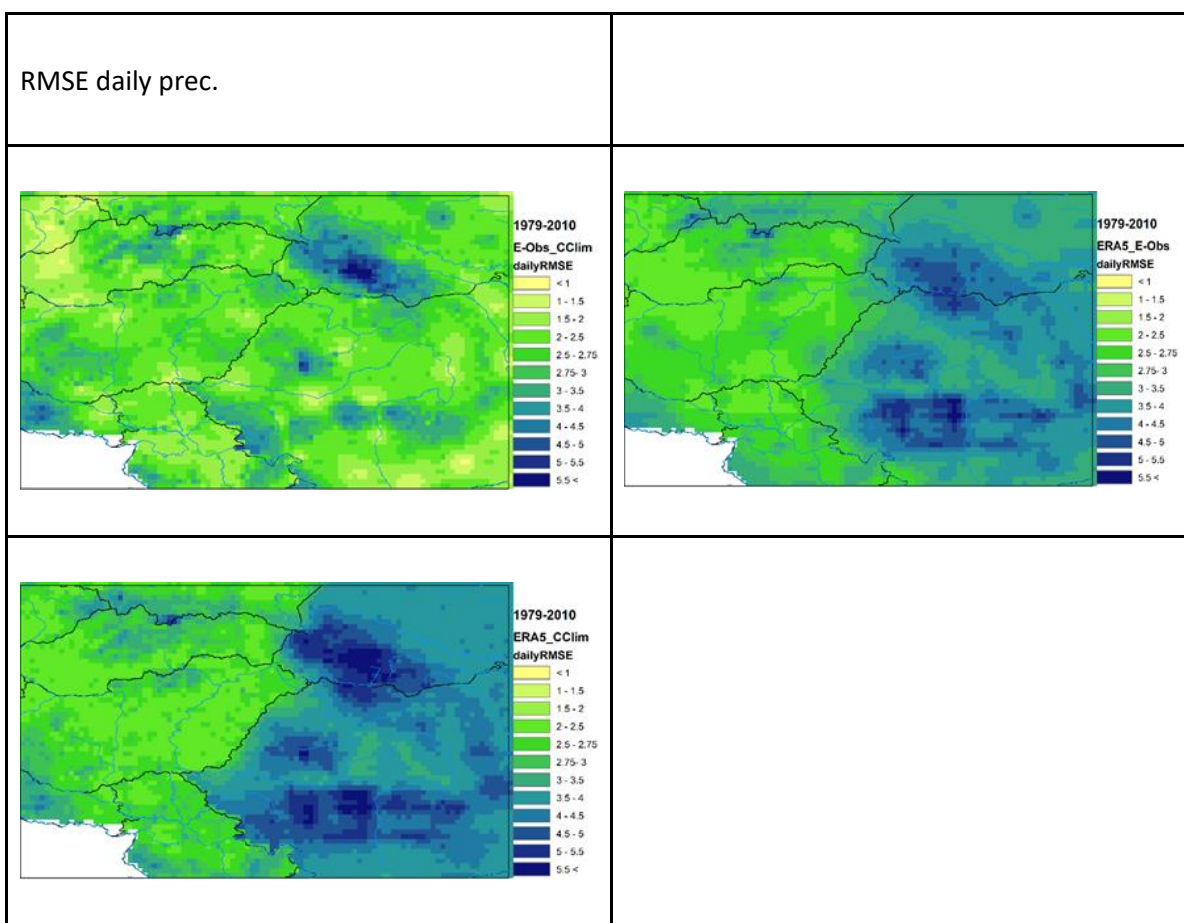


Figure 3.3.6.1 Daily root mean squared error (RMSE) in [mm] of E-OBS with the reference of CARPATCLIM (top left), of ERA5 with the reference of E-OBS (top right), of ERA5 with the reference of CARPATCLIM (bottom left). The statistical measure is computed on 0.1° grid over the time period 1979-2010.

E-OBS dataset can be characterized by 2 mm/day RMSE at least most of the region and 4.5 mm or above in wider area in the northeastern Carpathians in Ukraine and in smaller region in the southern Carpathians, Bihor Massif and Dinaric Alps (Figure 3.3.6.1, top left). Overall, ERA5 shows larger errors than E-OBS (Figure 3.3.6.1, bottom left). Large RMSE values turn up in the territory of Ukraine and Romania with around 4mm/day in the flat region and 5 mm/day or above at mountainous areas. The country borders become visible around Romania and between Ukraine-



Slovakia and Ukraine-Poland in the case of ERA5 analysis against both observational datasets ((Figure 3.3.6.1 top right (against E-OBS) and Figure 3.3.6.1 bottom left (against CARPATCLIM)). The reason possibly sum up from different factors, might be the performance of ERA5 over Romania and Ukraine influence that as well. The borders are not visible in the RMSE map depicting E-OBS compared to CARPATCLIM (Figure 3.3.6.1 top left), but turn up on map E-OBS to ERA5. We can state at least that the observational datasets are behaving similarly. ERA5 compared to E-OBS produces greater RMSE values over Romania and Ukraine, especially in the regions with higher elevations (Figure 3.3.6.1, top right). These findings confirm that the modelling of precipitation in the Carpathians and the Basin in between is challenging. Applying relatively fewer number of stations for gridding over Romania than in the other parts of CARPATCLIM could induce to make the borders visible as well, but not as the main factor. In addition, the borders cannot be explored on CARPATCLIM daily precipitation maps for a specific day, just on the many years daily RMSE maps.

We suggest analyzing additional statistics: the monthly RMSE, as the daily precipitation are correlated on the consecutive days, but the monthly totals can be counted as independent variables, thus the monthly RMSE can be considered as a relevant statistical measure rather than daily. The monthly RMSE values were derived for all the twelve months and then averaged (Figure 3.3.6.2). E-OBS can be described lower than 23 mm monthly RMSE sparsely. Note that the borders do not appear in the Figure 3.3.6.2, bottom left. Although greater values, above 35 mm can be explored in the territory of Romania and along the Carpathians in Ukraine in extended regions in both maps illustrates ERA5 compared to the observational datasets.

The Figure 3.3.6.3 describes the differences in the performance of various reanalysis datasets. The spatial distribution of the daily RMSE of ERA5Land (00-24 precipitation totals) against CARPATCLIM (Figure 3.3.6.3, left) is similar to ERA5 against CARPATCLIM (Figure 3.3.6.3, bottom left), also the magnitudes are in good agreement but noticeable that the borders cannot be traced on that. The daily RMSE of ERA5Land comparing to ERA5 is demonstrated in the right panel of the Figure 3.3.6.3 which depicts the differences of the reanalysis data for the Carpathian region. The mountainous area, particularly Dinaric Alps, the northeastern and southern Carpathians are diversely presented in ERA5Land and ERA5. 2mm or higher RMSE values appear about in the half of the domain compared ERA5Land to ERA5, with the greatest values in the high mountains.

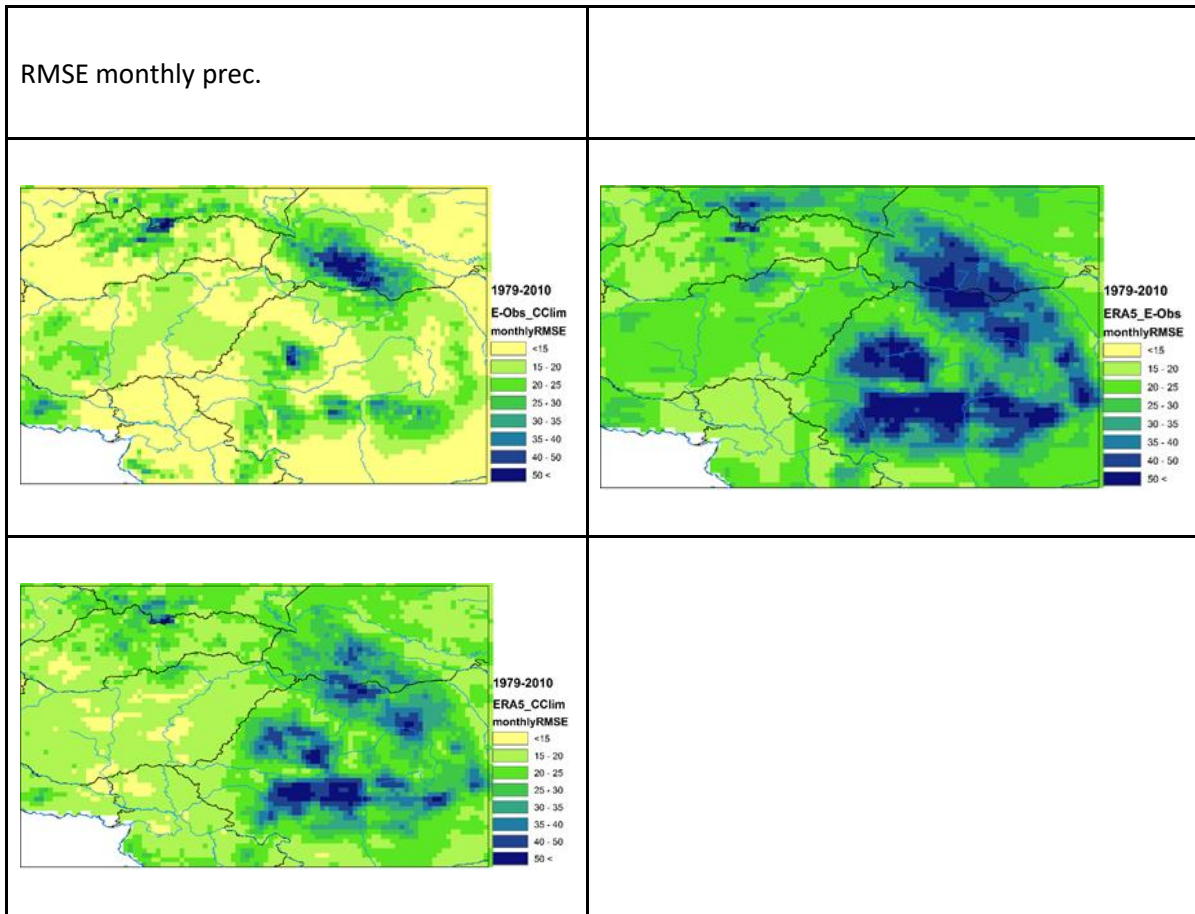


Figure 3.3.6.2 Yearly averaged monthly root mean squared error (RMSE) in [mm] based on monthly sum of E-OBS with the reference of CARPATCLIM (top left), of ERA5 with the reference of E-OBS (top right), of ERA5 with the reference of CARPATCLIM (bottom left). The statistical measure is computed on a 0.1° grid over the time period 1979-2010.

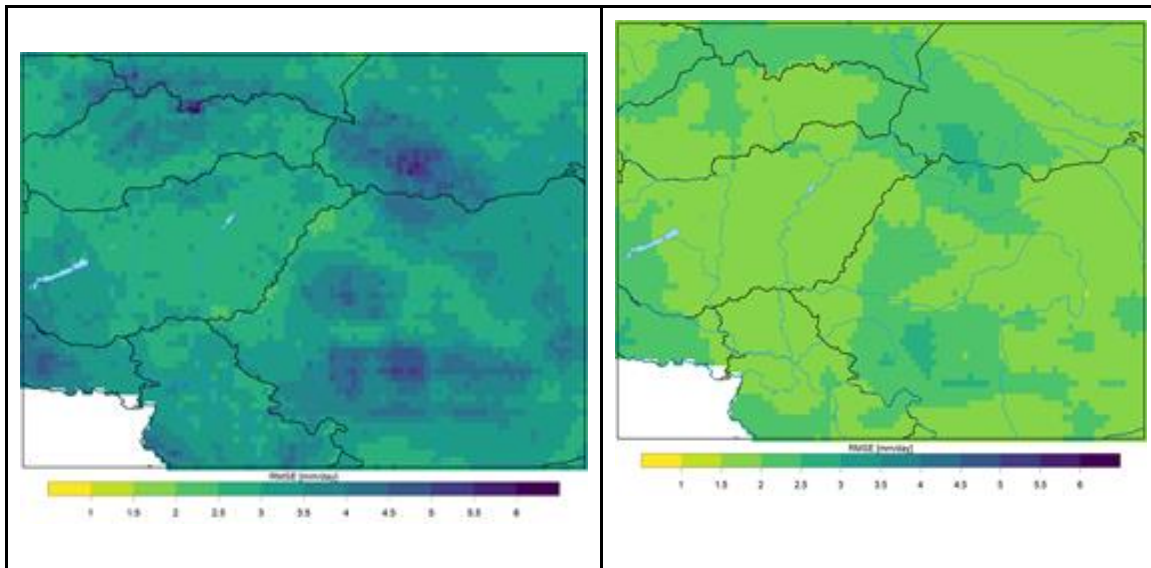
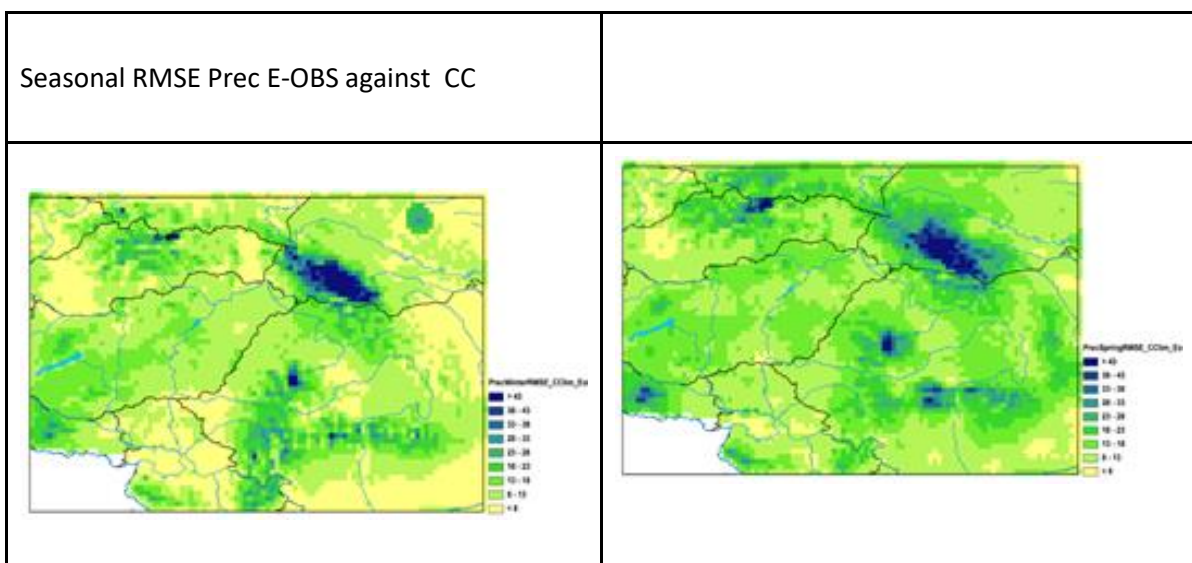


Figure 3.3.6.3 Daily root mean squared error (RMSE) in [mm] of ERA5Land with the reference of CARPATCLIM (left) and ERA5Land reference of ERA5 (right). The statistical measure is computed on a  $0.1^\circ$  grid over the time period 1981-2010.

#### RMSE seasonal

The Figure 3.3.6.4 and 3.3.6.5 illustrates the seasonal RMSE values for E-OBS against CARPATCLIM and for ERA5 against CARPATCLIM for the CDS users who are interested in applications requiring seasonal precipitation sums.



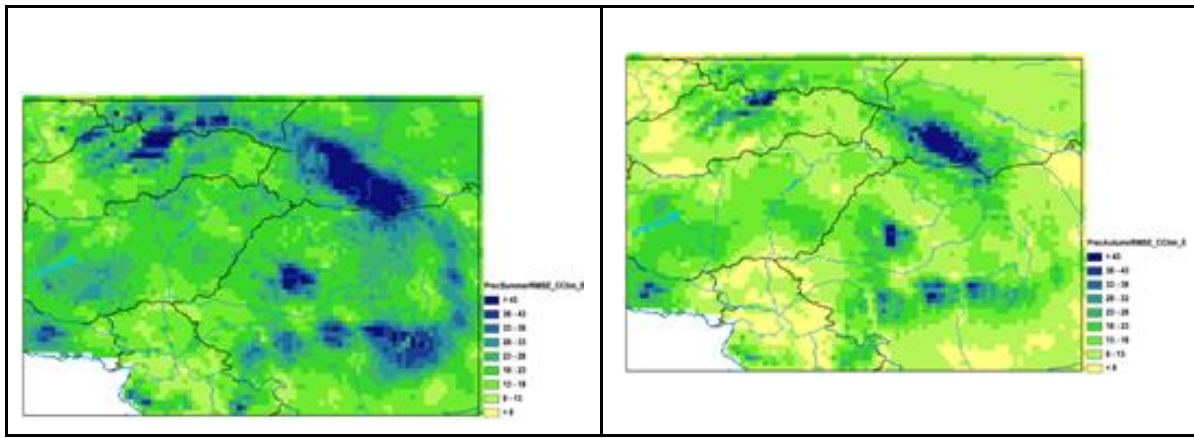


Figure 3.3.6.4 Seasonal root mean squared error (RMSE) in [mm] based on E-OBS with the reference of CARPATCLIM (MAM top left, JJA top right, SON bottom left, winter bottom right) The statistical measure is computed on 0.1° grid over the time period 1979-2010.

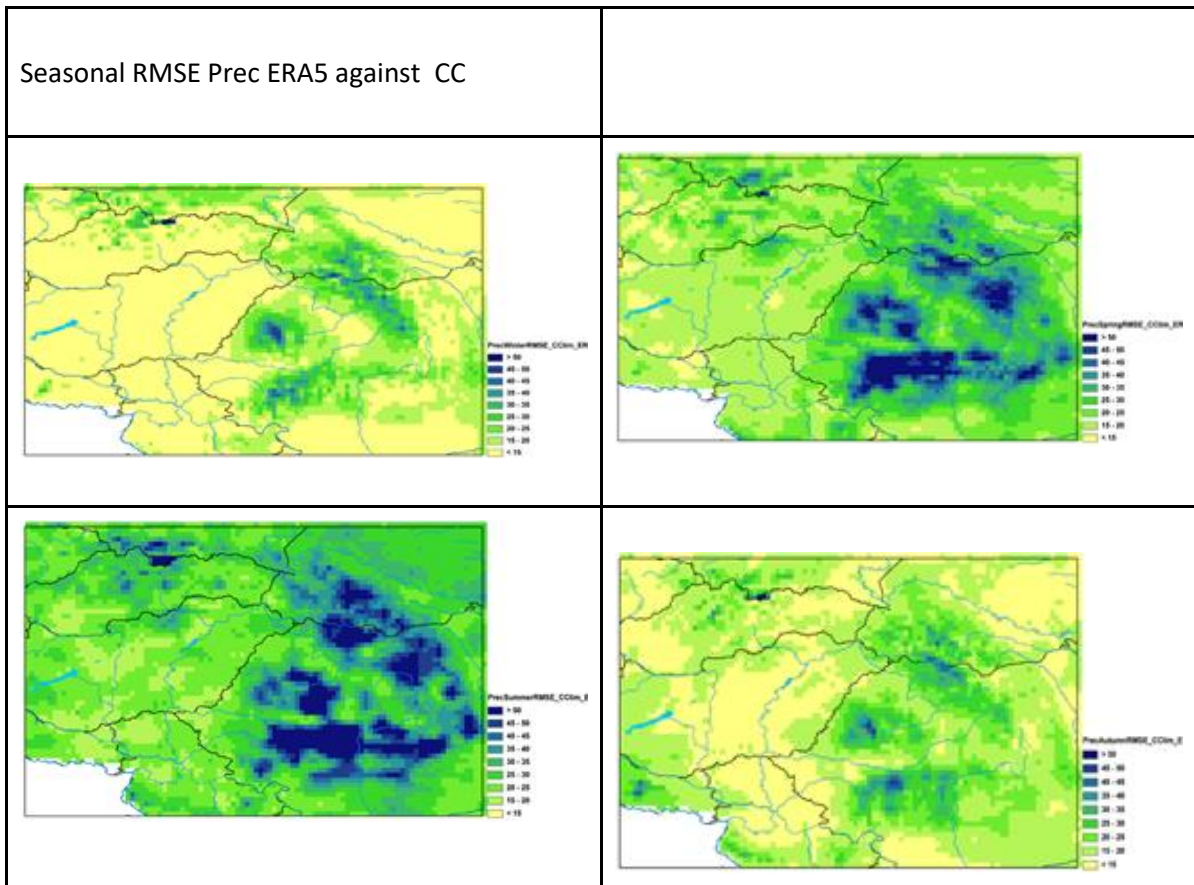
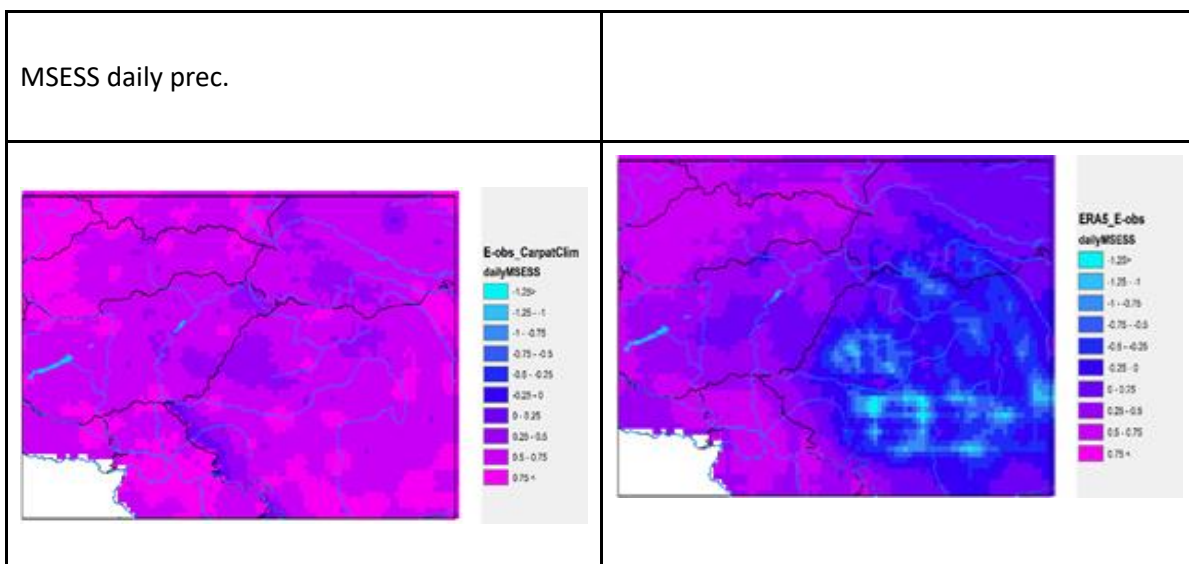


Figure 3.3.6.5 Seasonal root mean squared error (RMSE) in [mm] based on ERA5 with the reference of CARPATCLIM (MAM top left, JJA top right, SON bottom left, winter bottom right) The statistical measure is computed on 0.1° grid over the time period 1979-2010.

### 3.3.7 MSESS

MSESS of ERA5 against E-OBS is presented here as well for CARPATCLIM region. Negative MSESS values represent the grid points where the mean squared error exceeds the variance of the reference dataset. Comparing E-OBS to CARPATCLIM, the MSESS values are the highest in small patches, close to the station locations that were used in the gridding process (Figure 3.3.7.1, top left), otherwise the daily MSESS values vary around 0.5 or above in the majority of the region. The smallest values arise in the territory of Ukraine and Romania on the map, which shows the MSESS for ERA5 evaluated against CARPATCLIM (Figure 3.3.7.1, bottom left). The grid points located in Romania and in Ukraine are depicted with low values on the map, which illustrates the daily MSESS values for ERA5 against E-OBS (Figure 3.3.7.1, top right), similarly with the map which illustrates the evaluation of ERA5 against CARPATCLIM.

The monthly MSESS is a more relevant statistical measure than daily, as it was underlined in the analysis of the RMSE in the previous Section. Therefore, the MSESS computed from monthly precipitation is shown here (Figure 3.3.7.2) too. The greatest values can be explored when we compare the two observational datasets (Figure 3.3.7.2, top, left), typically in the flat regions out of Carpathians and in Serbia and at the north-west part of the domain. The yearly cycle of several score skills can be seen in Figure 3.3.7.3 and Figure 3.3.7.4.



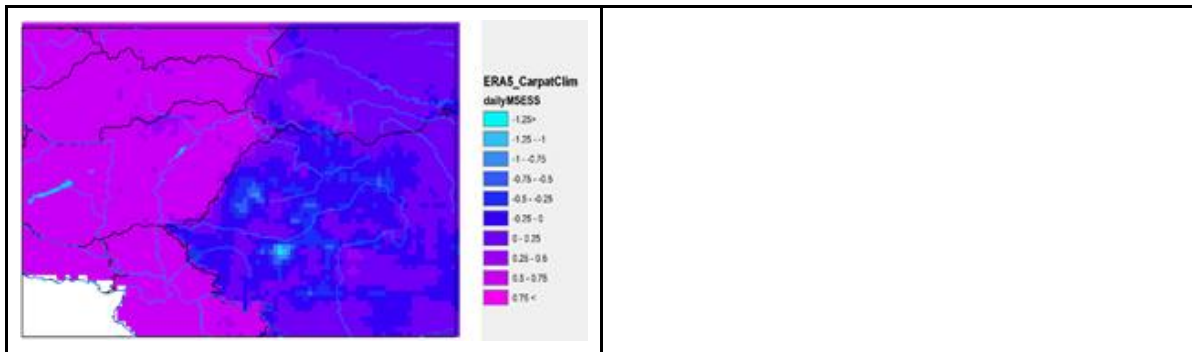
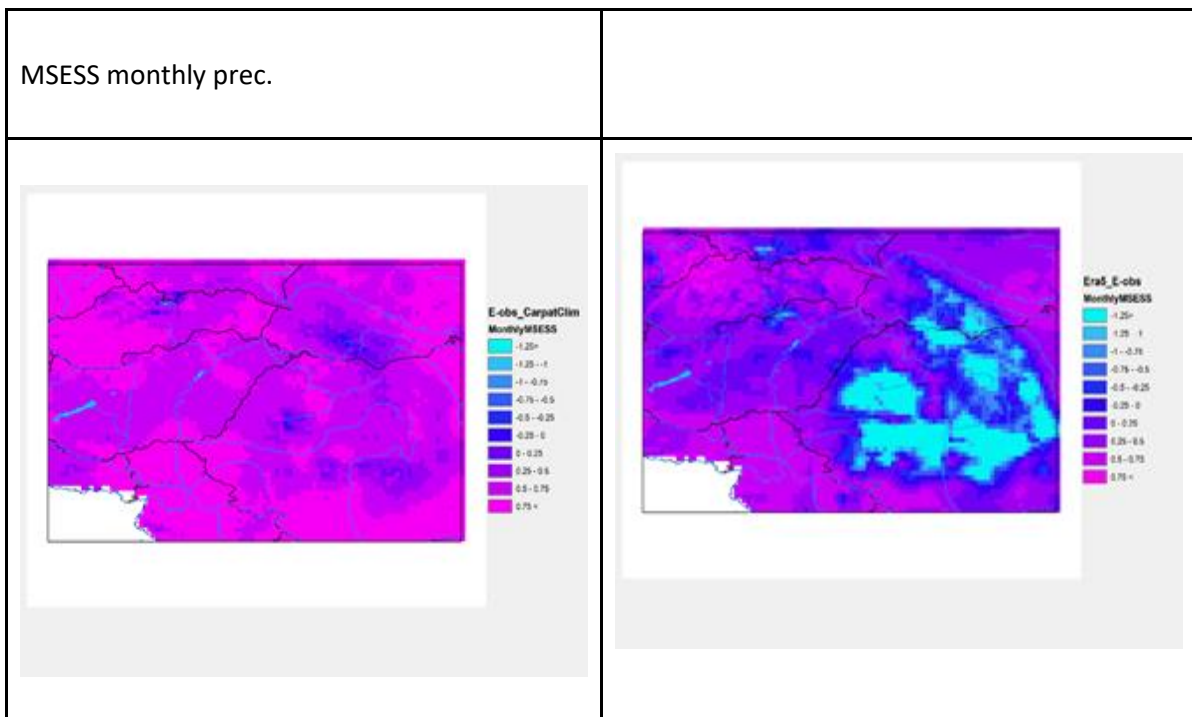


Figure 3.3.7.1 Daily Mean Square Error Skill Score (MSESS) based on daily precipitation of E-OBS with the reference of CARPATCLIM (top left), of ERA5 with the reference of E-OBS (top right), of ERA5 with the reference of CARPATCLIM (bottom left). The statistical measure is computed on a  $0.1^\circ$  grid over the time period 1979-2010.



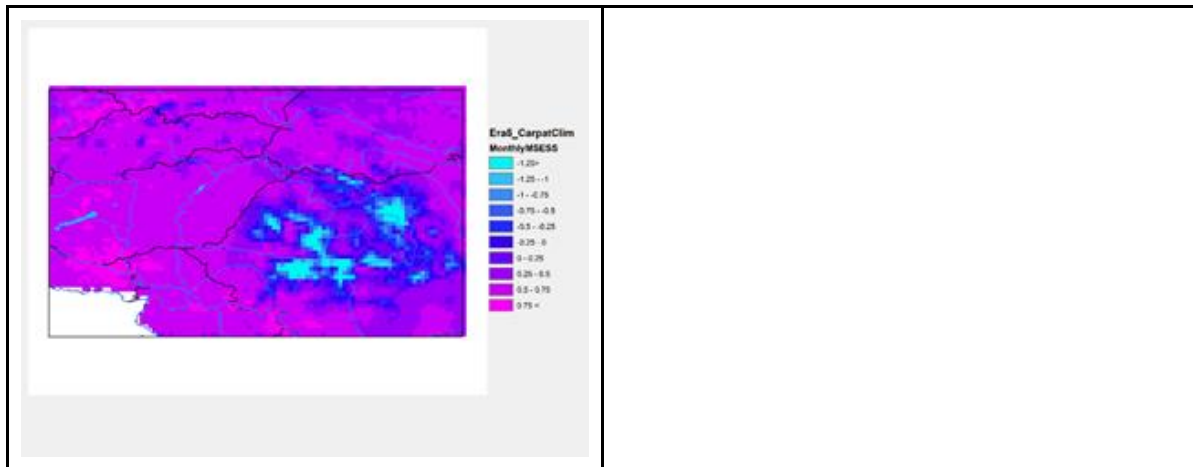
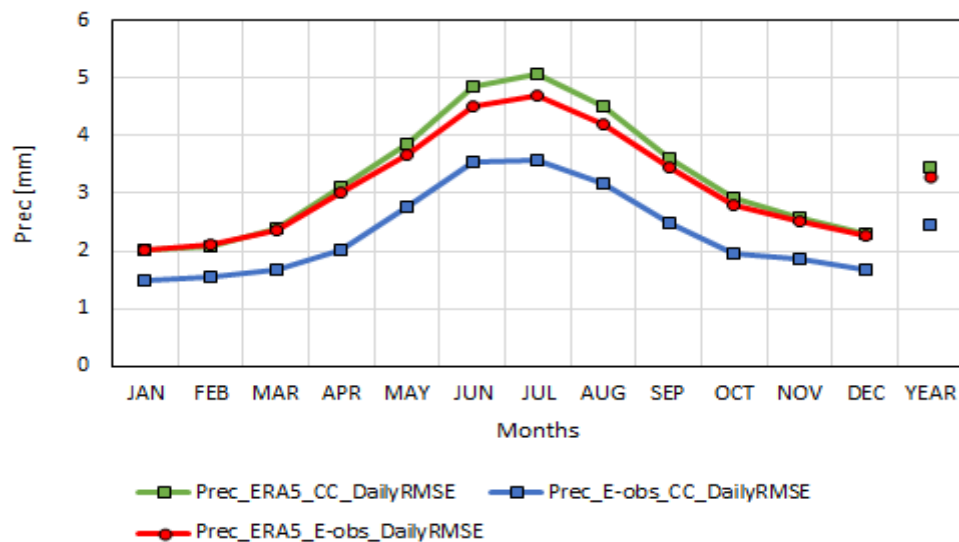


Figure 3.3.7.2 Yearly averaged monthly Mean Square Error Skill Score (MSESS) based on monthly precipitation of E-OBS with the reference of CARPATCLIM (top left), of ERA5 with the reference of E-OBS (top right), of ERA5 with the reference of CARPATCLIM (bottom left). The statistical measure is computed on a  $0.1^\circ$  grid over the time period 1979–2010.

### Scores on graphs



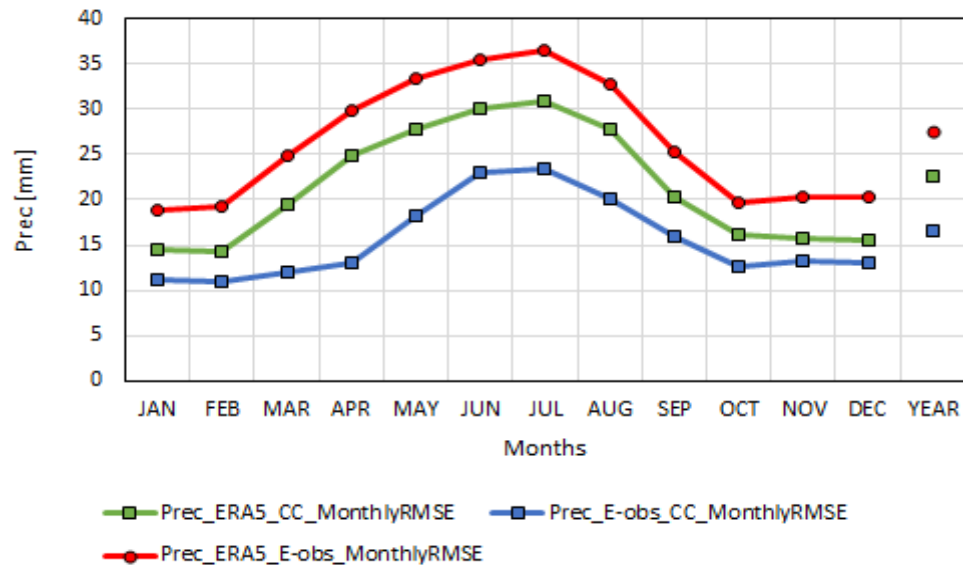
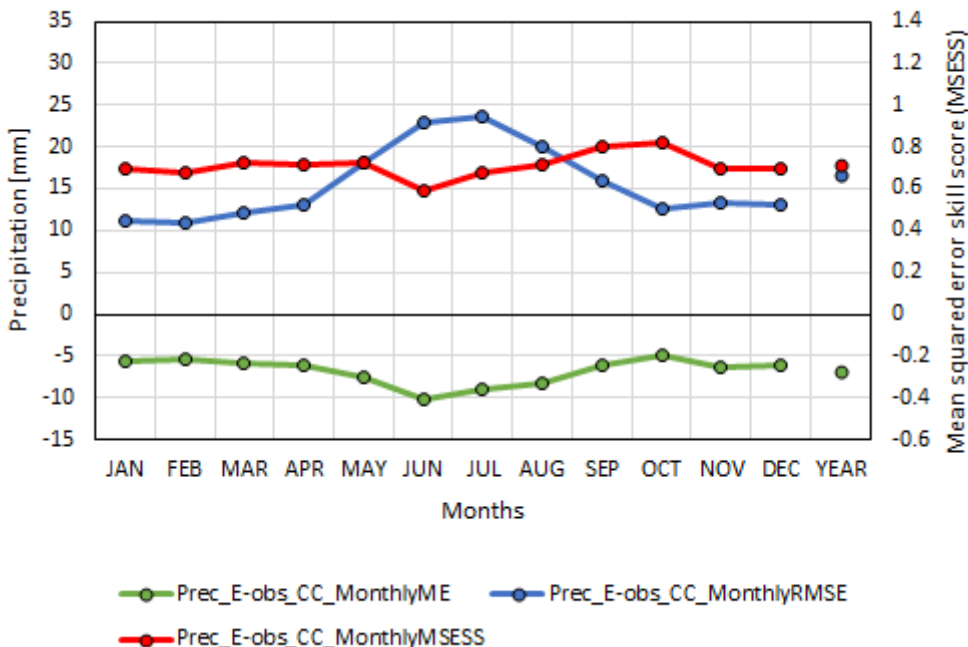


Figure 3.3.7.3 Daily (up) and monthly (bottom) RMSE of precipitation of E-OBS with the reference of CARPATCLIM and reference of ERA5, and ERA5 with the reference of CARPATCLIM. The statistical measure is computed on a 0.1° grid over the time period 1979-2010.



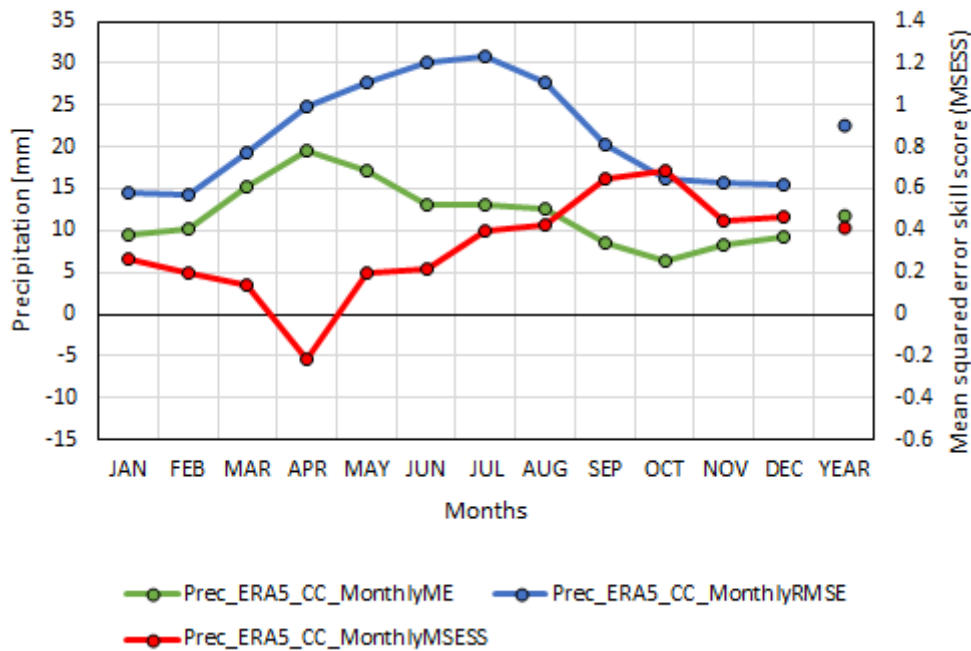


Figure 3.3.7.4 ME and MESS scores of monthly precipitation E-OBS with the reference of CARPATCLIM (top) and ERA5 with the reference of CARPATCLIM (bottom). The statistical measure is computed on a  $0.1^{\circ}$  grid over the time period 1979-2010.

### 3.3.8 Analysis of Variance (ANOVA)

The ANOVA method can be used effectively for the characterization of the spatio-temporal properties of CARPATCLIM, E-OBS and ERA5 datasets. The output statistics of the ANOVA procedure (see the Appendix for the methodology) complements well the evaluations. The main principle of the ANOVA method is that the total variance can be partitioning as the sum of the spatial variance of the temporal means and the spatial mean of the temporal variances on one hand; and the sum of the temporal variance of the spatial means and the temporal mean of the spatial variances on the other hand. The magnitude and spatial distribution of the specific components of the total variance can be analyzed for different time periods, years and seasons for instance. When a dataset can capture the spatio-temporal variability of a given climate parameter well, that can be settled as a dataset with better quality in general. This methodology is built into the modelling part of method MISH (the MISH interpolation method was applied for producing CARPATCLIM grids) in order to evaluate the modelling results automatically (Szentimrey 2016).

Aside from the yearly characteristics, the summer means and variances were analyzed in the case of precipitation. The summer was chosen, as the summer months are the wettest in the Carpathian region. The Table 3.3.8.1 contains the total means and total variances and their partitions for all three analyzed dataset. These statistical measures are applicable for pointing out the differences in the statistical structure of the datasets. The total means and total variances and theirs partitions for



precipitation can be compared and analyzed. The total variance is 40740.9 for CARPATCLIM (CCM), what is the sum of the “Spatial variance of temporal mean”: 23737.06 and “Spatial mean of temporal variances”: 17003.84 on the one hand, and the sum of „Temporal variance of spatial means”: 9637.43 and „Temporal mean of spatial variances”: 31102.78 on the other hand, as an example. The rest of the six measures in Table 3.3.8.1. are illustrated on graphs for yearly and for summer precipitation sums in Figure 3.3.8.1. and 3.3.8.2.

Some of the yearly measures are similar for all three dataset (Figure 3.3.8.1), such as the square “Root of spatial mean of temporal variances”, the „Spatial mean of temporal st. Deviations” and the „Temporal st. deviation of spatial means”. Larger differences turn up in the case of “Spatial st. deviation of temporal mean” and in the “Root temporal mean of spatial variances” and also in the „Temporal mean of spatial st. Deviation” between datasets, with the largest values in ERA5, CARPATCLIM and E-OBS respectively. The relationship of these statistics for the summer and for the year is the same:the largest values came up from ERA5 followed by CARPATCLIM and E-OBS in the end Figure 3.3.8.2.

Notations (see the Appendix for more details):

- $E_t(s)$  - temporal mean at location s
- $E_s(t)$  - spatial mean at time t
- $D_t(s)$  - temporal st. deviation at location s
- $D_s(t)$  - spatial st. deviation at time t

The  $E_t(s)$ ,  $D_t(s)$  are illustrated on maps, and  $E_s(t)$ ,  $D_s(t)$  are shown on graphs.

The derived statistics are as follows:

- $E$  - total mean
- $D_t$  - spatial mean of temporal st. deviations
- $D_s$  - temporal mean of spatial st. deviations
- $DE_t$  - spatial st. deviation of temporal means
- $DE_s$  - temporal st. deviation of spatial means

To make these measures more expressive the spatial means and spatial variances at the moment t are illustrated on graphs and temporal means and temporal variances at a specific location s are illustrated on maps. The Figure 3.3.8.3 shows the time series of the “ $E_s(t)$ -spatial mean” and “ $D_s(t)$ - spatial st. deviation” from 1979 to 2010. CARPATCLIM and E-OBS yearly and also summer spatial means are running parallel, with larger amounts representing CARPATCLIM than E-OBS during the whole analyzed period. The curves representing ERA5 spatial means are going bottommost far above CARPATCLIM. Larger overestimation (165 mm or higher) can be found in ERA5 yearly spatial means, mainly in the beginning of the period in 1988, 1985, 1987, 1981, 1989, 1996, 1980 and 1981. The spatial standard deviation of E-OBS and ERA5 running together until 1991, thereafter E-OBS curve is breaking down on the yearly graph. There is an increase in CARPATCLIM and a decrease in E-OBS between 1979 and 2010. The curves representing the observational datasets’ spatial standard deviations running together in summer, while the reanalysis data show higher values until



the turn of the millennium, then the differences are smaller between ERA5 and the observational datasets.

The maps of the temporal means (yearly) (Figure 3.3.8.4.) have been already presented in chapter 3.3.3. To conclude here as well: E-OBS is drier and ERA5 is wetter than CARPATCLIM at each elevation. E-OBS underestimates the yearly sum with 81.4 mm for the entire region, particularly at higher elevation above 1500 m, where the underestimation is 215.4mm in average. Similarly, even higher overestimation can be found in ERA5 at the highest mountainous areas (249.1 mm). The overall overestimation is 143.1 mm for the entire region, which is more than half as much compared to the underestimated precipitation in E-OBS.

On the map showing the temporal standard deviation (Figure 3.3.8.5), the E-OBS approximates the northern and eastern Carpathians well, while ERA5 produces similar values to CARPATCLIM in the southern Carpathians, complementing each other.

Substantial overestimation in ERA5 at higher altitudes and underestimation in E-OBS at flat regions becomes visible on the map illustrating the summer mean Figure 3.3.8.6. In the Figure 3.3.8.7, smaller standard deviations appear in the region of the southern Carpathians in E-OBS than in CARPATCLIM, contrary, the rest of the Carpathians are represented with smaller standard deviations in the reanalysis data.

The maps and graphs here help us to discover the differences, although the investigation of the reasons have to go more deeply into the derivation methods of the different datasets. These characteristics are depending on many factors, the station density, the quality of the data, the assimilation method in the case of reanalysis and also on the interpolation method, moreover some of these factors are changing in time.

	ANOVA Prec Year			ANOVA Prec Summer		
	CCM	E-OBS	ERA5	CarpatClim	E-OBS	ERA5
Total mean	699.36	617.98	842.46	247.06	219.66	285.79
Total variance	40740.9	31709.97	50803.8	9193.13	7773.55	12356.89
Spatial variance of temporal mean	23737.06	17425.21	34697.77	3676.25	3000.26	6893.81
Spatial mean of temporal	17003.84	14284.76	16106.02	5516.88	4773.29	5463.08



variances						
Temporal variance of spatial means	9637.43	7085.61	9207.61	2655.89	2137.81	2737.75
Temporal mean of spatial variances	31102.78	24624.45	41591.55	6537.47	5635.85	9619.2
Spatial st. deviation of temporal mean	154.07	132.00	186.27	60.63	54.77	83.03
Root spatial mean of temporal variances	130.40	119.52	126.91	74.28	69.09	73.91
Spatial mean of temporal st. Deviations	128.32	117.60	125.74	72.72	67.68	72.99
Temporal st. deviation of spatial means	98.17	84.18	95.96	51.54	46.24	52.32
Root temporal mean of spatial variances	176.36	156.92	203.94	80.85	75.07	98.08
Temporal mean of spatial st. Deviation	174.60	154.39	202.58	79.15	72.96	96.83

Table 3.3.8.1 Output of the ANOVA analysis for CARPATCLIM, E-OBS and ERA5 for yearly and summer precipitation.

### ANOVA\_PREC\_YEAR

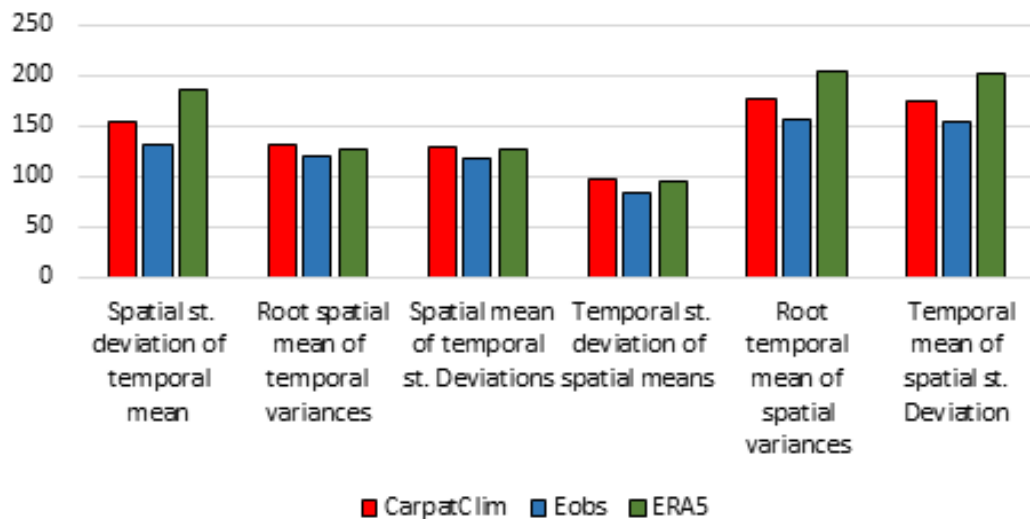


Figure 3.3.8.1 Some of the main statistics listed in Table 3.1.2. for yearly precipitation

### ANOVA\_PREC\_SUMMER

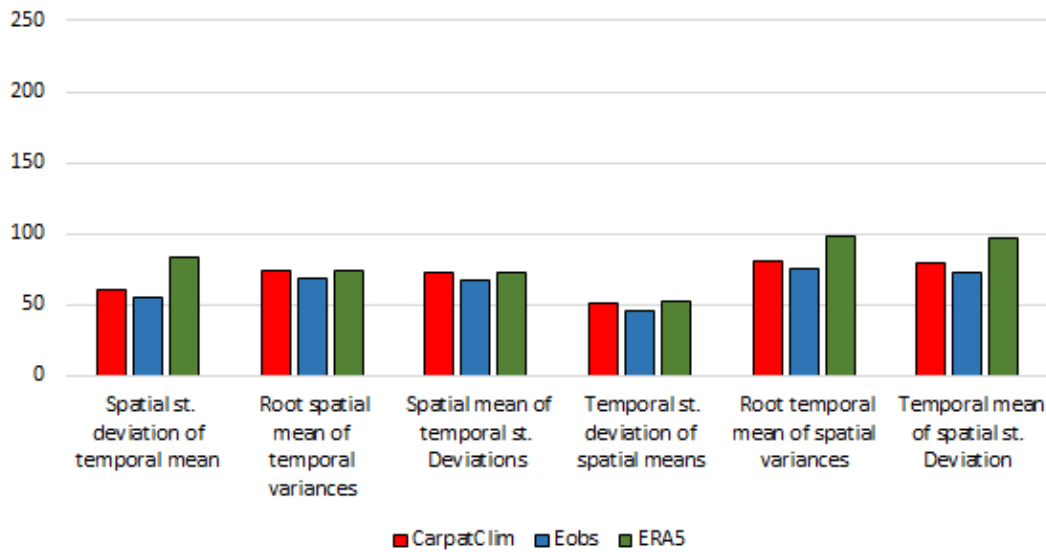
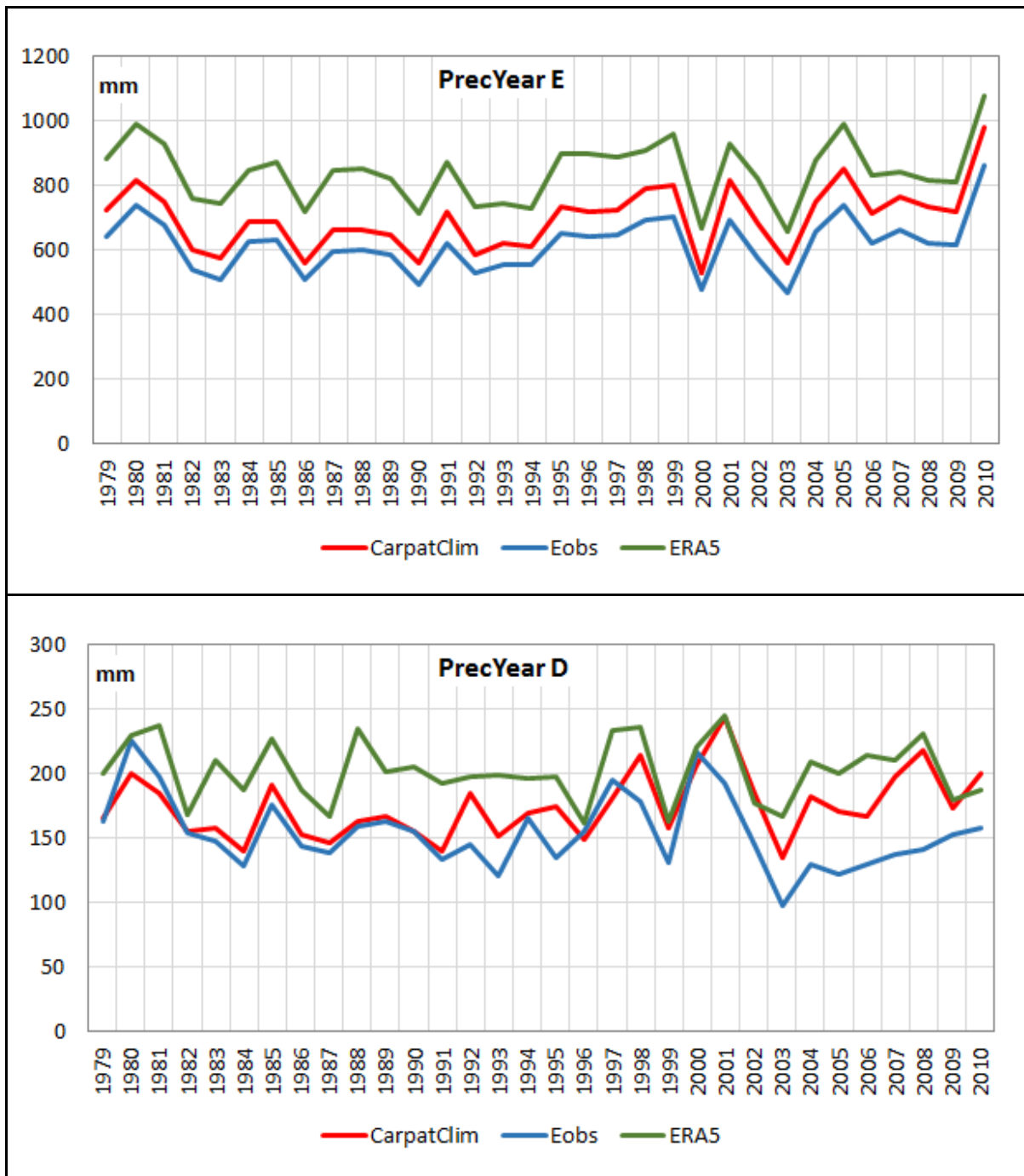


Figure 3.3.8.2 Some of the main statistics listed in Table 3.3.2. for summer precipitation.



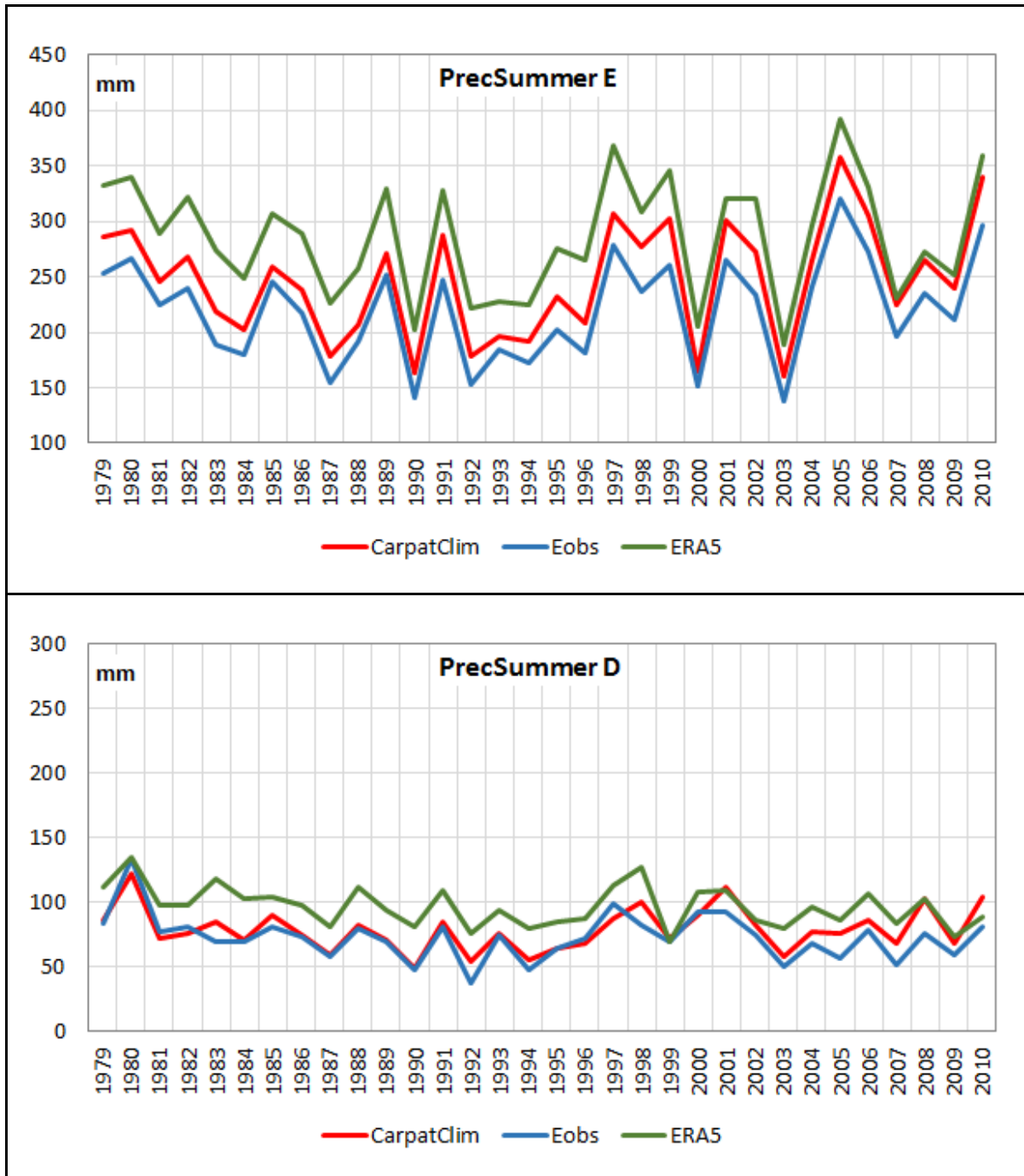


Figure 3.3.8.3. Yearly and summer Es (t)-spatial mean and Ds (t)- spatial st. deviation from 1979-2010 for CARPATCLIM, E-OBS and ERA5.

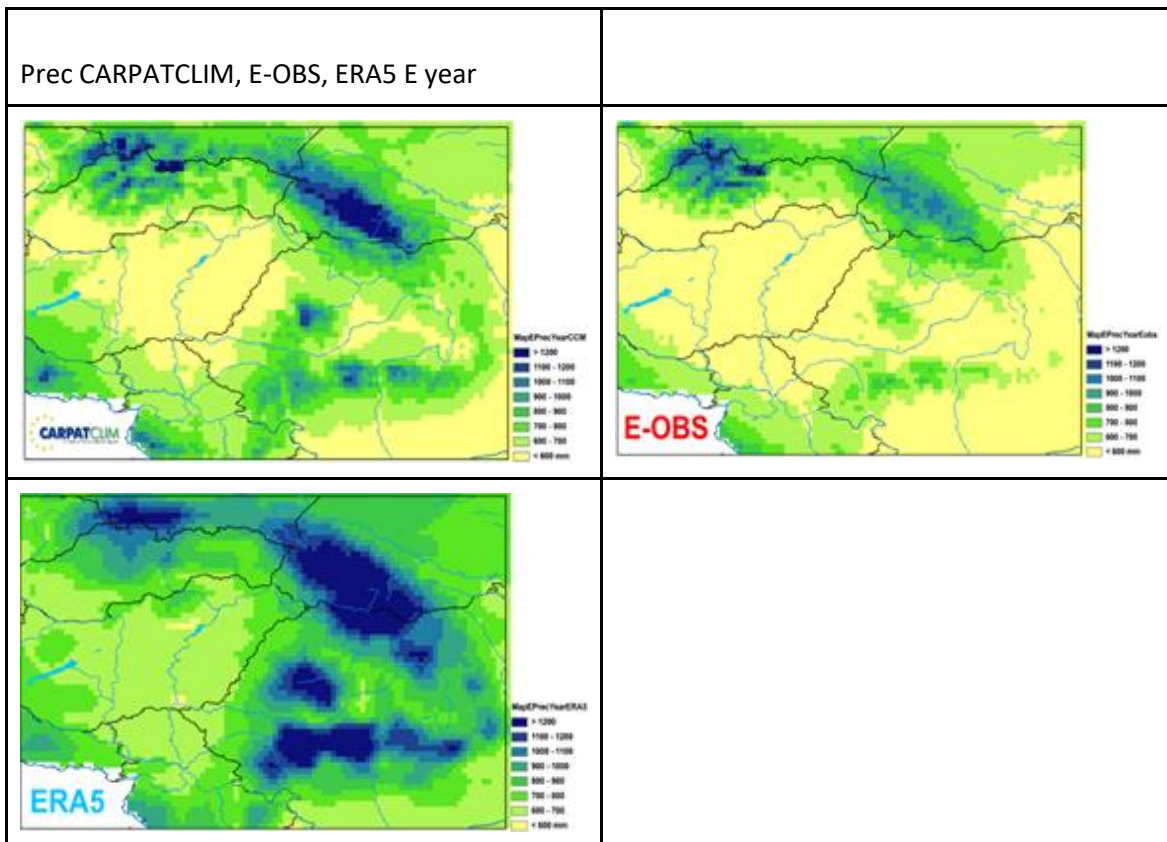
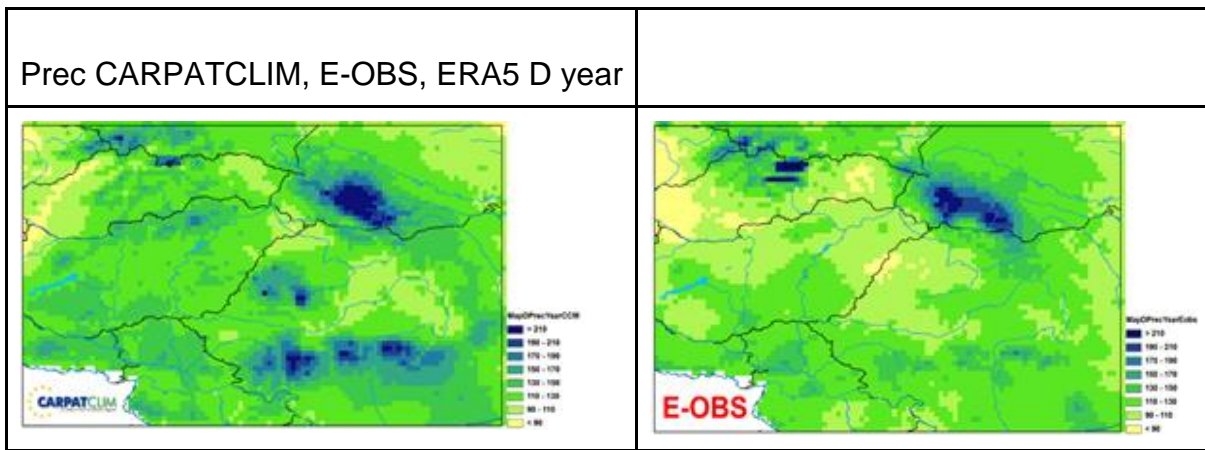


Figure 3.3.8.4 Et (s)-temporal mean of the yearly precipitation for CARPATCLIM, E-OBS and ERA5 for the period 1979-2010.



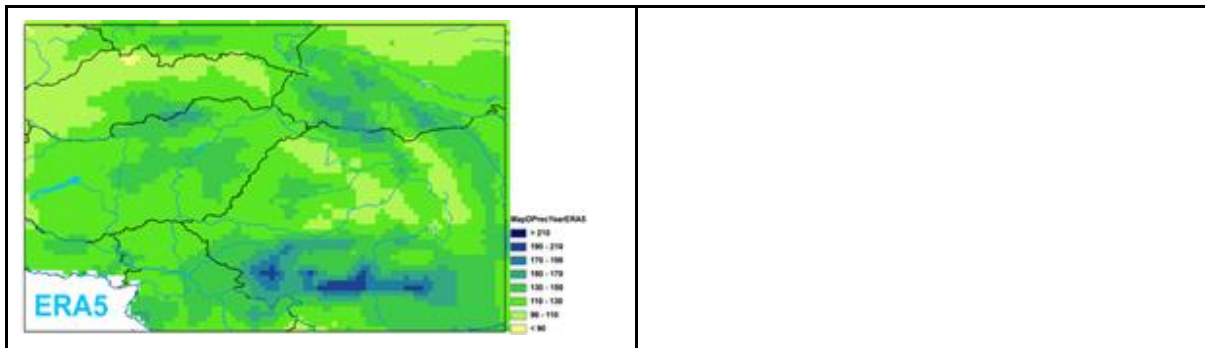


Figure 3.3.8.5 Dt (s)-temporal st. deviation of the yearly precipitation for CARPATCLIM, E-OBS and ERA5 for the period 1979-2010.

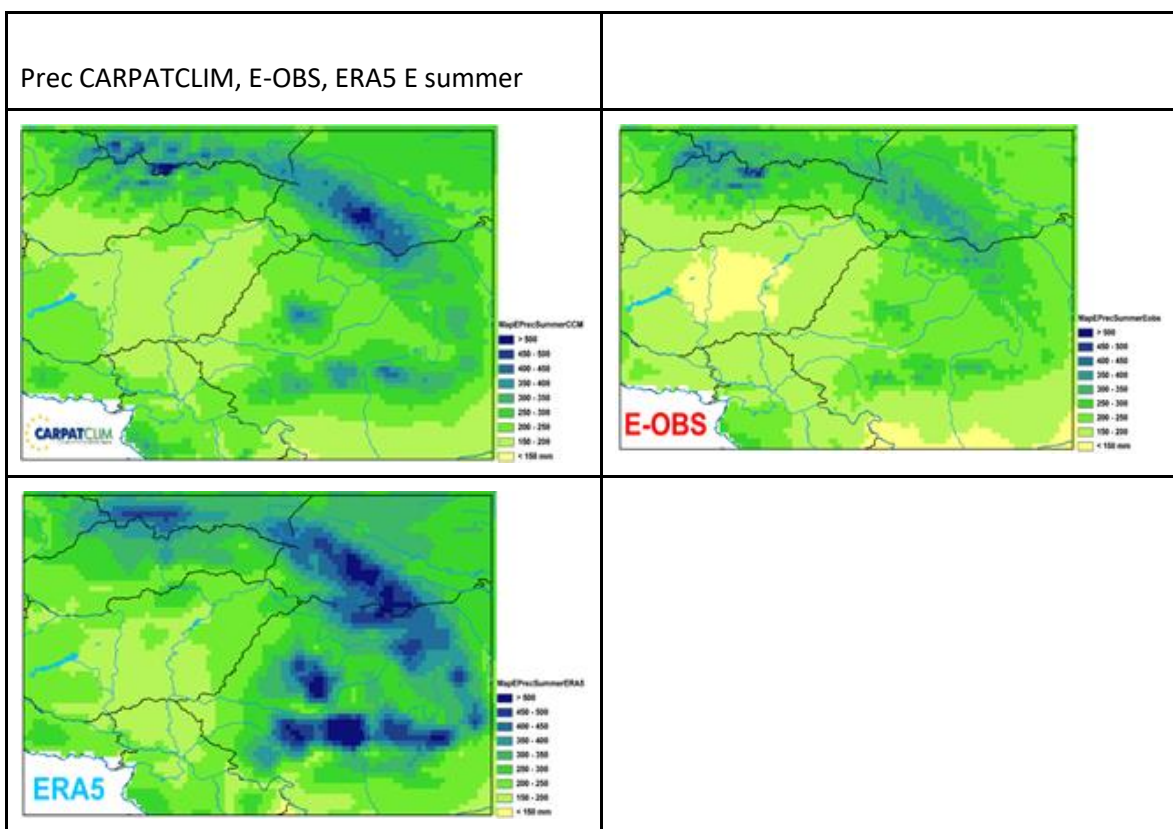


Figure 3.3.8.6 Et (s)-temporal mean of the summer (JJA) precipitation for CARPATCLIM, E-OBS and ERA5 for the period 1979-2010.

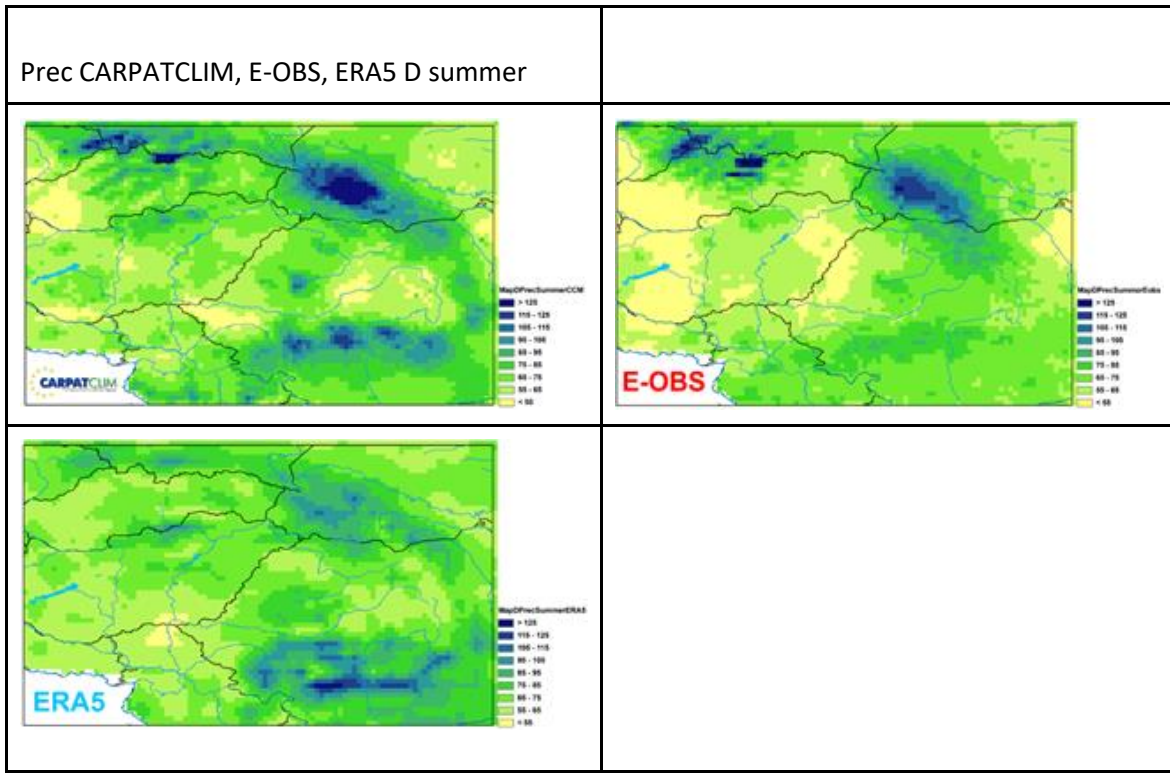


Figure 3.3.8.7 Dt (s)-temporal st. deviation of the summer (JJA) precipitation for CARPATCLIM, E-OBS and ERA5 for the period 1979-2010.

### 3.3.9 Maxima of daily precipitation

The Figure 3.3.9.1 allows us the comparison of the largest daily amount of precipitation existing in the different datasets. The maps showing the extractions highlight the differences. The appearance of the conspicuous value in Ukraine on the map, which illustrates E-OBS, is definitely the consequence of applying different QC and homogenization procedures as it seems to be erroneous data. E-OBS is more patchy and can be characterized with overall lower values than CARPATCLIM. In contrast to that, ERA5 produces higher daily extremes than CARPATCLIM, particularly in Romania and in the eastern part of the great Hungarian Plain. The regional average of the daily extremes by months can be seen in the Figure 3.3.9.2 Interesting to see that CARPATCLIM and ERA5 are very close. Consequently ERA5 performance is surprisingly good in this measure in regional average.

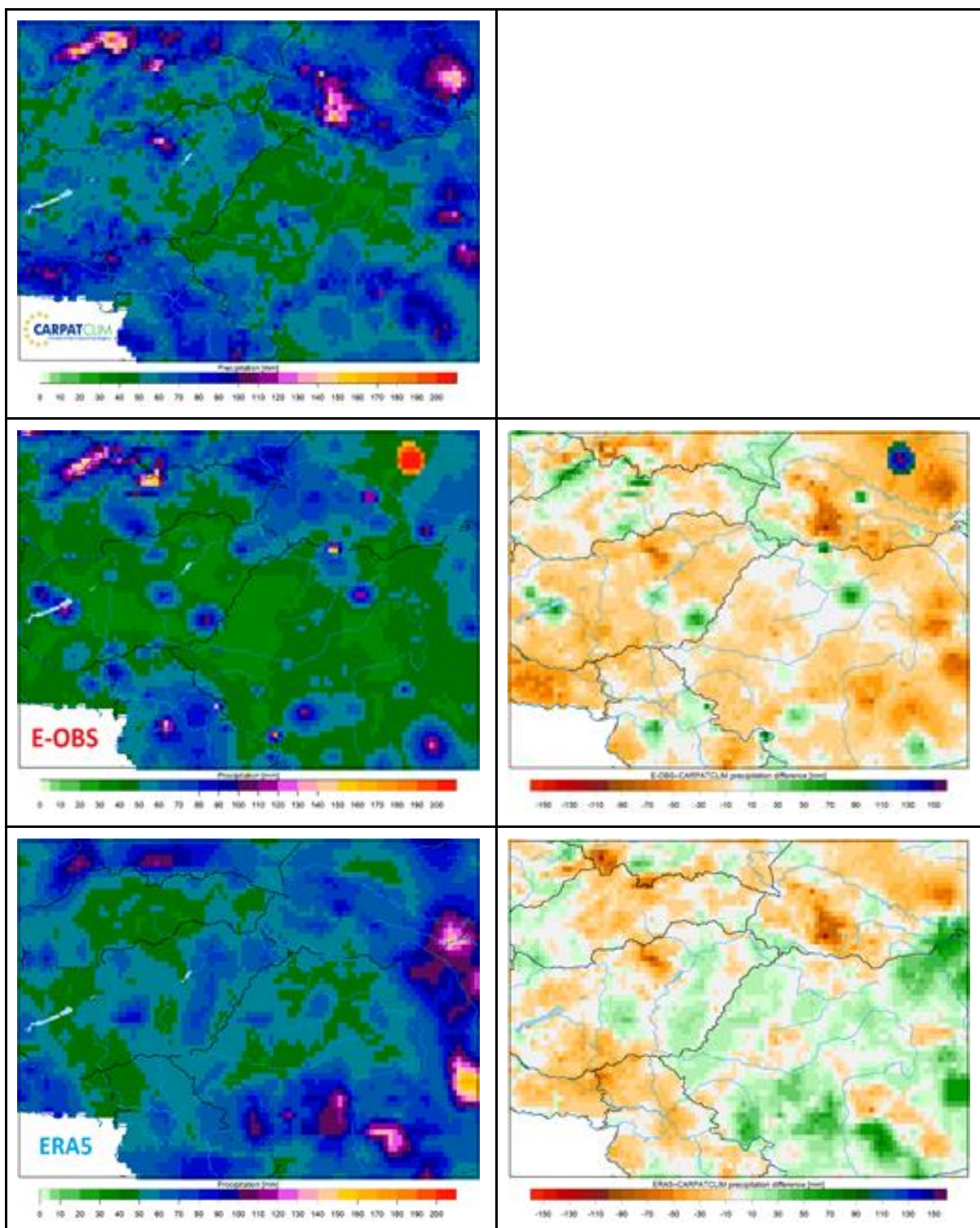


Figure 3.3.9.1 Largest daily precipitation sum during the period 1979-2010 for the analyzed datasets (left column) and the differences (right column) are as follows: E-OBS-CARPATCLIM and ERA5-CARPATCLIM.

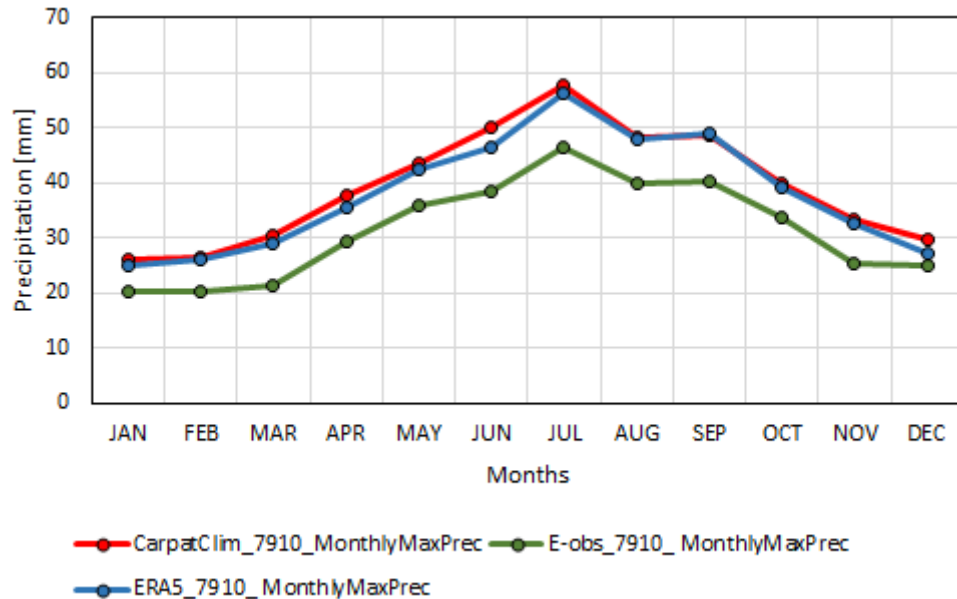
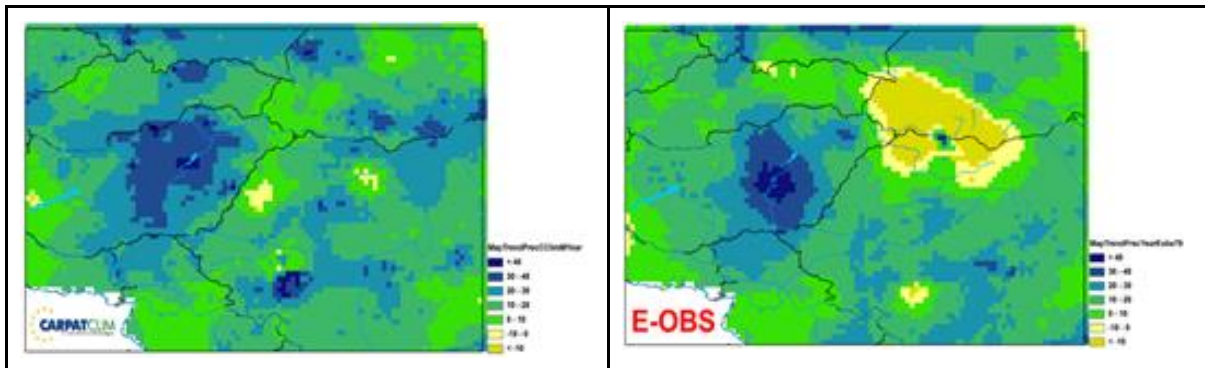


Figure 3.3.9.2 The regional average of the daily maximum precipitation for different datasets by month for CARPATCLIM domain for the period 1979-2010.

### 3.3.10 Trends

An exponential trend model was fitted to the annual precipitation sums at each grid points in this comparative study. The estimated changes over the whole period (1979-2010) in % can be seen in the Figure 3.3.10.1 for the different datasets. The spatial pattern of the precipitation changes remarkably diverge. An extended region with decreasing precipitation emerges in Ukraine, Transcarpatia in E-OBS. Possibly the less station data applied for gridding in E-OBS resulted in this unreasonable decreasing trend. ERA5 produces 10% or even major precipitation decrease in the eastern part of the Carpathian region, which is completely missing from CARPATCLIM. The precipitation increase is moderate in ERA5, 20% in the large part of the region, while there are around 30-40% increase in Polish Carpathians and in Tatras in CARPATCLIM.



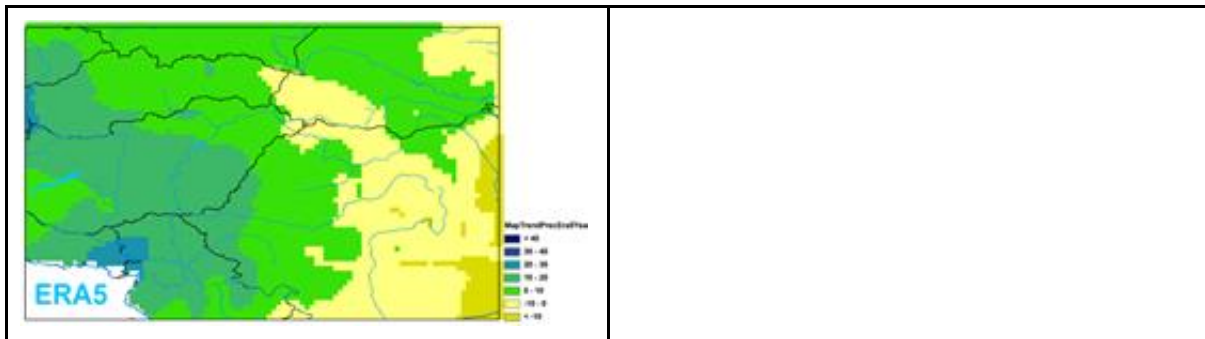


Figure 3.3.10.1 Result of exponential trend fitting for yearly precipitation in %/ 32 year. for CARPATCLIM (top left), E-OBS (top right) and ERA5 (bottom) over the time period 1979-2010.

### 3.3.11 Homogeneity test

The MASH (Multiple Analysis of Series for Homogenization, Szentimrey; 2014) software system for homogenization consists of functions for testing the residual inhomogeneity in any dataset. For doing this the closest grid points to 51 Hungarian meteorological stations (Figure 3.3.11.1) were selected from CARPATCLIM and also from E-OBS, then the gridded daily precipitation series from 1961-2010 were tested by MASH homogenization method. Test statistics are available only for Hungary as the station data were not collected into a common database in CARPATCLIM project. Therefore the comparison of the homogenization results for the stations and their closest grid points for the different datasets cannot be done out of Hungary.

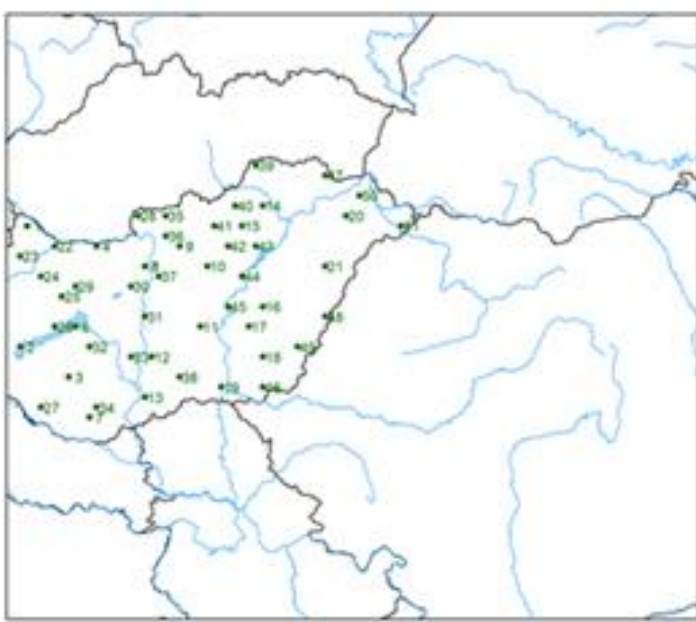


Figure 3.3.11.1 Map depicting the stations, which were used in the homogeneity test.



The test statistics for inhomogeneity of the gridded series are listed in the Table 3.3.11.1 and Table 3.3.11.2. The null hypothesis is that the examined gridded series are homogeneous. The critical value related to significance level 0.01 comes to 31. Test statistics (TS) can be compared to the critical value, the larger TS values are the more suspicious.

#### Test Statistics After Homogenization for E-OBS

Series	TSA	Series	TSA	Series	TSA
51	95.70	20	64.53	13	58.61
44	56.85	41	54.93	6	49.78
7	48.51	32	48.20	45	47.46
29	43.23	49	42.48	50	34.40
42	33.92	10	33.89	4	33.55
11	33.24	23	32.80	31	31.21
2	24.52	14	24.30	37	24.02
19	21.04	9	20.53	47	19.75
21	19.46	48	19.18	40	18.21
5	17.05	8	17.05	3	16.50
34	16.38	24	15.47	26	14.63
16	14.06	39	13.39	30	12.79
33	12.12	35	11.80	12	11.20
15	11.19	22	11.17	43	10.55
18	10.50	36	9.95	46	9.37
25	9.09	28	8.17	38	7.51
27	7.11	17	6.83	1	6.21

AVERAGE: 25.77

Table 3.3.11.1 The test statistics in decreasing order for E-OBS (after homogenization).

**Test Statistics After Homogenization for CARPATCLIM****Series TSA Series TSA Series TSA**

42	50.53	2	36.04	6	36.03
37	34.07	49	32.05	46	30.12
50	29.21	12	28.13	29	27.51
44	27.06	5	25.00	8	25.00
40	23.11	17	22.71	20	20.79
16	20.55	43	19.92	3	19.49
21	18.67	1	17.75	14	17.37
48	16.86	39	16.71	15	16.65
32	15.81	31	15.62	13	15.28
4	14.80	9	14.68	33	14.64
35	14.32	51	14.20	41	14.05
18	13.45	38	13.37	23	13.27
22	12.71	25	11.78	7	11.49
11	10.71	47	9.86	26	9.14



19	9.07	30	8.91	45	8.17
36	7.89	27	7.24	24	6.11
34	5.30	10	4.58	28	4.30

AVERAGE: 17.88

Table 3.3.11.2 The test statistics in decreasing order for CARPATCLIM (after homogenization)

The largest test statistics is 95.7 regarding E-OBS (Table 3.3.11.1), while 50.53 in CARPATCLIM (Table 3.3.11.2) taking the analyzed grid point series. The average of the statistics is smaller in CARPATCLIM (17.88) than in E-OBS (25.77) what suggest that E-OBS is bothered with residual inhomogeneity. Beyond doubt, the climate change signal strongly depends on whether the QC and the homogeneity procedure were applied, or not. Figure 3.3.9.1 in the chapter 3.3.9 confirms the weakness of the quality control in Ukraine Podolia, where some data obviously remained erroneous in E-OBS. Large discrepancies are standing out regarding the precipitation changes along the Carpathian chain in Slovakia, Ukraine and in Romania between CARPATCLIM and E-OBS (see Figure 3.3.11.1).

### 3.3.12 Main outcomes – precipitation in the Carpathians

E-OBS is drier and ERA5 is wetter than CARPATCLIM at each elevation. E-OBS underestimates the yearly sum with 81.4mm for the entire region, particularly at higher elevation above 1500m where the underestimation is 215.4mm in average. Similar or even higher overestimation can be found in ERA5 at the highest mountainous areas (249.1mm). The overall overestimation is 143.1mm for the entire region, which is more than half as much again the underestimation in E-OBS.

While the distribution of precipitation throughout the year is similar in all three examined datasets, the monthly average overestimation is 11.92mm in ERA5 and the underestimation is 6.7mm in E-OBS.

The monthly mean precipitation fallen for the selected watersheds confirm the general underestimation in E-OBS and overestimation in ERA5.

E-OBS is obviously drier than CARPATCLIM, particularly in plane regions in the center and at the southeastern border of the domain. The more rainy days in CARPATCLIM in higher elevation in the southern Carpathians is completely absent in E-OBS. This difference in rainy days seems to be linked to the reduced availability of stations in these areas.

Contrary, an overall overestimation of Q95 exists in the case of ERA5, most of all at higher altitudes, although the most intense precipitation in the north-eastern Carpathians in ERA5 is lower than in CARPATCLIM. The empirical probability of wet days in regional average is 0.31, 0.29 and 0.39 for CARPATCLIM, E-OBS and ERA5, respectively.

E-OBS dataset can be characterized by 2mm/day RMSE at least most of the region and 4.5mm or above in wider areas in the northeastern Carpathians in Ukraine and in smaller regions in the



southern Carpathians, Bihor Massif and Dinaric Alps. As for ERA5 large RMSE values turn up in the territory of Ukraine and Romania with around 4mm/day in the flat region and 5 mm/day or above at mountainous areas. Regarding the monthly RMSE values E-OBS can be described lower than 23 mm sparsely, but ERA5 compared to CARPATCLIM and to E-OBS produces 35 mm or above monthly RMSE in the territory of Romania and along the Carpathians in Ukraine in extended regions. These findings confirm that construction of a representative dataset in time and space alike and also the modelling of precipitation in the Carpathians and the Basin in between the chain of mountains is challenging. Comparing the model performances 2 mm or higher RMSE values appear about half of the domain ERA5Land against ERA5 with the greatest values in the high mountains.

The daily MESS values vary around 0.5 or above in the majority of the region taking E-OBS for CARPATCLIM as a reference. The smallest daily MESS values arise in the territory of Ukraine and Romania for ERA5 evaluated against CARPATCLIM.

E-OBS can be characterized with an overall lower maxima of daily precipitation than CARPATCLIM, beside this possibly a bad data remained in E-OBS in Ukraine. In contrast, ERA5 produces higher daily extremes than CARPATCLIM, particularly in Romania and in the eastern part of the great Hungarian Plain.

The spatial pattern of the precipitation changes remarkably diverge in the analyzed datasets. An extended region with decreasing precipitation emerges in Ukraine, Transcarpatia in E-OBS, possibly due to that less data were used for gridding in that region. ERA5 produces 10% or even major precipitation decrease in the eastern part of the domain, which is missing from the observational datasets.

Possibly the residual inhomogeneities in E-OBS contribute to the highly variable precipitation trend in the Carpathian region.

#### E-OBS

E-OBS underestimates the yearly sum with 81.4mm as an average for the period 1979-2010 for the entire region, particularly at higher elevation above 1500m, where the underestimation is 215.4mm in average. The monthly mean precipitation fallen for the selected watersheds also confirm the general underestimation of E-OBS. The more rainy days in CARPATCLIM in higher elevation in the southern Carpathians is completely absent in E-OBS. This difference in rainy days seems to be linked to the reduced availability of stations in these areas. E-OBS dataset can be characterized by 2 mm/day RMSE most of the region and 4.5mm or above in wider areas in the north-eastern Carpathians in Ukraine and in smaller regions in the southern Carpathians, Bihor Massif and Dinaric Alps. The daily MESS values vary around 0.5 or above in the majority of the region, taking E-OBS for CARPATCLIM as a reference. Considering the trend, an extended region with decreasing precipitation emerges in Ukraine, Transcarpatia in E-OBS, possibly due to that less data were used for gridding in that region. The probable residual inhomogeneities in E-OBS contribute to the highly variable precipitation trend in the Carpathian region.

#### ERA5

ERA5 is wetter than CARPATCLIM at each elevation. A very high overestimation (249.1 mm) can be found in ERA5 at the highest mountainous areas (>1500m) on yearly basis. The overall overestimation is 143.1 mm for the entire Carpathian region. The monthly mean precipitation fallen



at the selected watersheds confirms the general overestimation of ERA5. As for the sub-catchment studies the largest overestimation emerges in the region of Upper-Tisza sub-catchment in Ukraine in E-OBS to CARPATCLIM as a reference, with largest differences in the convective season. An overall overestimation of Q95 exists in the reanalysis, most of all at higher altitudes. Large RMSE values turn up in the territory of Ukraine and Romania with around 4mm/day in the flat region and 5 mm/day or above at mountainous areas in ERA5. The smallest daily MSESS values arise in the territory of Ukraine and Romania for ERA5 evaluated against CARPATCLIM. ERA5 produces 10% or even major precipitation decrease in the eastern part of the domain which is missing from the observational datasets.

## 4. Temperature

The aggregated variables at the basis of our analysis are: daily mean temperature (TG), daily maximum temperature (TX) and daily minimum temperature (TN). By using those variables, several other climate indices have been derived. The spatial domains considered are the Carpathians and Fennoscandia. E-OBS and ERA5 datasets have been compared to the regional observational gridded datasets, as it has been presented in Section 3 for precipitation.

When considering Fennoscandia, the set of core climate indices (Expert Team on Climate Change Detection and Indices, ETCCDI) suggested by the CCI/WCRP/JCOMM are calculated for E-OBS and ERA5 and evaluated against NGCD. The reference time period is the 30-year period 1981-2010.

The mean annual temperature is of course a key index. The temperature extremes are assessed by analyzing the mean maximum temperature and the mean minimum temperature over Fennoscandia. Furthermore, the temporal evolution of temperature is examined by means of the mean diurnal temperature range, which is obtained as the difference between the maximum and the minimum values. As a further step in our analysis, a range of Climate Impact Indices based on minimum and maximum temperature are calculated.

Among the calculated temperature indices are:

- Frost days (FD, number of days with minimum temperature < 0°C)
- Summer days (SU, number of days with maximum temperature > 25°C)
- Tropical nights (TR, number of days minimum temperature > 20°C)

The number of TR occurred in 2018, one of the hottest years on record.

The yearly cycle of temperature is investigated by taking into account the monthly mean temperature in the 3 subregions of Fennoscandia. In addition to that, the bias, the RMSE and the MSESS are calculated for all four seasons (DJF = winter, MMA = spring, JJA = summer, SON = autumn) and for all examined datasets aiming at assessing their ability in reconstructing the temperature fields.

For the Carpathian region, the daily maximum temperature (TX) and daily minimum temperature (TN) were considered in this comparative study. The daily mean temperature (TG) is not included



for the Carpathian region as it is derived from TX and TG in CARPATCLIM dataset. First, an ANOVA (ANalysis Of VAriance) was applied for CARPATCLIM domain for the examined datasets. The ANOVA is known as an adequate statistical methodology to explore the difference in the statistical structure of the datasets: The ANOVA can be used effectively for the characterization of the spatio-temporal statistical properties of CARPATCLIM, E-OBS and ERA5. The main principles of the ANOVA method is that the total variance can be partitioning as the sum of the spatial variance of the temporal means and the spatial mean of the temporal variances on one hand; and the sum of the temporal variance of the spatial means and the temporal mean of the spatial variances on the other hand. The comparison of the magnitude and spatial distribution of the specific components of the total variance can be analyzed for different time periods, years and seasons for example. The spatial means and spatial variances at the moment  $t$  are illustrated on graphs and temporal means and temporal variances at specific location  $s$  (the grid points in our case) are illustrated on maps (see Appendix for details on the ANOVA methodology).

The evaluation of the annual means is included in the ANOVA analysis. The yearly cycle, the mean annual diurnal temperature range (DTR), the Q95 and Q05 quantiles (daily and monthly) are shown on maps and graphs, the maxima and minima of the analyzed datasets are compared, then the TXx and TNn, SU and FD temperature indices are evaluated.

Beside these statistics, the verification scores of RMSE and MSESS (daily, monthly and seasonal) were computed and illustrated on maps and graphs for CARPATCLIM domain.

Furthermore, a linear trend model was fitted to the yearly mean TX and TN. The estimated changes over the whole period were computed and compared. Moreover, a homogeneity test of E-OBS gridded temperatures was performed for testing the residual inhomogeneity.

The methods used in this evaluation for the Carpathian region are described in detail in Szentimrey (2019).

## 4.1 Fennoscandia

This part of the study aims at assessing the quality of near-surface temperature in the European dataset E-OBS over Finland, Sweden and Norway by comparing it against the Nordic Gridded Climate Dataset (NGCD), that is specifically designed to model near-surface temperature in the Nordic region.

### 4.1.1 Climate Indices

The dictionary of climate indices can be found at

<https://surfobs.climate.copernicus.eu/userguidance/indicesdictionary.php>.

**Mean annual temperature.** The maps of the mean annual temperature over Fennoscandia in the time period 1978-2018, shown in Figure 4.1.1.1, show a remarkable agreement between all the

datasets. The differences are found only for the regions with the lowest temperature (i.e., the mountaintops and the northern Fennoscandia), where the values derived from ERA5 are smaller than those of the other datasets.

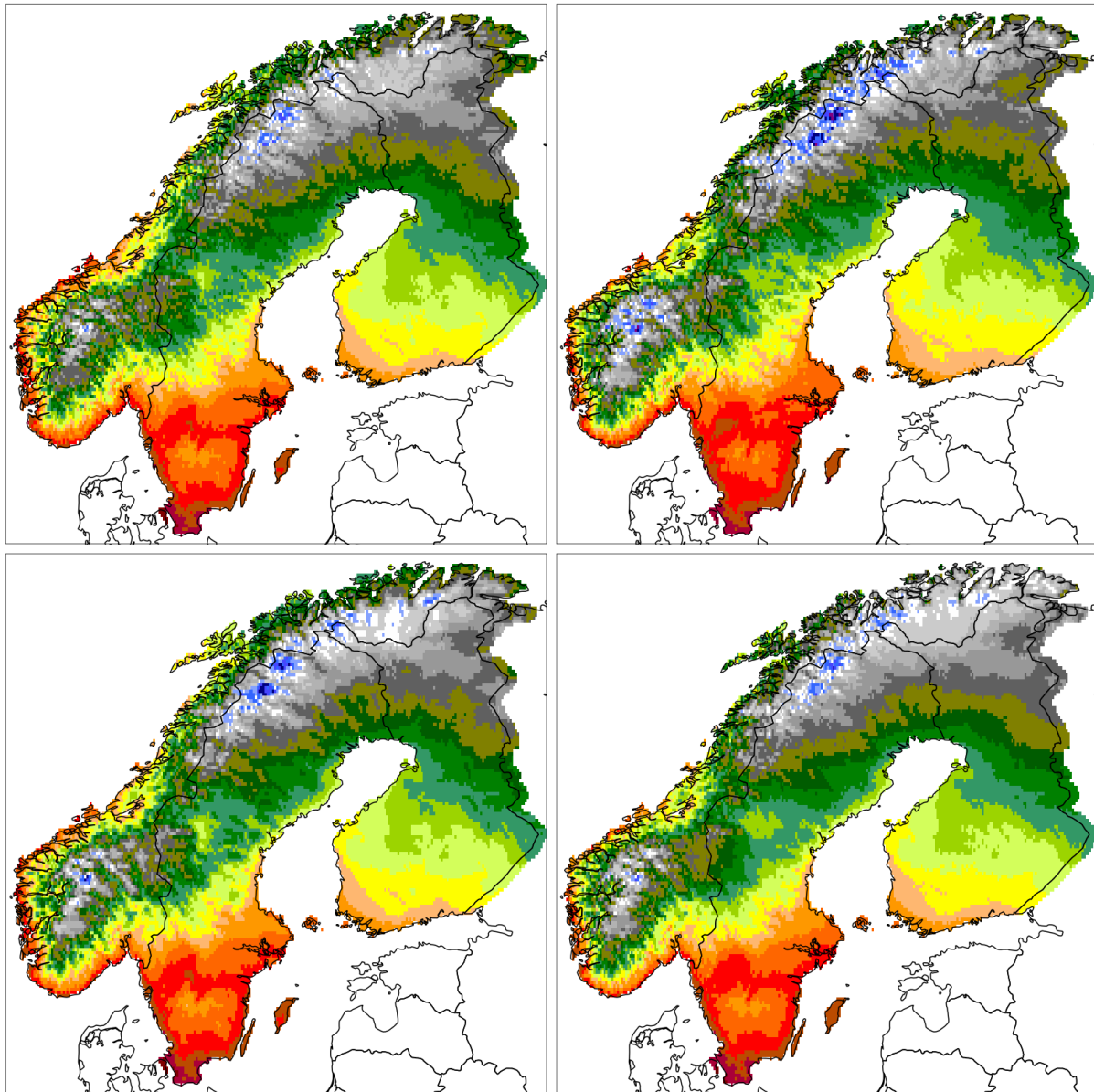


Figure 4.1.1.1: Mean annual temperature in the time period 1979-2018 for the datasets: E-OBS (top-left), ERA5-HRES (top-right), NGCD-1 (bottom-left), NGCD-2 (bottom-right).

**Temperature extremes.** The climate indices considered to investigate the ability of the models in reproducing the climatology of extreme precipitation are: TXn, TNn (Figure 4.1.1.2), TXx (Figure 4.1.1.3), TNx, TR, SU and CSU. The maps show that global reanalyses usually reproduce less extreme

situations than the observational gridded datasets. The global reanalyses differ also from the observational gridded datasets in those regions where there is a transition between heterogeneous surfaces, such as along the coast and in the proximity of the big lakes. E-OBS and NGCD are not too different. NGCD-2 is colder in the north of Norway. NGCD-1, sometimes, clearly shows the effect of individual stations.

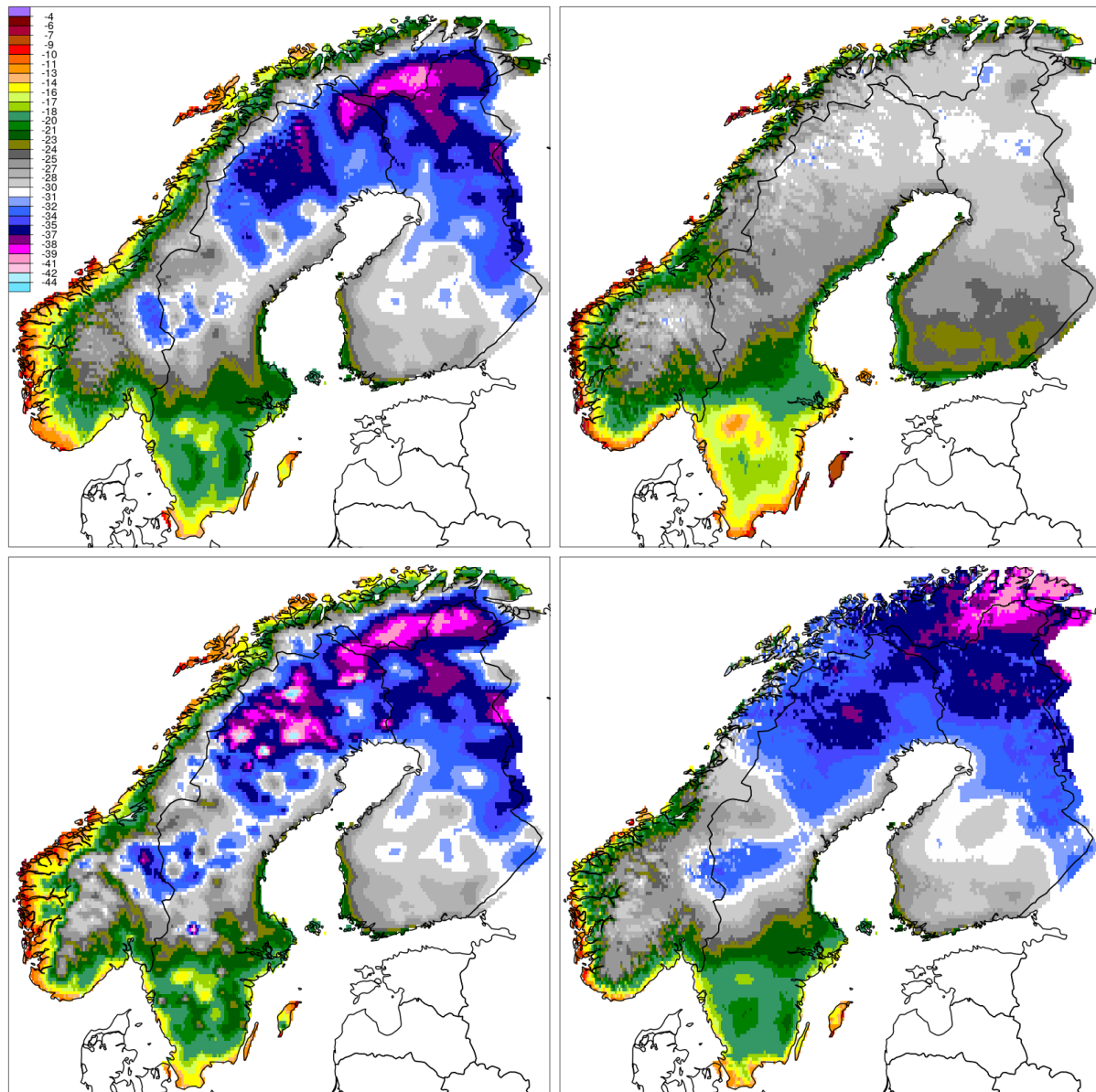


Figure 4.1.1.2: Mean annual TNn in the time period 1979-2018 for the datasets: E-OBS (top-left), ERA5-HRES (top-right), NGCD-1 (bottom-left), NGCD-2 (bottom-right).

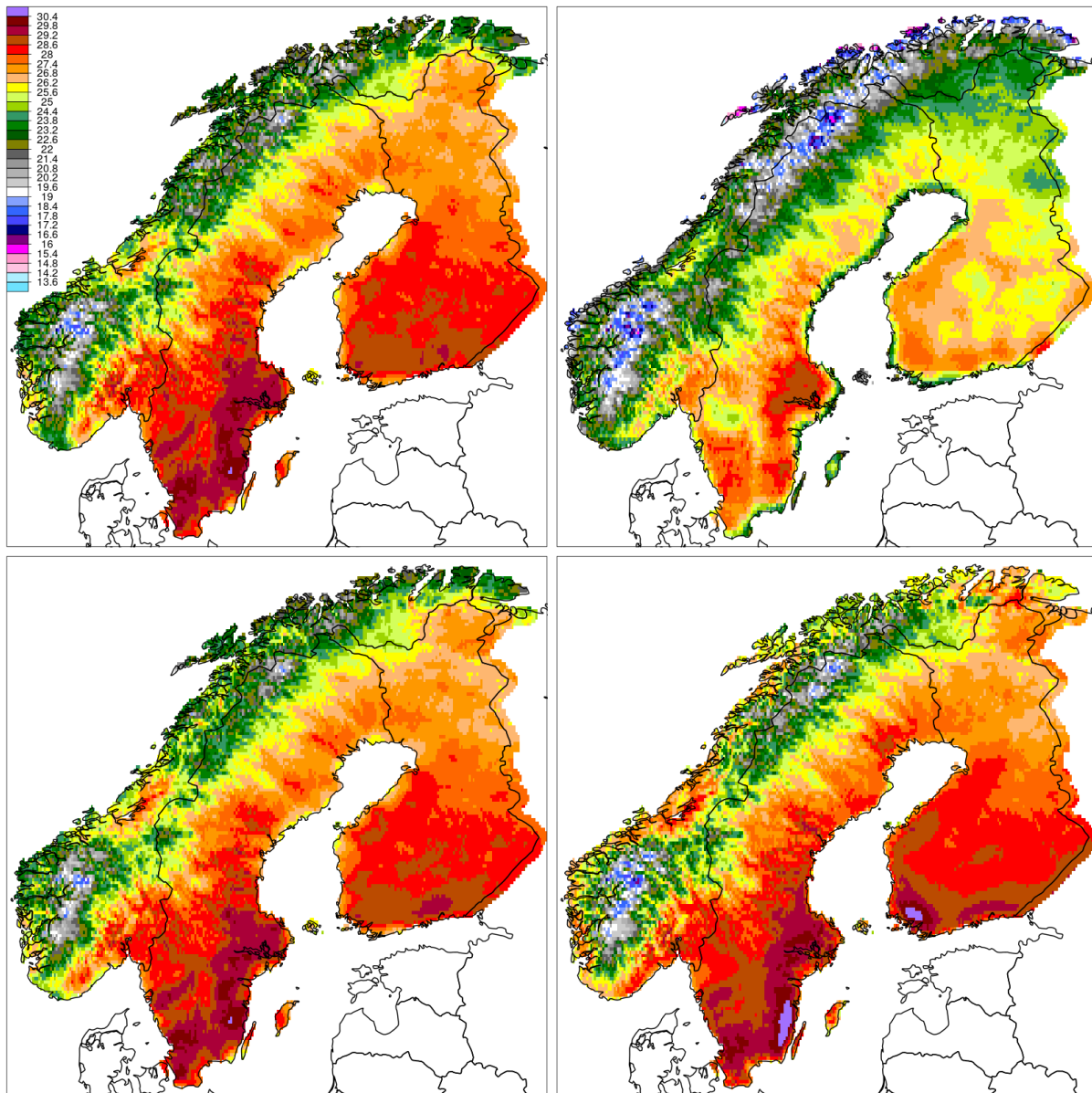


Figure 4.1.1.3: Mean annual TXx in the time period 1979-2018 for the datasets: E-OBS (top-left), ERA5-HRES (top-right), NGCD-1 (bottom-left), NGCD-2 (bottom-right).

**Mean diurnal temperature range (DTR).** DTR is obtained as the difference between the maximum and the minimum values and it shown in Figure 4.1.1.4. There is a systematic difference between the observational datasets and the global reanalyses that is also clearly visible from the DTR time series of the annual averages, aggregated over Fennoscandia (not shown here): ERA5 values are between 5 °C and 6 °C, while NGCD and E-OBS values are between 7.5 °C and 8.5 °C. With respect to the observational datasets, it is worth noticing that NGCD-2 clearly shows the footprint of topography, while NGCD-1 and E-OBS tend to show smoother fields. Furthermore, NGCD-2 is

different from both E-OBS and NGCD-1 along the coast of northern Norway, where NGCD-2 shows a much larger DTR than the other datasets. While the first remark might be seen as a point in favour of NGCD-2, the difference in the north of Norway is probably due to the inability of NGCD-2 to properly simulate the influence of the sea on coastal temperature because of the lack of stations there. The spatial distribution of DTR is rather similar for all datasets, the smallest values are: in western Norway, along the main mountain ridges; at the major lakes in southeast Finland; inland in the southern part of Sweden (the influence of the lakes on DTR is more evident in ERA5-LAND than in the other ERA5 datasets). In addition, for all datasets and for most part of the domain, it is possible to recognize a gradient in DTR over a narrow strip of land along the coast where the values tend to decrease the closer the grid points are to the seashore.

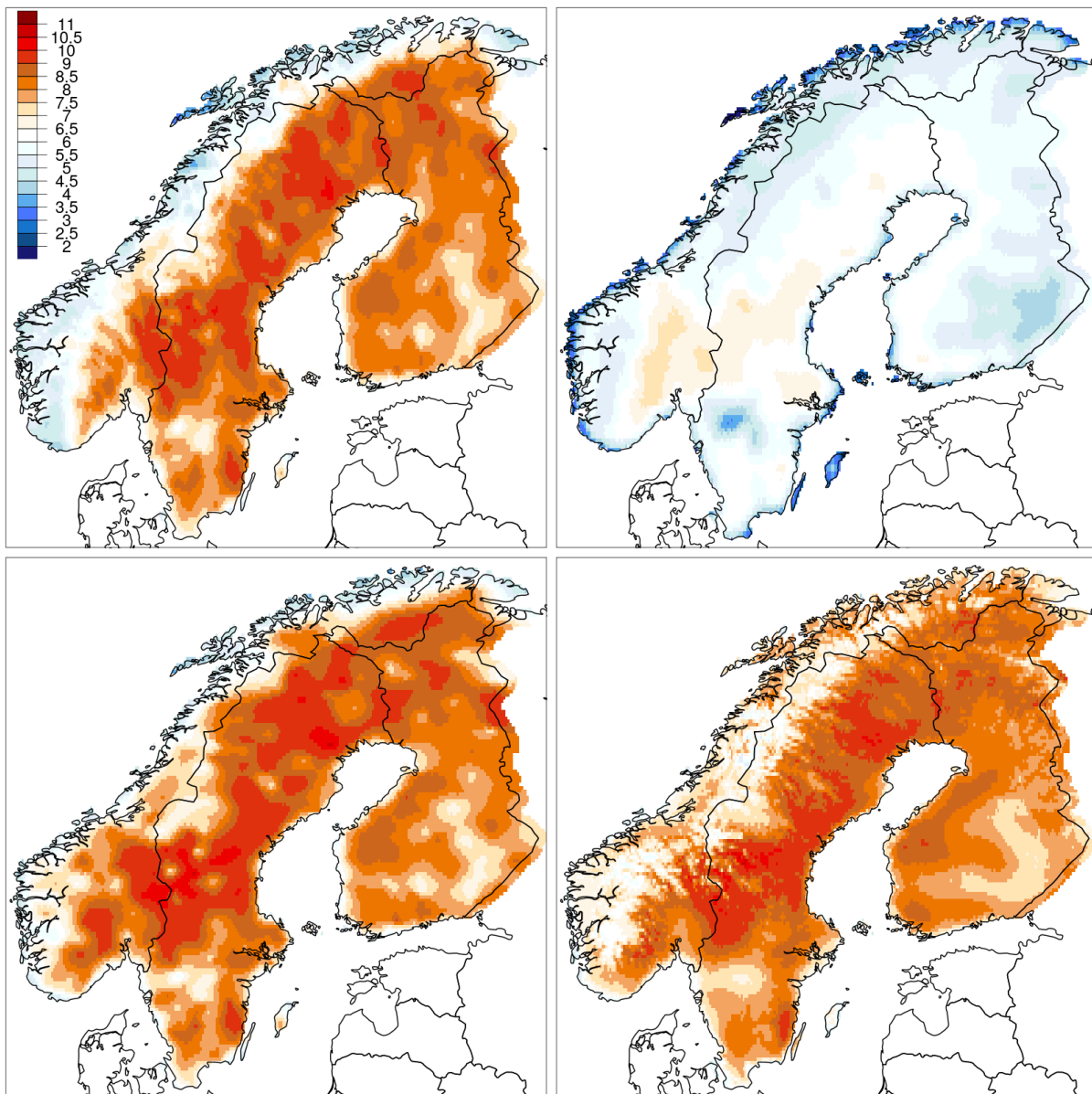




Figure 4.1.1.4: Mean annual DTR ( $^{\circ}\text{C}$ ) in the time period 1979-2018 for the datasets: E-OBS (top-left), ERA5-HRES (top-right), NGCD-1 (bottom-left), NGCD-2 (bottom-right).

**Frost Days (FD).** If we consider the mean annual number of frost and ice days, all the datasets behave in a similar way both in terms of time series and spatial distribution of values. With respect to the time series, the observational datasets tend to have slightly higher values of FD than ERA5, and slightly smaller values of ID. E-OBS agrees better with NGCD for ID than for FD, note that the first depends on TX while the second on TN. With respect to the consecutive number of frost days (CFD), E-OBS is the dataset with the smallest values of CFD aggregated over Fennoscandia and the maps show that the differences are mostly located in the mountainous regions where E-OBS systematically reports smaller values than the other datasets.

**Summer Days (SU).** The mean annual number of summer days (SU) show a significant difference between ERA5 and the observational datasets, and this difference grows linearly with the increase in SU. The time series shows that the observational gridded datasets have a greater variability than ERA5. All datasets seem to have greater SU values at the big cities (e.g., Helsinki, Stockholm and Oslo) than in their immediate surroundings, however this effect is more evident in the observational datasets. Lakes are marked in all datasets by a decrease in the number of SU. If we restrict our analysis to the observational gridded datasets, they are all very similar and the most noticeable differences are that NGCD-2 has higher SU values than the other datasets in those regions where SU is generally higher. The difference between ERA5 and observational datasets is significant in the consecutive number of summer days (CSU), as expected. E-OBS behaves similarly to NGCD-1, while NGCD-2 shows greater values of CSU along the coast than the other two observational datasets.

**Cold Nights (TN10p) and Warm Nights (TN90p).** Figure 4.1.1.5 shows the mean annual TN10p for E-OBS and NGCD. E-OBS is similar to NGCD-1, while ERA5 is similar to NGCD-2. The main difference is in southern Norway, where E-OBS and NGCD-1 show a larger percentage of cold nights than ERA5 and NGCD-2. The time series of the (spatially aggregated over Fennoscandia, not shown here) number of cold nights (TN10p), the number of cold days (TX10p) show a similar temporal trend in all datasets, which is that both TN10p and TX10p are gradually decreasing in time. At the same time, the time series of the aggregated number of warm nights (TN90p) and the number of warm days (TX90p) show a temporal trend in the opposite direction, with the gradual increase of TN90p and TX90p for the most recent years.

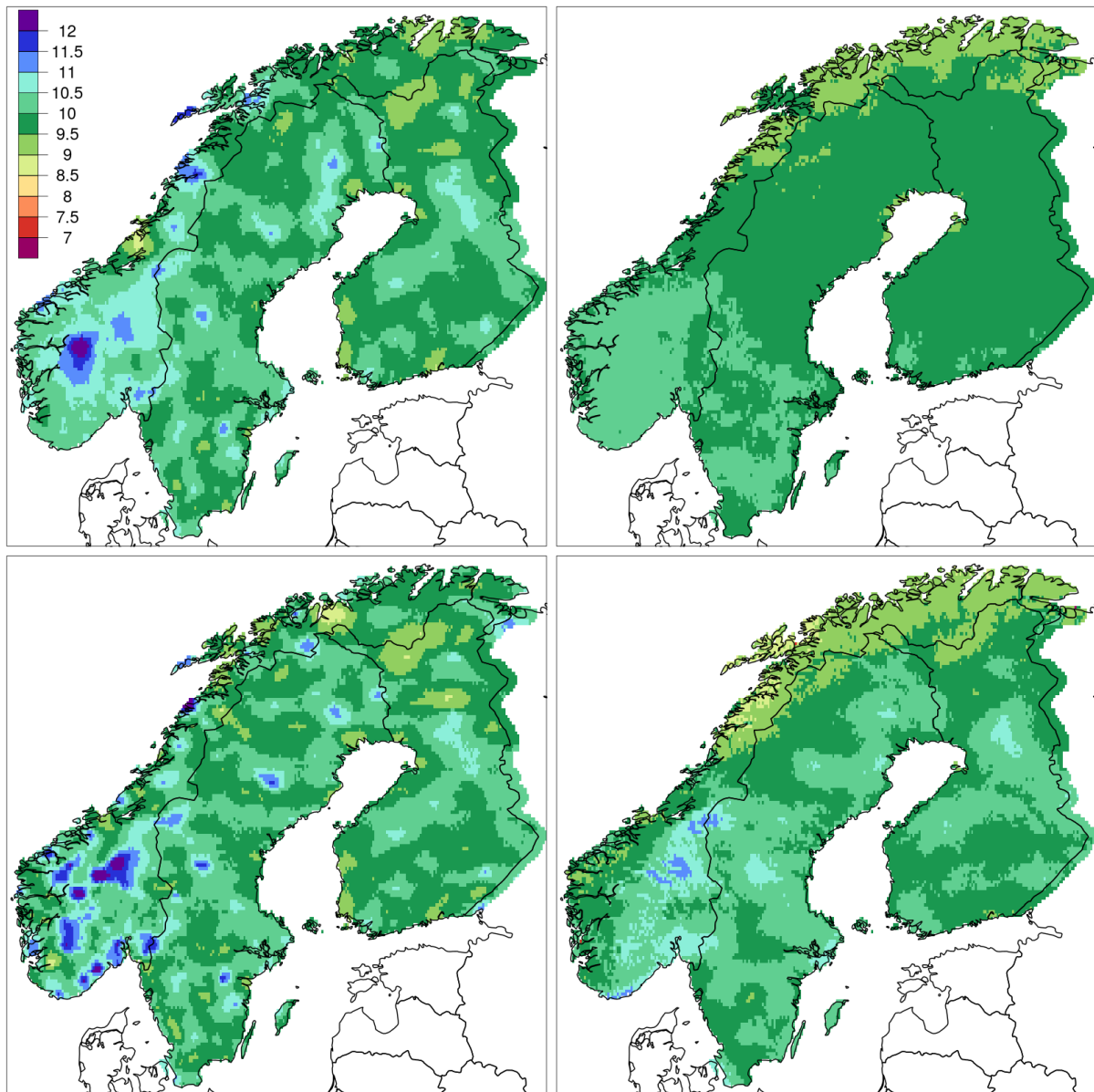


Figure 4.1.1.5: Mean annual TN10p (%) “cold nights” in the time period 1979-2018 for the datasets: E-OBS (top-left), ERA5-HRES (top-right), NGCD-1 (bottom-left), NGCD-2 (bottom-right).

#### 4.1.2 Yearly Cycle

The annual cycle of TG, TX and TN is shown in Figures 4.1.2.1, 4.1.2.2 and 4.1.2.3 respectively. The analysis has been made for all Fennoscandia, then for three regions (Figure 4.1.2.3): northern Norway (No-North), western Norway (No-West) and eastern Norway (No-East).

If we consider the whole Fennoscandian domain in Figures 4.1.2.1, 4.1.2.2 and 4.1.2.3, then it is rather difficult to distinguish between E-OBS and NGCD. ERA5 behaves similarly to NGCD with respect to the mean monthly temperature (Figure 4.1.2.1), while the extremes are filtered out a bit.



Monthly averaged maximum daily temperatures (Figure 4.1.2.2) are underestimated, while the monthly averaged minimum daily temperatures (Figure 4.1.2.3) are overestimated.

The subregion No-East is the Norwegian subregion where the four datasets are more similar. ERA5 still shows an underestimation of the monthly averaged maximum daily temperature, especially during winter and summer (between 1oC and 2oC).

In western Norway (No-West), the situation is more complex. The graphs of the mean and minimum monthly temperatures (Figures 4.1.2.1, 4.1.2.2 and 4.1.2.3) show that NGCD-1 and NGCD-2 differ, then E-OBS is similar to NGCD-1, while ERA5 is similar to NGCD-2. This effect is more pronounced in winter than during the summer. One possible explanation might be that both NGCD-1 and E-OBS take into account the distance from the ocean in their statistical interpolation scheme, while ERA5 and NGCD-2 do not give as much weight as the other two datasets to this geographical parameter. The maximum daily temperature (Figure 4.1.2.2) shows that the observational gridded datasets are in good agreement, while ERA5 underestimates the maximum temperatures by approximately 2oC or 3oC. However, during the summer E-OBS underestimates the maximum temperatures too and it is more similar to ERA5 than NGCD.

In northern Norway (No-North), E-OBS and NGCD-1 are very similar for all variables. ERA5 minimum temperatures (Figure 4.1.2.3) are also very similar to NGCD-1, the maximum temperatures (Figure 4.1.2.2) shows an underestimation throughout the whole year of approximately 2oC. ERA5 mean monthly temperatures (Figure 4.1.2.1) differ from NGCD-1 in the cold months, from January to April and from October to December. NGCD-2 shows a different behavior than the other datasets, with colder temperatures in winter, while during summer NGCD-2 and NGCD-1 are similar. The differences between NGCD-1 and NGCD-2 are discussed in further detail in Section 4.1.3.

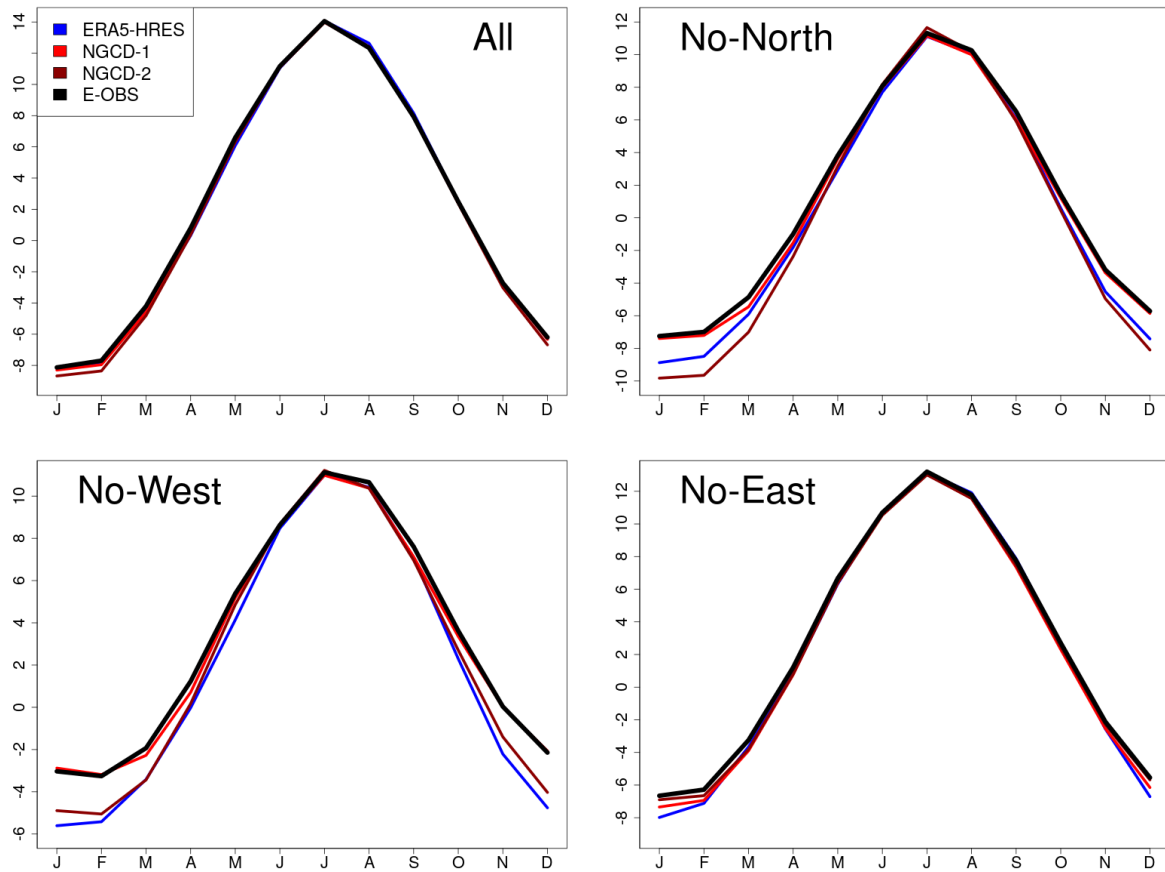


Figure 4.1.2.1. Mean monthly temperature (1979–2018) showing differences in the annual cycle. The values refer to averages over the entire Fennoscandia (top-left), and three subregions in Norway (North (top-right), West (bottom-left) and East (bottom-right), see Figure 2.1.2). The values were derived from the 0.1-degree versions of the datasets. Note the different scales between panels.

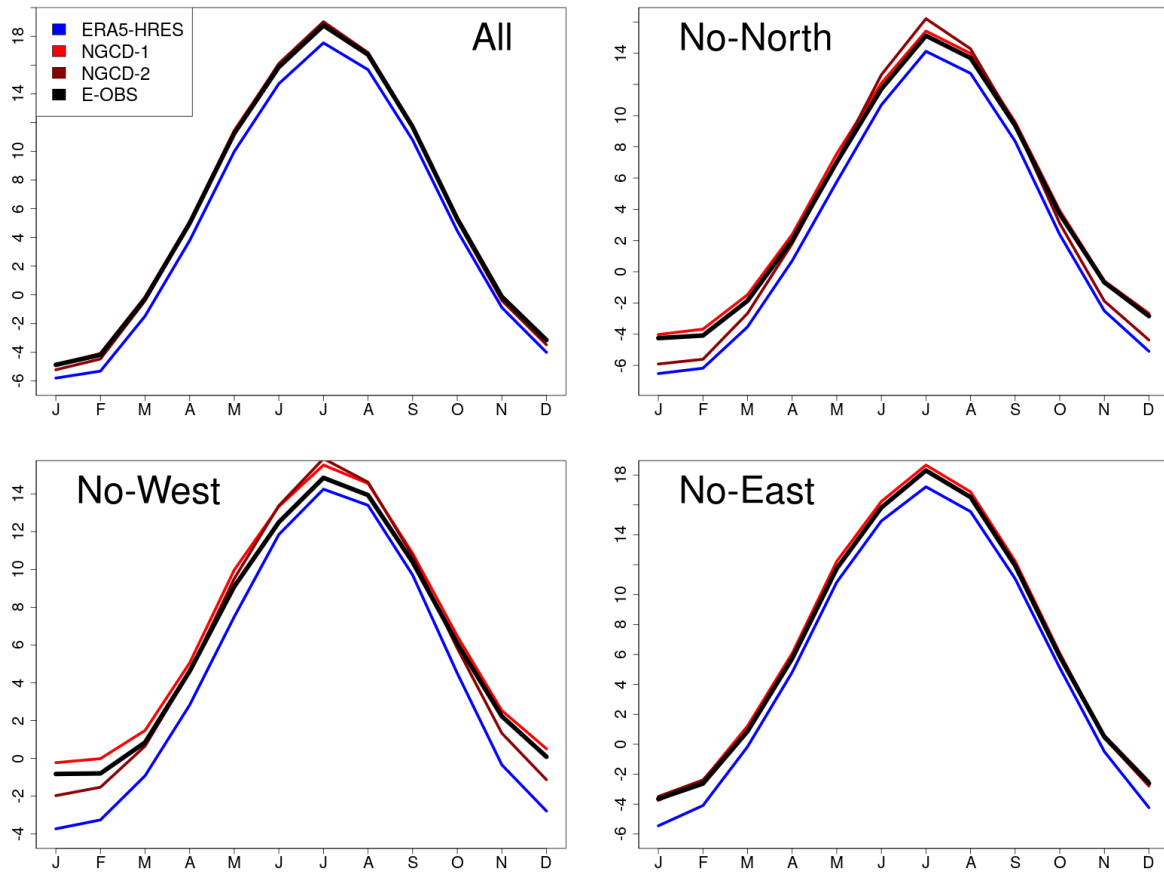


Figure 4.1.2.2. Monthly averaged maximum daily temperature (1979–2018) showing differences in the annual cycle. The values refer to averages over the entire Fennoscandia (top-left), and three subregions in Norway (North (top-right), West (bottom-left) and East (bottom-right), see Figure 2.1.2). The values were derived from the 0.1-degree versions of the datasets. Note the different scales between panels.

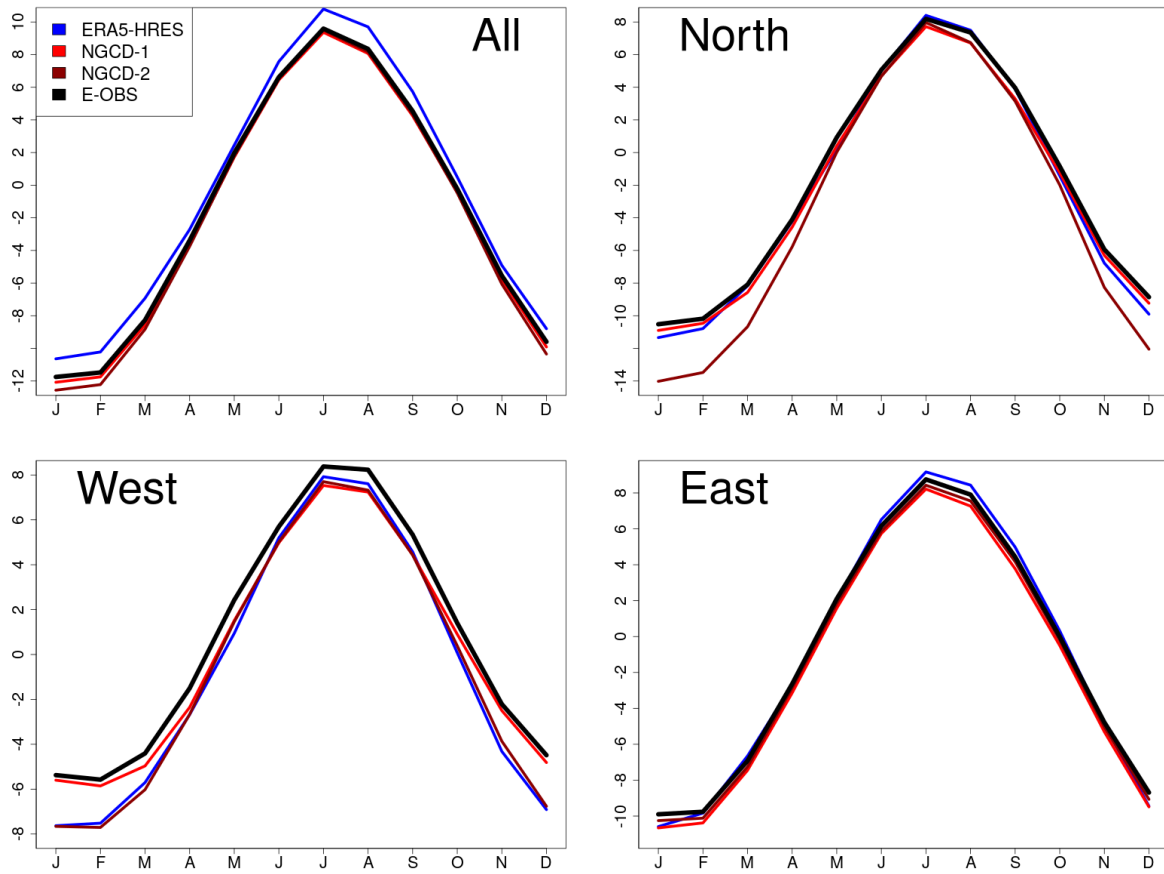


Figure 4.1.2.3. Monthly averaged minimum daily temperature (1979–2018) showing differences in the annual cycle. The values refer to averages over the entire Fennoscandia (top-left), and three subregions in Norway (top-right), West (bottom-left) and East (bottom-right), see Figure 2.1.2). The values were derived from the 0.1-degree versions of the datasets. Note the different scales between panels.

#### 4.1.3 Verification scores

For daily mean temperature we have computed bias, root mean squared error (RMSE) and the mean squared error skill score (MSESS).

**Bias - systematic deviations** (Figures 4.1.3.1, 4.1.3.2, 4.1.3.3 and 4.1.3.4). E-OBS and ERA5 are validated against NGCD. The biases are shown in the figures. For all models, the largest systematic differences take place in winter, while during the summer there is in general a better agreement between datasets. The different spatial analysis techniques used for NGCD-1 and NGCD-2 have also a strong impact on the evaluation and the verification results are significantly different between those two models. If compared to NGCD-1, E-OBS bias during winter shows a composite pattern with differences changing from  $-4^{\circ}\text{C}$  to  $4^{\circ}\text{C}$  over short distances (less than 20 km) in the mountains of Norway; E-OBS is in general warmer than NGCD-1, however there are some regions along the coast of Norway where the opposite occurs. Those abrupt variations are not present in E-OBS bias with respect to NGCD-2, however it is evident that E-OBS is systematically warmer during all

seasons except summer than NGCD-2 along the Norwegian coast and the bias increases the more we move towards north.

The comparison between ERA5 and NGCD shows that ERA5 is in general warmer in the lowlands and colder in the mountains and that the systematic differences are greater in winter. The same is true for ERA5-Land.

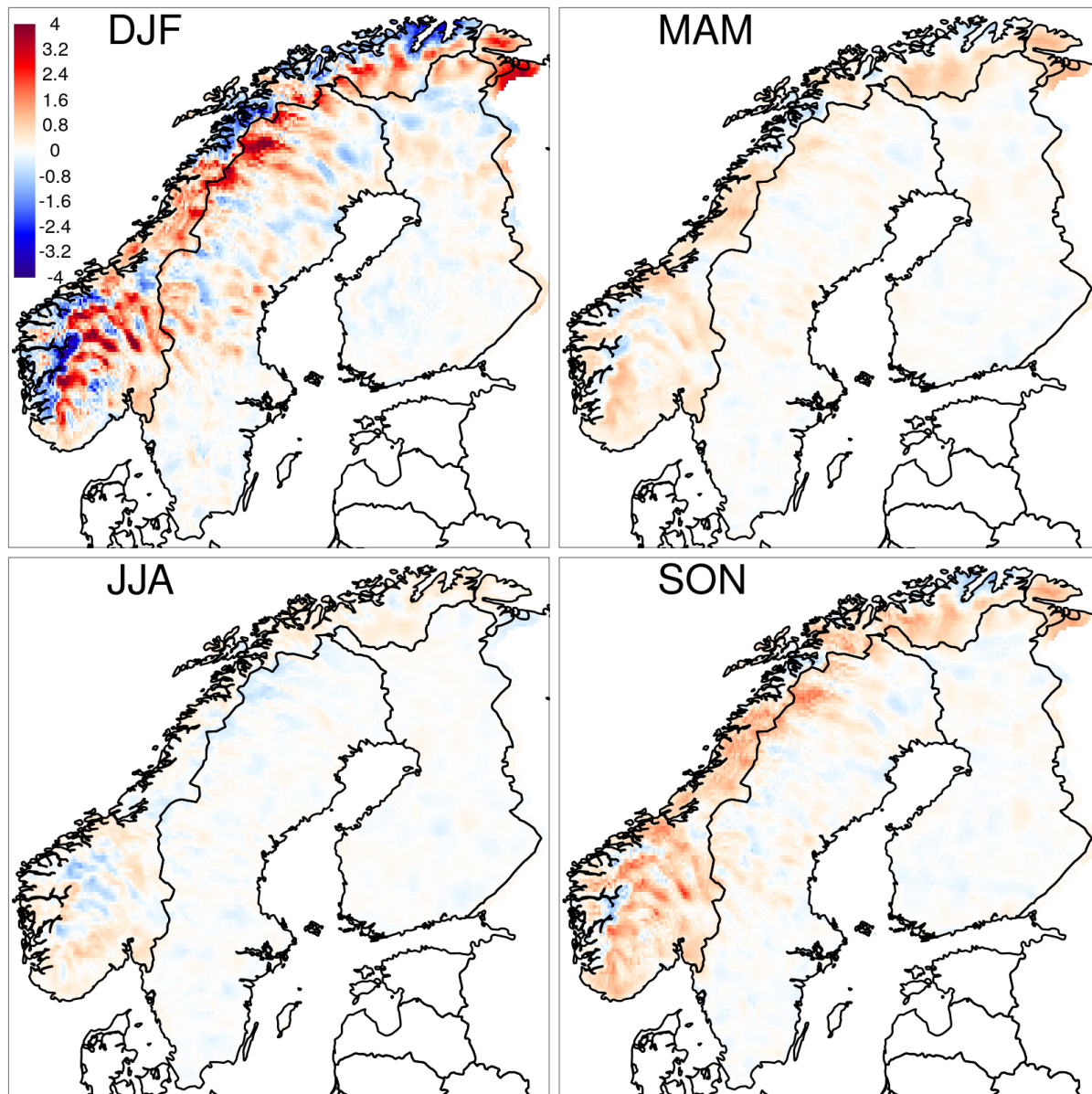


Figure 4.1.3.1. Bias ( $^{\circ}\text{C}$ ) for daily mean temperature. E-OBS is evaluated against NGCD-1 over the time period 1979-2018.

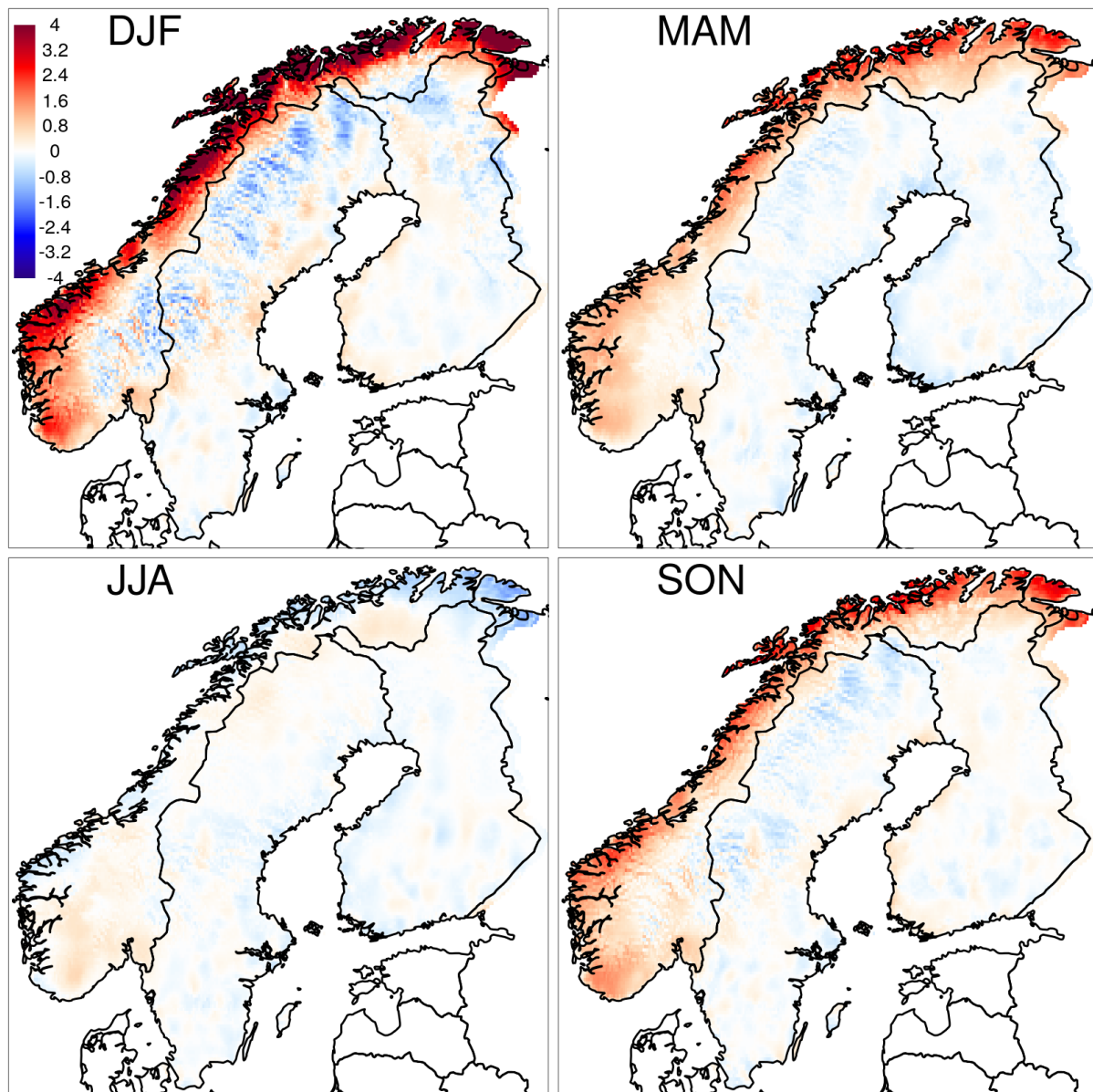


Figure 4.1.3.2. Bias ( $^{\circ}\text{C}$ ) for daily mean temperature. E-OBS is evaluated against NGCD-2 over the time period 1979-2018.

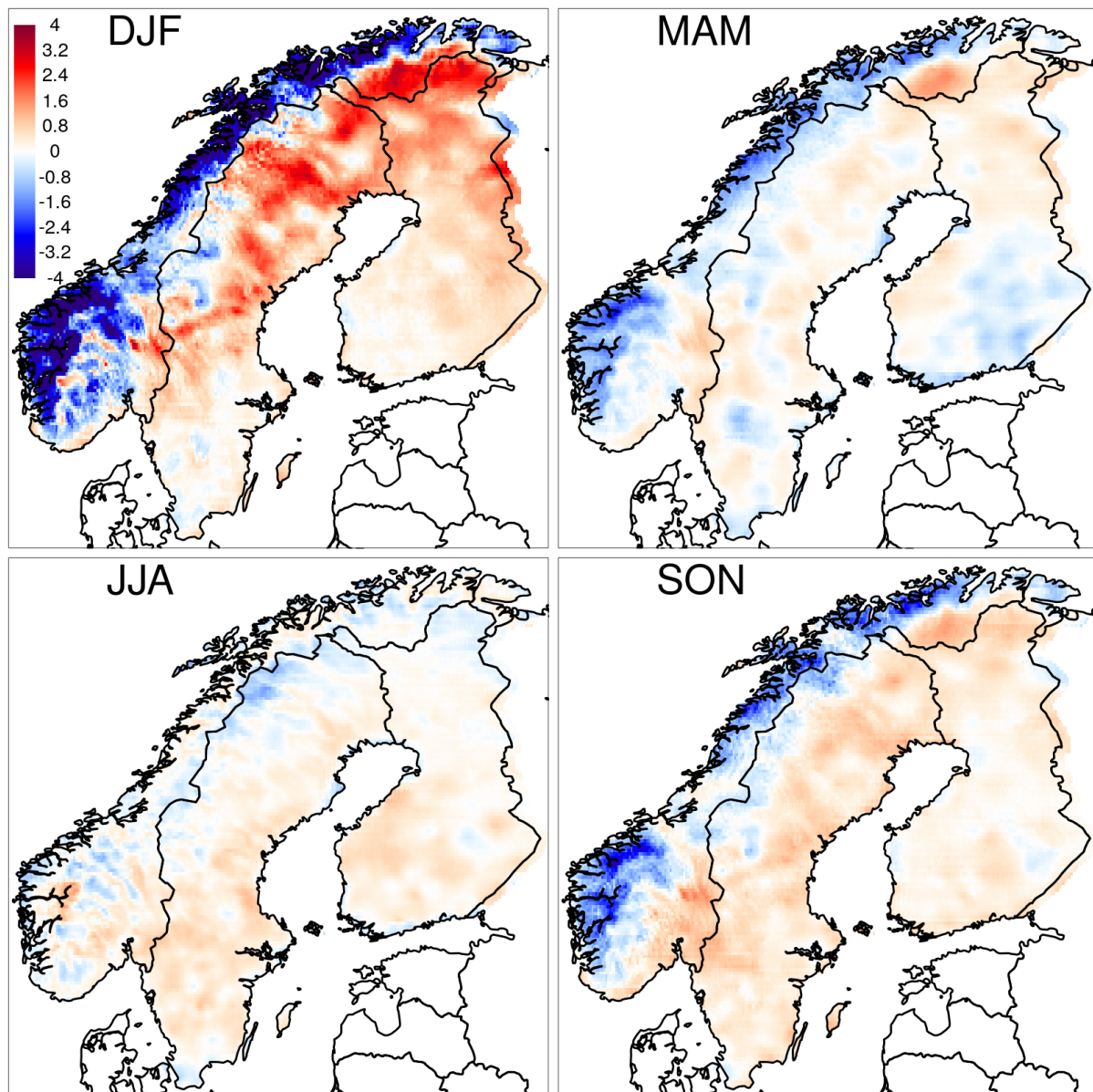


Figure 4.1.3.3. Bias ( $^{\circ}\text{C}$ ) for daily mean temperature. ERA5-HRES is evaluated against NGCD-1 over the time period 1979-2018.

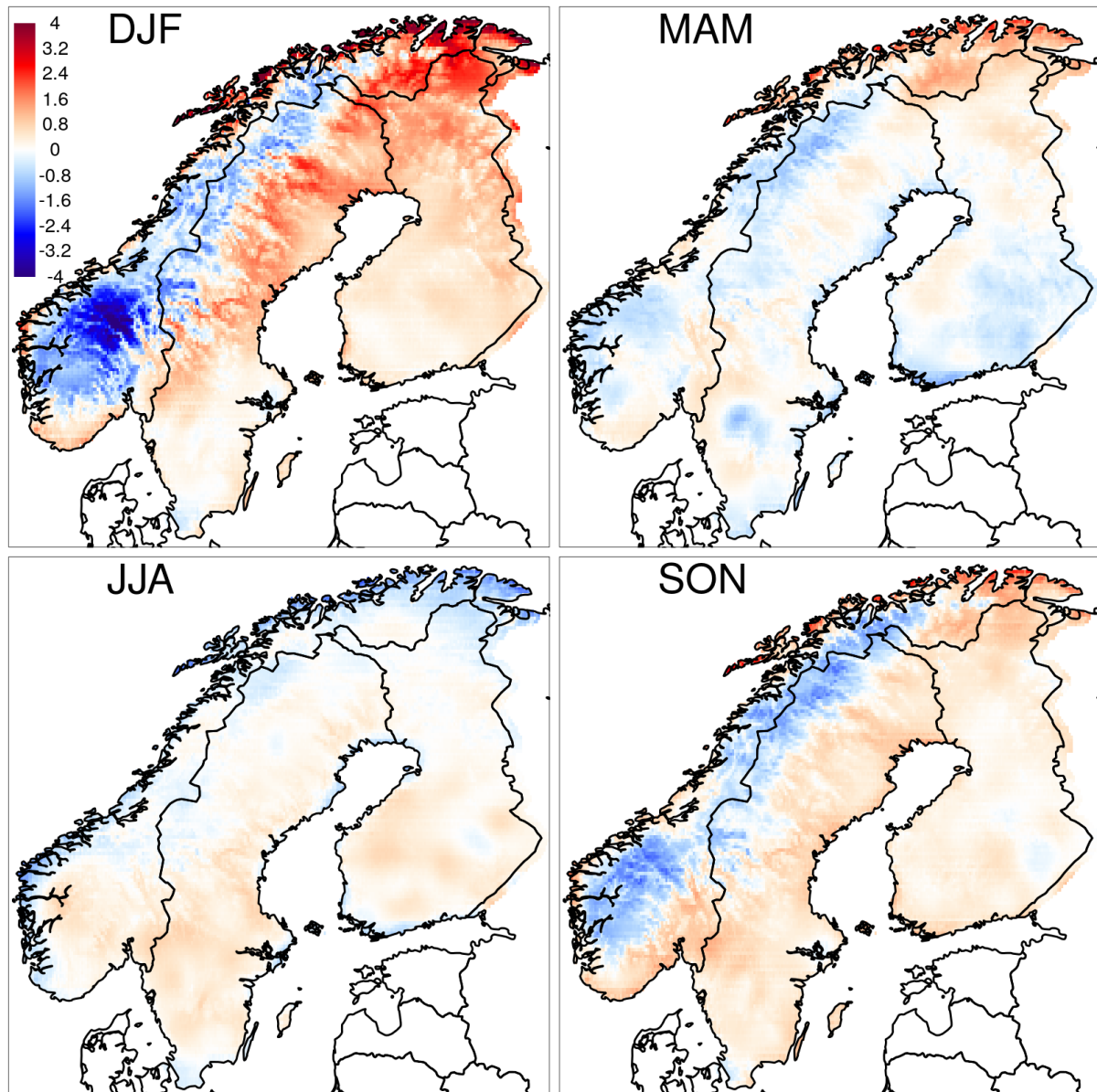


Figure 4.1.3.4. Bias ( $^{\circ}\text{C}$ ) for daily mean temperature. ERA5-HRES is evaluated against NGCD-2 over the time period 1979–2018.

**RMSE and MSESS (Figs. 4.1.3.5, 4.1.3.6 and 4.1.3.7).** If we consider the comparison between E-OBS and NGCD, one common feature shared by both RMSE and MSESS is that there is a clearly distinct behavior between Norway and the other two countries, that actually closely follows the Norwegian border. This is probably due to the fact that in Norway NGCD uses more stations than E-OBS, while for Sweden and Finland NGCD and E-OBS are based on the same set of stations. Note that ERA5 and ERA5-Land do not show the same difference between Norway and Sweden plus Finland, thus confirming our hypothesis on the effect of the station network. In Sweden and Finland, E-OBS vs NGCD RMSE is generally less than 1  $^{\circ}\text{C}$  in all seasons except winter, where it could be as high as 4  $^{\circ}\text{C}$  in the Swedish part of the Scandinavian mountains when we consider NGCD-2. However, the MSESS

is always above 0.8. In the case of Norway, the situation is more complex and E-OBS is more similar to NGCD-1, as indicated by the MSESS, with values generally higher than 0.7-0.8 except for the Norwegian mountains during winter. E-OBS compared to NGCD-2 in Norway shows the worst agreement in the winter along the coast, with values of MSESS as low as 0.2 and RMSE higher than 4 °C.

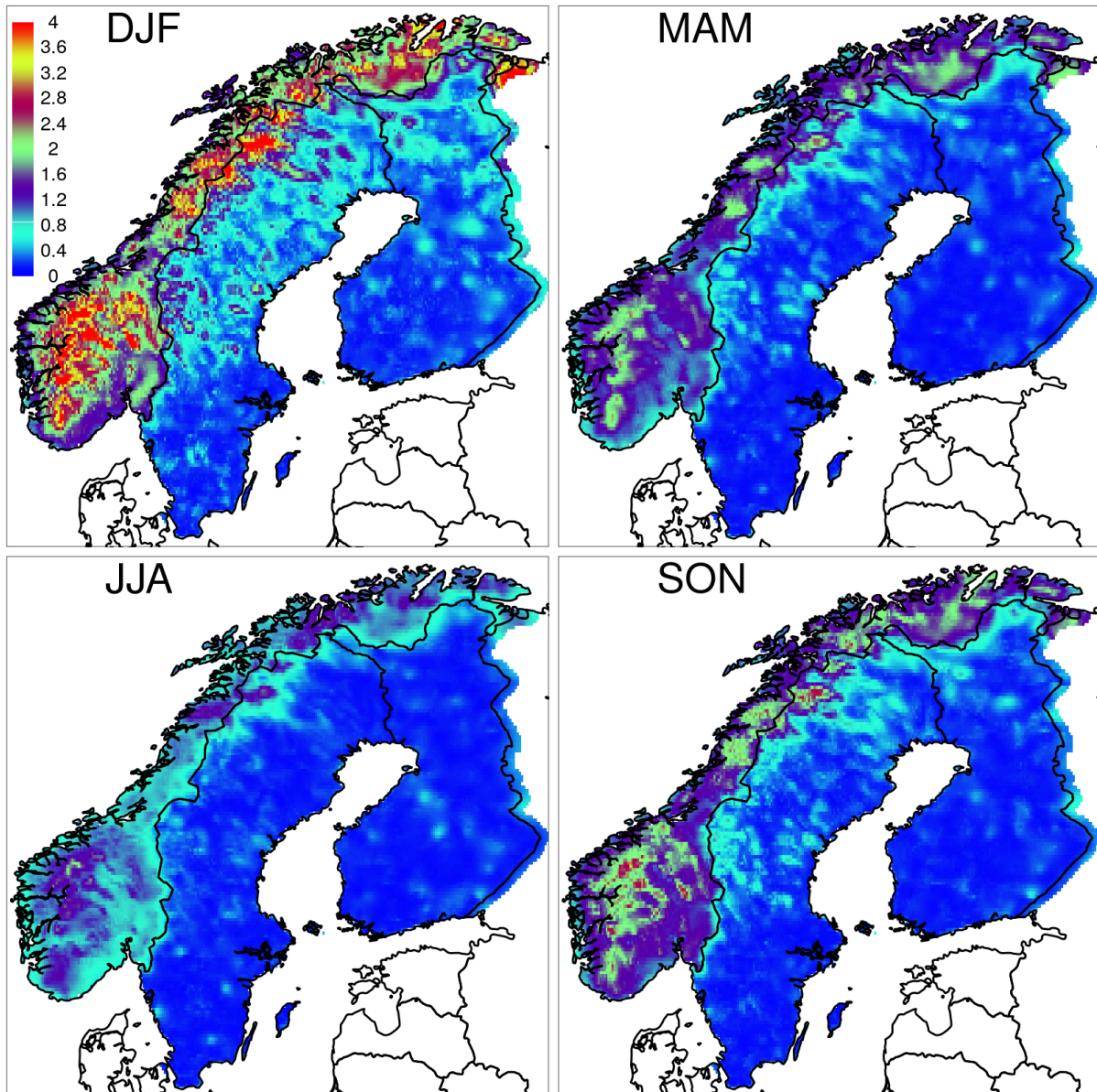


Figure 4.1.3.5. RMSE ( $^{\circ}\text{C}$ ) for daily mean temperature. E-OBS is evaluated against NGCD-1 over the time period 1979-2018.

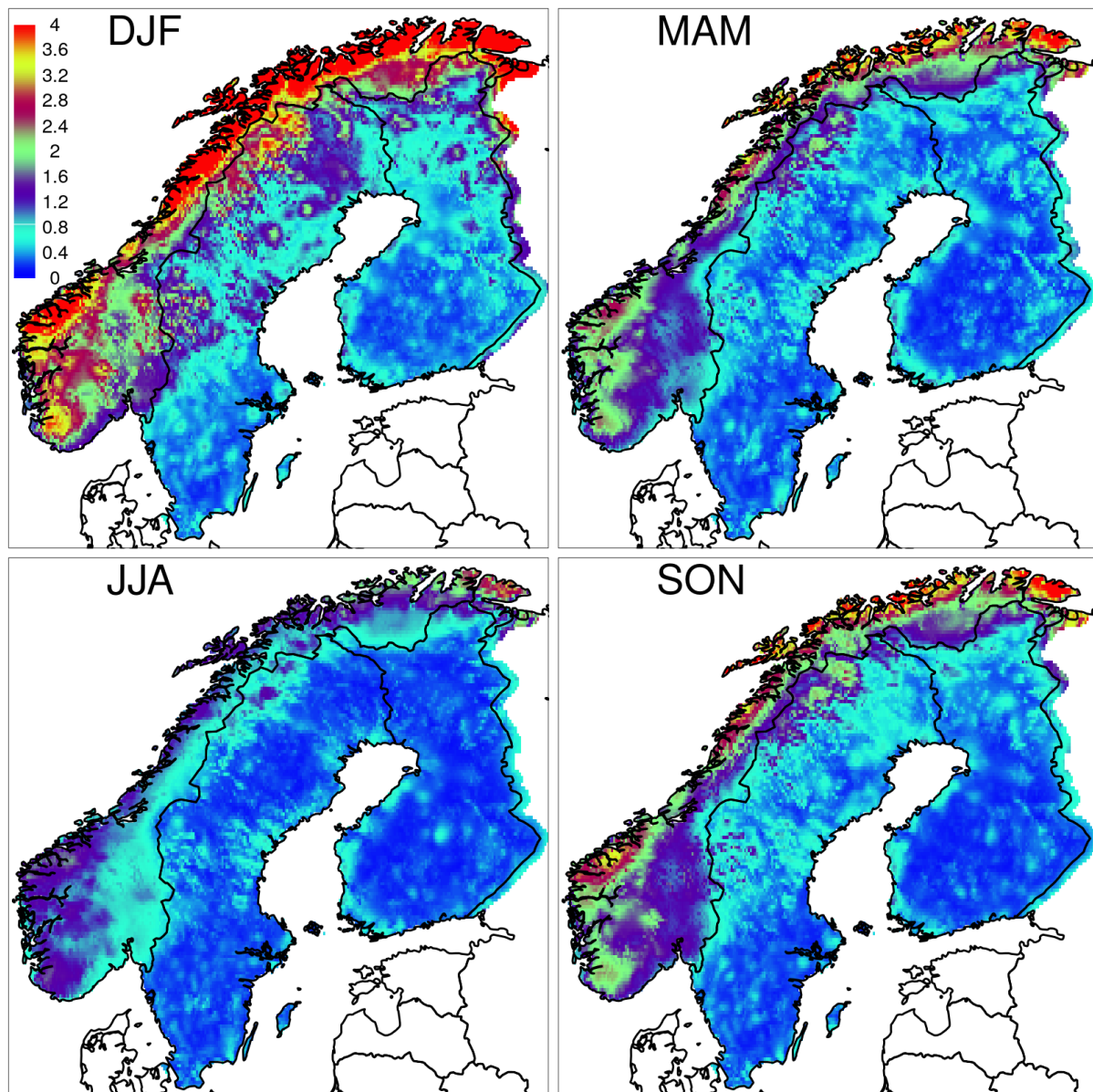


Figure 4.1.3.6. RMSE ( $^{\circ}\text{C}$ ) for daily mean temperature. E-OBS is evaluated against NGCD-2 over the time period 1979-2018.

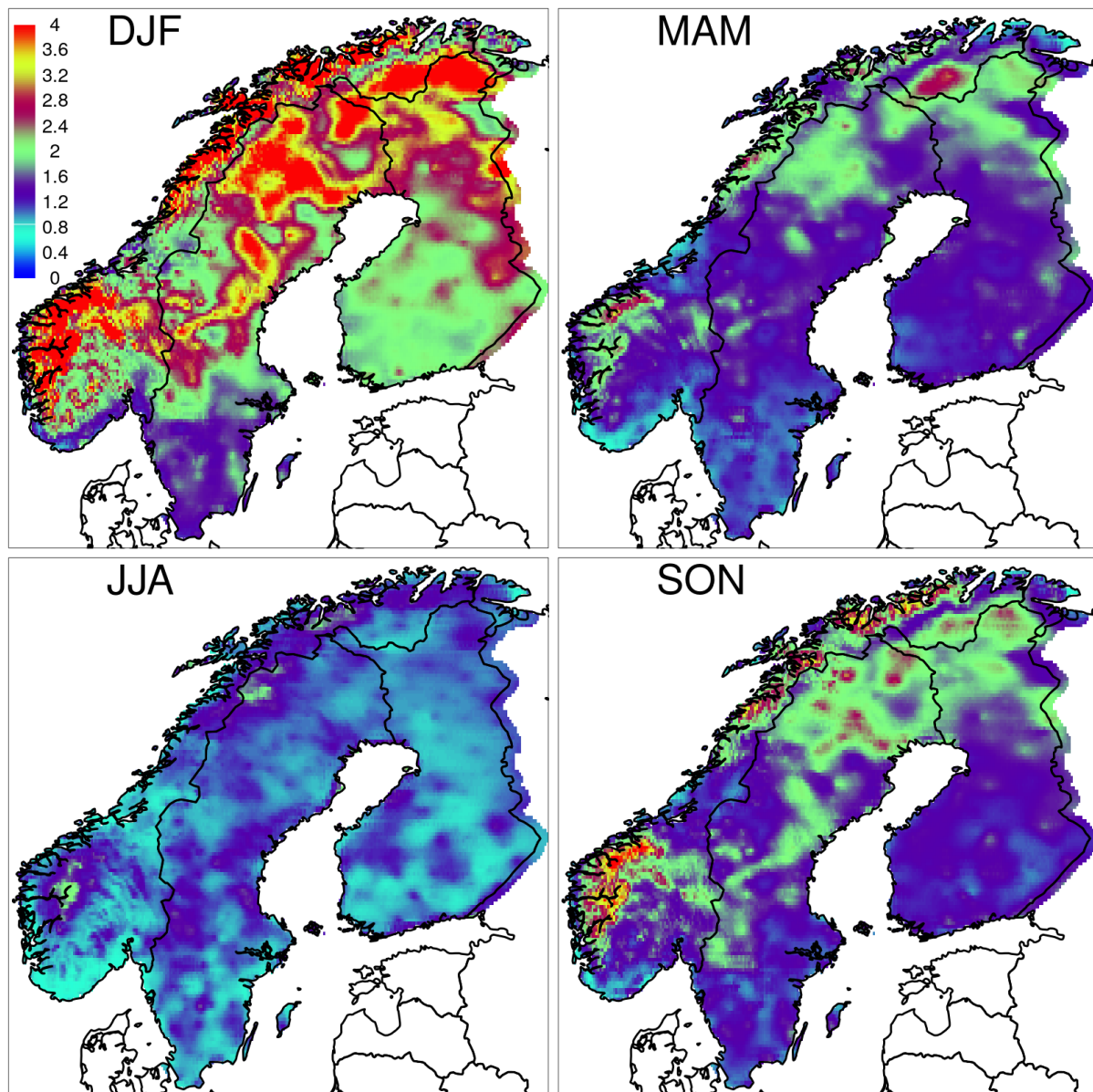


Figure 4.1.3.7. RMSE ( $^{\circ}\text{C}$ ) for daily mean temperature. ERA5-HRES is evaluated against NGCD-1 over the time period 1979-2018.

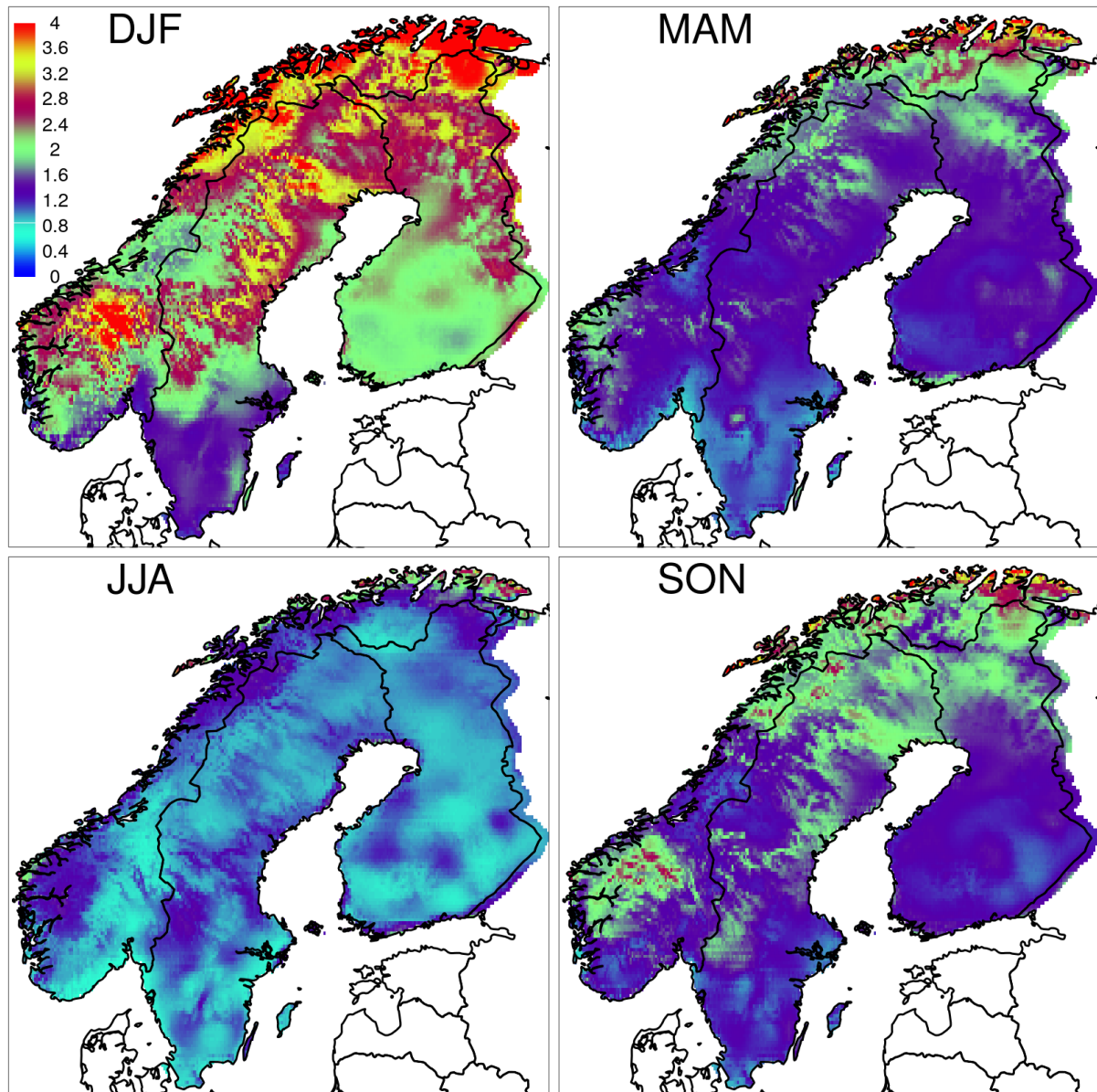


Figure 4.1.3.8. RMSE ( $^{\circ}$ C) for daily mean temperature. ERA5-HRES is evaluated against NGCD-2 over the time period 1979-2018.

ERA5 and ERA5-Land show in general high values of MSESS, although not as high as E-OBS. The best agreement between ERA5 and NGCD is in spring and autumn, the worst ERA5 performances are again in winter and over the Norwegian mountains. ERA5 and NGCD-1 also differ significantly along the coast of Norway in winter. There are also differences between ERA5 and NGCD in correspondence of the big lakes of Sweden (in the south of Sweden) and Finland.

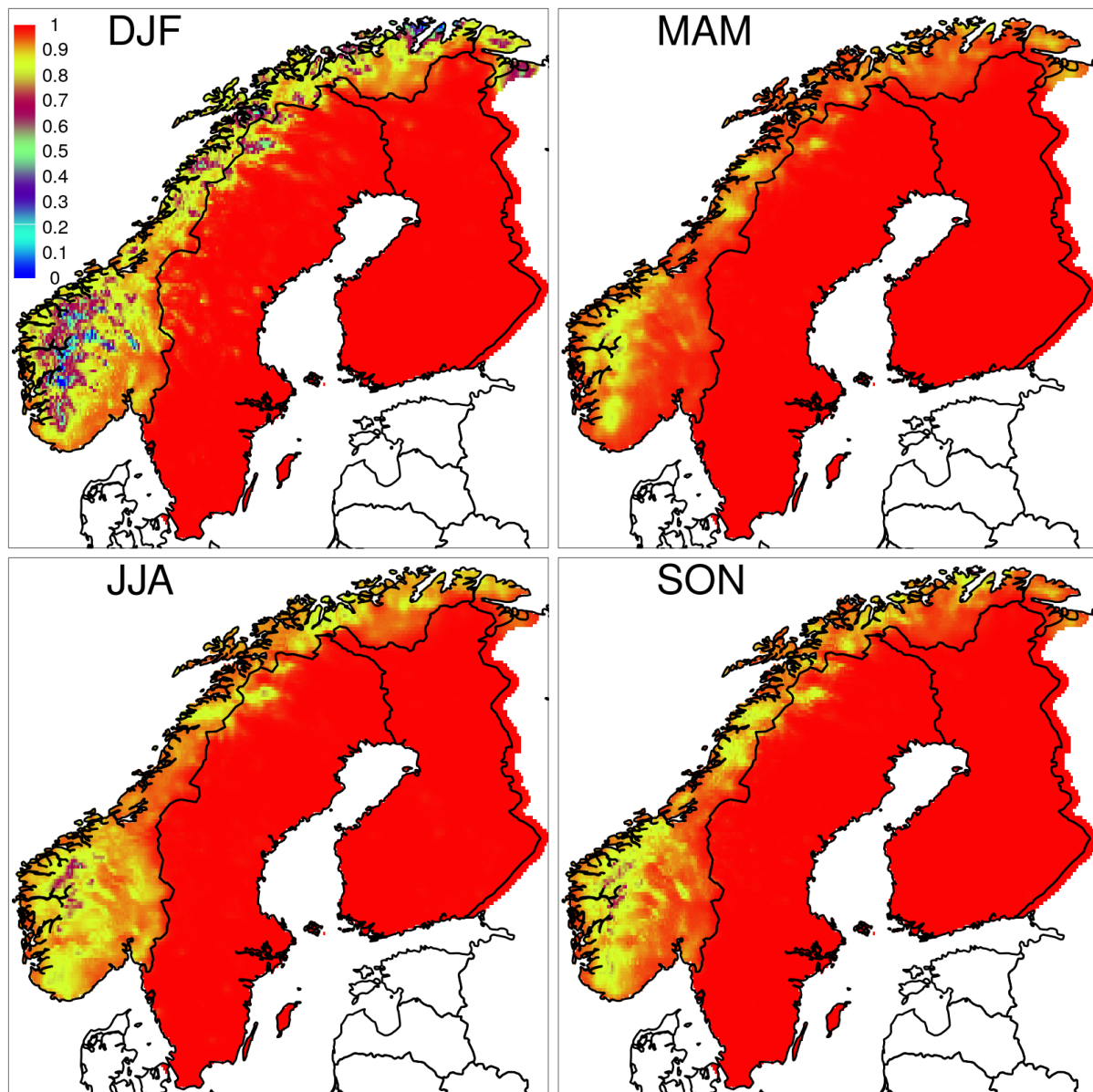


Figure 4.1.3.9. MESS for daily mean temperature. E-OBS is evaluated against NGCD-1 over the time period 1979-2018.

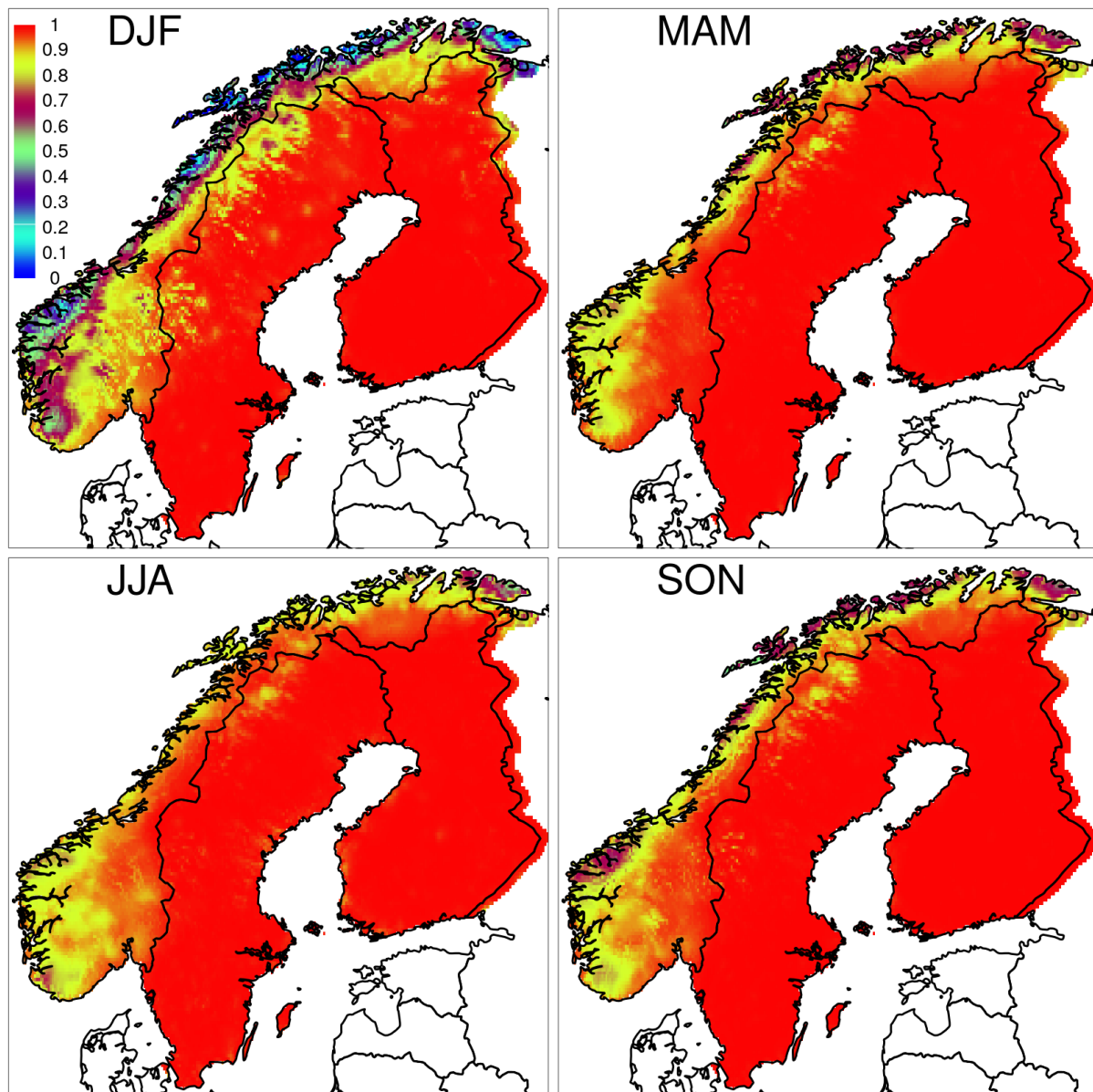


Figure 4.1.3.10. MESS for daily mean temperature. E-OBS is evaluated against NGCD-2 over the time period 1979-2018.

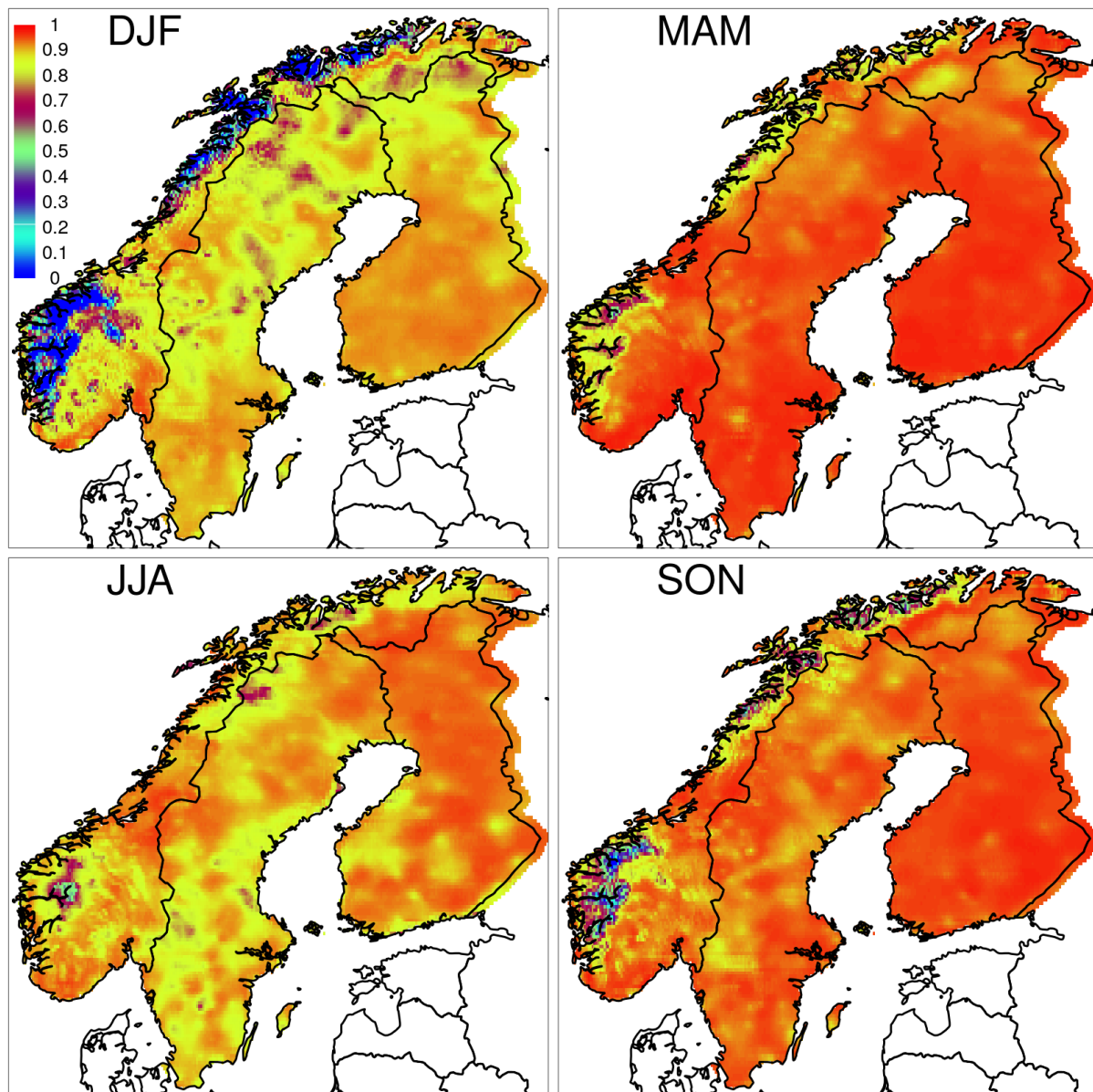


Figure 4.1.3.11. MSESS for daily mean temperature. ERA5-HRES is evaluated against NGCD-1 over the time period 1979-2018.

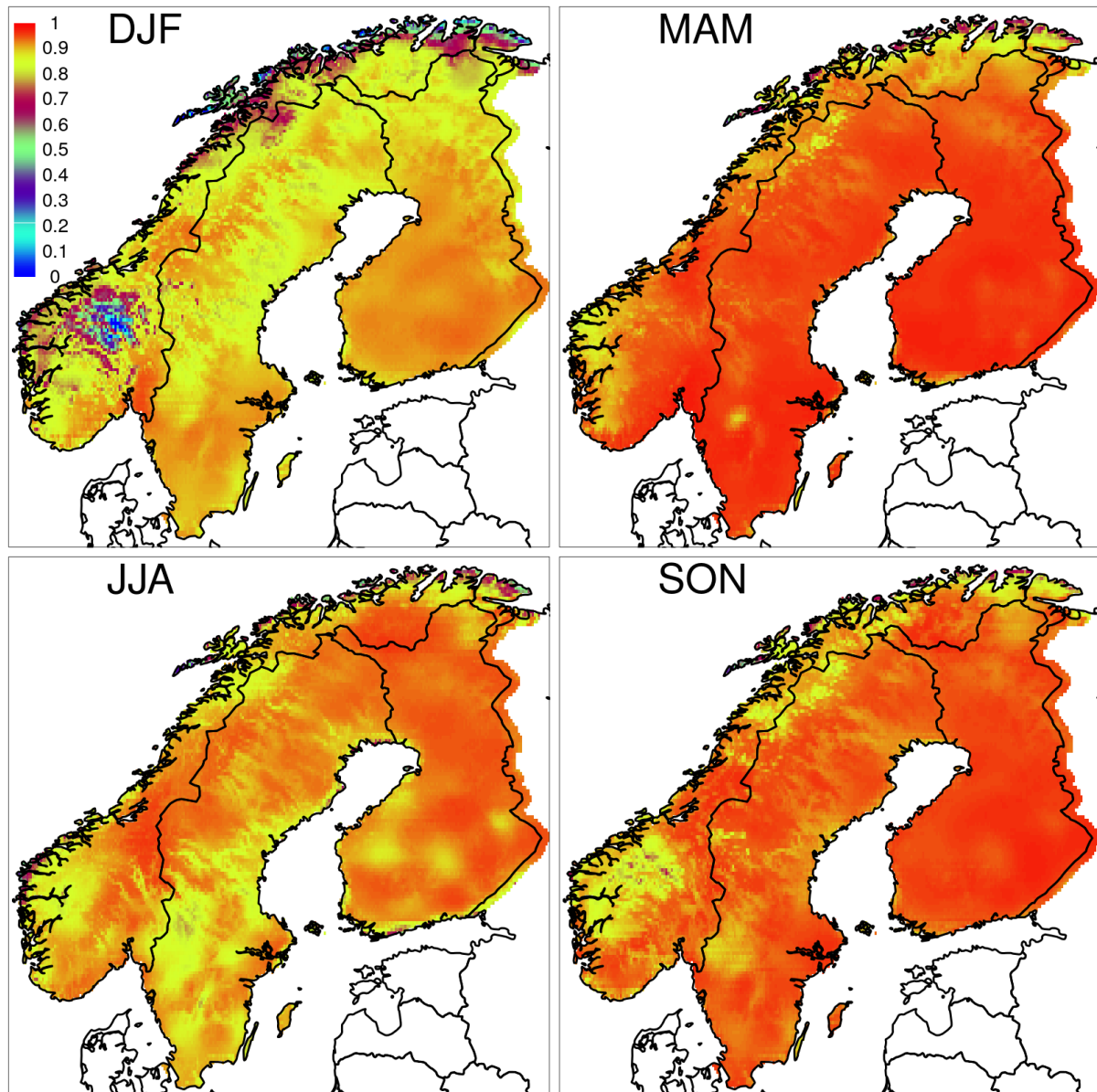


Figure 4.1.3.12. MSESS for daily mean temperature. ERA5-HRES is evaluated against NGCD-2 over the time period 1979–2018.

#### 4.1.4 Case study. Tropical nights in 2018

This case study considers the entire Fennoscandia and we have studied the different representation given by the datasets of the number of tropical nights in 2018, that has been a particularly hot year. As shown in Figure 4.1.4.1, according to E-OBS and the other observational datasets, for 2018 there are some grid points in southern Finland, Sweden and Norway where the number of tropical nights (TR) is greater than 10 nights. E-OBS and NGCD-1 show a similar behavior. NGCD-2 is also quite similar but TR is in general smaller. If compared to E-OBS and NGCD, ERA5 datasets present larger regions in the southern part of the domain with at least one tropical night, such as the whole

coastline of the Baltic sea and the regions in Finland and Sweden where the biggest lakes are located.

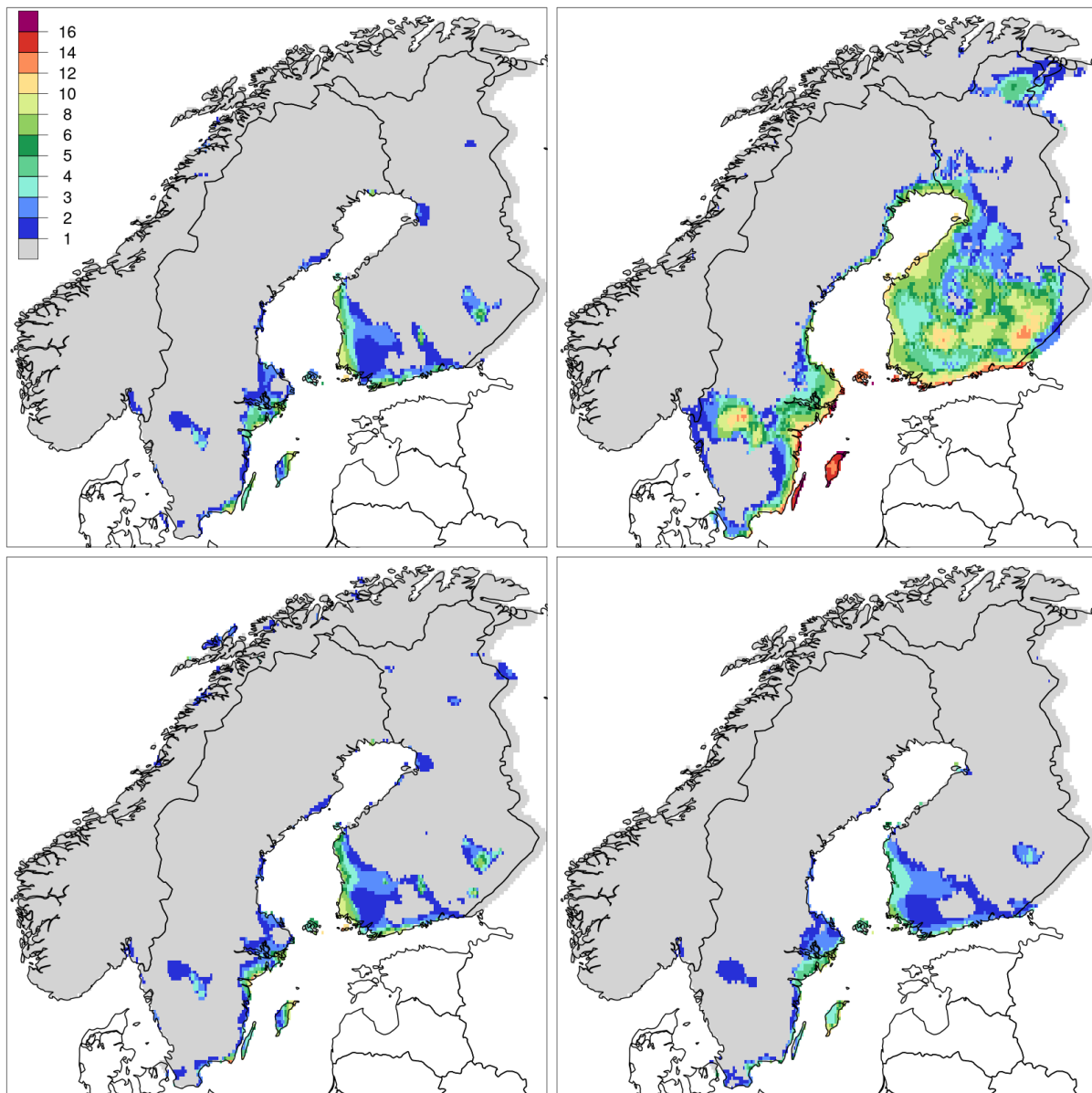


Figure 4.1.4.1. TR (days) in 2018 for the datasets: E-OBS (top-left), ERA5-HRES (top-right), NGCD-1 (bottom-left), NGCD-2 (bottom-right).

#### 4.1.5 Main outcomes – temperature in the Fennoscandia

##### E-OBS

E-OBS temperature climatology over Fennoscandia is very similar to those of NGCD-1 and NGCD-2 datasets. As for precipitation, it can be stated that E-OBS is able to represent the temperature mesoscale features over Fennoscandia. With respect to the cold, heat and multi-element indices, E-



OBS is comparable to NGCD, especially NGCD-1. With respect to temperature extremes, E-OBS and NGCD are also similar. In particular, E-OBS is similar to NGCD-1, because both statistical models represent the coastal effect in a comparable way. The minimum temperatures represented by NGCD-2 in the data sparse region of northern Norway are probably affected by significant uncertainties during winter, when small-scale processes play a relevant role. E-OBS daily fields of mean, minimum and maximum temperature over Sweden and Finland are similar to those of NGCD, with some differences only along the Scandinavian mountains. The situation over Norway is more complex, E-OBS daily fields during winter can differ significantly from NGCD, especially along the coast and in the mountainous region of the south. For the other seasons, the differences between E-OBS and NGCD are less pronounced also over Norway. It is worth remarking again that over Norway NGCD uses a different station network than those used by E-OBS.

## ERA5

ERA5 represents the temperature climatology over Fennoscandia relatively well, especially if used for studies on climatology at the synoptic and Meso-alpha scales. The temperature extremes are often filtered out. As a result, the diurnal temperature range of ERA5 is smaller than that of NGCD and some climate indices, such as the number of tropical nights, differ from NGCD in exceptional situations, such as in 2018. ERA5 climatology differs from NGCD in the regions of the big lakes in Sweden and Finland, it is not clear which representation is more accurate because the observational gridded datasets do not include temperature measurement over the lakes. ERA5 daily fields of temperature differ from NGCD, especially during winter and over Norway. As for E-OBS, also ERA5 shows the worst performances along the coast and in the mountainous regions of the Scandinavian mountains.

## 4.2 Carpathian region

This part of the study aims at assessing the quality of near-surface temperature in the European dataset E-OBS over Czech Republic, Slovakia, Poland, Ukraine, Romania, Serbia, Croatia and Hungary by comparing it against a regional climate dataset, CARPATCLIM, that is specifically designed to model near-surface temperature in the Carpathian region.

### 4.2.1 Analysis of Variance (ANOVA)

The ANOVA method can be used effectively for the characterization of the spatio-temporal properties of CARPATCLIM, E-OBS and ERA5 datasets. The output statistics of the ANOVA procedure (see the Appendix for the methodology). The magnitude and spatial distribution of the specific components of the total variance can be analyzed for different time periods, years and seasons for instance. When a dataset can capture the spatio-temporal variability of a given climate parameter well, that can be settled as a dataset with better quality in general. This methodology is built into the modelling part of method MISH (the MISH interpolation method was applied for producing CARPATCLIM grids) in order to evaluate the modelling results automatically (Szentimrey, 2016).



The main principle of the ANOVA method is that the total variance can be partitioning as the sum of the spatial variance of the temporal means and the spatial mean of the temporal variances on one hand; and the sum of the temporal variance of the spatial means and the temporal mean of the spatial variances on the other hand.

Besides the yearly characteristics, the spring and summer means and variances were analyzed in this study. The spring and summer were chosen from the seasons for presenting here, as the preliminary analysis showed greater differences between datasets in those seasons.

The Table 4.2.1.1 contains the total means and total variances and their partitions for all three analyzed dataset for daily maximum temperatures. The total variance is 6.28 for CARPATCLIM (CCM) what is the sum of the "Spatial variance of temporal mean": 5.43 and "Spatial mean of temporal variances": 0.86 on the one part, and the sum of „Temporal variance of spatial means": 0.78 and „Temporal mean of spatial variances": 5.5 on the other part, as an example. The rest of the measures in Table 4.2.1.1 are illustrated on graphs (Figure 4.2.1.1). The greatest differences turn out in summer in the case of the standard deviation of the temporal mean across the region and in the case of the mean of the spatial variance and spatial standard deviation for the period 1979-2010 (Figure 4.2.1.1). The daily maxima in ERA5 can be characterized with lower spatial variances than the observational datasets.

The spatial means and spatial variances at the moment t are illustrated on graphs and temporal means and temporal variances at a specific location s are illustrated on maps and are compared..

Notations (see the Appendix for more details):

- Et (s) - temporal mean at location s
- Es (t) - spatial mean at time t
- Dt (s) - temporal st. deviation at location s
- Ds (t) - spatial st. deviation at time t

The Et (s), Dt (s) are illustrated on maps, and Es (t), Ds (t) are shown on graphs.

The derived statistics are as follows:

- E - total mean
- Dt - spatial mean of temporal st. deviations
- Ds - temporal mean of spatial st. deviations
- DEt - spatial st. deviation of temporal means
- DEs - temporal st. deviation of spatial means

The Figure 4.2.1.2 shows the time series of the "Es (t)-spatial mean" and "Ds (t)- spatial st. deviation" from 1979 to 2010. CARPATCLIM and E-OBS yearly, spring and summer means of the daily maximum temperatures are running closely, but the curves based on ERA5 are going bottommost. The largest differences between CARPATCLIM and ERA5 can be seen in Figure 4.2.1.2 in summer, 0.63°C on average for the period 1979-2010. The spatial standard deviation characterizing E-OBS and ERA5 remains below CARPATCLIM in the whole period, particularly in spring. There is a large jump in spatial standard deviation of the spring average daily maximum temperatures in E-OBS in 2005, reaching 2.79°C.



The maps in the (Figure 4.2.1.3- 4.2.1.8) show the spatial distribution of the yearly and seasonal means and standard deviations of the daily maximum temperatures for CARPATCLIM region. Lower mean values at higher elevation are obvious in all three dataset. The warmest area goes up in the Great Hungarian plain to a larger extent in CARPATCLIM than it is appearing in E-OBS and in ERA5 for all seasons. Smallest standard deviation of the yearly average Tx shows up in the mountainous area at all three dataset, mentionable that the standard deviation of the yearly average Tx is low in ERA5 almost in the whole territory of Romania (Figure 4.2.1.4.). Patches with relative higher standard deviation values to the surroundings turn out on the yearly and spring maps in the foreground of the Eastern Carpathians in Romania in E-OBS (Figure 4.2.1.4. and Figure 4.2.1.6.). The largest differences of the standard deviations between ERA5 and the observational datasets can be explored in summer, with the lowest values in the Carpathians (Figure 4.2.1.8.). Although the patterns are similar to CARPATCLIM in E-OBS, except the hole displays over the Vojvodina region in Serbia and also the regions with smaller values in Ukraine..

The same tables, graphs and maps were prepared for daily minimum temperatures as for daily maximum temperatures by applying ANOVA analysis. The total variance is 3.56 in the case of yearly average daily minimum temperatures for CARPATCLIM (CCM), that is the sum of the "Spatial variance of temporal mean": 3.12 and „Spatial mean of temporal variances": 0.45 on one part, and the sum of „Temporal variance of spatial means": 0.39 and „Temporal mean of spatial variances": 3.17 on the other part (Table 4.2.1.1.). The measures in Table 4.2.1.1. and the graphs (Figure 4.2.1.9. and Figure 4.2.1.10.) indicates that the lowest daily minima and the smallest variances appear in CARPATCLIM and the highest ones in ERA5. The yearly and seasonal means derived from E-OBS and CARPATCLIM are close. The mean and standard deviation series run together from 1979-2010, ERA5 is running at the uppermost (Figure 4.2.1.10.).

The features of the topography can be explored on the map of the yearly mean minima (Figure 4.2.1.11.). Higher values than in CARPATCLIM ( $>7^{\circ}\text{C}$  yearly averages) are standing out between the Lake Balaton and the Danube River in E-OBS in Hungary and in extended regions in Serbia in ERA5 too. ERA5 overestimates the mean spring daily minima almost the whole territory of Hungary. E-OBS also provides higher spring average minima in the middle area of Hungary than CARPATCLIM (Figure 4.2.1.13.) The spatial distribution of the summer mean daily minima are similar in each dataset, although greater values are presented in E-OBS near the Lake Balaton and in Serbia, and also in ERA5 at the south-east of the domain (Figure 4.2.1.15.). The standard deviation of the yearly average daily minima is decreasing from north to south across the region (Figure 4.2.1.12.). The patches with higher standard deviation on the yearly map of E-OBS tracing out the locations of the measuring stations which are involved in E-OBS. The spring standard deviation maps are quite smooth, the highest values appear in the north-east of the domain at each dataset. The overall standard deviation of the average summer daily minima is smaller in ERA5 than in CARPATCLIM (Figure 4.2.1.16.). On the map illustrating E-OBS in the Figure 4.2.1.16. large jumps can be seen in relatively small distances which cannot link to the geographical position, rather depend on the amount of station data used for gridding.

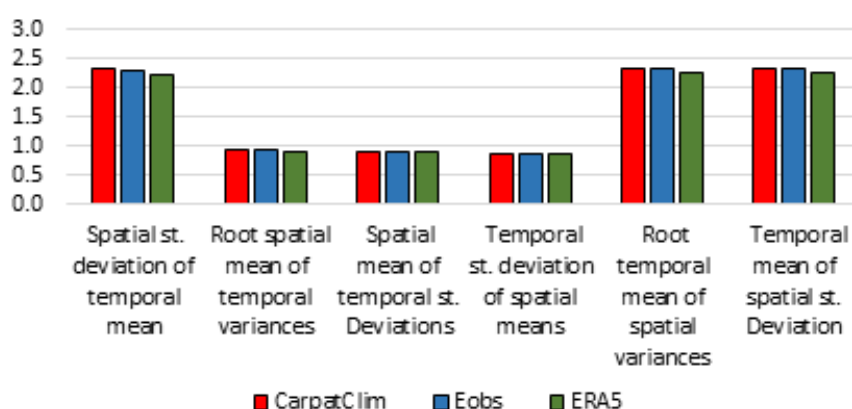
## ANOVA TX



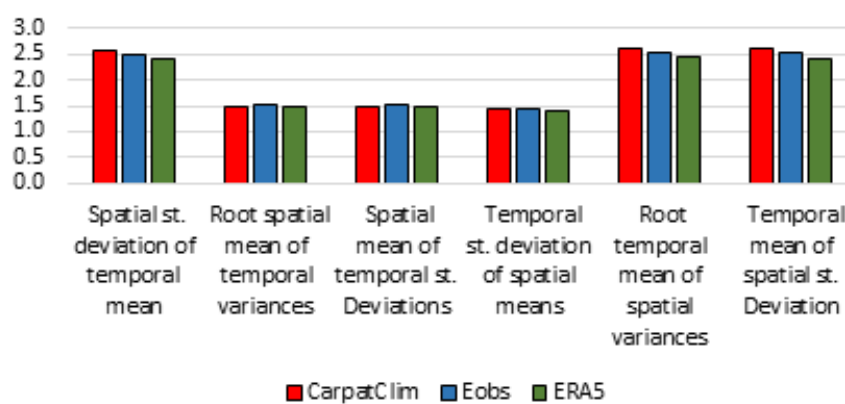
	Tx_Year			Tx_Spring			Tx_Summer		
	CCM	E-OBS	ERA5	CCM	E-OBS	ERA5	CCM	E-OBS	ERA5
Total mean	14.05	13.97	13.46	14.71	14.68	14.12	24.78	24.77	24.15
Total variance	6.28	6.18	5.86	8.92	8.49	7.91	9.17	8.46	8.15
Spatial variance of temporal mean	5.43	5.32	5.02	6.67	6.21	5.7	7.61	6.92	6.64
Spatial mean of temporal variances	0.86	0.86	0.83	2.25	2.28	2.21	1.57	1.55	1.51
Temporal variance of spatial means	0.78	0.76	0.75	2.06	2.04	2.02	1.33	1.28	1.23
Temporal mean of spatial variances	5.5	5.41	5.11	6.86	6.45	5.89	7.84	7.18	6.92
Spatial st. deviation of temporal mean	2.33	2.31	2.24	2.58	2.49	2.39	2.76	2.63	2.58
Root spatial mean of temporal variances	0.93	0.93	0.91	1.5	1.51	1.49	1.25	1.24	1.23
Spatial mean of temporal st. Deviations	0.92	0.92	0.91	1.5	1.51	1.48	1.25	1.24	1.22
Temporal st. deviation of spatial means	0.88	0.87	0.87	1.44	1.43	1.42	1.15	1.13	1.11
Root temporal mean of spatial variances	2.35	2.33	2.26	2.62	2.54	2.43	2.8	2.68	2.63
Temporal mean of spatial st. Deviation	2.34	2.32	2.26	2.61	2.53	2.42	2.79	2.67	2.62

Table 4.2.1.1. Results of ANOVA for yearly, spring and summer mean daily maximum temperatures for CARPATCLIM (CCM), E-OBS and ERA5 datasets in the period 1979-2010.

### ANOVA\_TX\_YEAR



### ANOVA\_TX\_SPRING



### ANOVA\_TX\_SUMMER

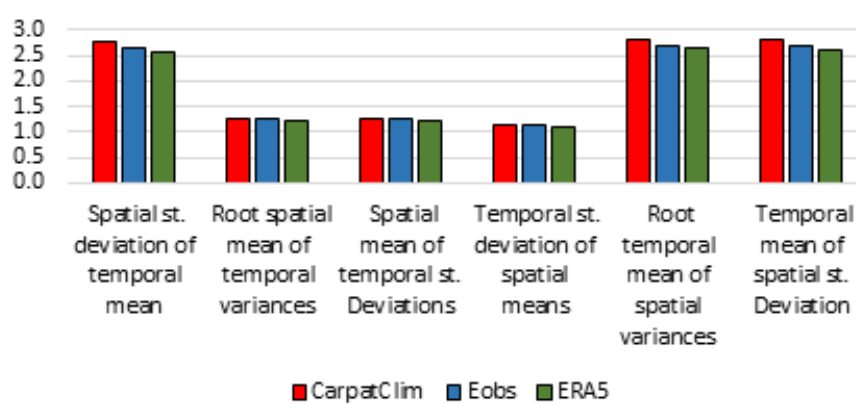
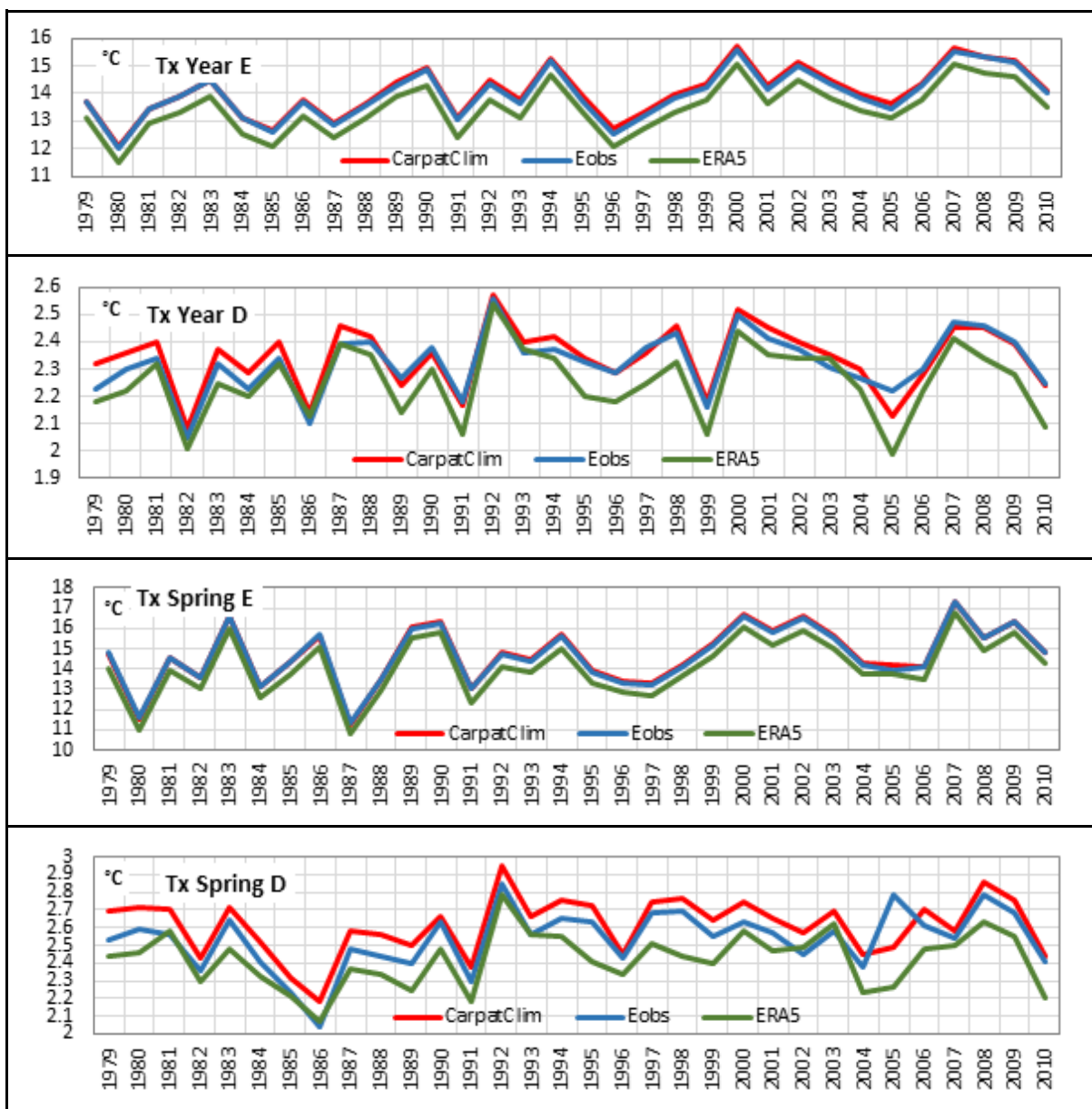




Figure 4.2.1.1 Output statistics of ANOVA of daily maximum temperatures for CARPATCLIM, E-OBS and ERA5 for the period 1979-2010.



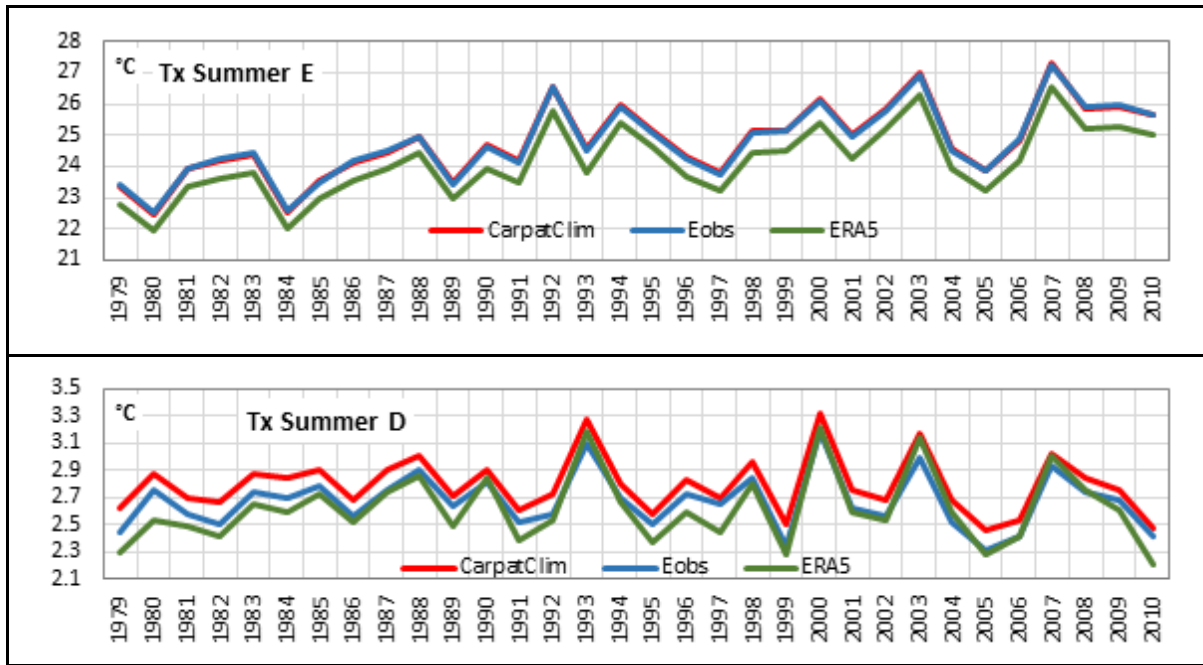
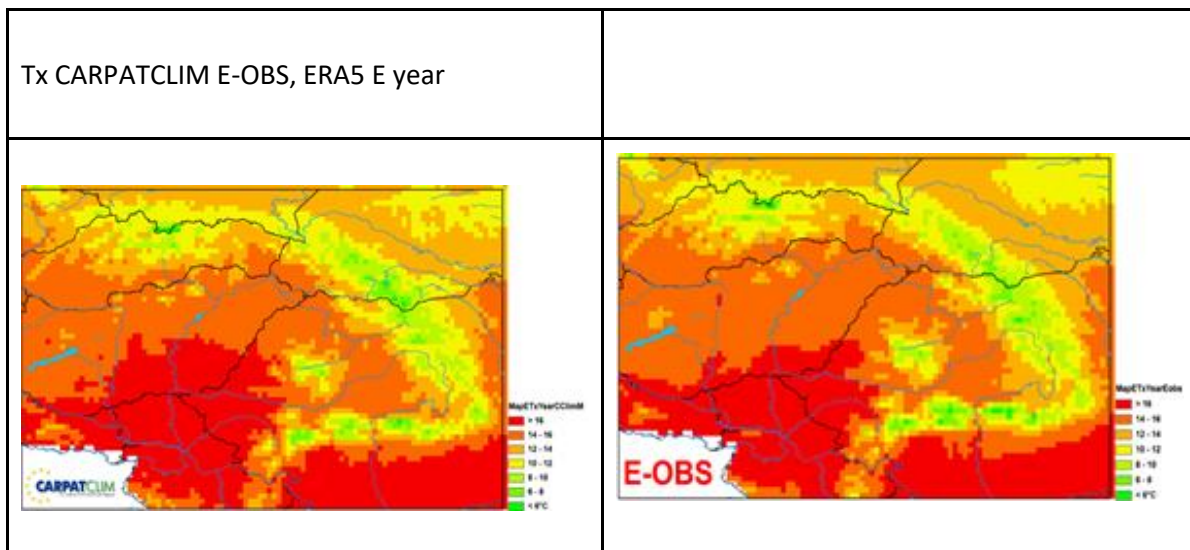


Figure 4.2.1.2 Yearly, spring and summer Es (t)-spatial mean and Ds (t)- spatial st. deviation from 1979-2010 for CARPATCLIM, E-OBS and ERA5.



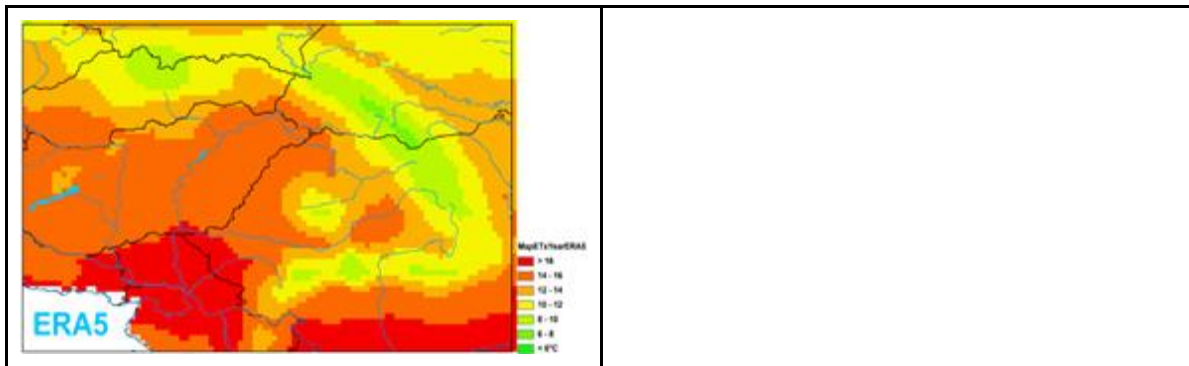


Figure 4.2.1.3 Et (s)-temporal mean of the yearly average daily maximum temperatures for CARPATCLIM, E-OBS and ERA5 datasets in the period 1979-2010.

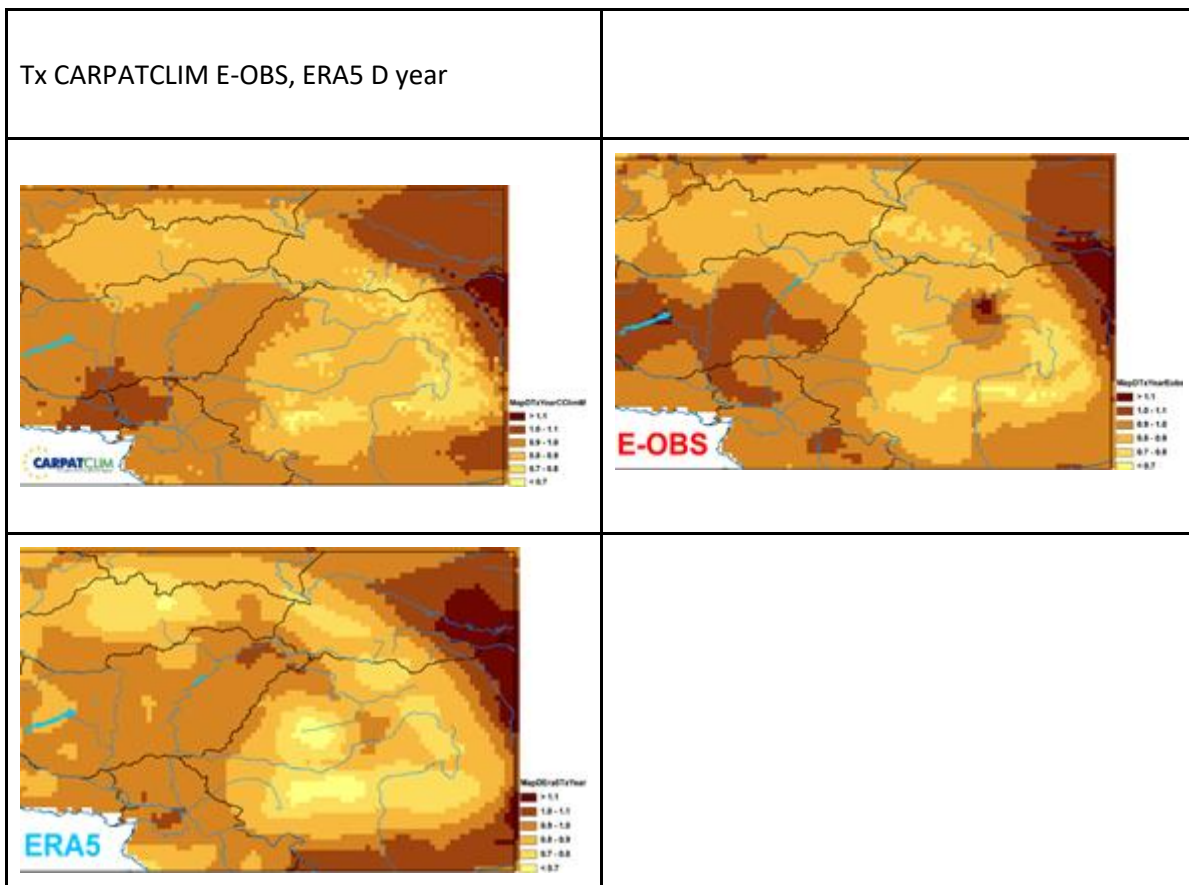


Figure 4.2.1.4. Dt (s)-temporal st. deviation of the yearly average daily maximum temperatures for CARPATCLIM, E-OBS and ERA5 datasets in the period 1979-2010.

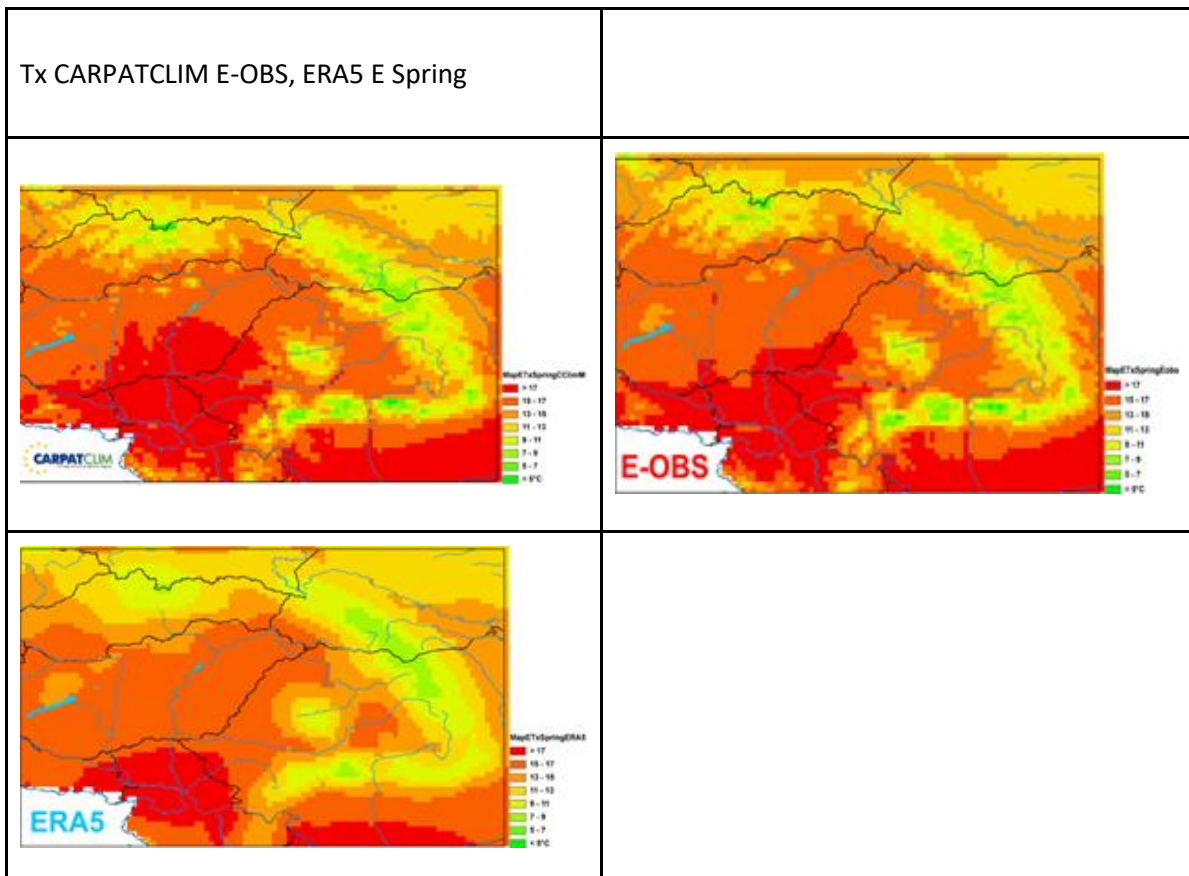
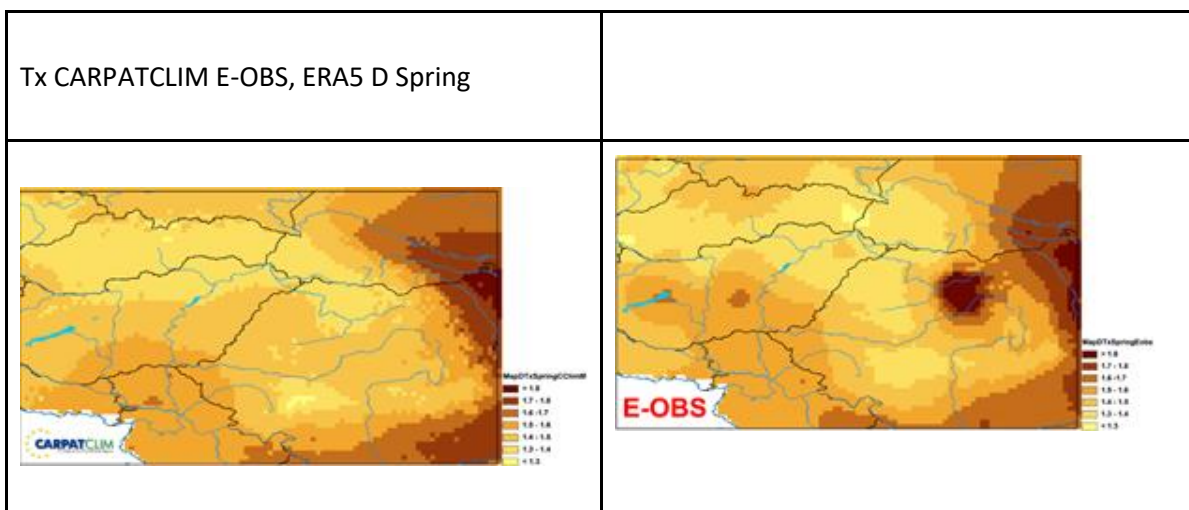


Figure 4.2.1.5. Et (s)-temporal mean of the spring average daily maximum temperatures for CARPATCLIM, E-OBS and ERA5 datasets in the period 1979-2010.



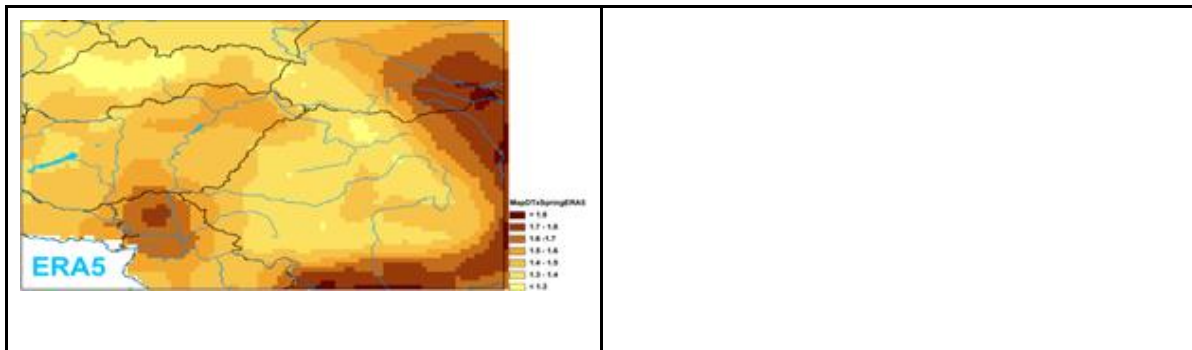


Figure 4.2.1.6. Dt (s)-temporal st. deviation of the spring average daily maximum temperatures for CARPATCLIM, E-OBS and ERA5 datasets in the period 1979-2010.

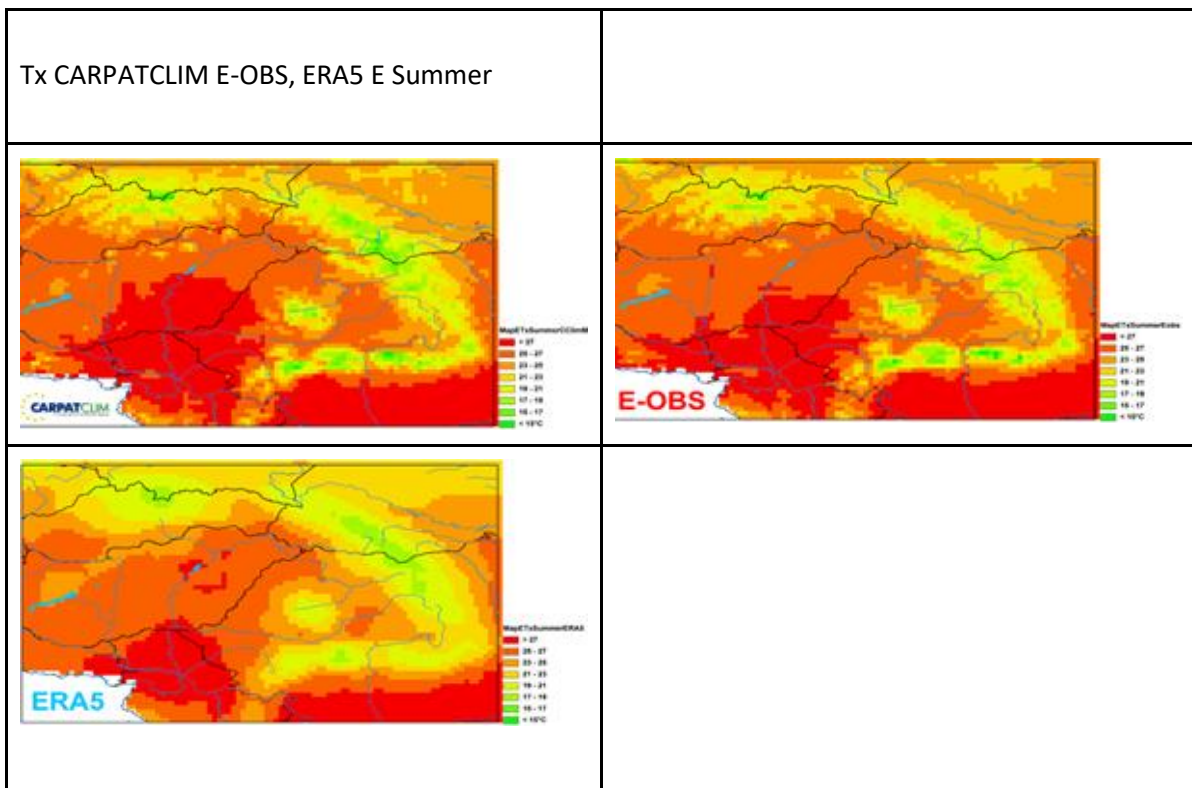
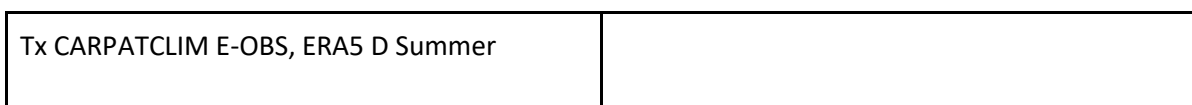


Figure 4.2.1.7. Et (s)-temporal mean of the summer average daily maximum temperatures for CARPATCLIM, E-OBS and ERA5 datasets in the period 1979-2010.



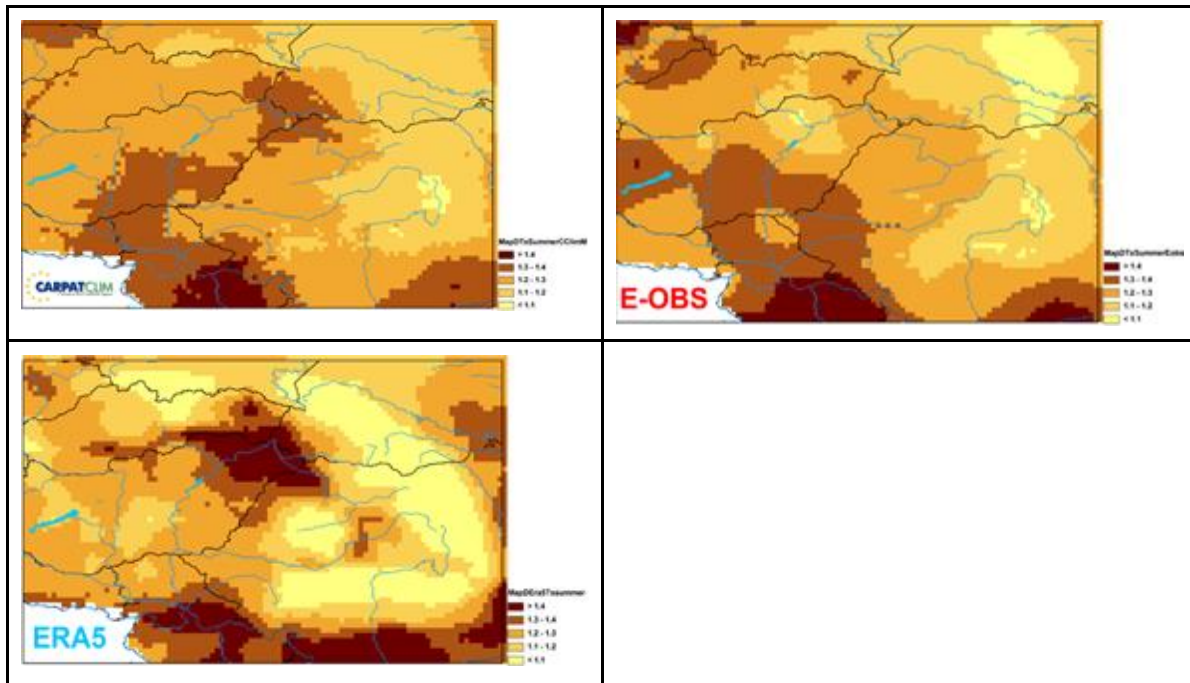


Figure 4.2.1.8. Dt (s)-temporal st. deviation of the summer average daily maximum temperatures for CARPATCLIM, E-OBS and ERA5 datasets in the period 1979-2010.

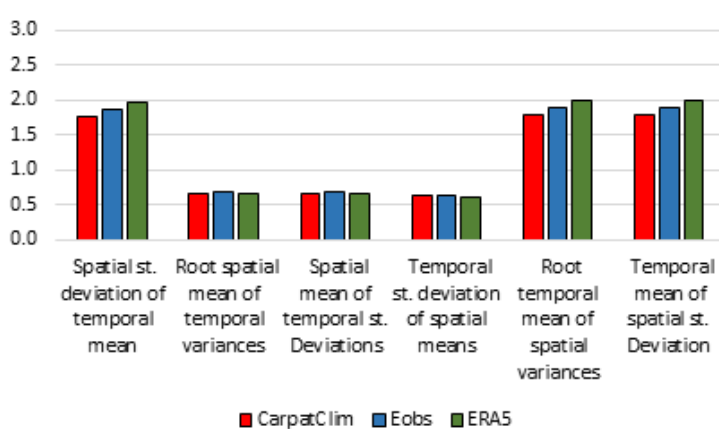
#### Anova TN

	Tn_Year			Tn_Spring			Tn_Summer		
	CCM	E-OBS	ERA5	CCM	E-OBS	ERA5	CCM	E-OBS	ERA5
Total mean	4.35	4.37	4.74	4.07	4.12	4.6	13.03	13.06	13.5
Total variance	3.56	4.01	4.36	4.43	4.79	5.14	4.28	4.64	5.18
Spatial variance of temporal mean	3.12	3.54	3.91	3.55	3.9	4.24	3.59	3.94	4.59
Spatial mean of temporal variances	0.45	0.47	0.45	0.87	0.89	0.9	0.68	0.7	0.59
Temporal variance of spatial means	0.39	0.4	0.38	0.78	0.77	0.78	0.61	0.59	0.5

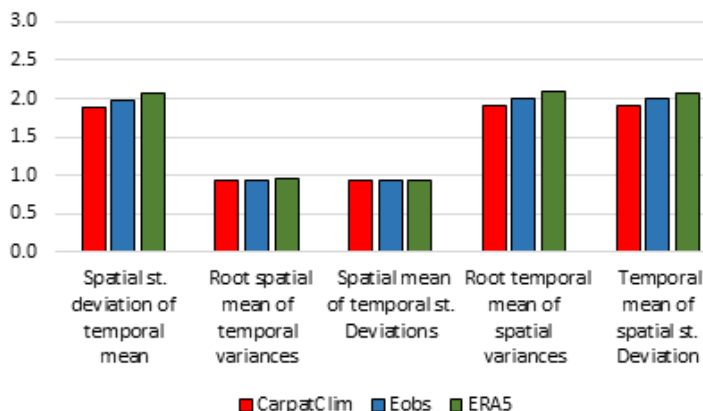
Temporal mean of spatial variances	3.17	3.61	3.98	3.65	4.02	4.35	3.67	4.05	4.68
Spatial st. deviation of temporal mean	1.77	1.88	1.98	1.89	1.97	2.06	1.9	1.99	2.14
Root spatial mean of temporal variances	0.67	0.68	0.67	0.93	0.94	0.95	0.83	0.84	0.77
Spatial mean of temporal st. Deviations	0.67	0.68	0.66	0.93	0.94	0.94	0.83	0.83	0.76
Temporal st. deviation of spatial means	0.63	0.63	0.62	0.88	0.88	0.89	0.78	0.77	0.71
Root temporal mean of spatial variances	1.78	1.9	2	1.91	2.01	2.09	1.91	2.01	2.16
Temporal mean of spatial st. Deviation	1.78	1.9	1.99	1.91	2	2.08	1.91	2.01	2.16

Table 4.2.1.2. Results of ANOVA for annual, spring and summer mean of daily minimum temperatures for CARPATCLIM (CCM), E-OBS and ERA5 datasets in the period 1979-2010

### ANOVA\_TN\_YEAR



## ANOVA\_TN\_SPRING



## ANOVA\_TN\_SUMMER

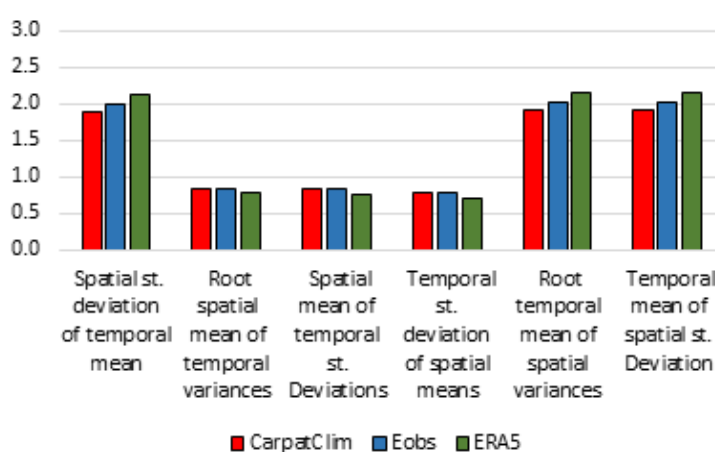
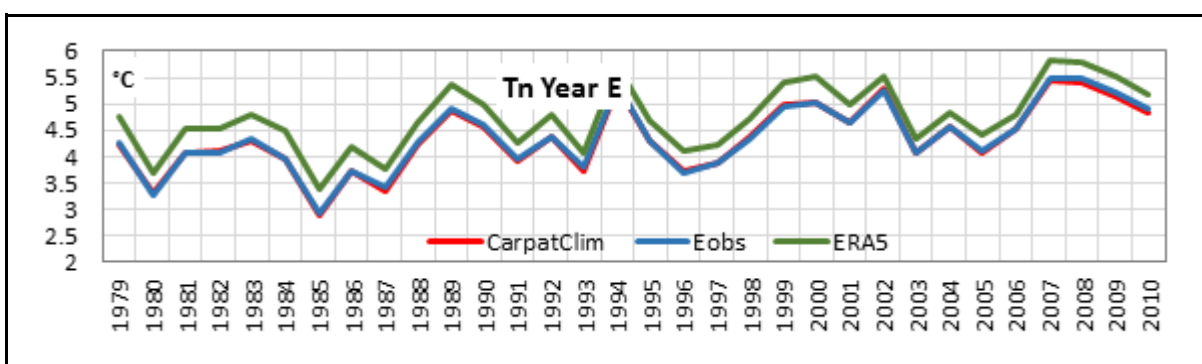
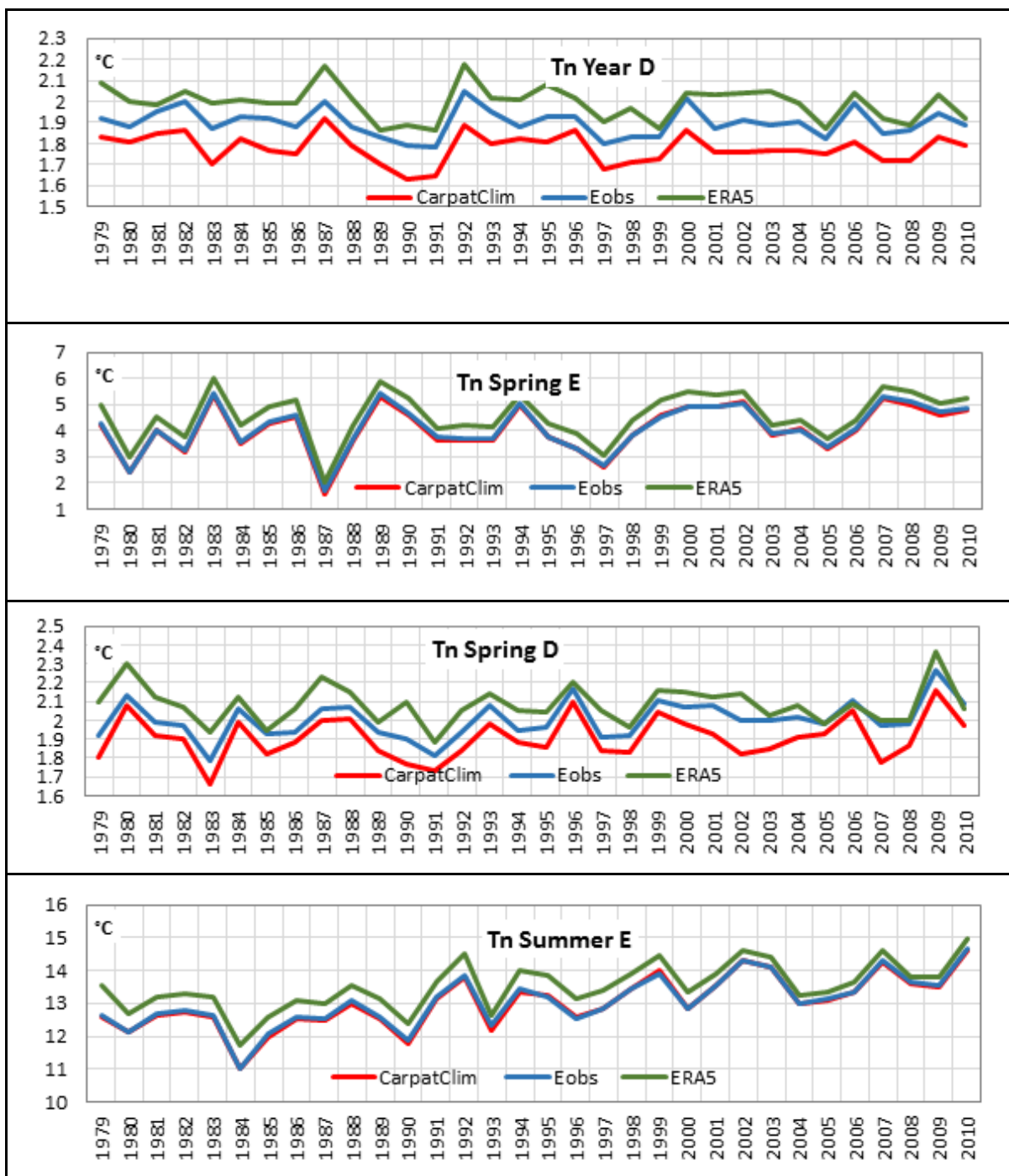


Figure 4.2.1.9. The output statistics of ANOVA of daily maximum temperatures for CARPATCLIM, E-OBS and ERA5 for the period 1979-2010.





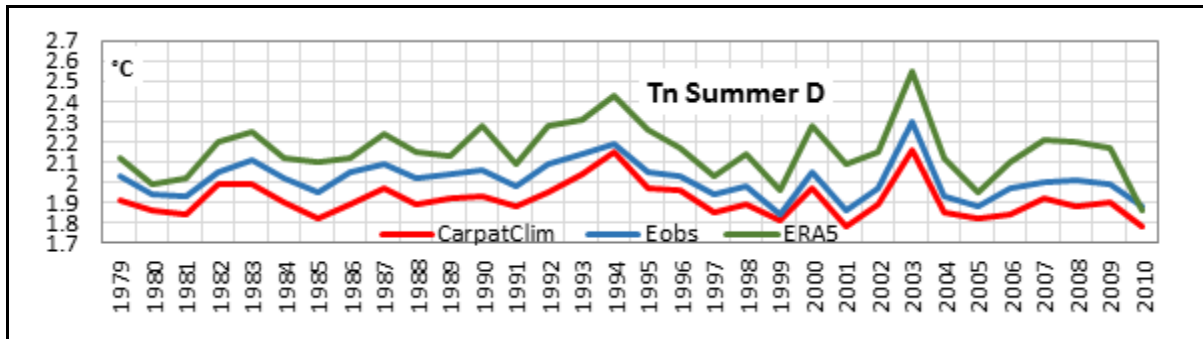


Figure 4.2.1.10. Yearly, spring and summer Es (t)-spatial mean and Ds (t)- spatial st. deviation for CARPATCLIM, E-OBS and ERA5 dataset in the period 1979-2010.

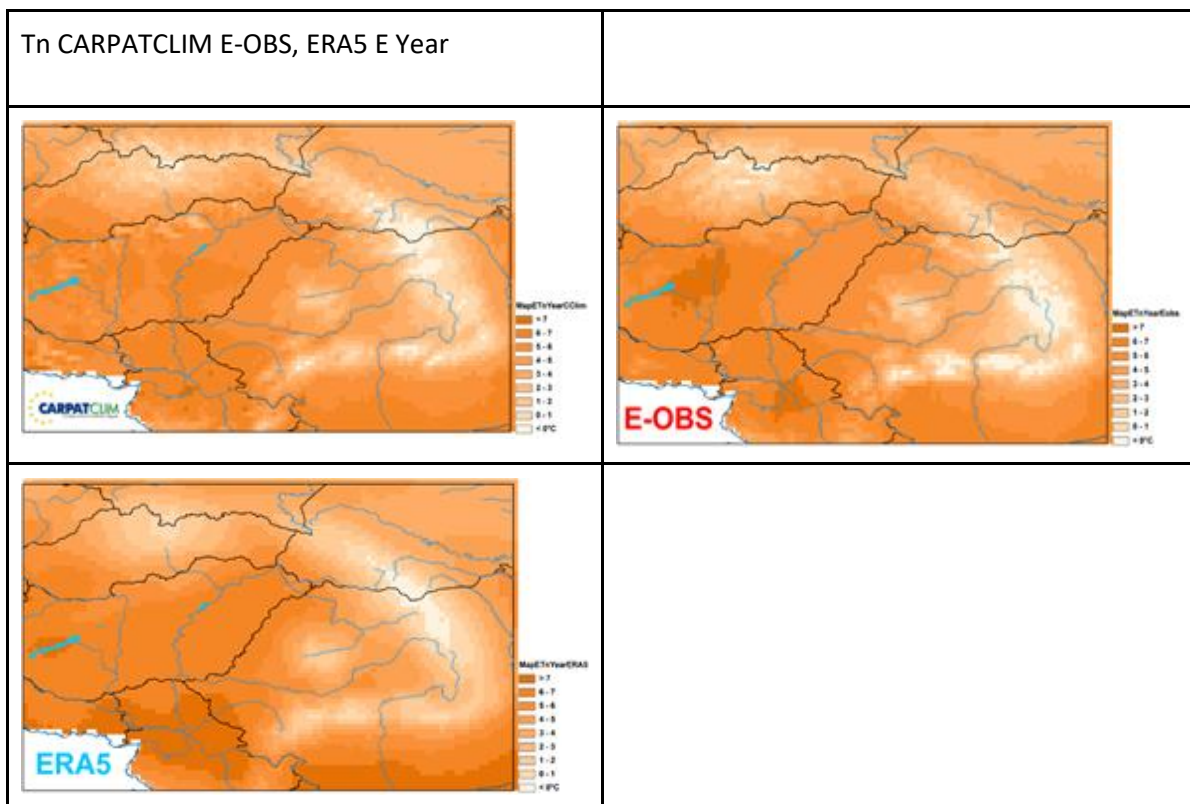


Figure 4.2.1.11. Yearly average (Et (s)-temporal mean) daily minimum temperatures for CARPATCLIM, E-OBS and ERA5 datasets in the period 1979-2010.

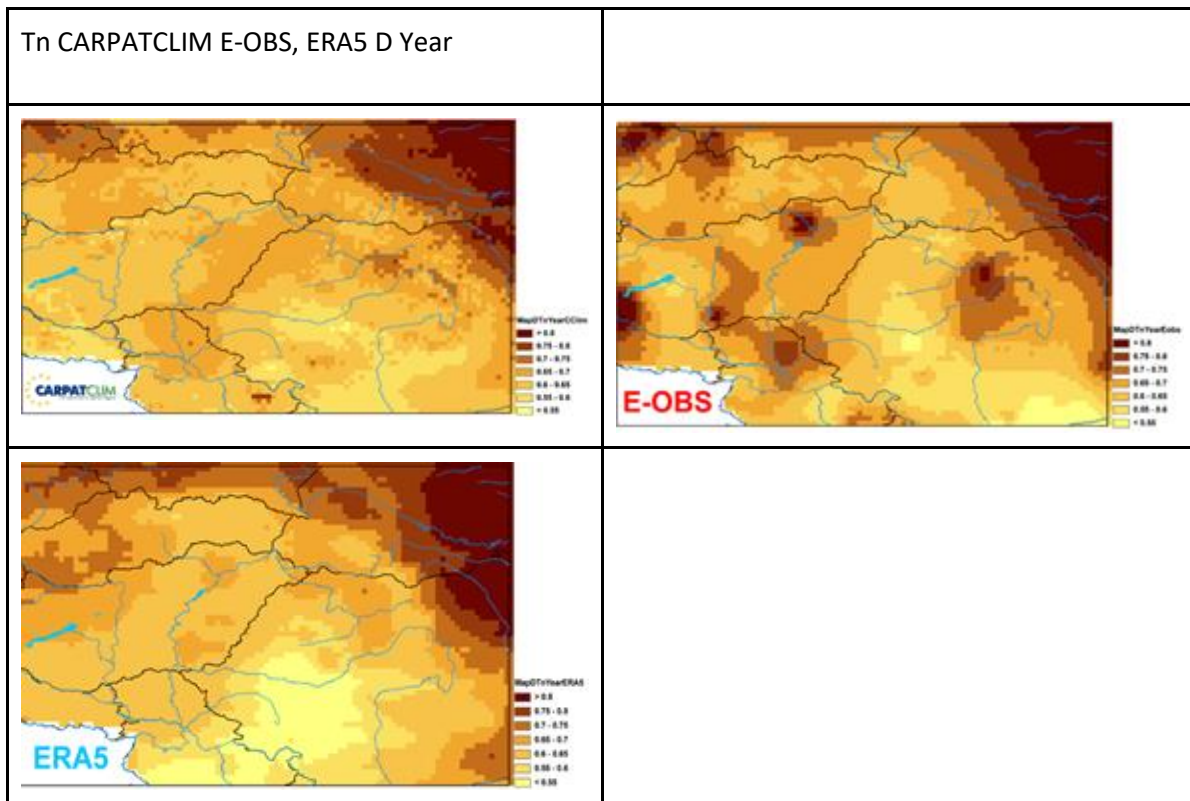


Figure 4.2.1.12. Dt (s)-temporal st. deviation of the yearly average daily minimum temperatures for CARPATCLIM, E-OBS and ERA5 datasets in the period 1979-2010.

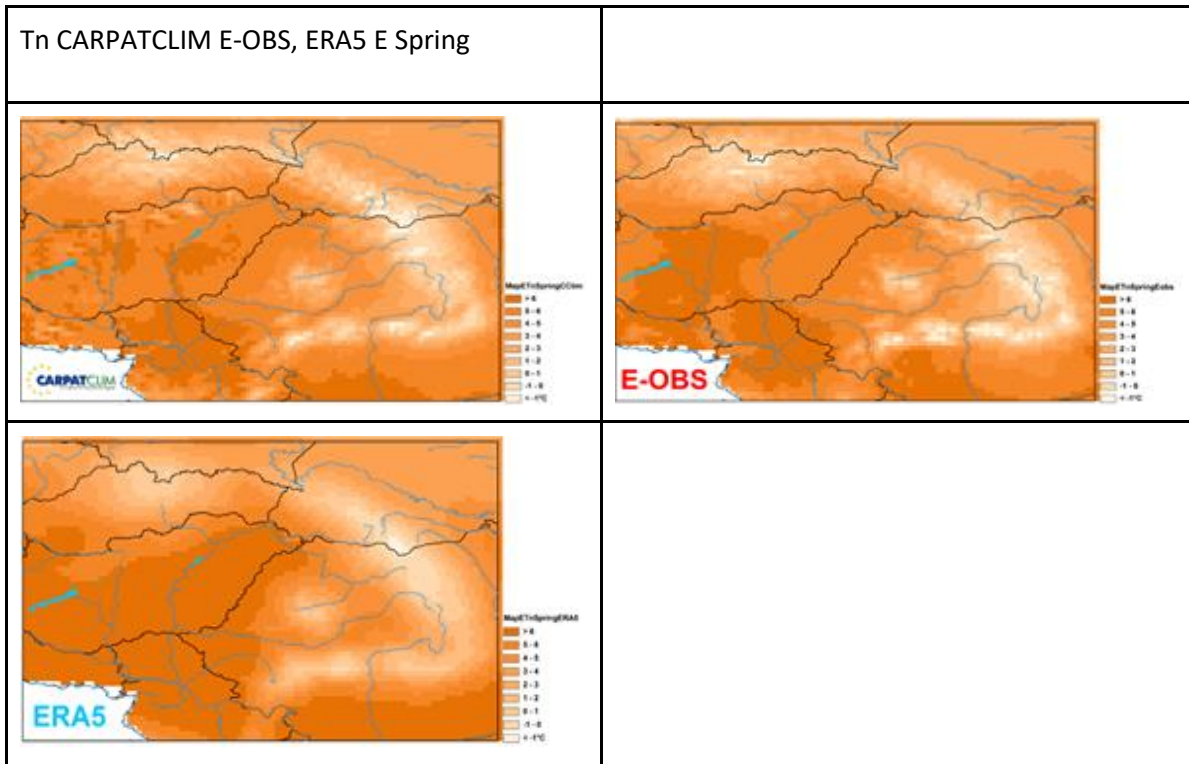


Figure 4.2.1.13. Spring average ( $Et$  (s)-temporal mean) daily minimum temperatures for CARPATCLIM, E-OBS and ERA5 datasets in the period 1979-2010.

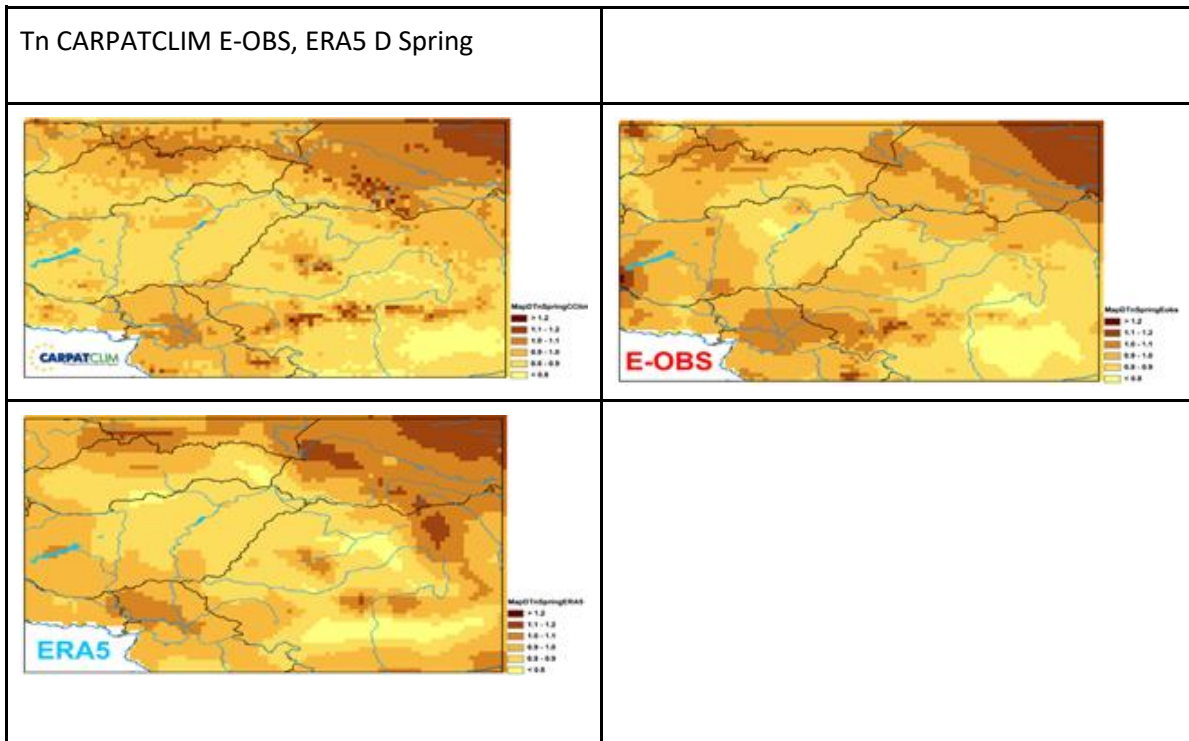


Figure 4.2.1.14. Dt (s)-temporal st. deviation of the spring average daily minimum temperatures for CARPATCLIM, E-OBS and ERA5 datasets in the period 1979-2010.

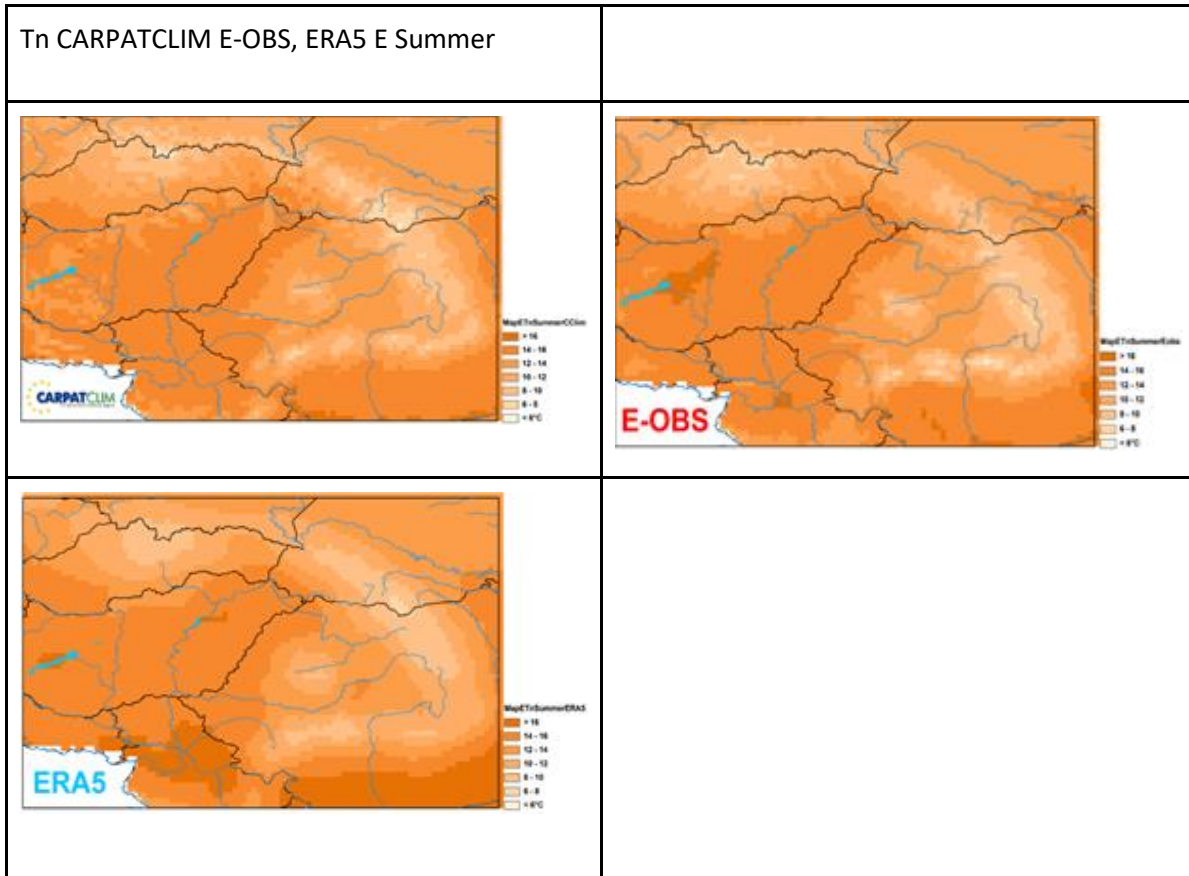
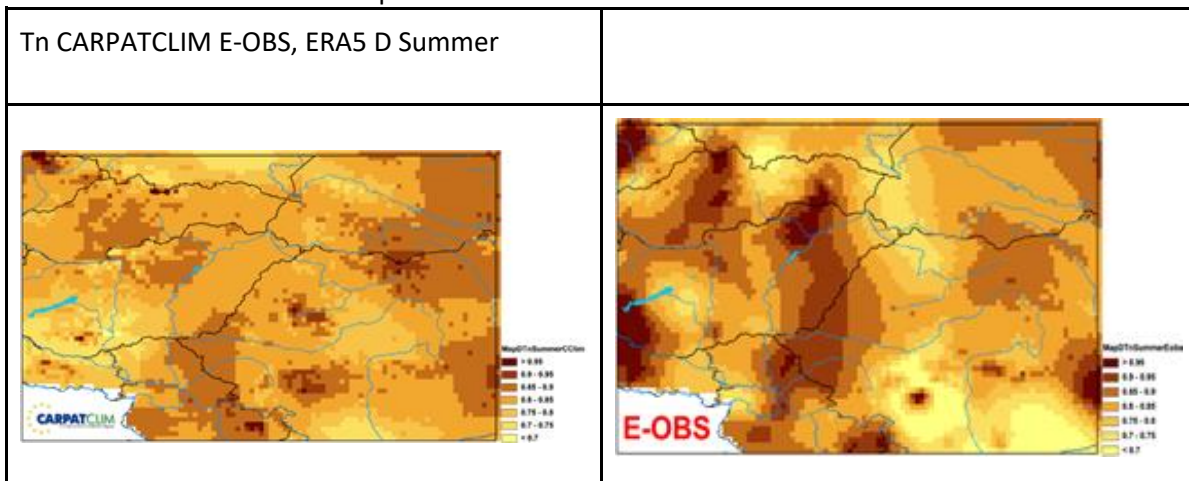


Figure 4.2.1.15. Summer average ( $E_t$  (s)-temporal mean) daily minimum temperatures for CARPATCLIM, E-OBS and ERA5 datasets in the period 1979-2010.



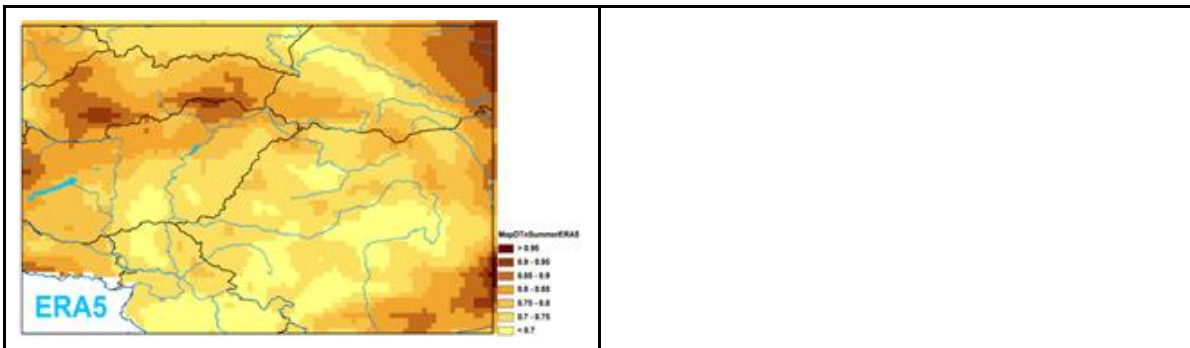
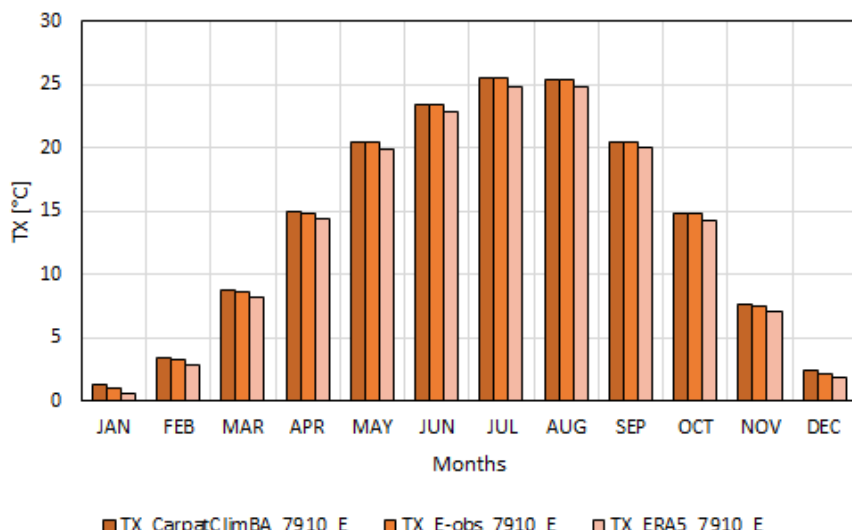


Figure 4.2.1.16. Dt (s)-temporal st. deviation of the summer average daily minimum temperatures for CARPATCLIM, E-OBS and ERA5 datasets in the period 1979-2010.

#### 4.2.2 Yearly cycle

The yearly and seasonal means and standard deviation maps are analyzed in the previous chapter. The monthly means of the daily maximum temperatures and their standard deviations averaged on the grid covering CARPATCLIM region can be seen in the Figure 4.2.2.1. CARPATCLIM and E-OBS produce almost the same monthly values. From November to January the differences between the two observational datasets are around 0.2°C in favor of CARPATCLIM, lesser in the other months. ERA5 monthly average maxima are lower at least half degree during the year in areal average (Figure 4.2.2.1, top). In the summer half year (more precisely from April to October) average monthly Tx can be characterized by 1.84°C standard deviation value, what is smaller than the rest of the year (2.53°C), otherwise there are no substantial differences in the monthly standard deviations between the datasets ( Figure 4.2.2.1 bottom).

Considering the monthly means of the daily minima CARPATCLIM provides the lowest minima at each month close to E-OBS. ERA5 overestimates the daily minimum temperatures at least by half degree from April to August (Figure 4.2.2.2, top). The monthly standard deviations are the highest in January and in February near to 3°C, then again half of it from April to October in all three datasets with a little overestimation in ERA5, except July and August (Figure 4.2.2.2, bottom).



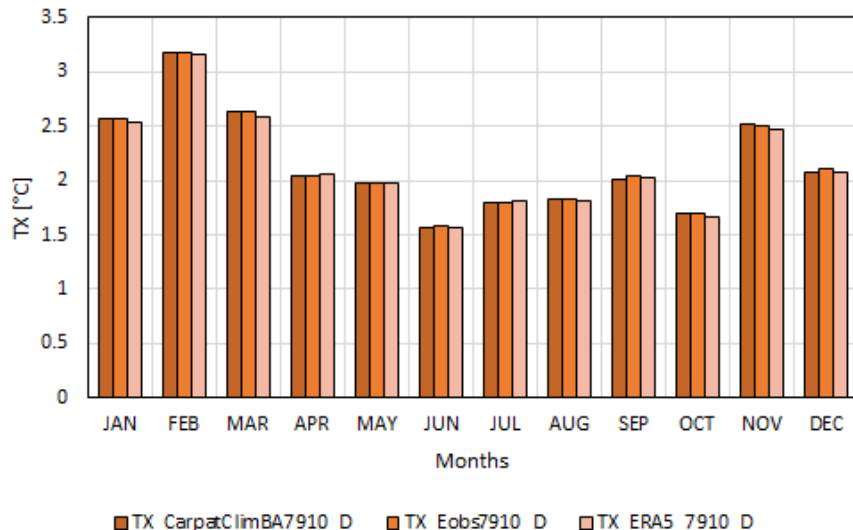
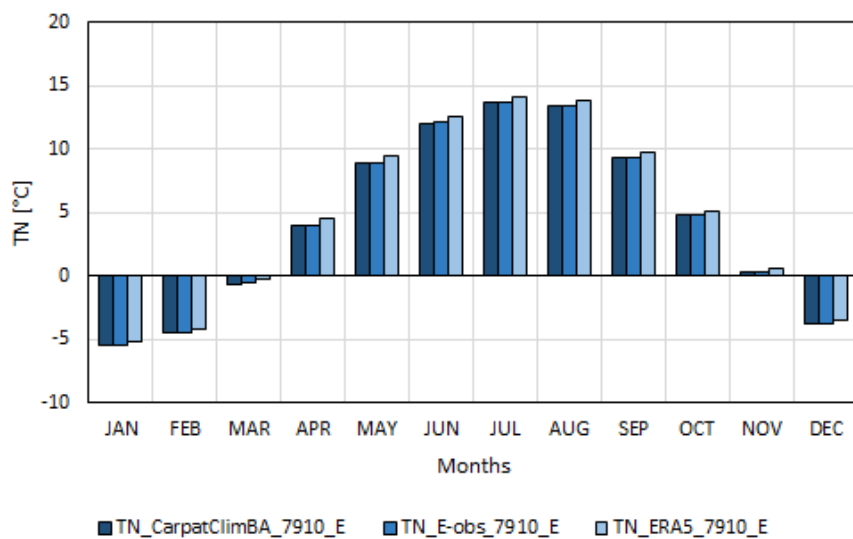


Figure 4.2.2.1. The monthly means of the daily maximum temperatures (top) and their standard deviations (bottom) averaged on CARPATCLIM domain for CARPATCLIM, E-OBS and ERA5 in the period 1979-2010.



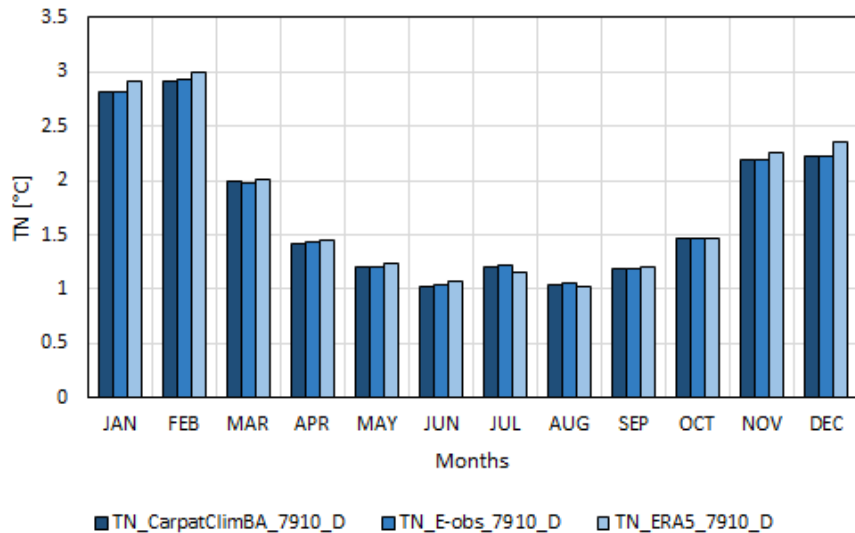
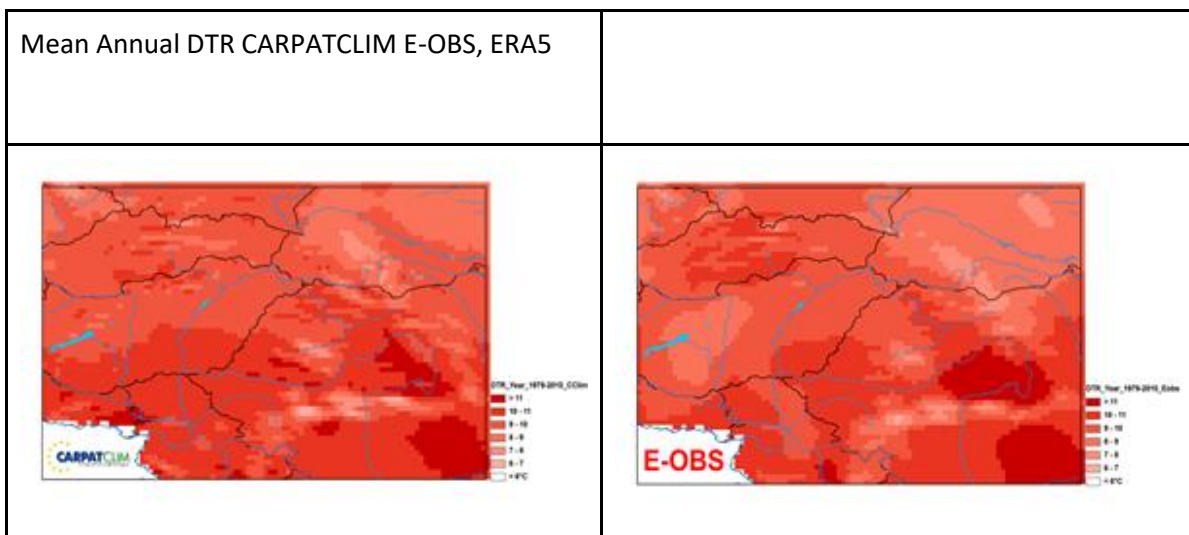


Figure 4.2.2.2. The monthly means of the daily minimum temperatures and their standard deviations averaged on CARPATCLIM domain for CARPATCLIM, E-OBS and ERA5 in the period 1979-2010.

#### 4.2.3 Mean annual DTR

The yearly mean of the diurnal temperature range is 9.77 in regional average in CARPATCLIM, 9.63 in E-OBS and 8.87 in ERA5. The ranking follows from that fact that the CAPATCLIM produces the lowest minima and highest maxima amongst the datasets we examined. The maps in Figure 4.2.3.1. show the spatial distribution of the mean annual DTR. The area illustrated with DTR above 10  $^{\circ}\text{C}$  is much wider below the half-court of Hungary in CARPATCLIM than in E-OBS and it is missing from ERA5 DTR map. The higher daily minima in E-OBS resulted in lower DTR values in the Transdanubia region in Hungary.



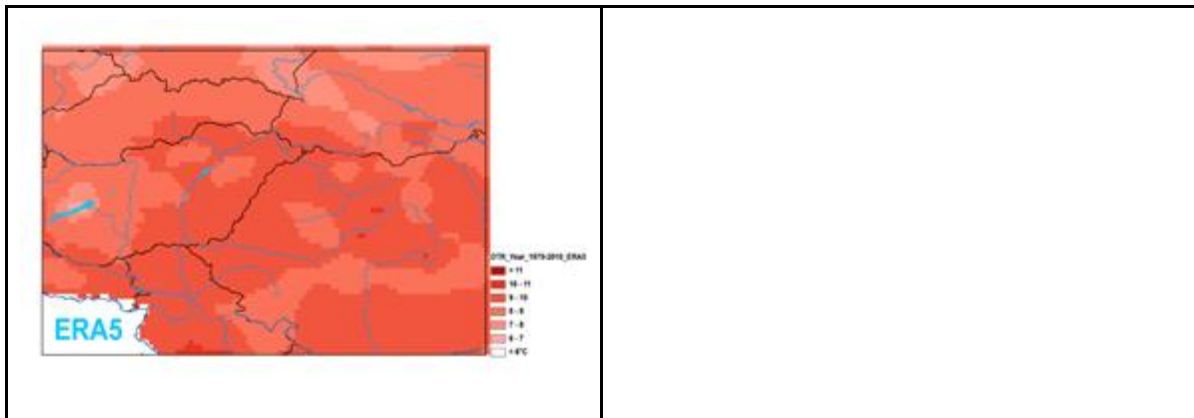


Figure 4.2.3.1. Mean annual diurnal temperature range ( $^{\circ}\text{C}$ ) for CarpatClim (top left) for E-OBS (top right) and ERA5 (bottom, left).

#### 4.2.4 Quantiles TX and TN

An important feature of a dataset is how it is able to describe the extremes. The Q95 quantile of the maximum temperatures represents the warm extremes and the Q05 of the minimum temperatures represents the cold extremes. The quantiles based on the monthly maxima (highest daily maximum per months) and monthly minima (lowest daily minimum per months) values as the samples are examined first and then all the daily data were considered as the sample to the quantile estimates. The spatial distribution of the Q95 quantiles of monthly (Figure 4.2.4.1) and daily (Figure 4.2.4.3) values are the same. Higher values appear in the flat region in the middle of the basin (between 36 and 38 $^{\circ}\text{C}$ ) and lower ones at higher altitudes (Figure 4.2.4.1). CARPATCLIM and E-OBS Q95 maps are detailed and similar. The spatial distribution of the Q95 quantiles in ERA5 is corresponding to the observational datasets, although there are underestimations in Slovakia and in Romania and besides these, the region with high values, above 40  $^{\circ}\text{C}$  appears at the south bound of domain in ERA5, what is missing from CARPATCLIM and E-OBS (Figure 4.2.4.1, bottom left). The spatial distribution of the Q95 quantiles of daily maxima is the same as the monthly maxima, but the daily Q95 quantiles are lower as it is expected. The highest values appear in the Great Hungarian Plain and on the Romanian Plain at each dataset with 30-32  $^{\circ}\text{C}$  Q95 values, although the Vojvodina region near to the Romanian border in Serbia is proven to be warmer as the Q95 quantile exceeds the 32 $^{\circ}\text{C}$ . The map of ERA5 daily Q95 quantiles is more schematic to the observational datasets. The main features of the orography are evident in Figure 4.2.4.3 (bottom, left) and also the measures of the values are the same as in the larger geographical region as the observational datasets.

The cold extremes, namely the coldest Q05 of monthly minima come up at the highest mountains necessarily in all three dataset, around -26 $^{\circ}\text{C}$ . The highest differences between CARPATCLIM and E-OBS can be found in Ukraine as a whole, and at the meeting of the Slovakian, Polish and Ukraine border, where E-OBS provides less cold Q05 monthly quantiles Figure 4.2.4.2 (top left and right). ERA5 is closer to CARPATCLIM in Ukraine than to E-OBS, but in the region of Eastern Beskids it is less extremely cold than CARPATCLIM (Figure 4.2.4.2 (bottom, left)).

The daily Q05 quantiles are colder in E-OBS at High Tatras in Slovakia (lower than -15°C in more grid points) than in CARPATCLIM, but warmer (by 2 °C approximately) in the North-eastern Carpathians around the highest peaks in E-OBS and in the territory of the Ukraine Podolian Highland also (Figure 4.2.4.4 top left and right). ERA5 Q05 map represents values in Ukraine closer to CARPATCLIM than E-OBS (Figure 4.2.4.4, bottom left). CARPATCLIM depicts the North-Western Carpathian much better in detail than ERA5.

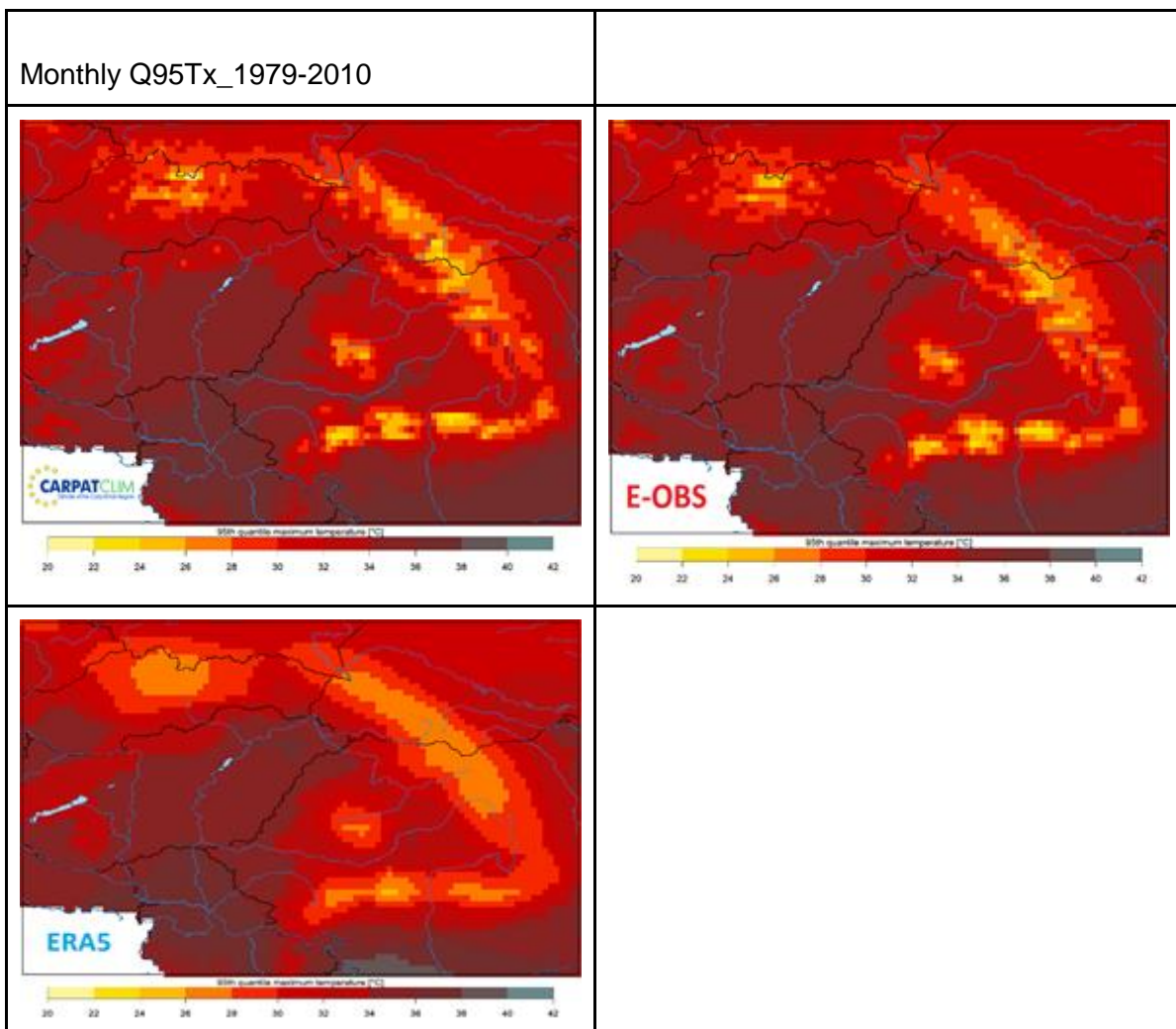


Figure 4.2.4.1. Q95 quantiles (monthly) based on the monthly maxima of the daily Tx for CARPATCLIM (top left), for E-OBS (top right) and ERA5 (bottom, left).

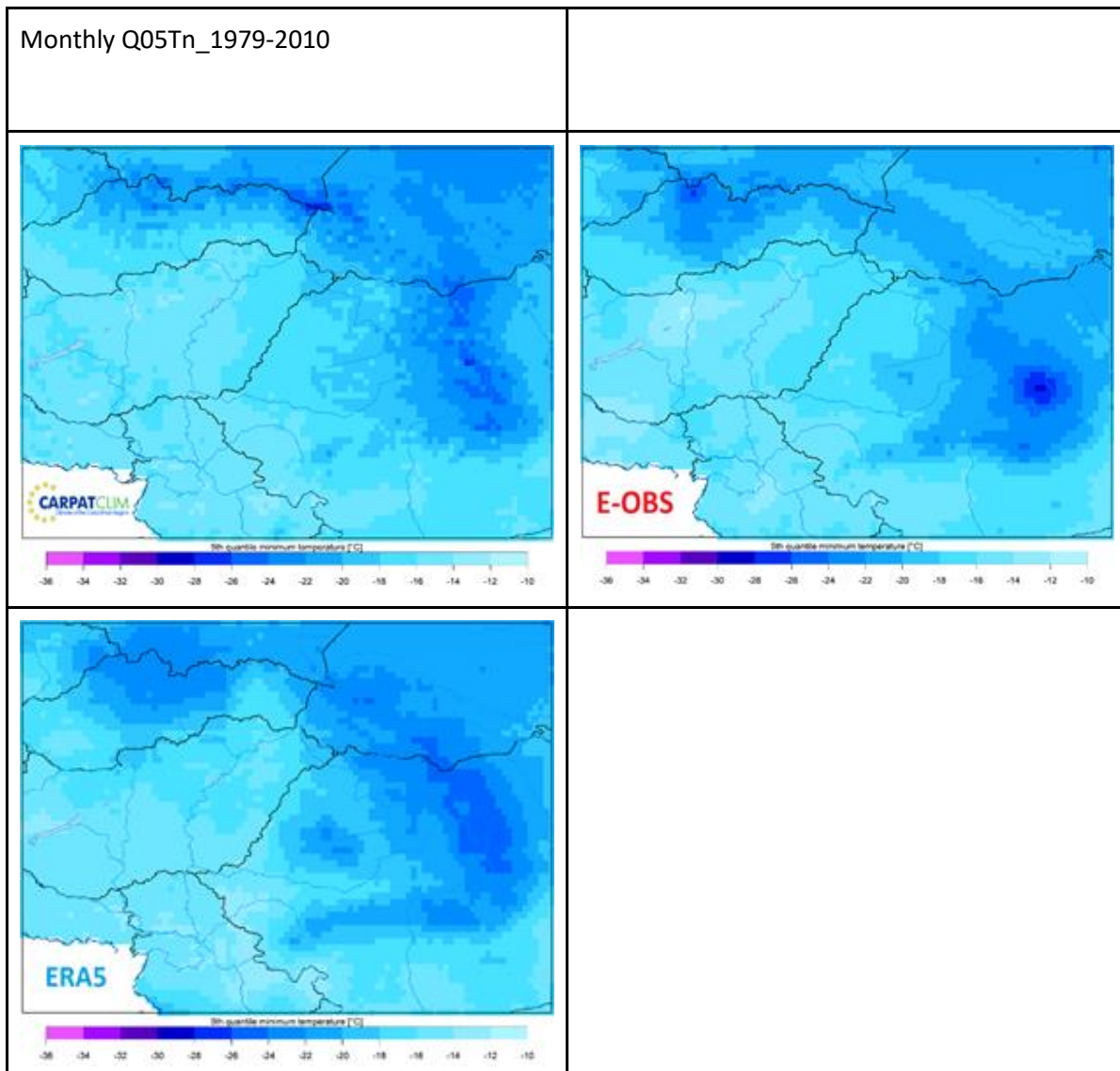


Figure 4.2.4.2. Q05 quantiles (monthly) based on the monthly minima of the daily Tn for CARPATCLIM (top left), for E-OBS (top right) and ERA5 (bottom, left).

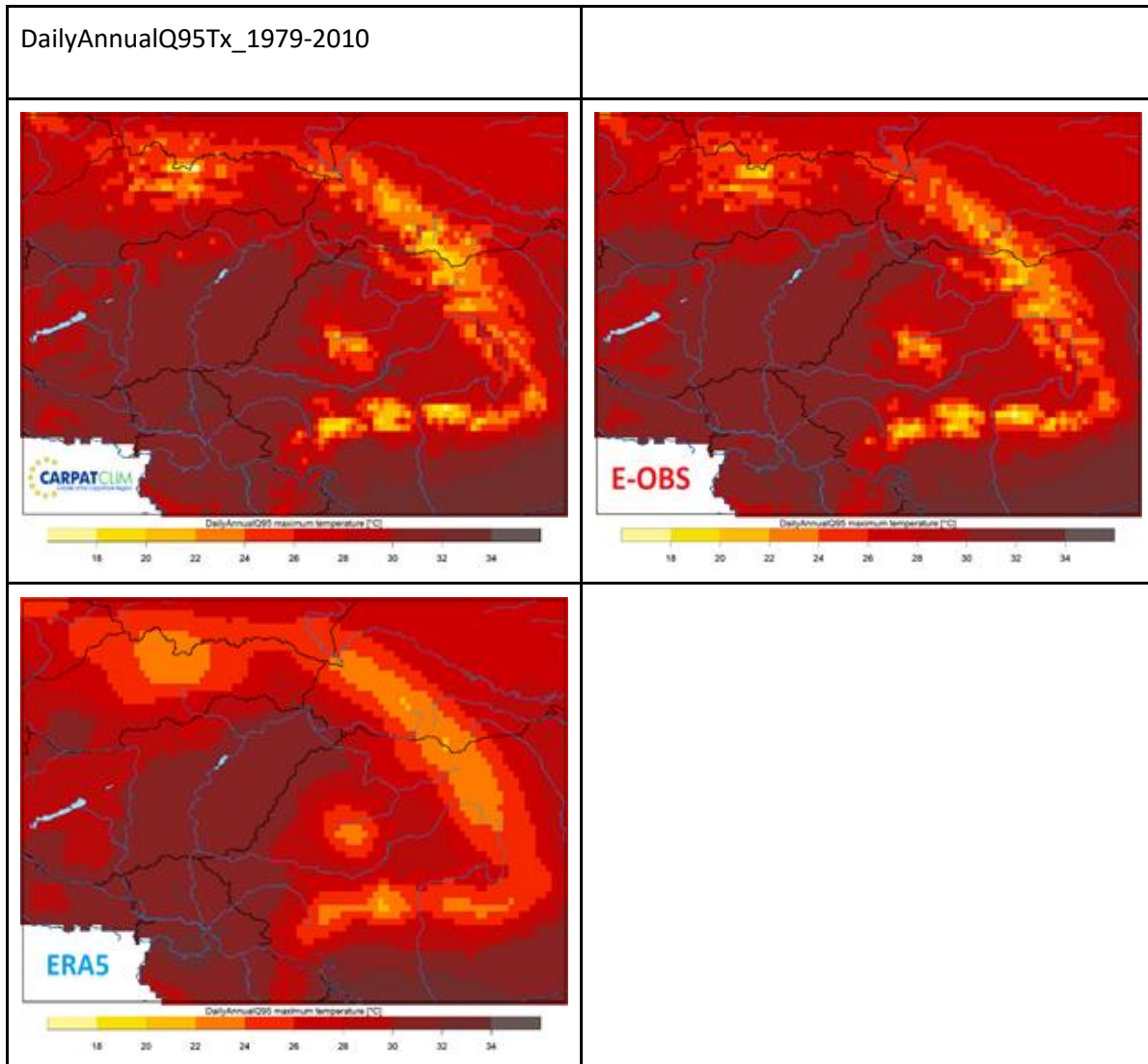


Figure 4.2.4.3. Q95 quantiles (daily) based on the daily maximum temperatures for CARPATCLIM (top left), for E-OBS (top right) and ERA5 (bottom, left).

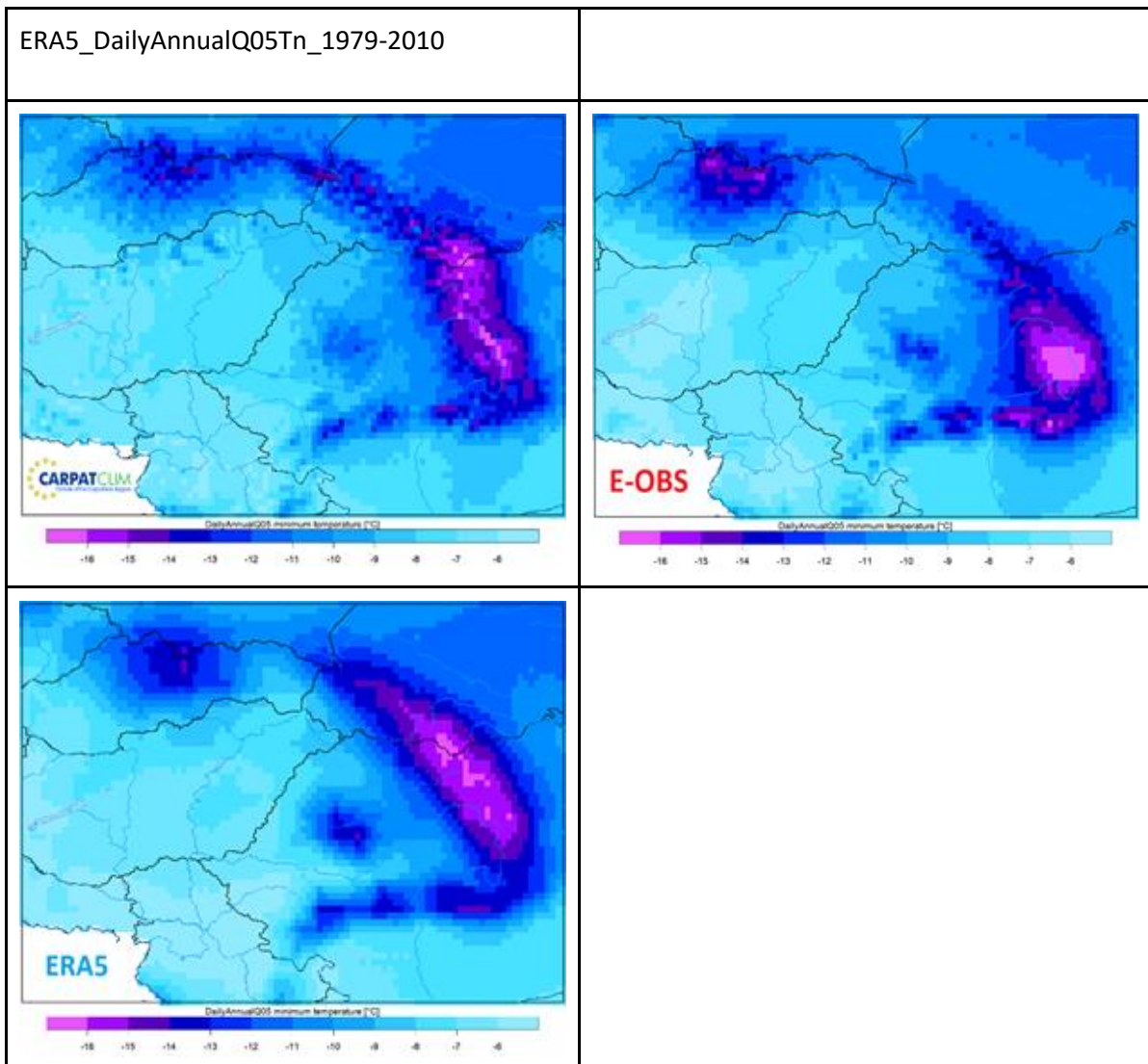


Figure 4.2.4.4. Q05 quantiles (daily) based on the daily minimum values for CARPATCLIM (top left), for E-OBS (top right) and ERA5 (bottom, left).

### Monthly graphs (quantiles)

The Q95 quantiles considering the monthly maxima of the daily  $T_x$  as a sample are shown in Figure 4.2.4.5. The monthly averaged Q95 from E-OBS are close to CARPATCLIM Q95 values during the year. ERA5 produces lower extremes, particularly from November to January when the underestimation is around 1 degree in Q95 of the monthly maximum temperatures. The Q05 of the monthly minimum temperatures in regional average are close in CARPATCLIM and in E-OBS. ERA5 less captures the cold extremes from June to October, the largest difference is 1.17°C in August in the case of the Q05 monthly minima (Figure 4.2.4.6).

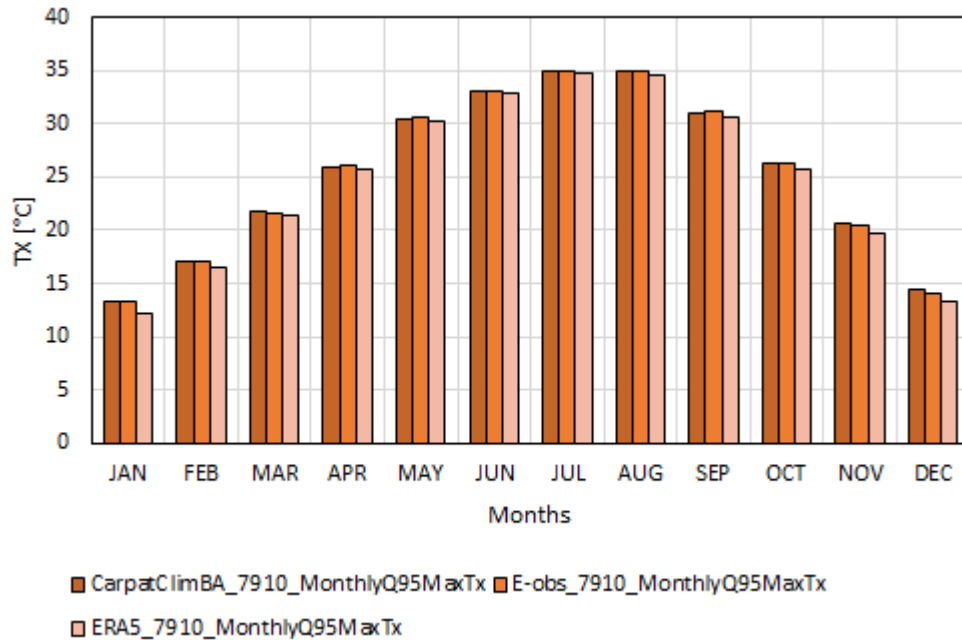


Figure 4.2.4.5. Yearly cycle of the Q95 quantiles (monthly) based on the monthly maxima of the daily Tx for CARPATCLIM, for E-OBS and ERA5 averaged for CARPATCLIM domain.

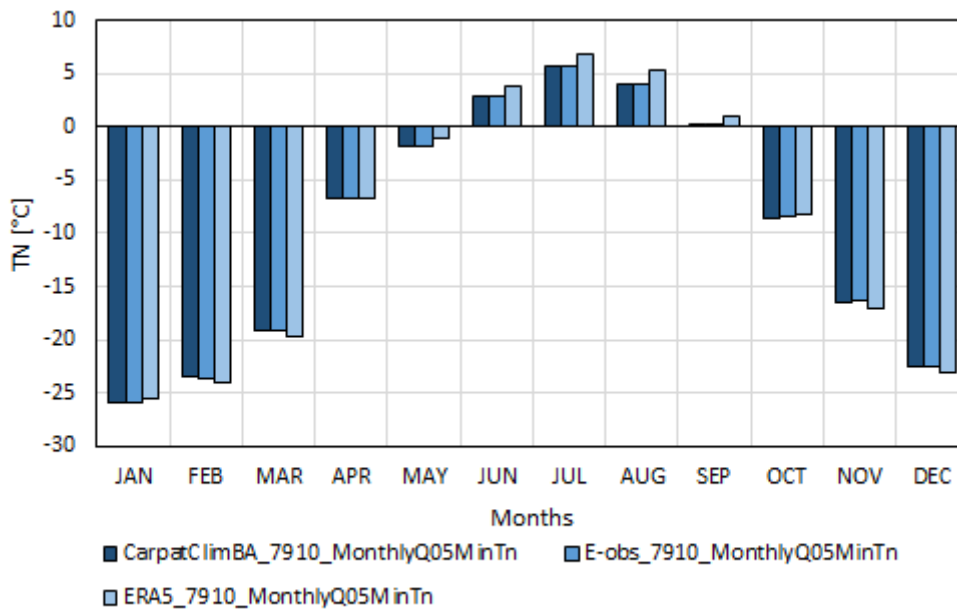
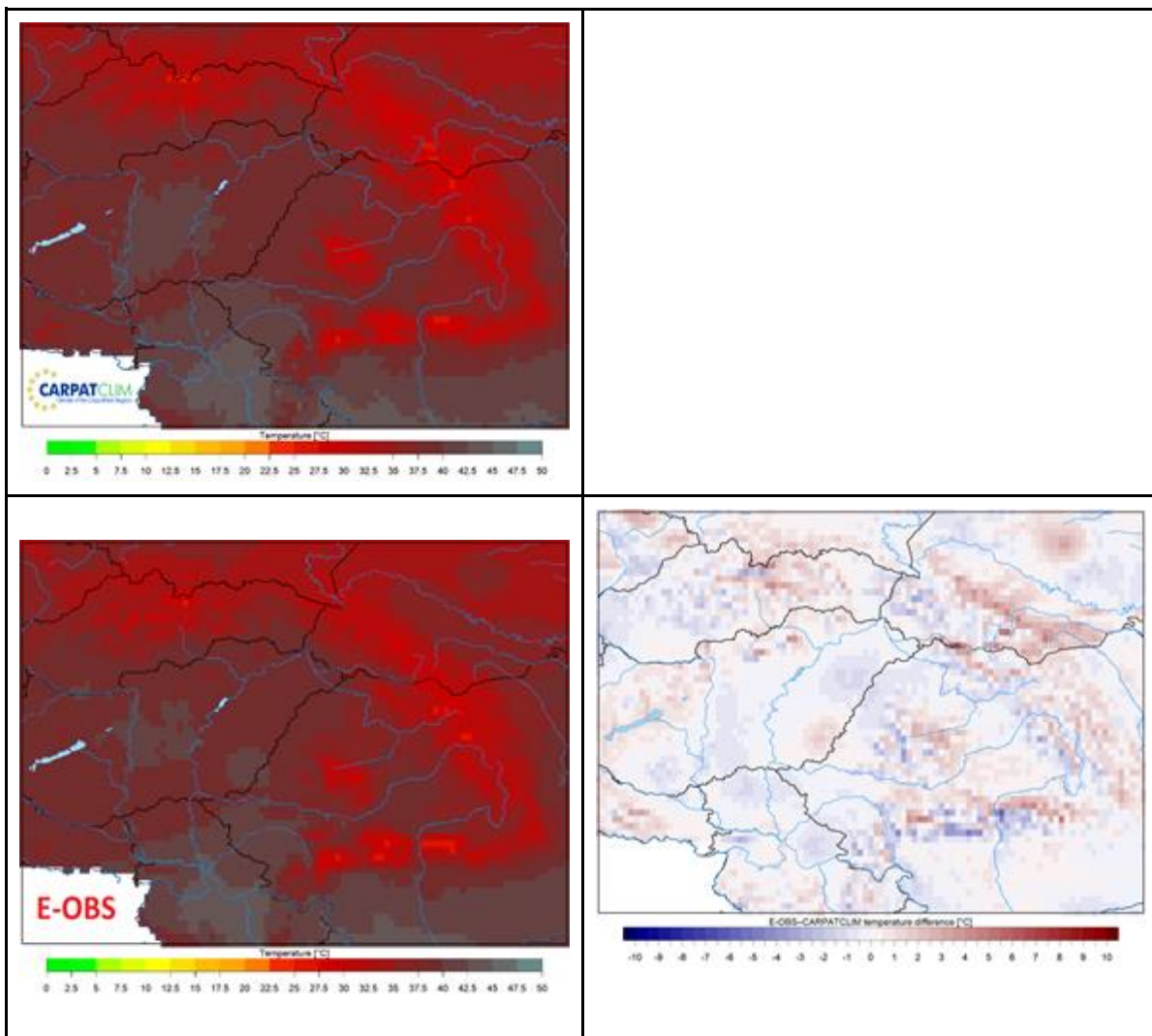


Figure 4.2.4.6. Yearly cycle of the Q05 quantiles (monthly) based on the monthly minima of the daily Tn for CARPATCLIM, for E-OBS and ERA5 averaged for CARPATCLIM domain.

#### 4.2.5 Climate indices

##### Maxima of TX and the differences

The absolute maxima (Figure 4.2.5.1) and absolute minima (Figure 4.2.5.2) in the period 1979-2010 are shown together with the differences to see the area where E-OBS and ERA5 produce higher or lower extreme temperatures than CARPATCLIM. Roughly the plain regions are represented lower absolute maxima in E-OBS than in CARPATCLIM, by contrast the hilly regions and in the high mountains E-OBS exceeds CARPATCLIM absolute maxima. The largest differences appear at high altitudes, some degree in both directions. There are some singularities in the southeast in Hungary near the Romanian border and in Podolia in Ukraine in the difference map of E-OBS and CARPATCLIM. The overall picture of ERA5 indicates that the highest temperatures are lower than in CARPATCLIM except in the upper catchment of the Tisa river in the northeast in Hungary and in Podolia in Ukraine and also the Romanian Plain.



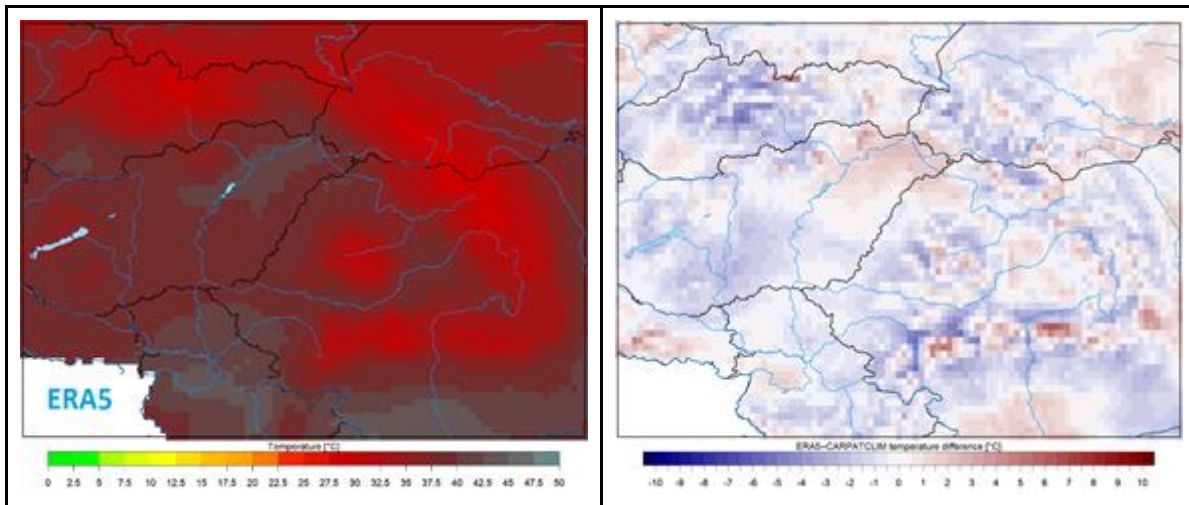
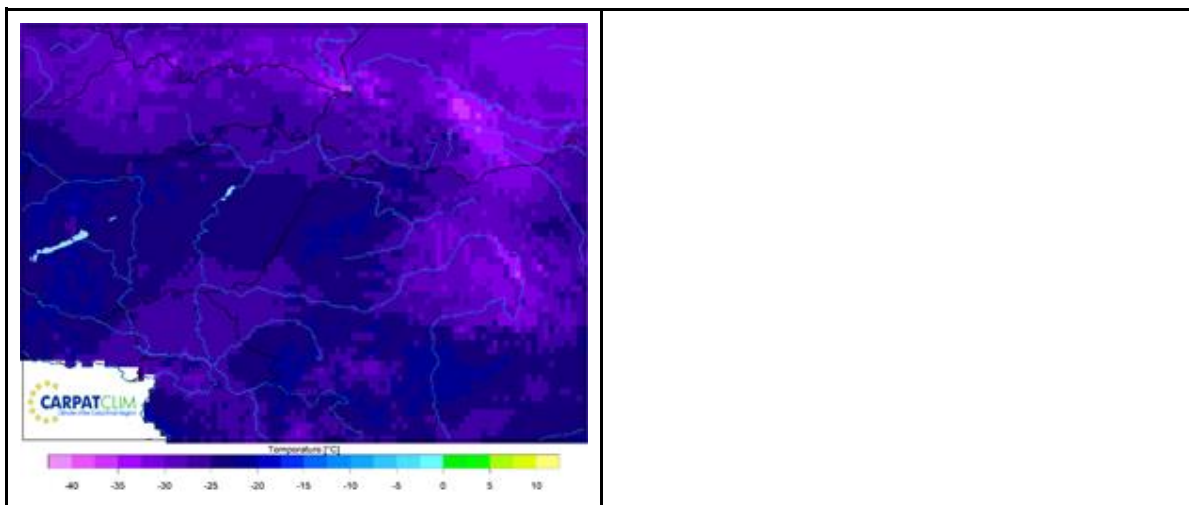


Figure 4.2.5.1. The highest temperatures (left) and the difference (E-OBS - ERA5) and CARPATCLIM (right) in the period 1979-2010.

#### Minima of TN for all three datasets and its differences

Considering the absolute minima, in the North-Eastern Carpathians the lowest temperature in the period 1979-2010 is less extremely cold in E-OBS and in ERA5 than in CARPATCLIM (Figure 4.1.27). The less extremely cold regions are wider in E-OBS than in ERA5, by 4-5 °C in wide regions. ERA5 is milder in the whole territory of Serbia. E-OBS and ERA5 is colder in the Tatra Mountain in Slovakia and more substantially in the Romanian plain behind the Southern Carpathians.



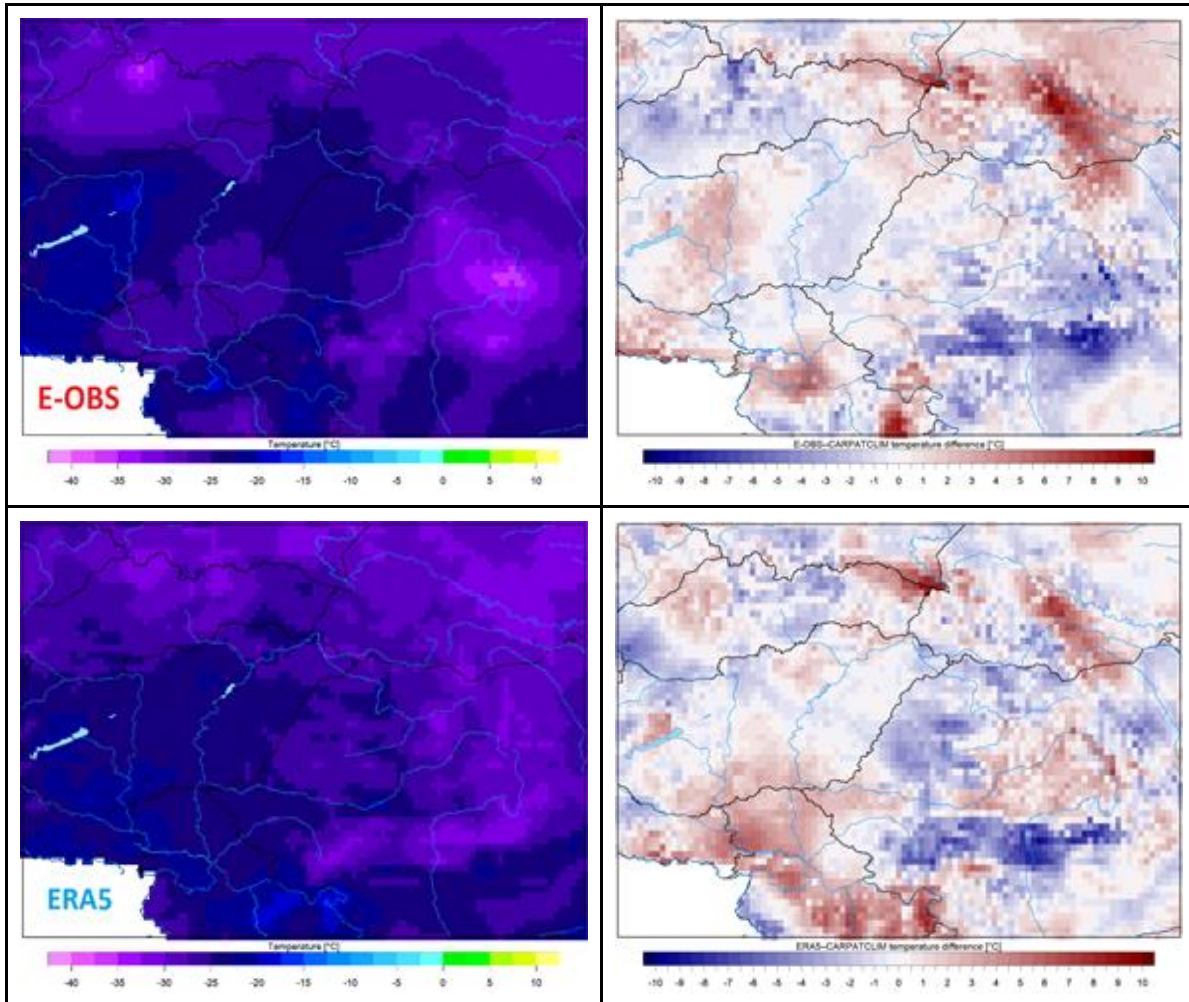


Figure 4.2.5.2. The lowest temperatures (left) and the difference E-OBS/ERA5 and CARPATCLIM (right) in the period 1979-2010.

### TXx and TNn indices

The average of the yearly maxima and minima can be seen for the examined datasets for the period 1979-2010 in Figure 4.2.5.3 and Figure 4.2.5.4. The spatial patterns are very similar in CARPTCLIM and E-OBS. ERA5 provides greater values in the northern half part of the Great Hungarian Plain and in middle Serbia. ERA5 is less detailed, naturally and the TXx are higher around the highest peaks than in the observational datasets. The Figure 4.2.5.4 confirms that the interpolation of the minimum temperature is more difficult than the maximum temperature. CARPATCLIM is well detailed and smooth along the Carpathians, while the north-eastern Carpathian are represented with less cold TNn values by 5 degree in large regions in E-OBS. In the corner of the eastern and southern Carpathians a spot with colder TNn values springs out in the map of E-OBS. ERA5 illustrates better, but less detailed pattern the North-eastern Carpathian than E-OBS with lower values than CARPATCLIM in the Southern Carpathians.

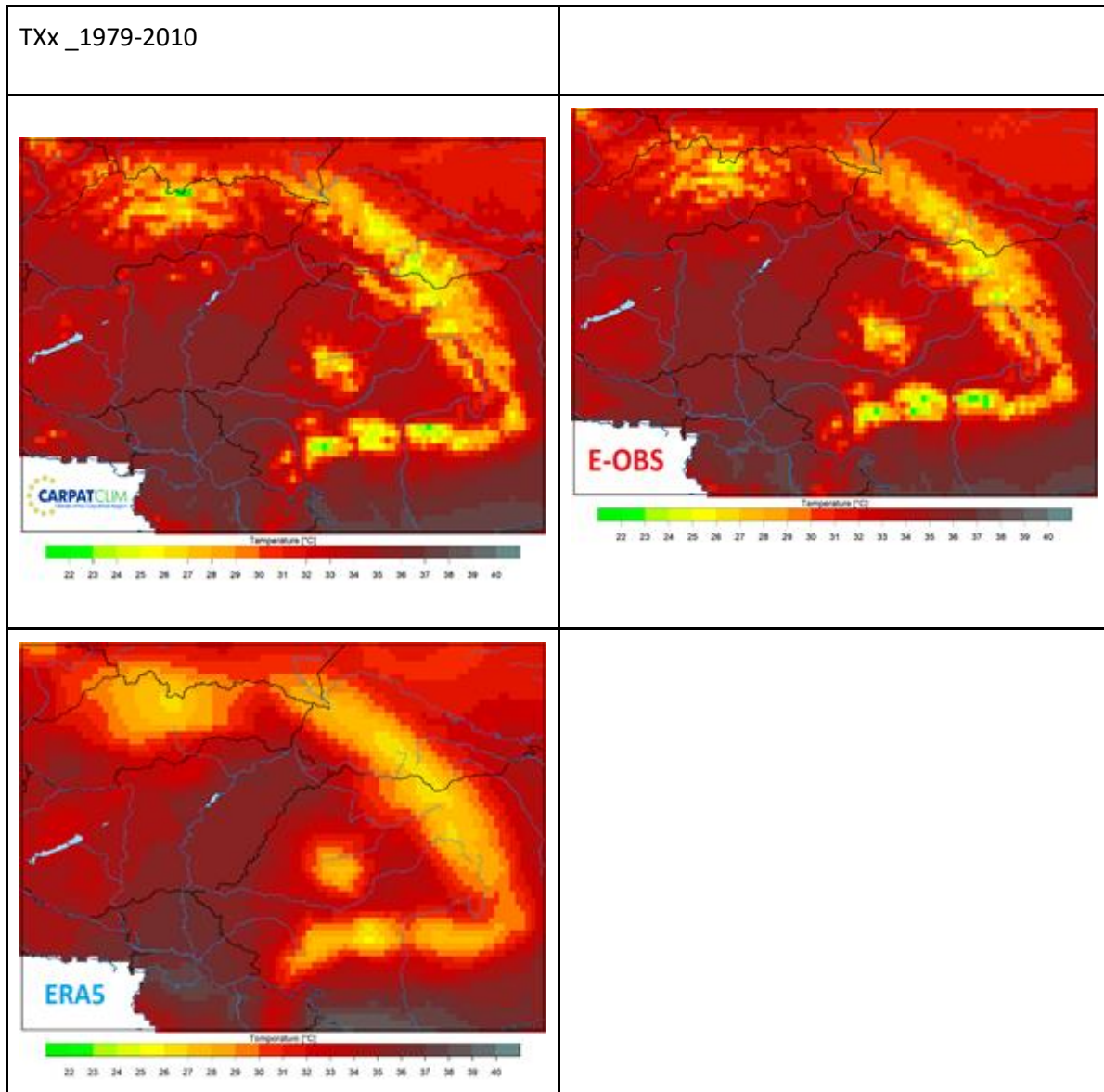


Figure 4.2.5.3. The TXx (average of the yearly maxima) temperature climate index for CARPATCLIM (top left), for E-OBS (top right) and ERA5 (bottom, left).

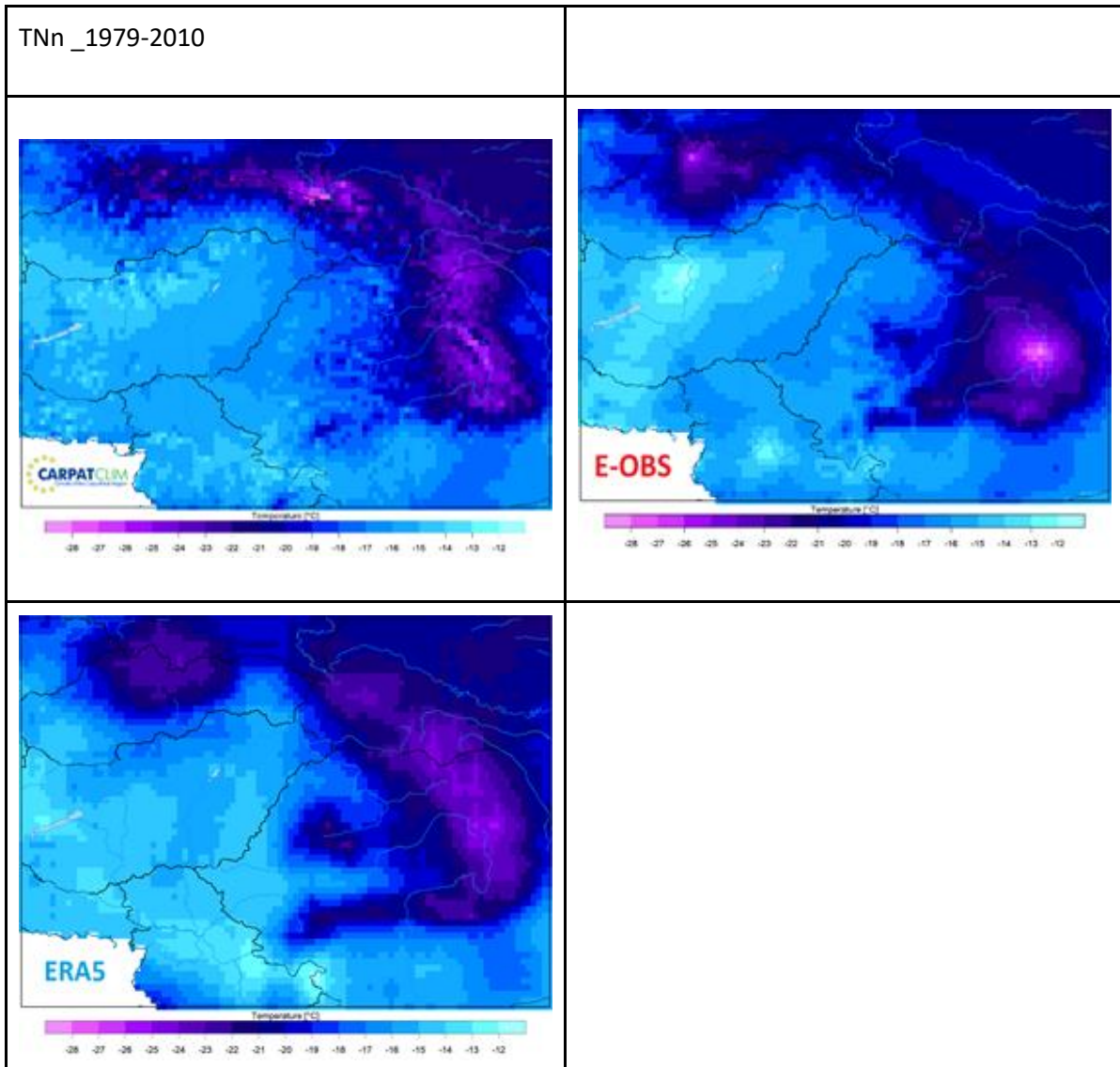


Figure 4.2.5.4. The TNn (average of the yearly minima) temperature climate index for CARPATCLIM (top left), for E-OBS (top right) and ERA5 (bottom, left) for the period 1979-2010.

### SU (summer days)

The spatial pattern of the summer days is similar on the set of maps in Figure 4.2.5.5 determined by the elevation above sea level as the main factor. CARPATCLIM and E-OBS are almost the same, but ERA5 produces fewer number of summer days in regional average, particularly in Romania. The frost days maps (Figure 4.2.5.6) of the observational datasets are alike, except the region depicted with less frost days in the middle of Hungary and in Serbia in E-OBS, unreasonably, the latest turns up in ERA5 too.

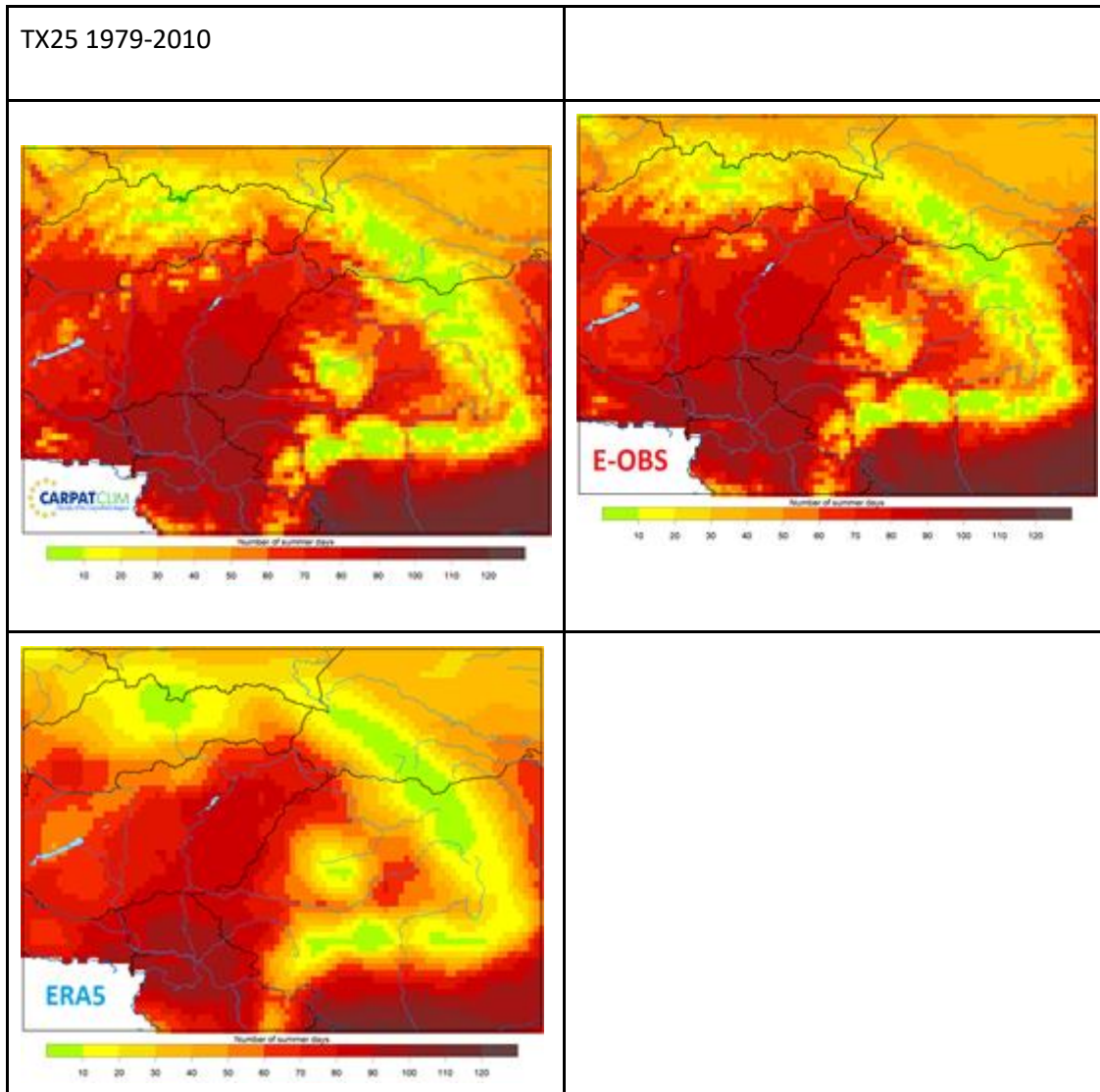


Figure 4.2.5.5. The summer days (SU) (number of days when the  $T_x > 25^{\circ}\text{C}$ ) temperature climate index for the for CARPATCLIM (top left), for E-OBS (top right) and ERA5 (bottom, left) in average for 1979-2010.

## FD (frost days)

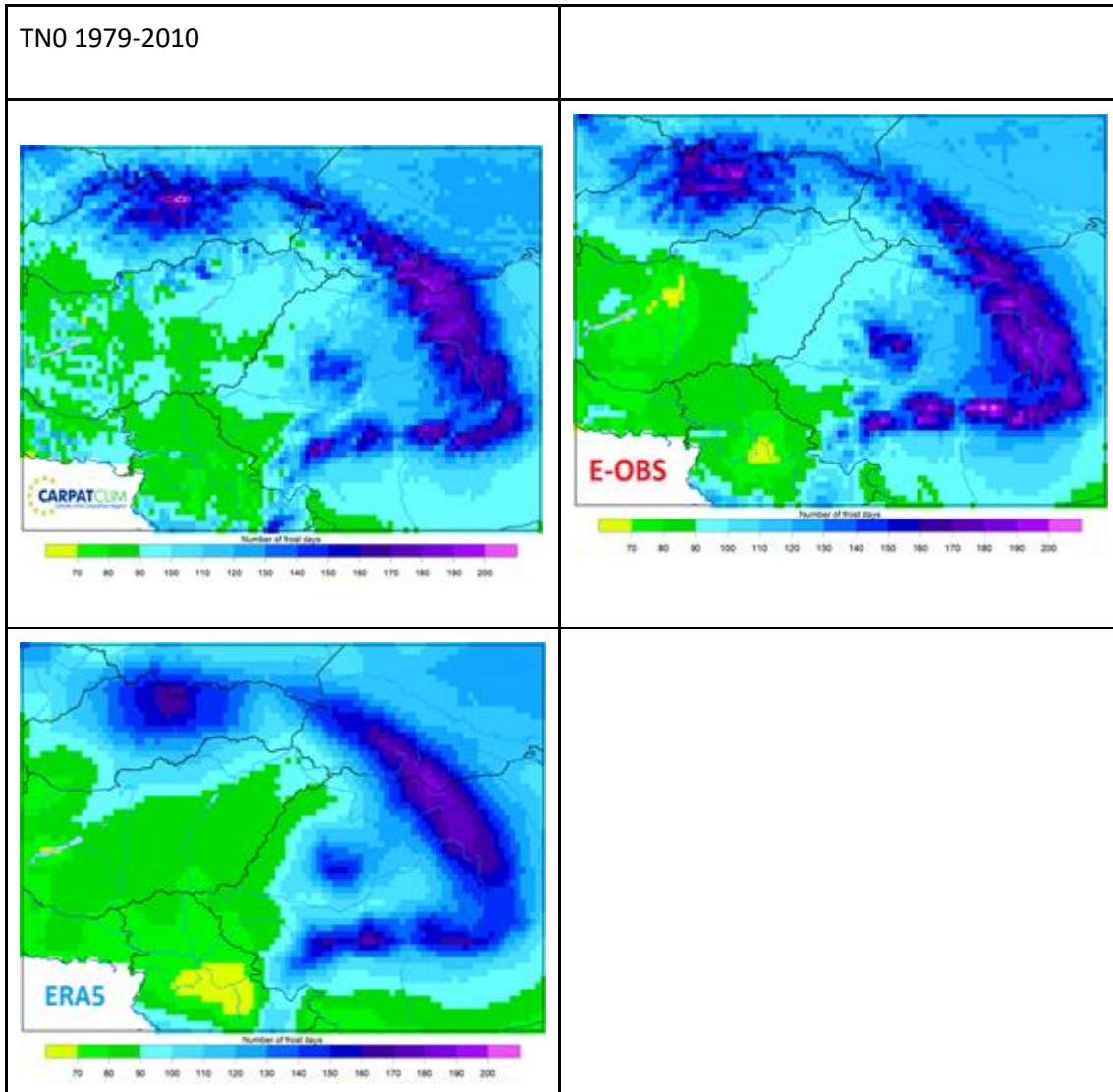


Figure 4.2.5.6. The frost days (FD) (number of days when the  $T_n < 0^\circ\text{C}$ ) average of the yearly minimum temperature climate index for the for CARPATCLIM (top left), for E-OBS (top right) and ERA5 (bottom, left) in average for 1979-2010

#### 4.2.6 RMSE

Daily, monthly and seasonal RMSE were computed for E-OBS and ERA5 against CARPATCLIM and ERA5 against E-OBS for the period 1979-2010. The maps in Figure 4.2.6.1-4.2.6.8. illustrate the RMSE for different time scales based on daily maximum and daily minimum temperatures. The observational datasets are closer to each other than ERA5 either to CARPATCLIM or E-OBS in general. The lowest RMSE values appear in the plain region, the orography is a determining factor here.

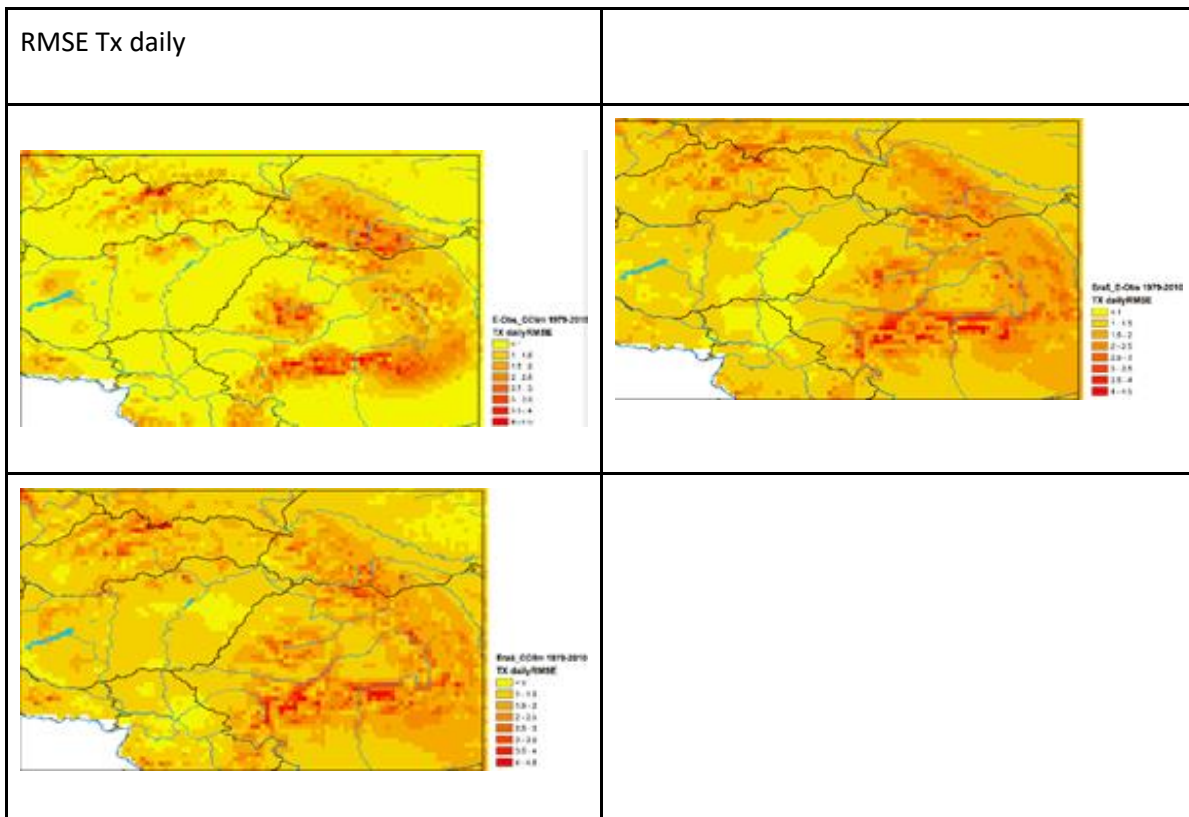
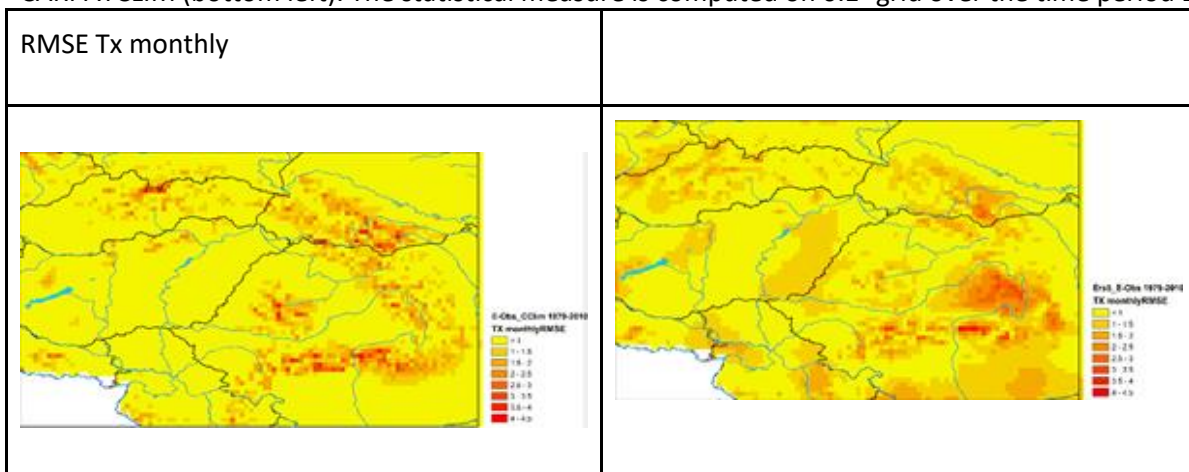


Figure 4.2.6.1. Daily root mean squared error (RMSE) in ( $^{\circ}\text{C}$ ) for daily Tx of E-OBS with the reference of CARPATCLIM (top left), of ERA5 with the reference of E-OBS (top right), of ERA5 with the reference of CARPATCLIM (bottom left). The statistical measure is computed on 0.1° grid over the time period 1979-2010.



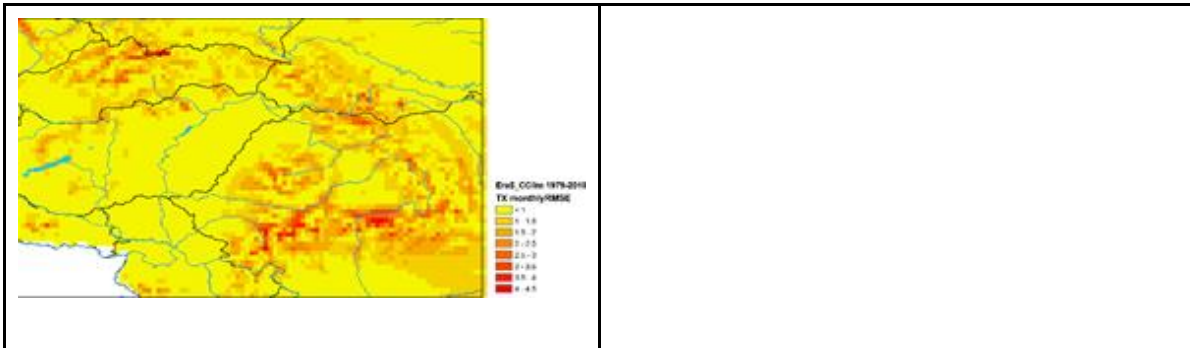


Figure 4.2.6.2. Yearly averaged RMSE ( $^{\circ}\text{C}$ ) for monthly Tx of E-OBS with the reference of CARPATCLIM (top left), of ERA5 with the reference of E-OBS (top right), of ERA5 with the reference of CARPATCLIM (bottom left). The statistical measure is computed on a  $0.1^{\circ}$  grid over the time period 1979-2010.

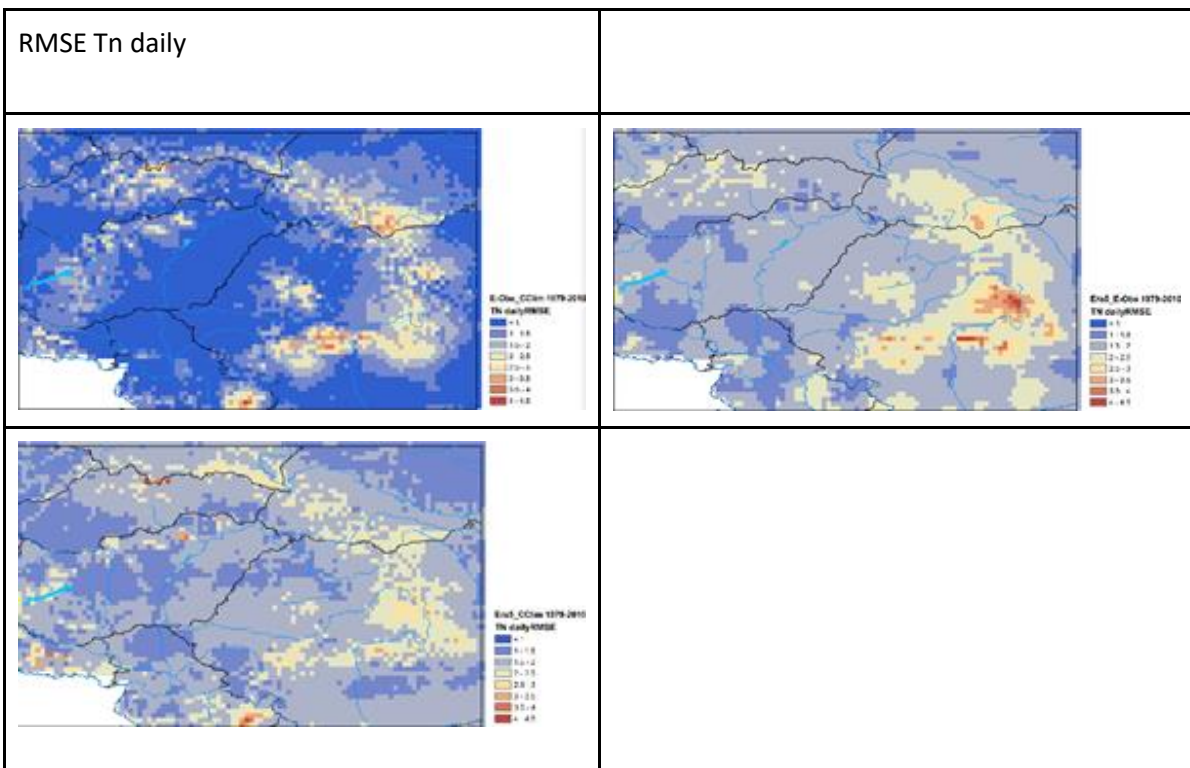
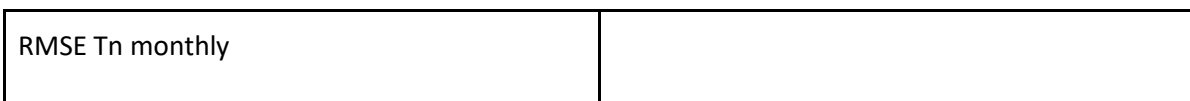


Figure 4.2.6.3. Daily root mean squared error (RMSE) in ( $^{\circ}\text{C}$ ) for daily Tn of E-OBS with the reference of CARPATCLIM (top left), of ERA5 with the reference of E-OBS (top right), of ERA5 with the reference of CARPATCLIM (bottom left). The statistical measure is computed on a  $0.1^{\circ}$  grid over the time period 1979-2010.



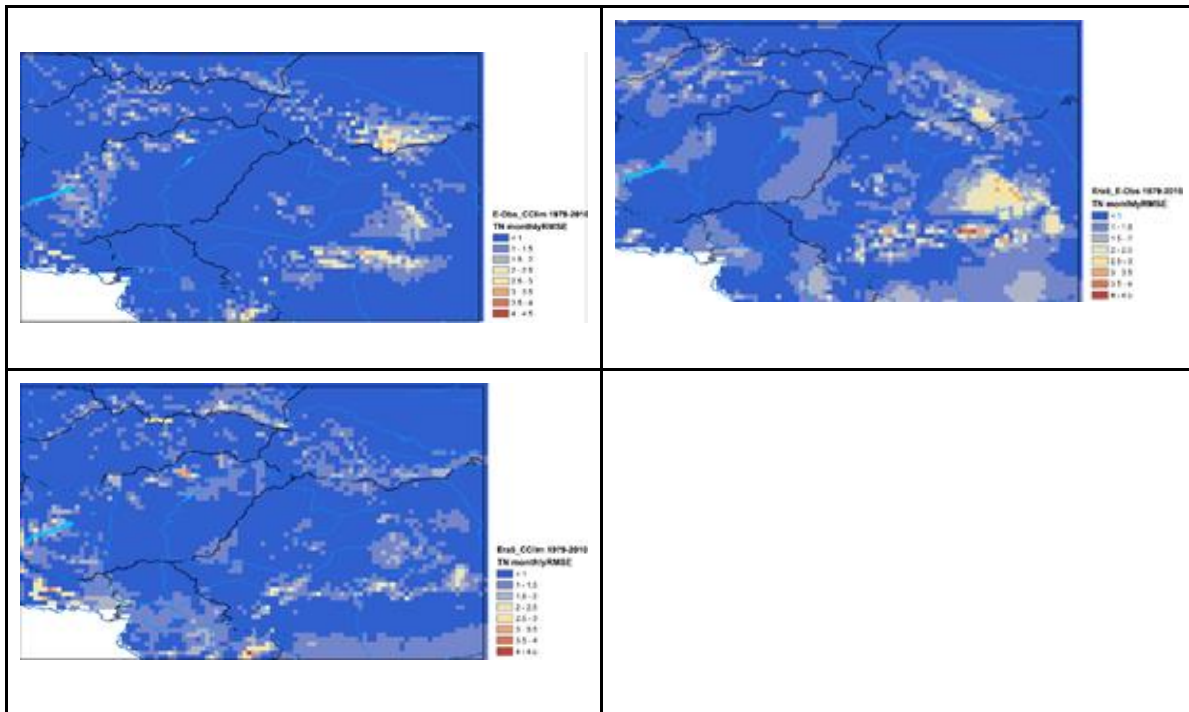
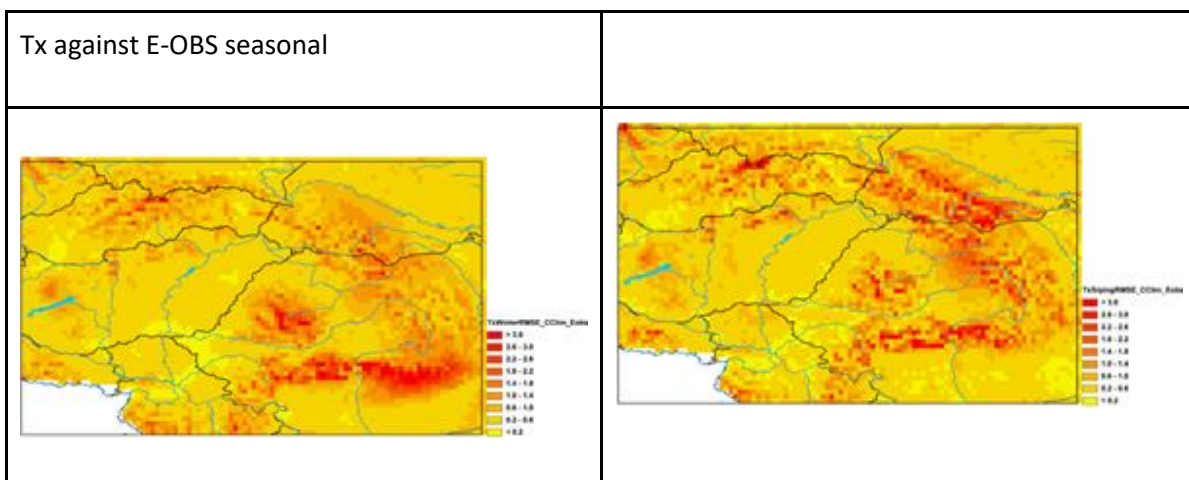


Figure 4.2.6.4. Yearly RMSE ( $^{\circ}\text{C}$ ) for monthly  $\text{Tn}$  of E-OBS with the reference of CARPATCLIM (top left), of ERA5 with the reference of E-OBS (top right), of ERA5 with the reference of CARPATCLIM (bottom left). The statistical measure is computed on a  $0.1^{\circ}$  grid over the time period 1979-2010.

### RMSE seasonal



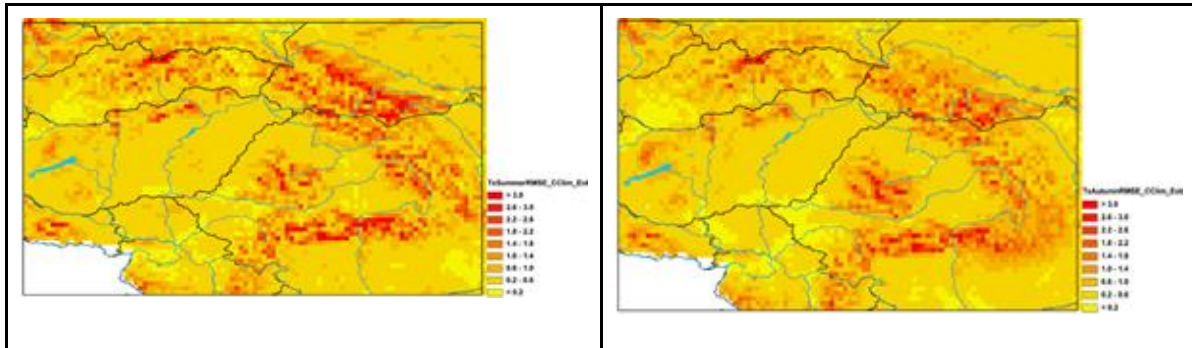


Figure 4.2.6.5. Seasonal daily root mean squared error (RMSE) in ( $^{\circ}$ C) for daily Tx of E-OBS with the reference of CARPATCLIM. (winter top left, spring top right, summer bottom left, autumn bottom right) The statistical measure is computed on a 0.1° grid over the time period 1979-2010.

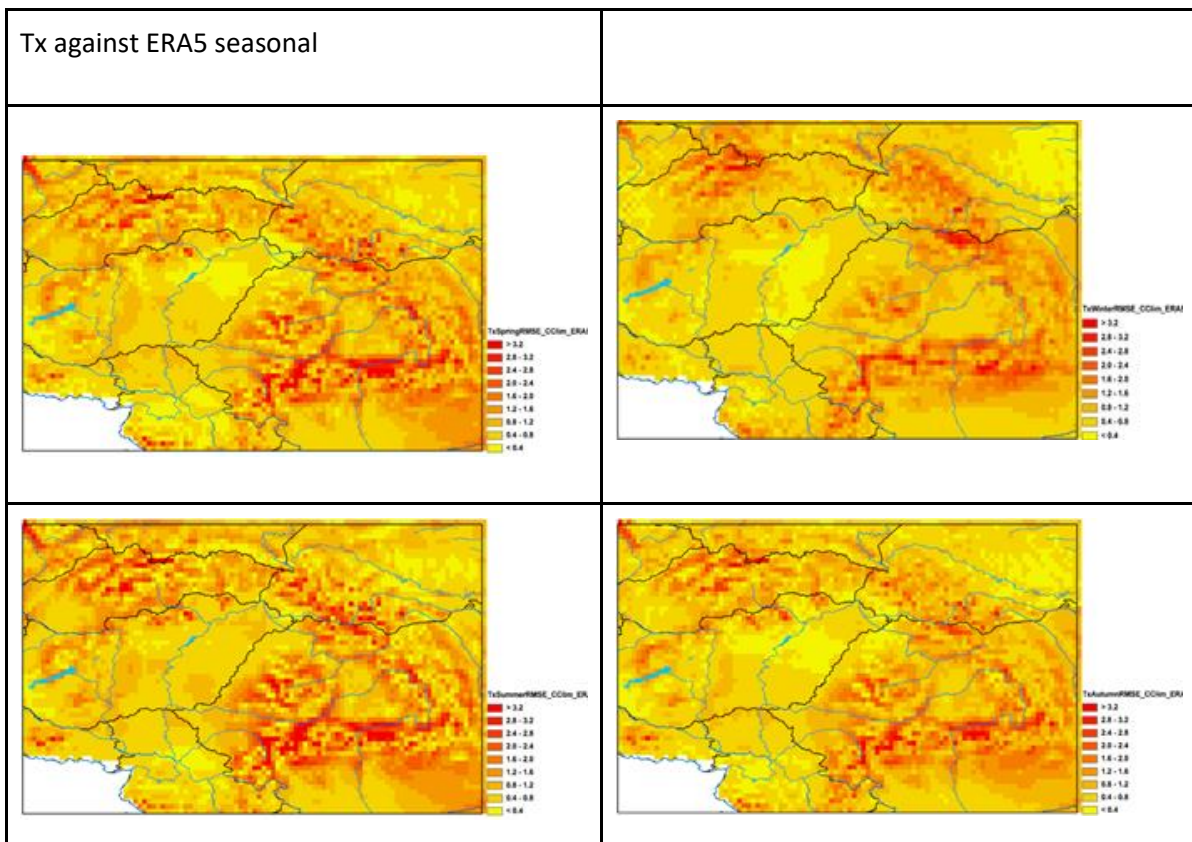


Figure 4.2.6.6. Seasonal daily root mean squared error (RMSE) in ( $^{\circ}$ C) for daily Tx of ERA5 with the reference of CARPATCLIM. (winter top left, spring top right, summer bottom left, autumn bottom right) The statistical measure is computed on a 0.1° grid over the time period 1979-2010.

Tn against E-OBS seasonal	
---------------------------	--

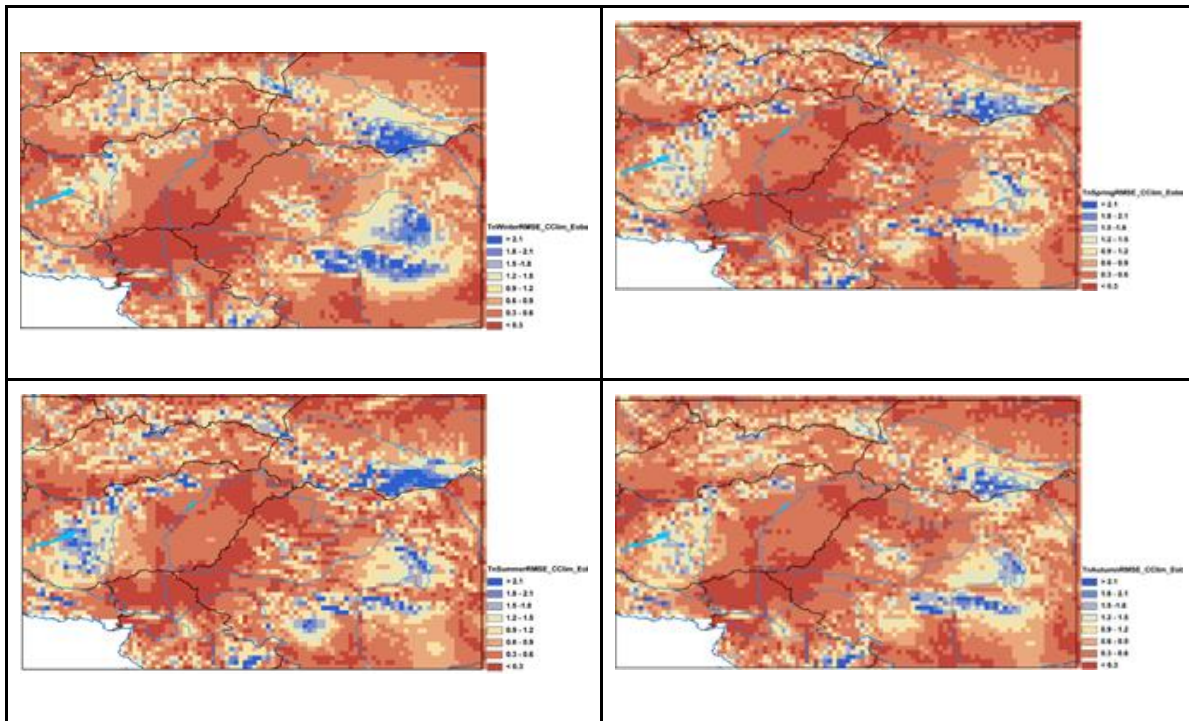
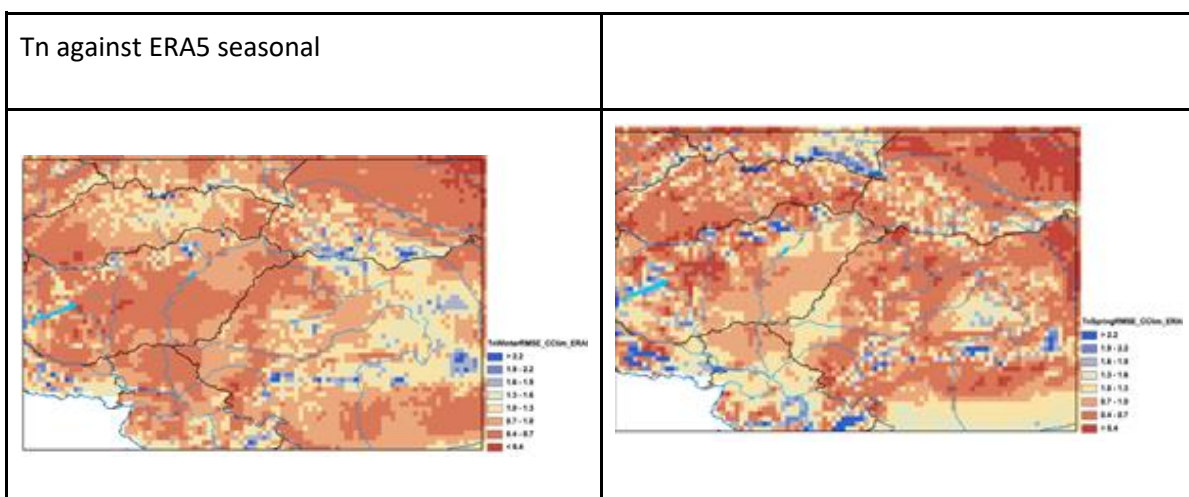


Figure 4.2.6.7. Seasonal daily root mean squared error (RMSE) in ( $^{\circ}\text{C}$ ) for daily Tn of E-OBS with the reference of CARPATCLIM. (winter top left, spring top right, summer bottom left, autumn bottom right) The statistical measure is computed on 0.1° grid over the time period 1979-2010.



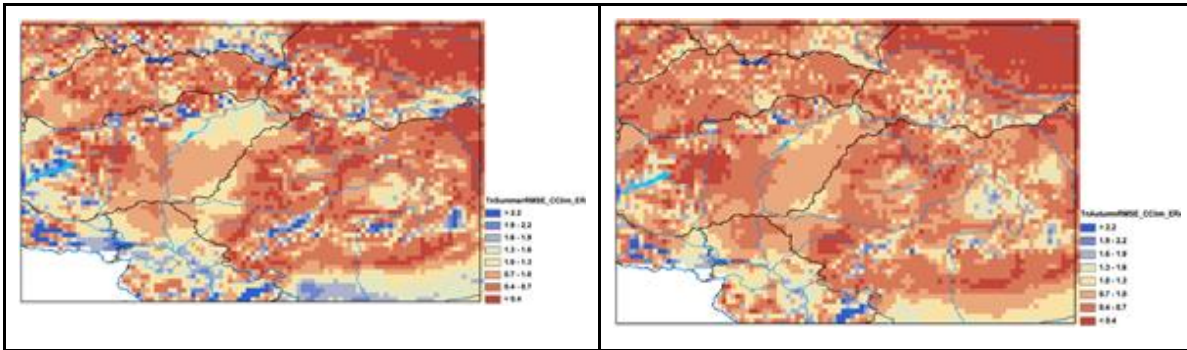
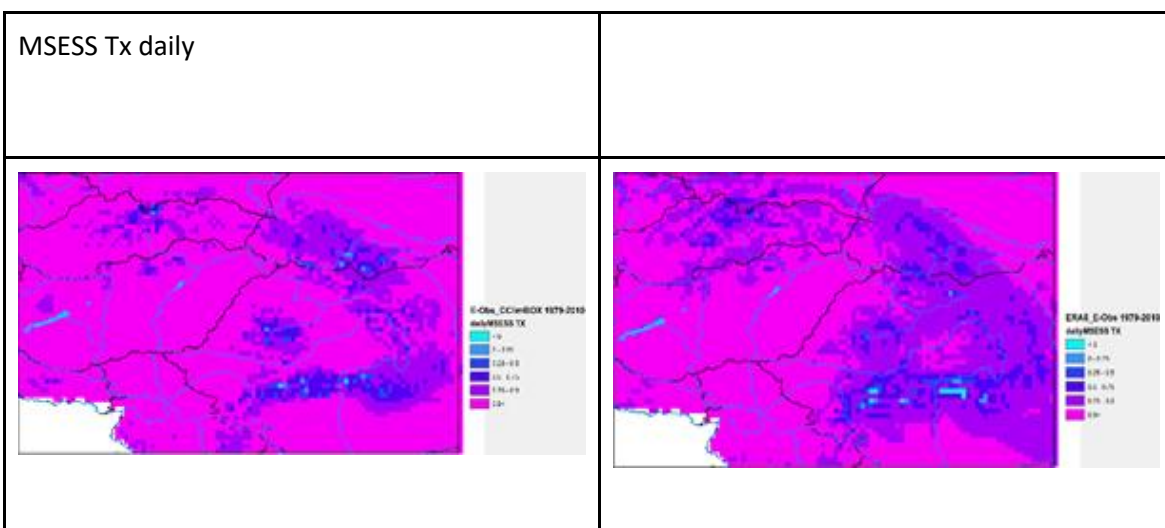


Figure 4.2.6.8. Seasonal daily root mean squared error (RMSE) in ( $^{\circ}$ C) for daily Tn of ERA5 with the reference of CARPATCLIM. (winter top left, spring top right, summer bottom left, autumn bottom right) The statistical measure is computed on a 0.1° grid over the time period 1979-2010.

#### 4.2.7 MSESS

Daily and monthly Mean Square Error Skill Score (MSESS) were computed for E-OBS and ERA5 against CARPATCLIM and ERA5 against E-OBS for the period 1979-2010. The maps in Figure 4.2.7.1 - 4.2.7.4 illustrate the MSESS for different time scales based on daily maximum and daily minimum temperatures. With this measure the amount of explained variation in each dataset can be described. The observational datasets are closer to each other than ERA5 either to CARPATCLIM or to E-OBS in general. The highest MSESS values appear in the plain region, the orography is one of the main determining factors. The Tn is a more problematic climate variable than Tx, as regards the difficulties arise of its interpolation and modelling. The spatial pattern of MSESS in Figure 4.2.7.4 confirms this statement. The yearly cycle of the monthly mean scores: ME, RMSE and MSESS for Tx and Tn can be seen in Figure 4.2.7.5 to follow the change of the performance of the analyzed datasets in time.



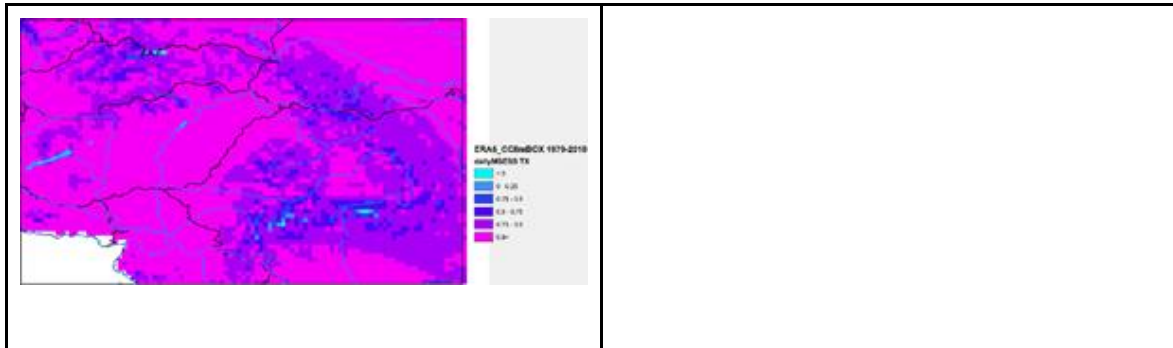


Figure 4.2.7.1 Daily MESS in for Tx daily of E-OBS with the reference of CARPATCLIM (top left), of ERA5 with the reference of E-OBS (top right), of ERA5 with the reference of CARPATCLIM (bottom left). The statistical measure is computed on a 0.1° grid over the time period 1979-2010.

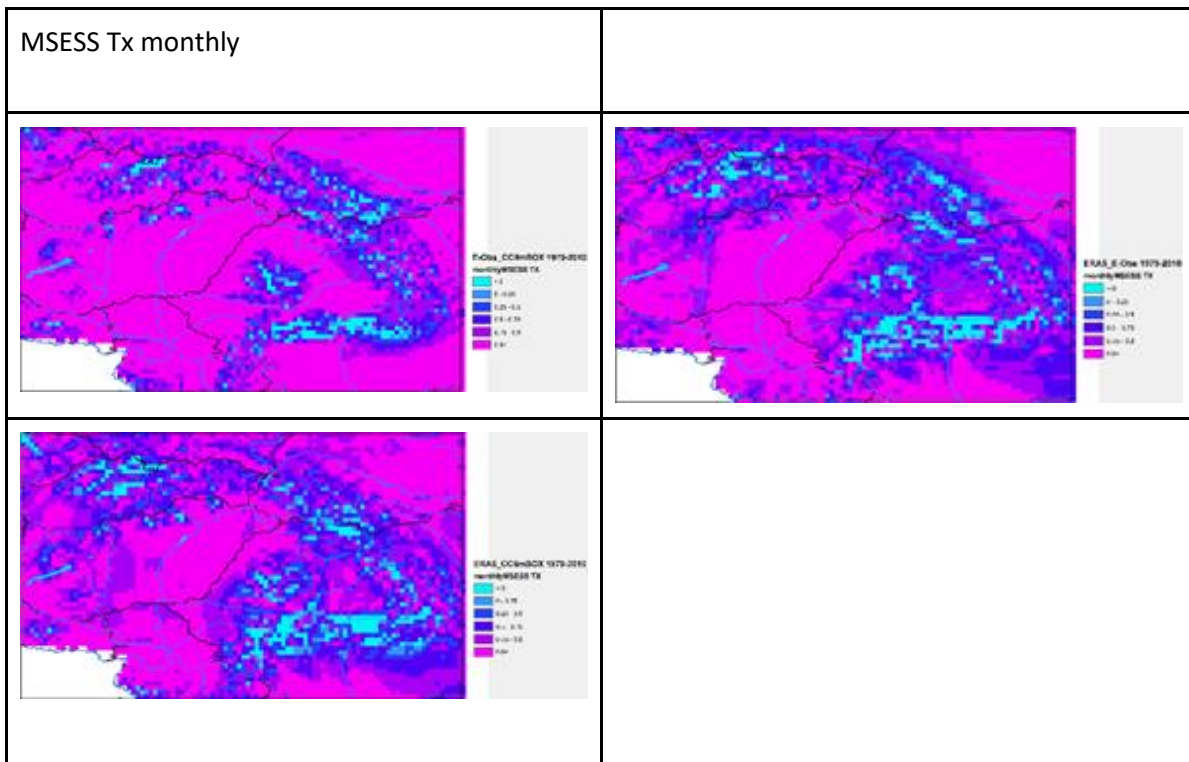


Figure 4.2.7.2. Yearly MESS for Tx monthly of E-OBS with the reference of CARPATCLIM (top left), of ERA5 with the reference of E-OBS (top right), of ERA5 with the reference of CARPATCLIM (bottom left). The statistical measure is computed on a 0.1° grid over the time period 1979-2010.

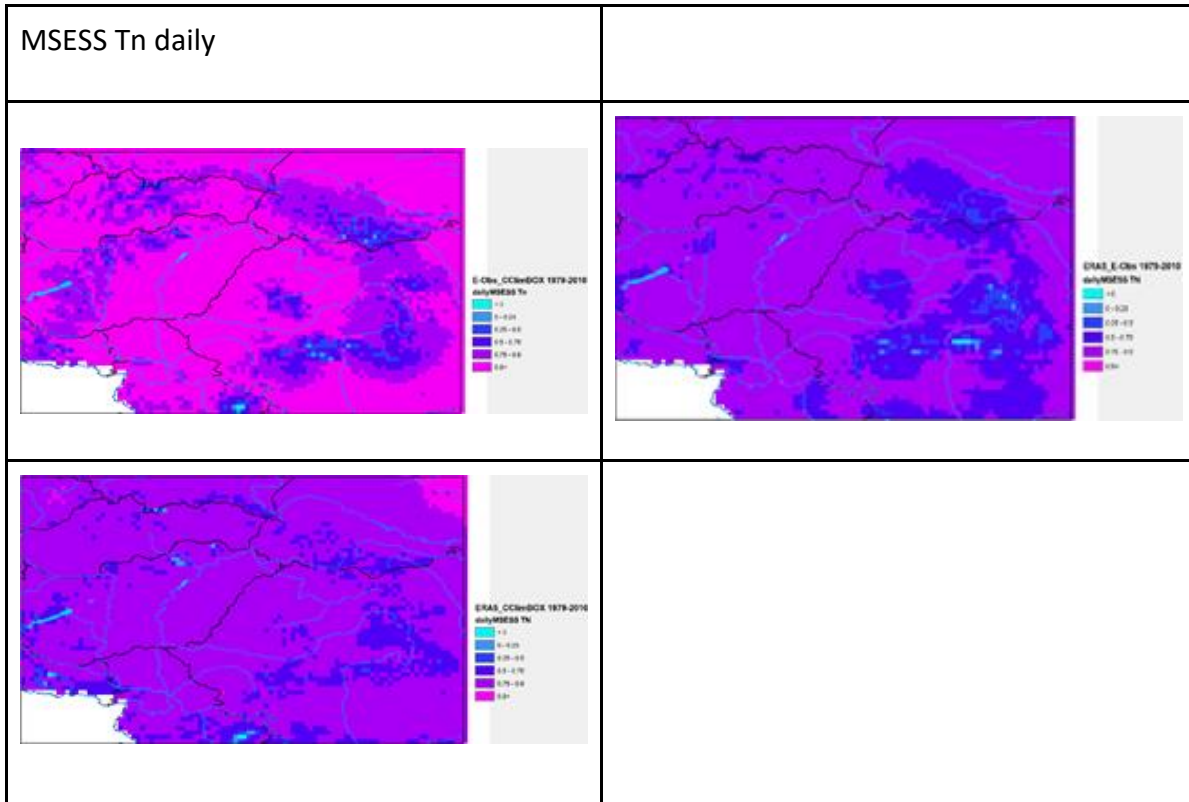
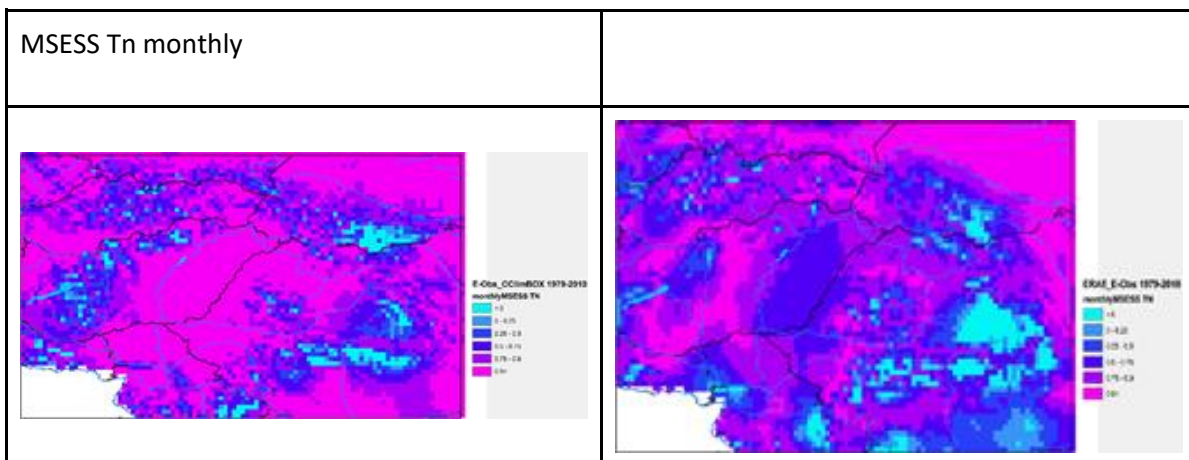


Figure 4.2.7.3. Daily MSESS for Tn daily of E-OBS with the reference of CARPATCLIM (top left), of ERA5 with the reference of E-OBS (top right), of ERA5 with the reference of CARPATCLIM (bottom left). The statistical measure is computed on a 0.1° grid over the time period 1979-2010.



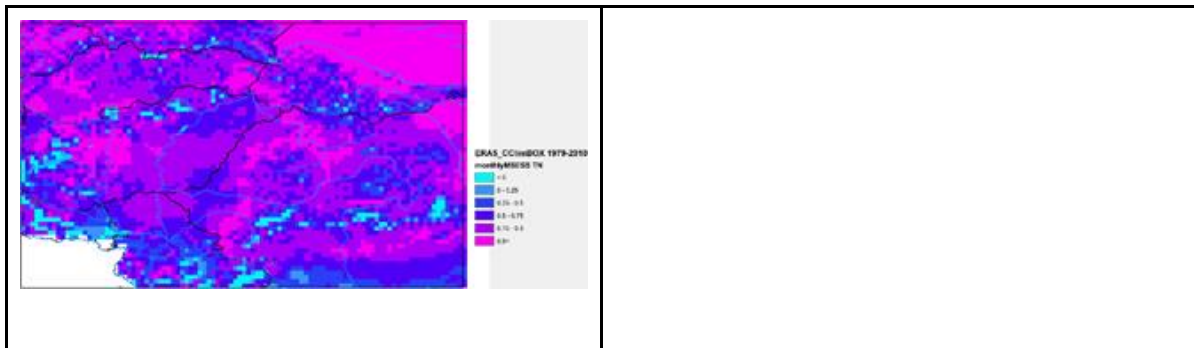
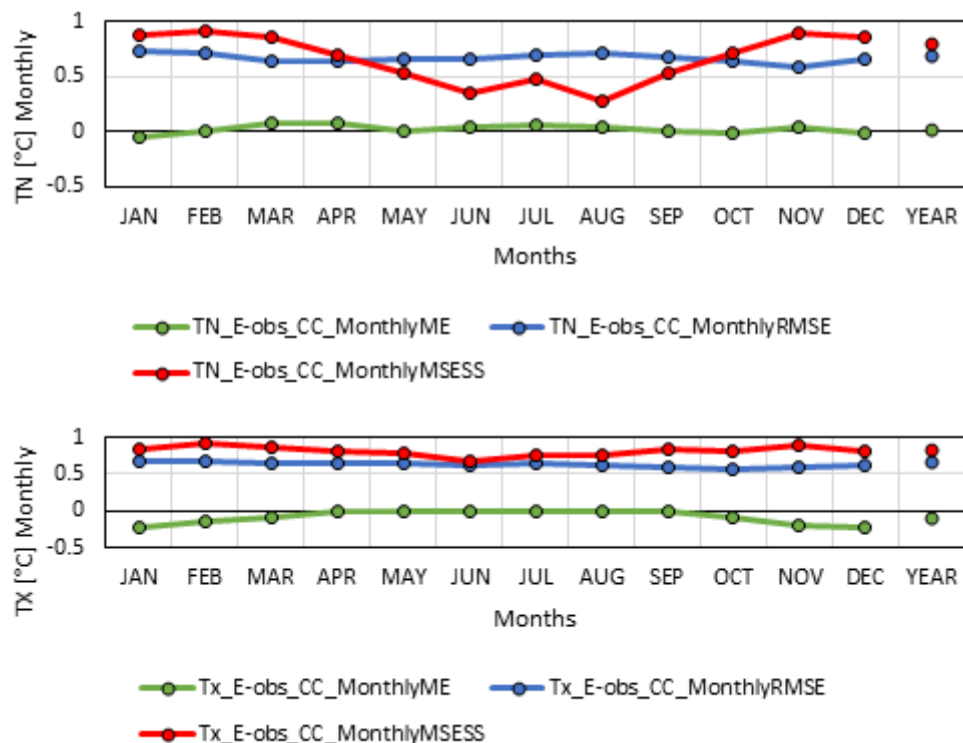


Figure 4.2.7.4. Yearly MESS for Tn monthly of E-OBS with the reference of CARPATCLIM (top left), of ERA5 with the reference of E-OBS (top right), of ERA5 with the reference of CARPATCLIM (bottom left). The statistical measure is computed on a  $0.1^{\circ}$  grid over the time period 1979-2010.



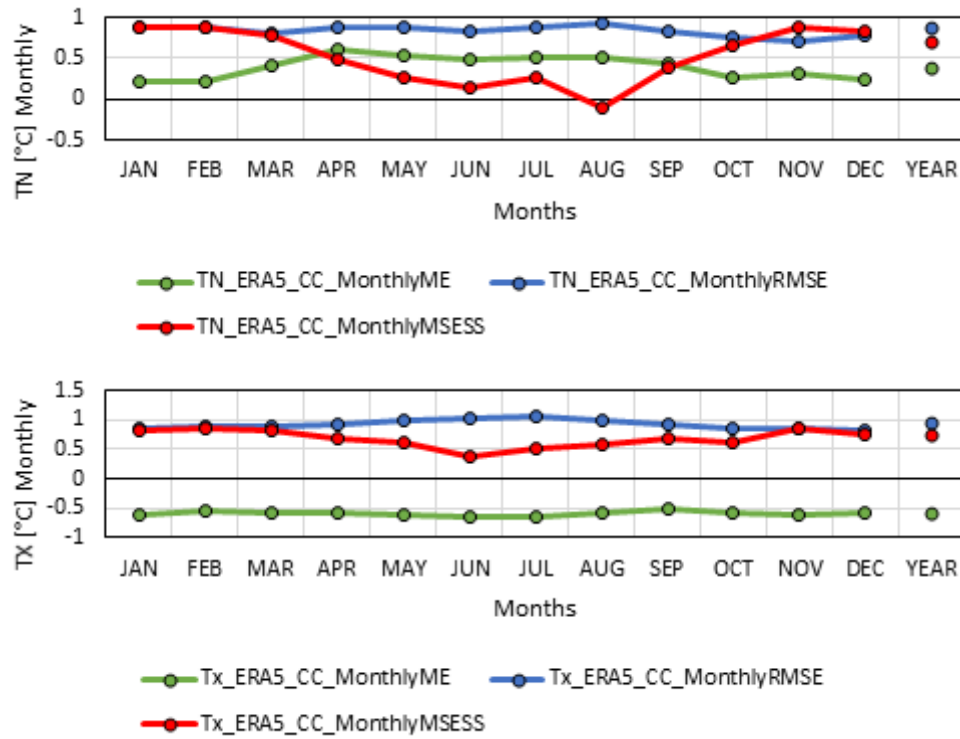


Figure 4.2.7.1. Monthly mean scores: ME, RMSE and MSESS for Tmax and Tmin, ERA5 and E-OBS is evaluated against CARPATCLIM over the time period 1979-2010.

#### 4.2.8 Trends

The trend maps in Figure 4.2.8.1-4.2.8.3 are remarkably different. The spatial distribution of the change of the daily maximum temperature from 1979 to 2010 is unexpectedly heterogeneous in E-OBS. Very high change, exceeding 2.5 °C comes up in mid-Hungary with the largest values at the Lake Balaton, while the change is less than 0.4 °C to the north-east in Hungary near the Slovakian border in the environment of Miskolc weather station (Figure 4.2.8.1, top right). The probable explanation of the high variability of the trend of the daily maxima in E-OBS is the less effective performance of QC and homogenization procedure. The trend fitted to ERA5 gridded time series indicates lower climate change signal in the Carpathian region as a whole (Figure 4.2.8.1, bottom left), though inexplicable high change appears where the Slovakian, Hungarian and Ukraine border meet.

The influence of the continental climate can be explored on CARPATCLIM summer change map (Figure 4.2.8.1, top left). The map illustrates E-OBS summer change is highly variable in the region and causelessly spotted, especially in the Carpathian Basin. For ERA5 the spatial distribution of the summer change is similar to yearly with the larger trend along the Slovak and Hungarian border, what is missing from CARPATCLIM.

Extremely high spatial variability turns up on the trend map representing the changes of the daily minimum temperatures for E-OBS (Figure 4.2.8.3, top right). Regions marked with very big and very low increase appear in Transdanubia in small a distance and in Slovakia, moreover E-OBS gives decreasing signal of minimum temperature in Romania narrow regions. ERA5 underestimate the change of the minimum temperature in wider region south from the midline of the domain.

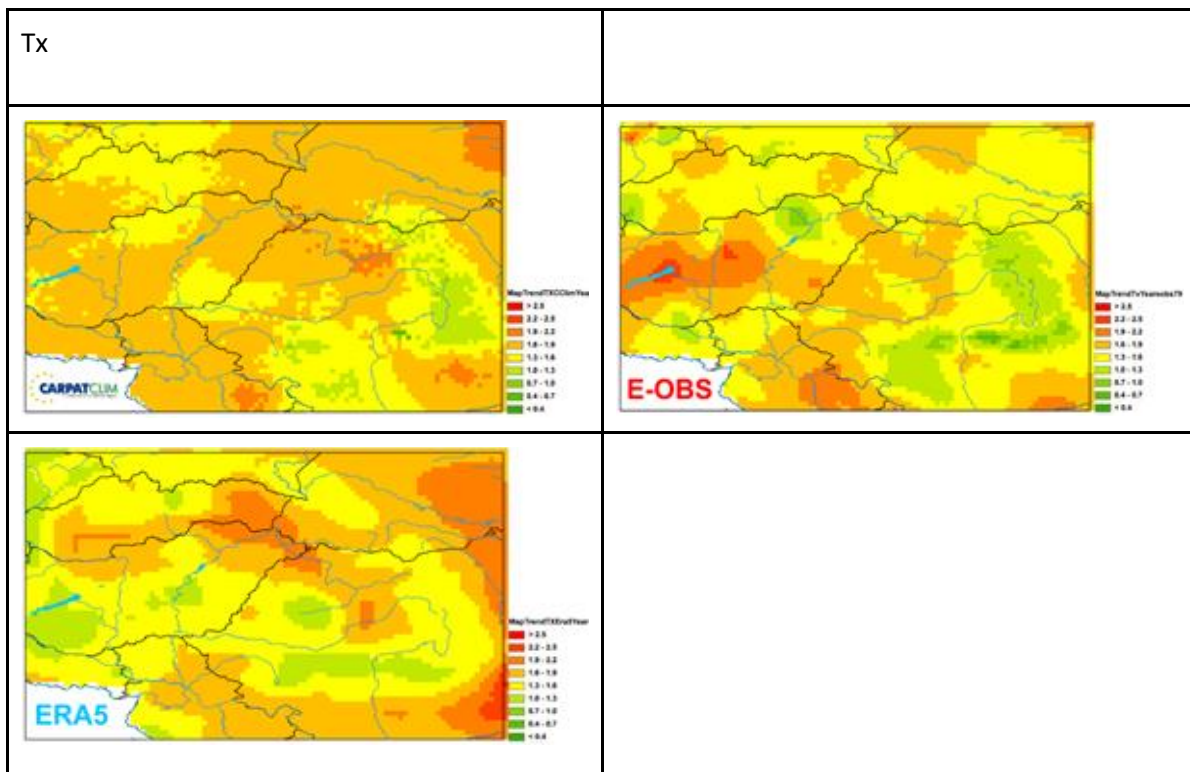
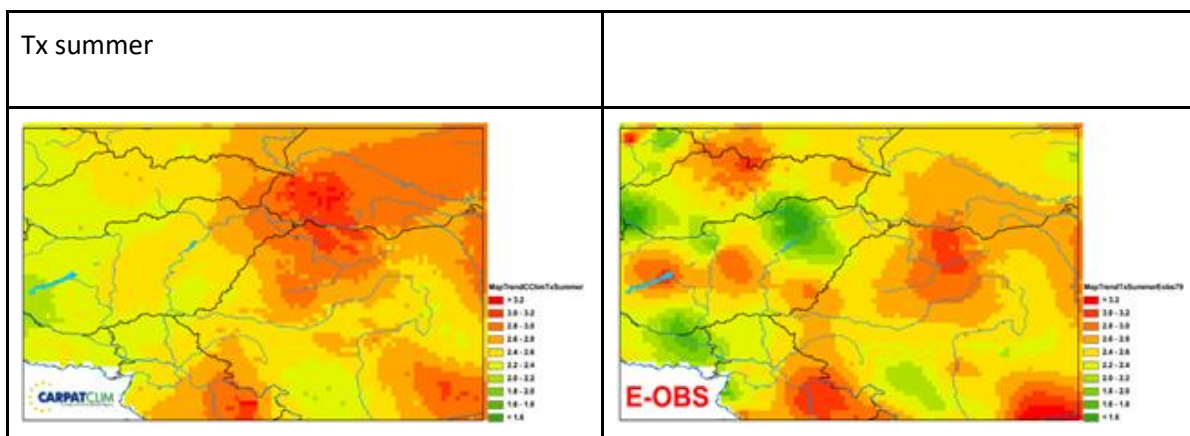


Figure 4.2.8.1. Linear trend for average annual Tx temperature in °C/32year. for CARPATCLIM (top left), E-OBS (top right) and ERA5 (bottom left) over the time period 1979-2010.



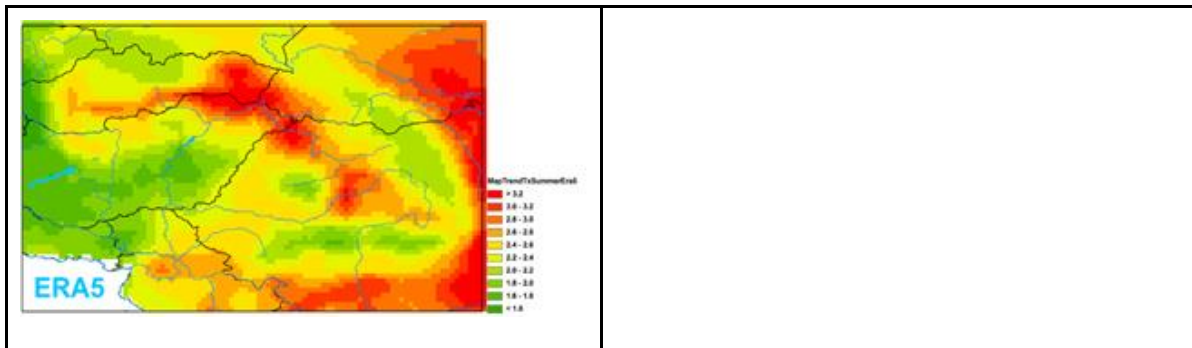


Figure 4.2.8.2. Linear trend for average summer Tx temperature in °C/32year for CARPATCLIM (top left), E-OBS (top right) and ERA5 (bottom left) over the time period 1979-2010.

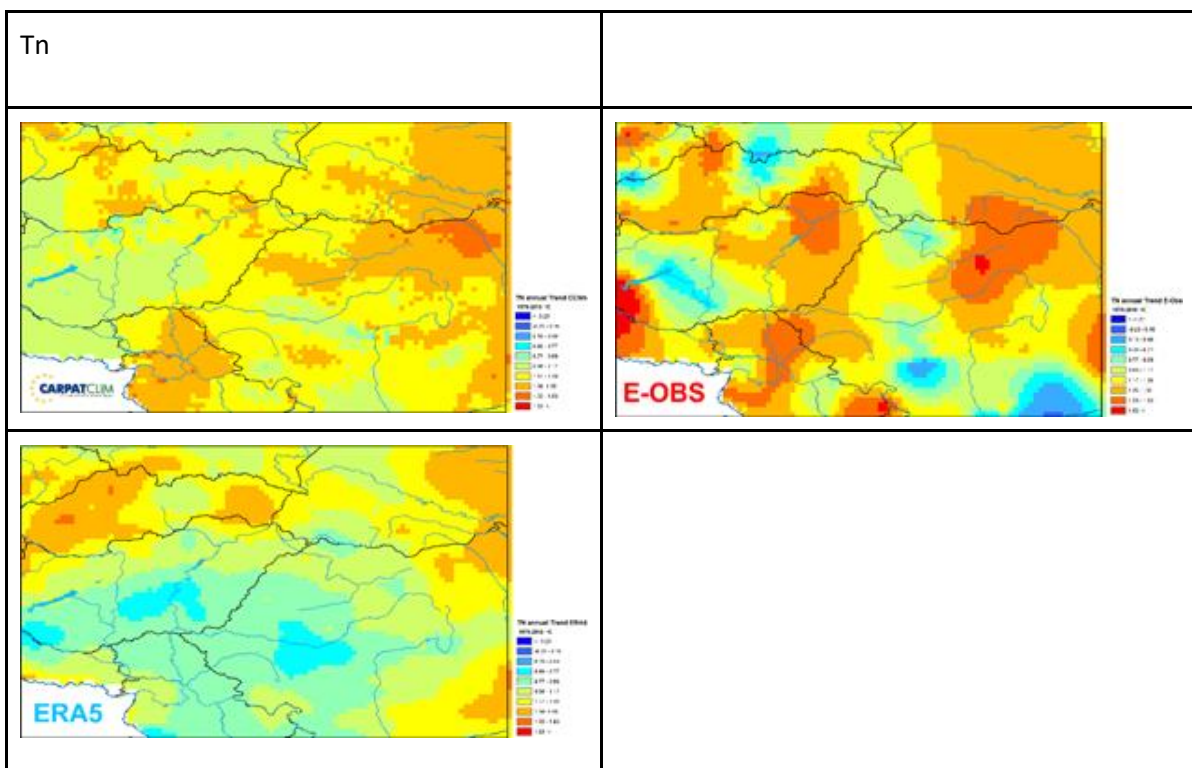


Figure 4.2.8.3. Linear trend for average annual Tn temperature in °C/32year for CARPATCLIM (top left), E-OBS (top right) and ERA5 (bottom left) over the time period 1979-2010.

#### 4.2.9 Homogeneity test

However, E-OBS gridded series were derived from homogenized station data series there is no information on the quality of the gridded series. The MASH (Multiple Analysis of Series for Homogenization, Szentimrey; 2014) software system for homogenization consists of functions for testing the residual inhomogeneity in any dataset. For making this test the closest grid points to 51 Hungarian meteorological stations (Figure 4.2.9.1) were selected from CARPATCLIM and also from E-OBS, then the gridded daily maximum and minimum temperature series from 1961-2010 (the longest overlap between the datasets) were tested by MASH homogenization method. Test

statistics are available only for Hungary to make a comparison, as the station data were not collected into a common database in CARPATCLIM project. Therefore the comparison of the homogenization results for the stations and their closest grid points for the different datasets cannot be done out of Hungary.

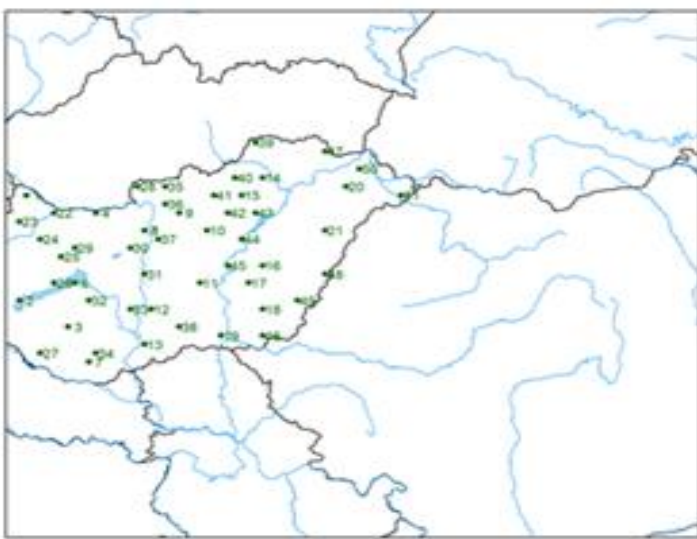


Figure 4.2.9.1. The location of the stations, which were used in the homogeneity test.

The test statistics for inhomogeneity of the gridded series are listed in the Table 4.2.9.1 and Table 4.2.9.2. The null hypothesis is that the examined gridded series are homogeneous. The critical value related to significance level 0.05 comes to 20.86 Test statistics (TS) can be compared to the critical value. The larger TS values are the more suspicious. The highest TSA values are of the order of hundreds in many cases in E-OBS (Table 4.2.9.1) and appear at grid-points near the stations where inhomogeneities were found and eliminated by MASH during preparation of CARPATCLIM.

### **Homogeneity test for TN**

#### **Test Statistics After Homogenization for TN in E-OBS**

<b>Series</b>	<b>TSA</b>	<b>Series</b>	<b>TSA</b>	<b>Series</b>	<b>TSA</b>
37	529.82	6	417.25	13	366.72
36	342.52	11	322.14	15	291.76
14	265.76	38	261.02	41	182.02
22	176.71	20	170.18	24	163.54
26	152.44	5	150.96	8	150.96
34	148.13	9	128.54	33	124.65



40	106.52	1	103.2	23	99.75
27	96.67	49	84.07	10	81.79
47	68.82	31	63.15	25	60.87
51	60.76	43	58.93	17	48.55
21	48.25	2	48.13	46	45.73
7	45.64	16	45.49	39	44.83
29	44.81	4	39.63	50	36.39
32	34.76	12	33.59	3	31.32
18	30.68	19	26.91	42	26.48
45	26.06	35	25.69	44	25.12
30	23.55	48	23.47	28	21.75

AVERAGE: 117.77

Table 4.2.9.1. The test statistics in decreasing order for E-OBS (after homogenization).

#### Test Statistics After Homogenization for TN in CARPATCLIM

Series	TSA	Series	TSA	Series	TSA
32	50.61	22	49.95	26	44.76
30	44.52	16	44.49	14	39.18
38	38.36	19	37.46	12	36.28
28	33.64	11	32.76	21	31.34
36	28.60	24	27.90	41	27.75
48	27.68	45	25.34	10	24.17
3	22.76	18	22.23	33	22.13
23	21.34	4	21.15	35	20.99
43	20.22	37	20.12	17	18.96
7	18.86	5	17.85	8	17.85
1	17.63	20	16.47	27	16.01
40	15.91	49	14.09	42	13.29
6	13.08	50	12.99	46	12.01
2	11.72	31	11.31	9	11.23

34 11.04 47 10.39 29 9.87

44 9.60 25 9.18 15 8.93

51 8.66 13 8.65 39 8.12

**AVERAGE:** 22.34

Table 4.2.9.2. The test statistics in decreasing order for E-OBS (after homogenization).

Possibly the residual inhomogeneities and erroneous data cause the extremely variable trend for E-OBS compared to CARPATCLIM. The largest TSA values appear grid points near Miskolc (15), Siófok (6), Baja (13) where the Figure 4.2.9.2 is patchy. The MASH found these stations inhomogeneous. During MASH QC and homogenization these errors were filtered and the series were adjusted in CARPATCLIM project. Inexplicable large and low changes can be seen in E-OBS. Note that the trends are analyzed and compared for CARPATCLIM, E-OBS and ERA5 in the previous chapter for a shorter overlapping period from 1979-2010. The Figure 4.1.47.. shows that in spite of the curves of the yearly mean Tn curves are running together for CARPATCLIM and E-OBS the statistical structure of the compared dataset are quite different. The maps and the graph of the regionally averaged standard deviation underline that (Figure 4.2.9.3).

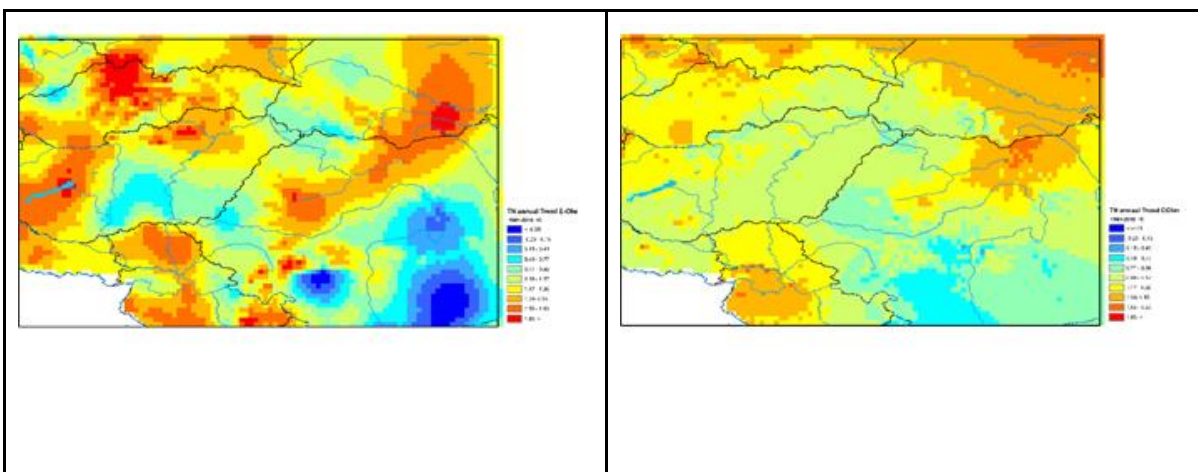
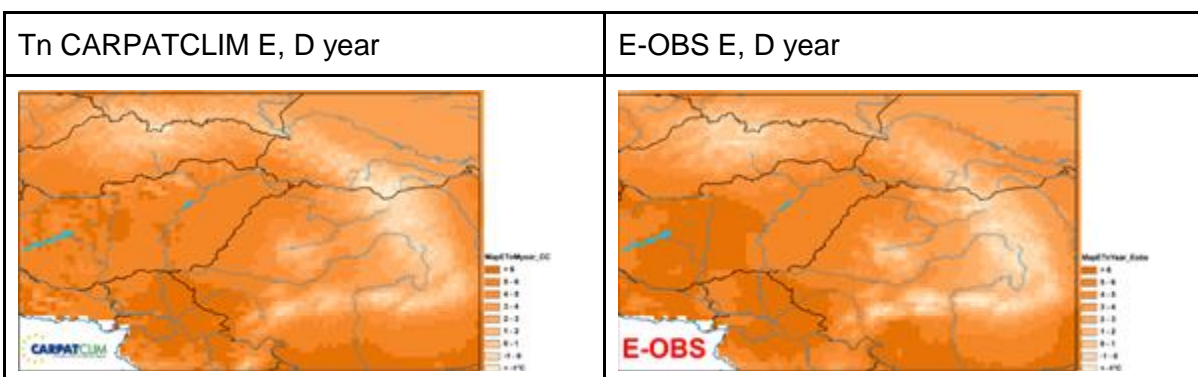


Figure 4.2.9.2. Linear trend (change in the whole period) for average annual average TN temperature in °C for E-OBS (left) and CARPATCLIM (right) over the time period 1961-2010, the longest overlapping period.



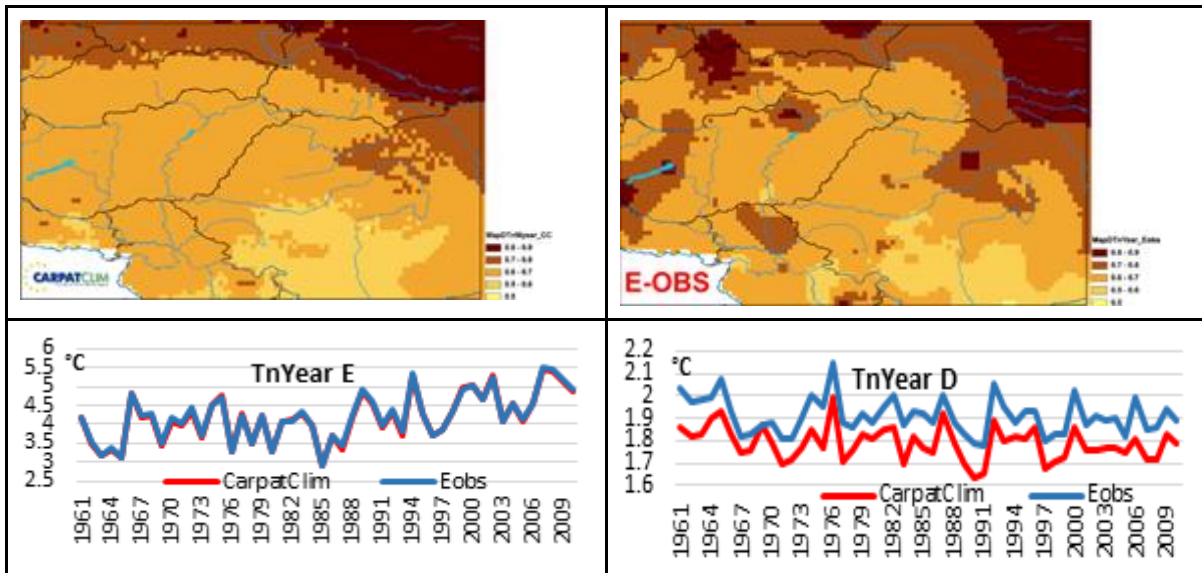


Figure 4.2.9.3. Yearly mean and standard deviation maps for CARPATCLIM and E-OBS in the period 1961-2010 (the longest overlapping period) and the time series of these statistics.

### Homogeneity test for TX

The test statistics for inhomogeneity of the gridded series are listed in the Table 4.2.9.3 and Table 4.2.9.4. The null hypothesis is that the examined gridded series are homogeneous. The critical value related to significance level 0.05 comes to 20.86. Test statistics (TS) can be compared to the critical value, the larger TS values are the more suspicious. The highest TSA values are of the order of hundreds in many cases in E-OBS (Table 4.2.9.3), 108.51 in average. Big values appear at grid-points near the stations where inhomogeneities were found and eliminated by MASH during preparation of CARPATCLIM.

### Test Statistics After Homogenization for TX in E-OBS

Series	TSA	Series	TSA	Series	TSA
15	526.81	6	268.89	19	265.44
20	195.03	5	191.02	8	191.02
42	178.28	1	177.43	37	173.22
7	170.07	36	166.41	9	158.71



49	152.98	10	148.89	44	143.36
11	141.64	31	134.15	26	127.74
43	116.86	47	113	21	104.12
22	102.59	34	100.64	2	92.4
4	91.47	14	89.13	45	83.82
16	83.31	18	78.16	23	75.5
13	70.1	41	64.16	24	64.15
39	62.49	17	54.81	33	52.92
50	50.62	25	50.29	3	48.34
30	46.81	28	44.2	40	42.94
38	41.97	51	38.69	12	34.42
35	24.71	32	23.47	48	22.92
29	21.24	27	17.89	46	14.83

AVERAGE: 108.51

Table 4.2.9.3. The test statistics in decreasing order for E-OBS (after homogenization).

#### Test Statistics After Homogenization for TX in CARPATCLIM

Series TSA Series TSA Series TSA



29	49.91	49	47.61	11	43.01
13	36.51	12	33.36	34	33.28
6	33.23	30	32.27	28	31.43
22	31.04	19	29.14	33	28.66
2	26.63	41	26.2	20	26.05
38	25.26	17	24.71	48	24.58
24	22.09	45	21.17	9	21.14
31	20.98	36	20.69	21	20.21
14	20.18	43	19.75	16	19.62
25	19.46	7	18.98	50	18.63
26	18.42	3	17.94	35	17.83
40	16.6	5	16.47	8	16.47
44	16.34	23	16.21	32	16.09
37	15.78	10	15.36	46	14.33
39	14.09	18	13.85	15	13.78
4	13.66	1	13.54	42	12.4
27	11.7	47	10.78	51	8.02

AVERAGE: 22.26

Table 4.2.9.4. The test statistics in decreasing order for E-OBS (after homogenization)

Due to the residual inhomogeneities the trend maps show quite large differences in the climate signal depending on the dataset we consider Figure 4.2.9.4 for the average annual of daily maximum temperature too. The station inhomogeneities in Hungary (Miskolc, Baja and Siófok) explain the spots with unlike change in E-OBS and in CARPATCLIM.

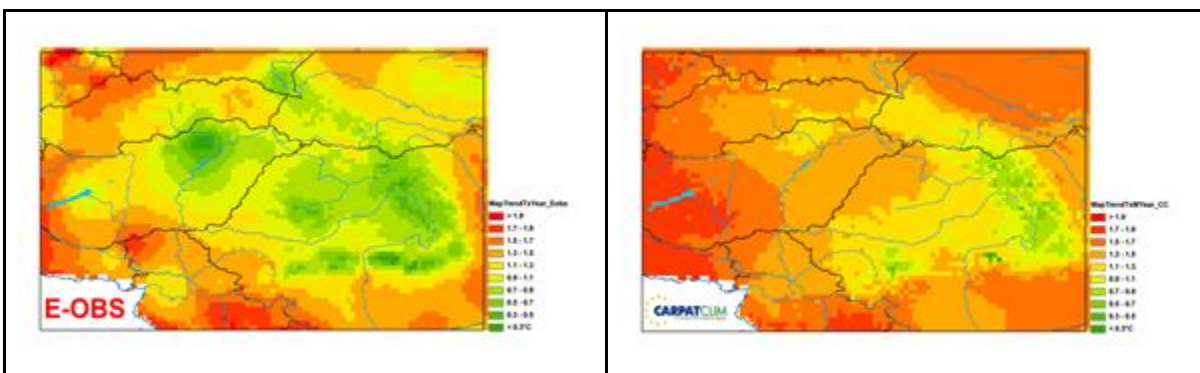


Figure 4.2.9.4. Linear trend (change in the whole period) for average annual TX temperature in °C for E-OBS (left) and CARPATCLIM (right) over the time period 1961-2010.

#### 4.2.10 Main outcomes – temperature in the Carpathians

The spatial distribution of the yearly mean Tx and Tn is similar regarding the datasets including in this comparative study. Lower mean values for Tx and Tn are obvious in all three datasets at higher elevation. The warmest area goes up in the Great Hungarian plain to a larger extent in CARPATCLIM than it is appearing in E-OBS and in ERA5 for Tx. The standard deviation of the yearly average Tx is low in ERA5 almost in the whole territory of Romania.

Regarding the yearly mean minimum temperatures higher values than in CARPATCLIM ( $>7^{\circ}\text{C}$  yearly averages) are standing out between the Lake Balaton and the Danube River in E-OBS in Hungary and in extended regions in Serbia in ERA5 as well. ERA5 overestimates the mean spring daily minima almost on the whole territory of Hungary. E-OBS also provides higher spring average minima in the middle area of Hungary than CARPATCLIM. The spatial distribution of the summer mean daily minima are similar in each dataset, although greater values are present in E-OBS near the Lake Balaton and in Serbia, and also in ERA5 at the south-east of the domain.

As a regard for the yearly cycle CARPATCLIM and E-OBS produce almost the same monthly mean Tx values. ERA5 monthly average maxima are lower at least half degree during the year on average. Considering the monthly mean of the daily minima CARPATCLIM provides the lowest minima at each month close to E-OBS. ERA5 overestimates the daily minimum temperatures at least by half a degree from April to August.



The yearly mean of the diurnal temperature range is 9.77 in regional average in CARPATCLIM, 9.63 in E-OBS and 8.87 in ERA5. The ranking follows from that fact that the CAPATCLIM produces the lowest minima and highest maxima amongst the datasets we examined.

The spatial distribution of the Q95 based on CARPATCLIM and E-OBS Tx values are well detailed and similar. The spatial distribution of the Q95 quantiles in ERA5 is corresponding to the observational datasets, although there are underestimations in Slovakia and in Romania and besides these, the region with high values, above 40 °C appears at the south bound of domain in ERA5. The daily Q05 quantiles are colder in E-OBS at High Tatras in Slovakia than in CARPATCLIM, but warmer in the North-eastern Carpathians around the highest peaks in E-OBS and in the territory of the Ukraine Podolian Highland. In Ukraine, ERA5 Q05 spatial pattern represents values closer to CARPATCLIM than to E-OBS. CARPATCLIM depicts the North-Western Carpathians in more detail than ERA5.

Temperature indices: Roughly the plain regions are represented lower absolute maxima in E-OBS than in CARPATCLIM, by contrast the hilly regions and in the high mountains E-OBS exceeds CARPATCLIM absolute maxima in the period 1979-2010. In the north-eastern Carpathians the lowest temperatures are less extremely cold in E-OBS and in ERA5 than in CARPATCLIM. The spatial pattern of the yearly average number of summer days is described similarly in all three dataset. The frost days of the observational datasets are similar, except the region depicted with less frost days in the middle of Hungary and in Serbia in E-OBS. Less frost days in Serbia emerge in the reanalysis too.

As for the RMSE values, the observational datasets are closer to each other than ERA5 either to CARPATCLIM or E-OBS in general. The lowest RMSE values appear in the plain region, the orography is a determining factor here. The highest MSESS values appear in the plain region, the orography is one of the main determining factors. The Tn is a more problematic climate variable than Tx, as regards the difficulties arise of its interpolation and modelling.

The temperature trends are remarkably different for the examined datasets. The spatial distribution of the change of the daily maximum and minimum temperatures from 1979 to 2010 is unexpectedly heterogeneous in E-OBS, possibly due to the residual inhomogeneity of the gridded data. Extremely high spatial variability turns up on trend map represents the changes of the daily minimum temperatures for E-OBS. For ERA5 the spatial distribution of the summer change is similar to yearly with the larger trend along the Slovak and Hungarian border, what is missing from CARPATCLIM. ERA5 underestimates the change of the minimum temperature in a wider region south from the midline of the domain.

#### E-OBS

The warmest area goes up in the Great Hungarian plain to a larger extent in CARPATCLIM than it is appearing in E-OBS for Tx. Higher mean Tn values than in CARPATCLIM (>7°C yearly averages) are



standing out between the Lake Balaton and the Danube River in E-OBS in Hungary and in extended regions in Serbia in ERA5 as well.

E-OBS also provides higher spring average minima than CARPATCLIM in the middle area of Hungary.

The spatial distribution of the Q95 based on CARPATCLIM and E-OBS Tx values are well detailed and similar. The daily Q05 quantiles are colder in E-OBS at High Tatras in Slovakia than in CARPATCLIM, but warmer in the North-eastern Carpathians around the highest peaks and in Ukraine at the Podolian Highland.

Roughly the plain regions are represented lower absolute maxima in E-OBS than in CARPATCLIM, by contrast the hilly regions and in the high mountains E-OBS exceeds CARPATCLIM absolute maxima. In the north-eastern Carpathians the lowest temperatures are less extremely cold than in CARPATCLIM.

The frost days of the observational datasets are similar, except the region with less frost days in central Hungary and in Serbia.

As for the RMSE values, the observational datasets are closer to each other than ERA5 either to CARPATCLIM or E-OBS in general. The highest MSESS values appear in the plain region, the orography is one of the main determining factors. The Tn is a more problematic climate variable than Tx, as regards the difficulties arise of its interpolation and modelling.

The spatial distribution of the change of the daily maximum and minimum temperatures from 1979 to 2010 is unexpectedly heterogeneous in E-OBS, possibly due to the residual inhomogeneity of the gridded data. Extremely high spatial variability turns up on trend map represents the changes of the daily minimum temperatures.

## ERA5

The warmest area goes up in the Great Hungarian plain to a larger extent in CARPATCLIM than it is appearing in ERA5 for TX. The standard deviation of the yearly average Tx is low in ERA5 almost in the whole territory of Romania. Higher mean Tn values than in CARPATCLIM ( $>7^{\circ}\text{C}$  yearly averages) are standing out in extended regions in Serbia in ERA5. ERA5 overestimates the mean spring daily minima almost on the whole territory of Hungary.

In the northeastern Carpathians the lowest temperatures are less extremely cold than in CARPATCLIM. Less frost days in Serbia emerge in the reanalysis.

As for the RMSE values, the observational datasets are closer to each other than ERA5 either to CARPATCLIM or E-OBS in general. The highest MSESS values appear in the plain region, the orography is one of the main determining factors. The Tn is a more problematic climate variable than Tx, as regards the difficulties arise of its interpolation and modelling. ERA5 underestimates the change of the minimum temperature in a wider region south from the midline of the domain.



## 5. Conclusion

The evaluation of the updated E-OBS dataset and the new global reanalysis ERA5 against regional datasets has been performed by calculating climate indices and statistical measures considering the variables of daily precipitation and temperature. In the following subsections the results of this evaluation are summarized and conclusions drawn, according to the dataset and the variable.

### E-OBS

#### PRECIPITATION

The spatial representation of precipitation of E-OBS generally agrees well with the reference datasets. Enhanced amounts of precipitation along the mountain ridges and certain mesoscale features like the dry inner-Alpine conditions are realistically reproduced. Also, well-known precipitation “hot spots” in the High Tatras, along the Norwegian coast, as well as in the Southern Alps and in the Julian Alps are realistically shown in E-OBS.

However, E-OBS lacks some outstanding moist anomalies like e.g. the Massif Central in the Alps and the Southern Carpathians in the Carpathians. Furthermore, a general underestimation of precipitation magnitude is visible in all three regions. Given that the error and the skill patterns of E-OBS compared to the reference datasets suddenly change at country borders, the performance of E-OBS seems to rely strongly on the data availability. This is especially visible when considering the skill scores in the Alpine region, where significantly fewer stations are included in Northern Italy, in parts of France, Switzerland and Austria, as well as in Croatia (Figure 1 and Figure 2). In Germany and Slovenia, on the other hand, the skill scores uniformly reach a perfect score because the same stations are fed into E-OBS as into APGD. Similarly, E-OBS coincides very well with NGCD-1 and 2, especially in the flat areas of Sweden and Finland, where the same station network is included in E-OBS as in NGCD.

To conclude, E-OBS very realistically reproduces daily precipitation in Fennoscandia, as it is based on a very similar set of observational data as the reference datasets. In contrast to that, E-OBS scores worse in the Alpine region where the difference in the station network heavily depends on the nation. Overall, it is not surprising that E-OBS comes off worst in remote and mountainous areas, where fewer in-situ measurements are taken into account, as opposed to flat, densely populated areas. As long as large-scale phenomena over Europe are examined, E-OBS is assumed to be the most suitable dataset to date. Investigations on mesoscale phenomena and especially the calculation of long-term trends should be avoided or treated with caution. The latter arises due to temporal inconsistencies in the station network.

#### TEMPERATURE

When considering general temperature distribution of E-OBS, a remarkable agreement between E-OBS and the reference datasets is found especially in the Carpathians, but also in Fennoscandia. This finding holds also when looking at extremes with only minor differences in the north of Norway



and along the Carpathian rim. Concerning the DTR, it is worth noticing that E-OBS and NGCD-1 show smoother fields compared to accentuated DTR patterns in NGCD-2 due to clear topography imprint and less pronounced coastal effects. The largest systematic differences occur in winter, as opposed to the summer in Fennoscandia. However, the different behavior of NGCD-1 and NGCD-2 also affects the evaluation of E-OBS. While E-OBS is warmer than NGCD-2, except for summer, with the bias increasing towards the North, E-OBS is warmer than NGCD-1 throughout the entire year, apart from some areas along the Norwegian coast. Given these findings, major differences of E-OBS compared to the regional reference datasets again arise in areas of complex topography and along the Norwegian coast that is heavily influenced by oceanic climate. The better performance of the regional datasets can be clearly explained by regionally adapted interpolation methods.

Similar to the analysis of precipitation, E-OBS very realistically reproduces the general temperature distribution in Fennoscandia, as it is based on a very similar set of observational data as the reference datasets. However, this dependence on the station network is even more pronounced, as the deviation of E-OBS from NGCD is larger in Norway, where NGCD includes significantly more station data, compared to Sweden and Finland. In the Carpathian region the spatial distribution of the yearly means and the yearly cycles are similar. CARPATCLIM captures the daily extremes better than E-OBS, the largest discrepancies can be found in the trends.

## ERA5

### PRECIPITATION

ERA5 agrees surprisingly well with the precipitation patterns of the reference datasets. The dominant patterns of enhanced precipitation due to orography in contrast to the dry conditions in the flat lee regions, as well as the wet oceanic regions along the Norwegian coast are realistically reproduced by ERA5. The major drawback of ERA5 is the constant overestimation of the precipitation amounts. While the mean annual precipitation of ERA5 is only partly higher compared to the references, it clearly overestimates the wet-day frequency in all three regions. Consequently, it can be assumed that light precipitation is especially overrepresented. Another problem of ERA5 is the misrepresentation of those small regions that are prone to heavy precipitation. The comparatively coarse original grid resolution of ERA5 and the therewith related spatial smoothing, together with the absence of station data in reanalyses, lead to missing of local precipitation extremes. Thus, problems arise when single grid points are investigated, as e.g. the small-sized catchment of Tagliamento in the Julian Alps. Nevertheless, the finer grid resolution of ERA5 compared to former global reanalyses seems to boost its performance significantly. While it is not recommended to use ERA5 when investigating local extremes, it proves to be an interesting alternative regarding the analysis of precipitation over Europe in general.

### TEMPERATURE

Regarding temperatures, ERA5 has lower mean and maximum and higher minimum values if compared to the reference datasets, especially in colder regions (e.g. along orographic elevations



and in northern Fennoscandia). When it comes to extreme temperature quantiles, they are less extreme in ERA5 compared to the observational datasets, because of ERA5 represents areal averages with a larger spatial support than the references. Furthermore, ERA5 shows larger deviations from the reference in regions of transitive temperature regimes, as e.g. along the coast and in the proximity of the big lakes. The different behavior between ERA5 and the reference datasets is enhanced when looking at the spatial distribution of DTR. There, major lakes in Southeast Finland and inland in the southern part of Sweden are better visible in ERA5-LAND than in the other ERA5 datasets.

The bias between ERA5 and NGCD shows that ERA5 is in general warmer in the lowlands and colder in the mountains, and that the systematic differences are greater in winter. The same is true for ERA5-Land. Even if ERA5 shows a good overall performance compared to NGCD and CARPATCLIM in case of temperature, it comes off worse than E-OBS, especially in Fennoscandian winter.

To conclude, ERA5 is suitable when analyzing temperature in areas of less complex topography and where oceanic influence is minimized.



## 6. References

- Copernicus Climate Change Service (C3S) (2017): ERA5: Fifth generation of ECMWF atmospheric reanalyses of the global climate . Copernicus Climate Change Service Climate Data Store (CDS). [Date of access: 30.5.2020] <https://cds.climate.copernicus.eu/cdsapp#!/home>
- Cornes, R. C., van der Schrier, G., van den Besselaar, E. J. M., & Jones, P. D. (2018). An ensemble version of E-OBS temperature and precipitation datasets. *Journal of Geophysical Research: Atmospheres*, 123, 9391–9409. <https://doi.org/10.1029/2017JD028200>
- European Environment Agency (2016). European river catchment, updates: Iceland, Malta and Romania. European Environment Agency and European Topic Centre land use and spatial information. Retrieved from. <https://www.eea.europa.eu/data-and-maps/data/european-river-catchments-1#tab-qis-data>
- Frei, C. (2014). Interpolation of temperature in a mountainous region using non-linear profiles and non-Euclidean distances. *International Journal of Climatology*, 34(5), 1585–1605. <https://doi.org/10.1002/joc.3786>
- Frei, C., & Isotta, F. A. (2019). Ensemble spatial precipitation analysis from rain gauge data: Methodology and application in the European Alps. *Journal of Geophysical Research: Atmospheres*, 124. <https://doi.org/10.1029/2018JD030004>
- Haylock, M. R., Hofstra, N., Klein Tank, A. M. G., Klok, E. J., Jones, P. D., & New, M. (2008). A European daily high-resolution gridded data set of surface temperature and precipitation for 1950–2006. *Journal of Geophysical Research*, 114, D20119. <https://doi.org/10.1029/2009JD011799>
- Hersbach, H., Bell, B., Berrisford, P., Hirahara, S., Horányi, A., Muñoz-Sabater, J., Nicolas, J., Peubey, C., Radu, R., Schepers, D., Simmons, A., Soci, C., Abdalla, S., Abellán, X., Balsamo, G., Bechtold, P., Biavati, G., Bidlot, J., Bonavita, M., De Chiara, G., Dahlgren, P., Dee, D., Diamantakis, M., Dragani, R., Flemming, J., Forbes, R., Fuentes, M., Geer, A., Haimberger, L., Healy, S., Hogan, R. J., Hólm, E., Janisková, M., Keeley, S., Laloyaux, P., Lopez, P., Lupu, C., Radnoti, G., de Rosnay, P., Rozum, I., Vamborg, F., Villaume, S., Thépaut, J.-N. (2020). ERA5 Global Reanalysis.
- Hochberg, Yoav Benjamini and Yosef (1995): Controlling the False Discovery Rate: A Practical and Powerful Approach to Multiple Testing. *Journal of the Royal Statistical Society* 57, no. 1. 289–300.
- Isotta, F. A., Frei, C., Weilguni, V., Perćec Tadić, M., Lassegues, P., Rudolf, B., et al. (2014). The climate of daily precipitation in the Alps: Development and analysis of a high-resolution grid dataset from pan-alpine rain-gauge data. *International Journal of Climatology*, 34(5), 1657–1675. <https://doi.org/10.1002/joc.3794>



Isotta, F. A., Vogel, R., & Frei, C. (2015). Evaluation of European regional reanalyses and downscalings for precipitation in the Alpine region. *Meteorologische Zeitschrift*, 24(1), 15–37. <https://doi.org/10.1127/metz/2014/0584>

Isotta et al. (2020). LAPrec. in preparation

Klein Tank, A.M.G., J.B. Wijngaard, G.P. Koennen, R. Boehm, G. Demaree, A. Gocheva, M. Mileta, S. Pashiardis, L. Hejkrlik, C. Kern-Hansen, R. Heino, P. Bessemoulin, G. Müller-Westmeier, M. Tzanakou, S. Szalai, T. Pálsdóttir, D. Fitzgerald, S. Rubin, M. Capaldo, M. Maugeri, A. Leitass, A. Bukantis, R. Aberfeld, A.F.V. van Engelen, E. Forland, M. Mietus, F. Coelho, C. Mares, V. Razuvayev, E. Nieplova, T. Cegnar, J. Antonio López, B. Dahlström, A. Moberg, W. Kirchhofer, A. Ceylan, O. Pachaliuk, L.V. Alexander, P. Petrovic (2002): Daily surface air temperature and precipitation dataset 1901–1999 for European Climate Assessment (ECA). – *Int. J. Climatol.* 22, 1441–1453.

Klok, E.J., Klein Tank, A.M.G. (2008): Updated and extended European dataset of daily climate observations. – *Int. J. Climatol.* 29, 1182–1191. DOI:10.1002/joc.1779

Lakatos, M., Szentimrey, T., Bihari, Z. and Szalai, S. (2013) Creation of a homogenized climate database for the Carpathian region by applying the MASH procedure and the preliminary analysis of the data. *Idojaras*, 117, 143–158.

Mátrai,A. (2015): Analysis of probabilistic precipitation forecasts on the sub-catchments of Danube and Tisza rivers. Diploma work (in Hungarian)

Lussana C., Saloranta T., Skaugen T., Magnusson J., Tveito O.E. and Andersen J. (2018a) seNorge2 daily precipitation, an observational gridded dataset over Norway from 1957 to the present day *Earth Syst. Sci. Data* 10 235–49

Lussana, C., Tveito, O. E., and Ubaldi, F. (2018b) Three-dimensional spatial interpolation of 2m temperature over Norway, *Q. J. Roy. Meteor. Soc.*, 144, 344–364, <https://doi.org/10.1002/qj.3208>

Rodwell, M. J., Richardson, D. S., Hewson, T. D. and Haiden T (2014) "A new equitable score suitable for verifying precipitation." *Quarterly Journal of the Royal Meteorological Society* 136, 1344–1363.

Spinoni, J., Szalai, S., Szentimrey, T., Lakatos, M., Bihari, Z., Nagy, A., Németh, Á., Kovács, T., Mihic, D., Dacic, M., Petrovic, P., Kržič, A., Hiebl, J., Auer, I., Milkovic, J., Štepánek, P., Zahradníček, P., Kilar, P., Limanowka, D., Pyrc, R., Cheval, S., Birsan, M.-V., Dumitrescu, A., Deak, G., Matei, M., Antolovic, I., Nejedlík, P., Šťastný, P., Kajaba, P., Bochnícek, O., Galo, D., Mikulová, K., Nabivanyts, Y., Skrynyk, O., Krakovska, S., Gnatiuk, N., Tolasz, R., Antofie, T., Vogt, J. (2015): Climate of the Carpathian Region in the period 1961–2010: climatologies and trends of 10 variables. *International Journal of Climatology* 35(7), 1322-1341



Squintu, A. A., van der Schrier, G., Brugnara, Y., Klein Tank, A. (2019) Homogenization of daily temperature series in the European Climate Assessment & Dataset. *Int J Climatol*, 39, 1243–1261. <https://doi.org/10.1002/joc.5874>

Squintu, A. A. (2020) Building Long Homogeneous Temperature Series across Europe: A New Approach for the Blending of Neighboring Series. *Journal of Applied Meteorology and Climatology*, 59.1, 175-189. <https://doi.org/10.1175/JAMC-D-19-0033.1>

Szentimrey, T. (1999) Multiple Analysis of Series for Homogenization (MASH). *Proceedings of the Second Seminar for Homogenization of Surface Climatological Data, Budapest, Hungary, WMO, WCDMP-No. 41*, 27–46.

Szentimrey, T. (2008): Development of MASH homogenization procedure for daily data. *Proceedings of the Fifth Seminar for Homogenization and Quality Control in Climatological Databases, Budapest, 2006, WCDMP-No. 71, WMO/TD-NO. 1493*, 123–130.

Szentimrey, T. and Bihari, Z. (2007) Mathematical background of the spatial interpolation methods and the software MISH (Meteorological Interpolation based on Surface Homogenized Data Basis). In: *Proceedings from the Conference on Spatial Interpolation in Climatology and Meteorology, Budapest, Hungary, 2004. COST Action 719, COST Office*, pp. 17–27

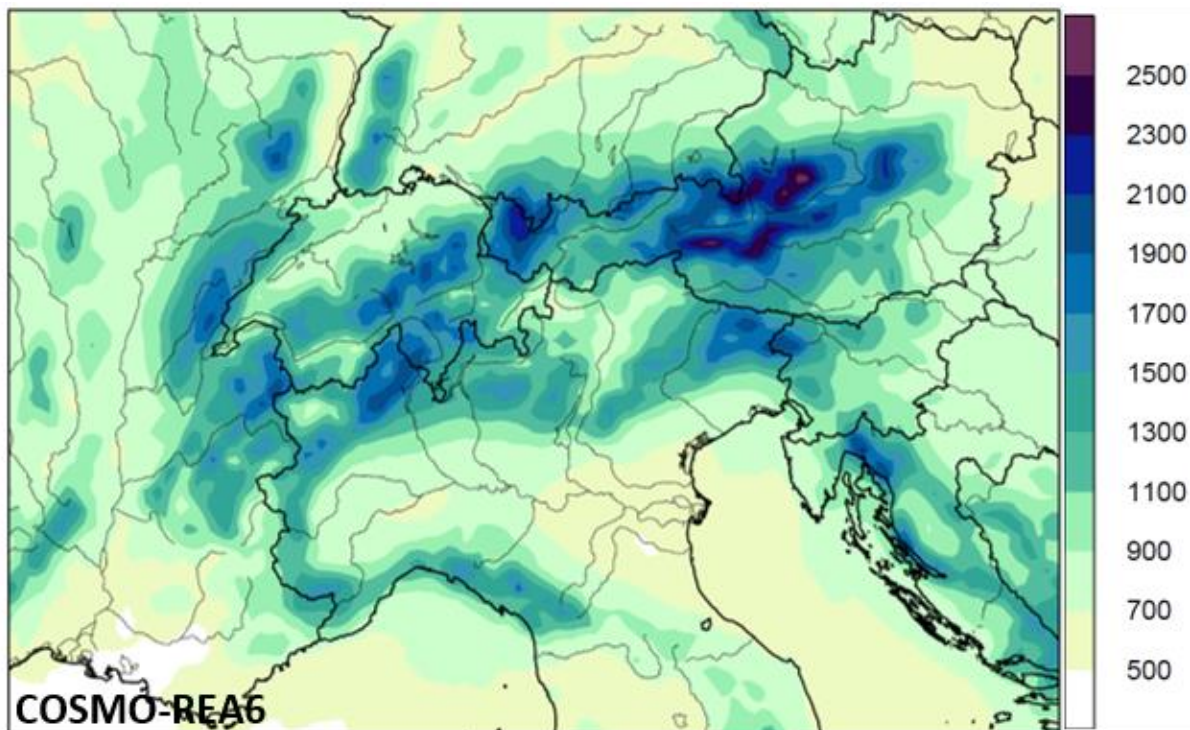
Szentimrey, T. (2014): Manual of homogenization software MASHv3.03, Hungarian Meteorological Service, p.69.

Szentimrey, T. (2019): Mathematical methodology and software for comparison of gridded datasets (manuscript)

Tveito, O.E., E.J. Førland, R. Heino, I. Hanssen-Bauer, H. Alexandersson, B. Dahlström, A. Drebs, C. Kern-Hansen, T. Jónsson, E. Vaarby-Laursen and Y. Westman (2000) Nordic Temperature Maps, DNMI Klima 9/00 KLIMA, Norwegian Meteorological Institute

Tveito, O.E., Bjørdal, I., Skjelvåg, A.O., Aune, B. (2005): A GIS-based agro-ecological decision system based on gridded climatology. – *Meteor. Appl.* 12, 57–68.

## Appendix



Appendix 1: Mean annual precipitation (mm per year; 1997-2008). COSMO-REA6 is shown on 0.1° regular grid.

**ANOVA (Analysis Of Variance) examination Tamás Szentimrey**

VARIMAX Limited Partnership

szentimrey.t@gmail.com

Using the basic theorem of ANOVA the total spatio-temporal variance can be partitioned (1) equivalently as follows.

- Sum of spatial variance of temporal means and spatial mean of temporal variances.

The temporal means and temporal variances (or st. deviations) in the space can be visualised by maps.

- Or sum of temporal variance of spatial means and temporal mean of spatial variances.

The series of spatial means and spatial variances (or st. deviations) can be visualised by graphics.

The above ANOVA methodology can be used for the gridded monthly, seasonal and annual series calculated from the daily series. Mean series for temperature, while sum series for precipitation. The calculated maps and graphics for E-OBS and CarpatClim datasets can be compared.

In addition the ANOVA methodology can be used also for the monthly maximum and minimum series (Section 3) furthermore for the difference series of the datasets (Section 2).

### 1.1 Mathematical description



$Z(s_j, t)$  ( $j = 1, \dots, N$ ;  $t = 1, \dots, n$ ) – data series ( $s_j$ : location;  $t$ : time)

$\hat{E}(s_j) = \frac{1}{n} \sum_{t=1}^n Z(s_j, t)$  ( $j = 1, \dots, N$ ) – temporal mean at location  $s_j$

$\hat{D}^2(s_j) = \frac{1}{n} \sum_{t=1}^n (Z(s_j, t) - \hat{E}(s_j))^2$  ( $j = 1, \dots, N$ ) – temporal variance at location  $s_j$

$\hat{E}(t) = \frac{1}{N} \sum_{j=1}^N Z(s_j, t)$  ( $t = 1, \dots, n$ ) – spatial mean at moment  $t$

$\hat{D}^2(t) = \frac{1}{N} \sum_{j=1}^N (Z(s_j, t) - \hat{E}(t))^2$  ( $t = 1, \dots, n$ ) – spatial variance at moment  $t$

$\hat{E} = \frac{1}{N \cdot n} \sum_{j=1}^N \sum_{t=1}^n Z(s_j, t) = \frac{1}{N} \sum_{j=1}^N \hat{E}(s_j) = \frac{1}{n} \sum_{t=1}^n \hat{E}(t)$  – total mean

$\hat{D}^2 = \frac{1}{N \cdot n} \sum_{j=1}^N \sum_{t=1}^n (Z(s_j, t) - \hat{E})^2$  – total variance

$\frac{1}{N} \sum_{j=1}^N (\hat{E}(s_j) - \hat{E})^2$  – spatial variance of temporal means

$\frac{1}{N} \sum_{j=1}^N \hat{D}^2(s_j)$  – spatial mean of temporal variances

$\frac{1}{n} \sum_{t=1}^n (\hat{E}(t) - \hat{E})^2$  – temporal variance of spatial means

$\frac{1}{n} \sum_{t=1}^n \hat{D}^2(t)$  – temporal mean of spatial variances

### Partitioning of Total Variance (Theorem)



$$\hat{D}^2 = \frac{1}{N} \sum_{j=1}^N (\hat{E}(s_j) - \hat{E})^2 + \frac{1}{N} \sum_{j=1}^N \hat{D}^2(s_j) = \frac{1}{n} \sum_{t=1}^n (\hat{E}(t) - \hat{E})^2 + \frac{1}{n} \sum_{t=1}^n \hat{D}^2(t) \quad (1)$$

The analysis of these terms is recommended to characterize the spatiotemporal variability.

Spatial terms: spatial variance of temporal means  $\frac{1}{N} \sum_{j=1}^N (\hat{E}(s_j) - \hat{E})^2$

and temporal mean of spatial variances  $\frac{1}{n} \sum_{t=1}^n \hat{D}^2(t)$ .

Temporal terms: spatial mean of temporal variances  $\frac{1}{N} \sum_{j=1}^N \hat{D}^2(s_j)$

and temporal variance of spatial means  $\frac{1}{n} \sum_{t=1}^n (\hat{E}(t) - \hat{E})^2$ .

These statistics are included by the output ANOVA.res.

### Example

ANOVA results for CarpatClim dataset, annual mean series of daily minimum values (Tn)

Total mean: 4.18

Total variance: 3.92

Spatial variance of temporal means: 3.46

Spatial mean of temporal variances: 0.46

Temporal variance of spatial means: 0.40

Temporal mean of spatial variances: 3.52

Spatial st. deviation of temporal means: 1.86

Root spatial mean of temporal variances: 0.68

Spatial mean of temporal st. deviations: 0.67

Temporal st. deviation of spatial means: 0.63

Root temporal mean of spatial variances: 1.88

Temporal mean of spatial st. deviations: 1.87

### Visualization



Maps of temporal means (E) and st. deviations (D):

$\hat{E}(\mathbf{s}_j)$ ,  $\hat{D}(\mathbf{s}_j)$  ( $j = 1, \dots, N$ ) (output ANOVA.res)

Graphics of spatial means (E) and st. deviations (D):

$\hat{E}(t)$ ,  $\hat{D}(t)$  ( $t = 1, \dots, n$ ) (Output: ANOVA.ser)